

**CRANFIELD UNIVERSITY**  
College of Aeronautics

PhD Thesis



Demil Y. Djafri

**Multi-disciplinary Design of Wings for Transport Aircraft  
Operating at High Subsonic Speed**

Supervisor : Prof. D. Howe

December 1995

This thesis is submitted in partial fulfilment of the requirements for  
the Degree of Doctor of Philosophy

## ACKNOWLEDGEMENT

I would like to express my sincere and deep appreciation to Professor D. Howe for his guidance, supervision, advice, and encouragement for the research of this thesis.

Many thanks must be given to Mr. H. Smith, Professor J. P. Fielding and other staff at the College of Aeronautics for their invaluable help.

And finally, I wish to express my appreciation to my parents, and to my wife Rika for taking care of me and our baby boy Faiz.

## ABSTRACT

In this thesis a methodology for designing wings for transport aircraft operating at high subsonic speed is investigated. Several methods are studied, including more accurate methods such as the computational methods. These are used as an addition to the semi-empirical methods.

Several attempts have been made to build a computerised aircraft design in the past. Most of the conceptual aircraft design programs that are available are based on the semi-empirical method only. As faster computers become available, a method for designing a high subsonic aircraft wing is studied by including computational aerodynamic and computational structural analysis in the integration process. SPARV is used as the computational aerodynamic program and NASTRAN is used as the computational structural analysis program.

The objectives of this thesis are to study a method of performing the conceptual design of wings for transport aircraft operating at high subsonic speed and to demonstrate that aerodynamics analysis using Computational Fluid Dynamics (CFD) and structures analysis using the Finite Element Method (FEM), can be coupled with the aircraft synthesis program in a seamless distributed computing environment. The achievement of these objectives is demonstrated by applying the methodology to specific wing design.

This method has been validated and tested for transport aircraft operating at high subsonic speed, but application on military transports may also be valid. An example case study is presented in this thesis.

Improvement of the method for future development is also considered in the thesis. These include the use of a more powerful computational aerodynamics package.

# TABLE OF CONTENTS

ACKNOWLEDGEMENT ..... i

ABSTRACT ..... ii

TABLE OF CONTENTS ..... iii

LIST OF FIGURES ..... vii

LIST OF TABLES ..... ix

NOTATIONS ..... x

1. INTRODUCTION ..... 1

    1.1 Introduction ..... 1

    1.2 Description of the work ..... 6

2. PAST COMPUTERISED AIRCRAFT DESIGN / LITERATURE  
STUDY ..... 13

    2.1 Introduction ..... 13

    2.2 ADROIT (Ref. 4) ..... 13

    2.3 Pasaribu (Ref. 9) ..... 14

    2.4 DESAID (Ref. 8) ..... 15

    2.5 MVO (Ref. 7) ..... 16

    2.6 ACSYNT (Ref. 27) ..... 17

    2.7 GASP (Ref. 37) ..... 19

    2.8 NASA Langley Research Center ..... 19

    2.9 Other related research studies ..... 21

3. HIGH SUBSONIC AIRCRAFT DESIGN PROCESS ..... 23

    3.1 Introduction ..... 23

    3.2 Parametric Study ..... 23

    3.3 Fuselage Design ..... 28

    3.4 Wing Design ..... 30

    3.5 Engine Selection ..... 30

    3.6 Weight and Balance ..... 31

    3.7 Undercarriage Design ..... 32

    3.8 Performance Analysis ..... 34

    3.9 Tailplane Design ..... 35

    3.10 Design Optimisation ..... 38



4. WING DESIGN PROCESS ..... 42

4.1 Introduction ..... 42

4.2 Aerofoil selection ..... 44

4.3 Wing Area ..... 46

4.4 Thickness ratio, Sweep and Mach number trade-offs 48

4.5 Wing Aspect Ratio and Span ..... 51

4.6 Spanload and Taper Ratio ..... 52

4.7 Wing Incidence Angle ..... 53

5. COMPUTATIONAL AERODYNAMIC PROCESS ..... 54

5.1 Introduction ..... 54

5.2 Computational Aerodynamics Program ..... 54

5.2.1 Navier Stokes Equations ..... 57

5.2.2 Euler Equations ..... 57

5.2.3 Full Potential Equations ..... 57

5.2.4 Laplaces Equations ..... 57

5.3 Panel Method ..... 58

5.4 Panel Method Modelling ..... 58

5.5 Aircraft Cruise Lift Coefficient Estimation ..... 60

5.6 Validation ..... 60

6. COMPUTATIONAL STRUCTURAL ANALYSIS PROCESS ... 67

6.1 Introduction ..... 67

6.2 Structural Layout ..... 69

6.2.1 Chordwise location of spars ..... 70

6.2.2 Rib pitch ..... 72

6.2.3 Rib direction ..... 74

6.3 Finite Element Modelling ..... 78

6.3.1 NASTRAN Sol-200 ..... 80

6.3.2 Optimisation for minimum weight ..... 82

6.3.3 NASTRAN Finite Element Model ..... 84

6.4 Fatigue ..... 92

6.5 Design Results ..... 94

7. PROGRAM INTEGRATION METHODOLOGY ..... 95

7.1 Introduction ..... 95

7.2 Program Design Philosophy ..... 95

7.2.1 Portability ..... 96

7.2.2 The Target Computer ..... 96

7.2.3 The Programming Language ..... 97

7.3 Design Problem Formulation ..... 98

7.4 Characteristics of Integration Method ..... 102

7.5 Data Transfer Techniques ..... 102

7.5.1 Aircraft Synthesis Data ..... 103

7.5.2 Stability and Control Data ..... 105

7.5.3 Pressure Load Data ..... 105

7.5.4 Deflection / Deformation Data .....	106
7.6 Interface Program .....	106
7.6.1 Pressure Load Interface .....	107
7.6.2 Deflection / Deformation Interface .....	108
7.7 Static Aeroelasticity Analysis .....	108
7.7.1 Direct Solution .....	109
7.7.2 Iterative Analysis .....	109
7.7.3 MODIFY module .....	110
7.8 Convergence and Optimality .....	121
7.9 Twist Optimisation .....	124
8. CASE STUDIES .....	126
8.1 Introduction .....	126
8.2 Validation (VC-10) .....	126
8.2.1 SPARV Model .....	127
8.2.2 NASTRAN Model .....	131
8.3 Interface Program Results .....	137
8.3.1 Pressure Loads .....	137
8.3.2 Structure Deflection .....	140
8.4 Static Aeroelastic Iteration Results .....	141
8.5 Divergence Test .....	143
8.6 Test Case Results .....	143
8.6.1 Parametric Study .....	143
8.6.2 Stability and Control .....	149
8.6.3 Aircraft Synthesis .....	152
8.6.4 Aerodynamic .....	153
8.6.5 Structure .....	154
8.6.6 Comparison with semi-empirical method ....	156
9. DISCUSSION .....	157
10. CONCLUSION .....	160
REFERENCES .....	163
A. PARAMETRIC STUDY .....	171
A.1 Introduction .....	171
A.2 Parametric Study Criteria .....	171
A.2.1 Landing Field Length .....	172
A.2.2 Take Off Field Length .....	172
A.2.3 Second Segment Climb Gradient .....	173
A.2.4 Missed Approach .....	174
A.2.5 Cruise Performance .....	175
A.2.6 Initial Cruise Altitude Capability (ICAC) ..	177
A.2.7 One Engine Inoperative (OEI) Ceiling .....	178
A.3 Method for finding optimum point .....	179

A.4 Parametric Study Input File ..... 180

A.5 Parametric Study Output File ..... 183

A.6 PARAMETRIC stand alone program ..... 189

B. WING LAYOUT CALCULATIONS ..... 190

    B.1 Introduction ..... 190

    B.2 Wing Layout input files ..... 190

    B.3 Wing Layout output file ..... 196

C. SPARV PRE AND POST PROCESSORS ..... 201

    C.1 Introduction ..... 201

    C.2 PRESPARV input file ..... 202

    C.3 PRESPARV output file ..... 202

        C.3.1 Wing points generation ..... 203

        C.3.2 Fuselage points generation ..... 209

        C.3.3 HTP points generation ..... 209

        C.3.4 VTP points generation ..... 210

    C.4 Co-ordinate points of deflected wing. .... 211

    C.5 PRESPARV stand alone program ..... 211

    C.6 POST SPARV ..... 211

D. NASTRAN PRE AND POST PROCESSORS ..... 213

    D.1 Introduction ..... 213

    D.2 PRENASTRAN input file ..... 213

    D.3 PRENASTRAN output file ..... 218

    D.4 POSTNASTRAN ..... 224



# LIST OF FIGURES

FIGURE 1.1	FORECAST DELIVERY BY AEROPLANE SIZE (1990-2005)	2
FIGURE 1.2	RELATIVE COST	4
FIGURE 1.3	PROPOSED FLOWCHART	9
FIGURE 1.4	PROPOSED FLOWCHART	10
FIGURE 1.5	PROPOSED FLOWCHART	11
FIGURE 1.6	PROPOSED FLOWCHART FOR WINGLAYOUT	12
FIGURE 3.1	(W/S) COMPARISON	25
FIGURE 3.2	$V_{APP}^2$ VS. LFL	26
FIGURE 3.3	( $T_O/W$ ) COMPARISON	27
FIGURE 3.4	$CL_{MAX}$ VS. SWEEP C/4	35
FIGURE 3.5	PARAMETRIC STUDY	41
FIGURE 3.6	DEMONSTRATED $CL_{MAX}$ LEVELS	41
FIGURE 4.1	( $T_O/W$ ) VS. (W/S)	47
FIGURE 4.2	SCALE UP OF AEROFOIL SECTION	49
FIGURE 4.3	SWEEP ANGLE VS. AR	52
FIGURE 5.1	FLOW EQUATIONS	56
FIGURE 5.2	SPARV WITH 25 PANELS CHORDWISE	61
FIGURE 5.3	SPARV WITH 13 PANELS CHORDWISE	62
FIGURE 5.4	PRESSURE DISTRIBUTION COMPARISON (OPEN TRAILING EDGE)	63
FIGURE 5.5	SPARV WING CROSS SECTION MODEL (OPEN TRAILING EDGE)	64
FIGURE 5.6	PRESSURE DISTRIBUTION COMPARISON (CLOSE TRAILING EDGE)	65
FIGURE 5.7	SPARV WING CROSS SECTION MODEL (CLOSE TRAILING EDGE)	66
FIGURE 6.1	AIRBUS SPAR LOCATION	71
FIGURE 6.2	B747 RIB LAYOUT	75
FIGURE 6.3	AIRBUS RIB LAYOUT	76
FIGURE 6.4	BOEING 777 CUTAWAY	77
FIGURE 6.5	RELATION BETWEEN ANALYSIS AND OPTIMISATION	81
FIGURE 6.6	VON MISSES STRESS OF MEMBRANE ELEMENTS	87
FIGURE 6.7	VON MISSES STRESS OF PLATE ELEMENTS	88
FIGURE 6.8	TIP DEFLECTION OF MEMBRANE ELEMENTS	89
FIGURE 6.9	TIP DEFLECTION OF PLATE ELEMENTS	90
FIGURE 6.10	EXAMPLE OF NASTRAN MODEL	91
FIGURE 6.11	FATIGUE IMPLICATION	93
FIGURE 7.1	FLOWCHART OF THE MAIN MODULE	101
FIGURE 7.2	FLOWCHART OF AIRCRAFT SYNTHESIS	104
FIGURE 7.3	AERODYNAMIC AND STRUCTURAL PANEL	107
FIGURE 7.4	CONVERGED WING (WING A)	118
FIGURE 7.5	DIVERGED WING (WING B) STUDY	119
FIGURE 7.6	FLOWCHART OF MODIFY MODULE	120
FIGURE 7.7	AERODYNAMIC AND FINITE ELEMENT PANEL	122
FIGURE 7.8	WING CONVERGENCE	123
FIGURE 7.9	TWIST OPTIMISATION	125
FIGURE 8.1	VC-10 AERODYNAMICS PANEL TOP VIEW	128
FIGURE 8.2	VC-10 AERODYNAMICS PANEL 3-VIEW	129

FIGURE 8.3 VC-10 SPANWISE DISTRIBUTION .....	130
FIGURE 8.4 SOL-200 OBJECTIVE FUNCTION HISTORY .....	134
FIGURE 8.5 VC-10 STRUCTURAL PANEL .....	136
FIGURE 8.6 SPANWISE LIFT COEFFICIENT OF VC-10.....	137
FIGURE 8.7 VC-10 ITERATION OF SPANWISE DISTRIBUTION.....	138
FIGURE 8.8 VC-10 CHORDWISE DISTRIBUTION .....	139
FIGURE 8.9 TIP DEFLECTION.....	142
FIGURE 8.10 GNPLOT RESULTS OF PARAMETRIC STUDY.....	149
FIGURE 8.11 GNPLOT RESULT OF PRESPARV.....	154
FIGURE 8.12 XL-PRE PROCESSOR .....	155
FIGURE 8.13 COMPUTATIONAL VS. SEMI-EMPIRICAL METHOD.....	156
FIGURE A.1 PARAMETRIC STUDY .....	180
FIGURE C.1 ORIGINAL AEROFOIL CO-ORDINATE .....	203
FIGURE C.2 SINE DISTRIBUTION.....	205
FIGURE C.3 AEROFOIL CO-ORDINATE POINT .....	205
FIGURE C.4 THICKNESS RATIO EFFECT.....	206
FIGURE C.5 SWEEP EFFECT - TWIST=0, DIHEDRAL=0 .....	207
FIGURE C.6 DIHEDRAL EFFECT - TWIST=0, DIHEDRAL=4 .....	208
FIGURE C.7 TWIST ANGLE EFFECT - TWIST=5, DIHEDRAL=4.....	208
FIGURE C.8 FUSELAGE PANELS .....	209



LIST OF TABLES

TABLE 3.1 AIRCRAFT M.A.C., LEMAC, AND C.G. RANGE..... 32

TABLE 4.1 REAR SPAR DEPTH..... 44

TABLE 6.1 SPAR LOCATION..... 71

TABLE 6.2 KINK, FLAP, AND AILERON LOCATION..... 73

TABLE 6.3 RIBS LAYOUT ..... 78

TABLE 6.4 ALL MEMBRANE VS. ALL PLATE STUDY ..... 86

TABLE 7.1 DIVERGENCE STUDY ..... 111

TABLE 7.2 CONVERGED WING (WING A) STUDY ..... 112

TABLE 7.3 DIVERGED WING (WING B) STUDY..... 113

TABLE 7.4 RESULTS OF TIP LIMITATION ..... 115

TABLE 7.5 DISPLACEMENT CONSTRAINT ..... 117

TABLE 8.1 SOL-200 DESIGN VARIABLE HISTORY ..... 131

TABLE 8.2 SOL-200 OBJECTIVE FUNCTION HISTORY..... 133

TABLE 8.3 VC-10 TIP DEFLECTION..... 140

TABLE A.1 CLIMB GRADIENT REQUIREMENT ..... 174

TABLE A.2 PARAMETRIC STUDY EXAMPLE INPUT FILE ..... 181

TABLE A.3 INPUT VARIABLES FOR PARAMETRIC STUDY..... 182

TABLE A.4 PARAMETRIC STUDY EXAMPLE OUTPUT FILE ..... 183

TABLE B.1 EXAMPLE OF AEROFOIL.DAT ..... 191

TABLE B.2 EXAMPLE OF RAE9515.DAT ..... 192

TABLE B.3 EXAMPLE OF RELATIVE.DAT ..... 193

TABLE B.4 EXAMPLE OF FUSE.DAT ..... 193

TABLE B.5 EXAMPLE OF VTP.DAT ..... 194

TABLE B.6 EXAMPLE OF HTP.DAT ..... 195

TABLE B.7 EXAMPLE OF ENGINE.DAT ..... 196

TABLE B.8 WING LAYOUT EXAMPLE OUTPUT FILE ..... 196

TABLE C.1 EXAMPLE OUTPUT OF PRESERV..... 210

TABLE D.1 EXAMPLE OF INITIAL.DAT ..... 214

TABLE D.2 EXAMPLE OF SPARV.CPX FILE ..... 216

TABLE D.3 EXAMPLE OUTPUT OF PRENASTRAN..... 219

NOTATIONS

AR	Aspect Ratio
b	Span
C	Section chord
C <sub>D</sub>	Aeroplane drag coefficient
C <sub>d</sub>	Section drag coefficient
CD <sub>i</sub>	Induced drag coefficient
CG	Centre of Gravity
C <sub>K</sub>	Chord at kink location
C <sub>L</sub>	Aeroplane lift coefficient
C <sub>l</sub>	Section lift coefficient
C <sub>L,A</sub>	Approach Lift Coefficient
C <sub>L,MAX L</sub>	Maximum Landing Lift Coefficient
C <sub>L,T</sub>	Maximum Take Off Lift Coefficient
C <sub>M</sub>	Pitching moment coefficient
C <sub>R</sub>	Root Chord
C <sub>T</sub>	Tip chord
D	Drag
ESAR	Equivalent Still Air Range
e	Spanload efficiency factor
L	Aeroplane lift
l	Section lift
LE	Leading Edge
LEMAC	Distance of Leading Edge of the MAC to nose
LFL	Landing Field Length
M	Mach Number
N	Number of Engine
MAC	Mean Aerodynamic Chord
OEW	Operating Empty Weight
q	Dynamic pressure
RN	Reynolds Number
S	Wing Area
SREF	Reference Area
SAR	Still Air Range
t/c	Thickness to chord ratio
TOFL	Take Off Field Length
T <sub>o</sub>	Thrust at Static Sea Level
V <sub>A</sub>	Approach Speed
V <sub>1</sub>	Decision Speed
W	Gross Weight
W <sub>G</sub>	Gross Weight
W <sub>L</sub>	Landing Weight

$\alpha$	Angle of Attack
$\alpha_B$	Body angle of Attack
$\alpha_W$	Wing Angle of Attack
$\Lambda$	Sweep Angle
$\Gamma$	Dihedral Angle
$\lambda$	Taper Ratio
$\eta$	Semi-span fraction
$\sigma$	density ratio
$\gamma$	climb gradient

# *Chapter 1*

# 1. INTRODUCTION

## 1.1 Introduction

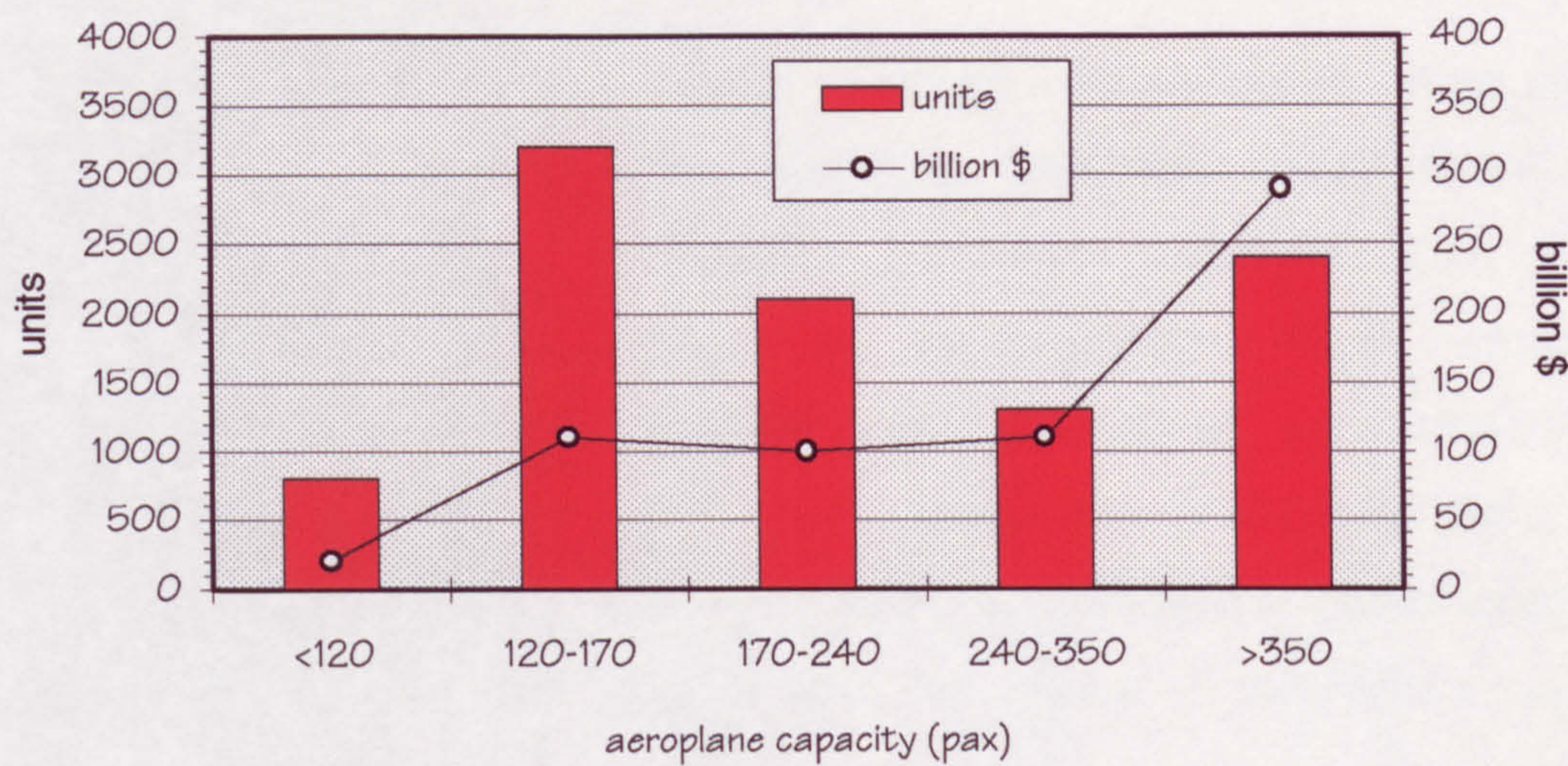
Aircraft design is a complex and iterative process where new designs take a long time to evolve, typically 15 years for an airliner (Ref. 4). This iterative design involves conceptual, preliminary and detail design phases. In order to reduce the time involved in aircraft design, in this thesis a computerised program is developed which covers conceptual design and preliminary design steps. Preliminary design step is covered in the form of computational aerodynamics and computational structural analysis.

In developing a methodology for designing high subsonic transport aircraft wings several methods are studied, including more accurate methods such as the computational methods. These are used as and in addition to the semi-empirical method. The design emphasis is on the high subsonic transport aeroplane.

High subsonic aircraft are chosen for study because a very large proportion of aircraft sales in the world come from this category of aircraft (Ref. 69). As can be seen from Fig. 1.1, the small aircraft (less than 120 seats) only share a very small portion of the aircraft to be delivered until 2005. Most of the aircraft are of higher capacity which fall into high-subsonic aeroplanes.



Forecast delivery by aeroplane size (1990 - 2005)



(source : Ref. 69)

**Figure 1.1      Forecast delivery by aeroplane size (1990-2005)**

Several attempts have been made to develop a computerised aircraft design process. A more accurate method to design high subsonic aircraft wings is required in order to cut the number of iterations in the design process. Most of the conceptual aircraft design programs that are available are based on the semi-empirical method. As faster computers become available, a revised method for designing high subsonic aircraft wings is studied by including computational aerodynamic and computational structural analysis in the iteration process.

In general transport wing design process is a continually evolving process. The process has evolved with considerable experience which includes analytical computational aerodynamics and computational structural analysis.



Computational methods are improving so that the wing design process will continue to change and improve with time.

Although the empirical wing design procedures enable a first cut try at good wing design, the procedure does not guarantee a successful design without considerable wind tunnel testing. It should be anticipated that several cycles of wind tunnel testing are required to achieve a successful wing design. The primary deficiencies of computational aerodynamics include no adequate modelling of separated and vortex flow, and no shock / boundary layer interaction scheme.

With the advent of computational aerodynamics the process used to achieve a successful wing design has been improved. The suggested wing design procedures provide a much better first cut design and also provide an outline of the technique for using computational tools to assist in refining the wing.

Because the cost of rectifying a fault is lowest at the earliest possible stage in an aircraft's life, the suggested wing design procedures is aimed at giving a good first cut design in order to avoid a modification at a later stage which will cost a lot more money. Cost of an error during the initial design is about one thousandth of the cost that could be caused if it goes into service (Ref. 31).

As can be seen in Fig. 1.2, the cost grows logarithmically. An effort during the initial design



phase is considered necessary to give an accurate as possible solution.

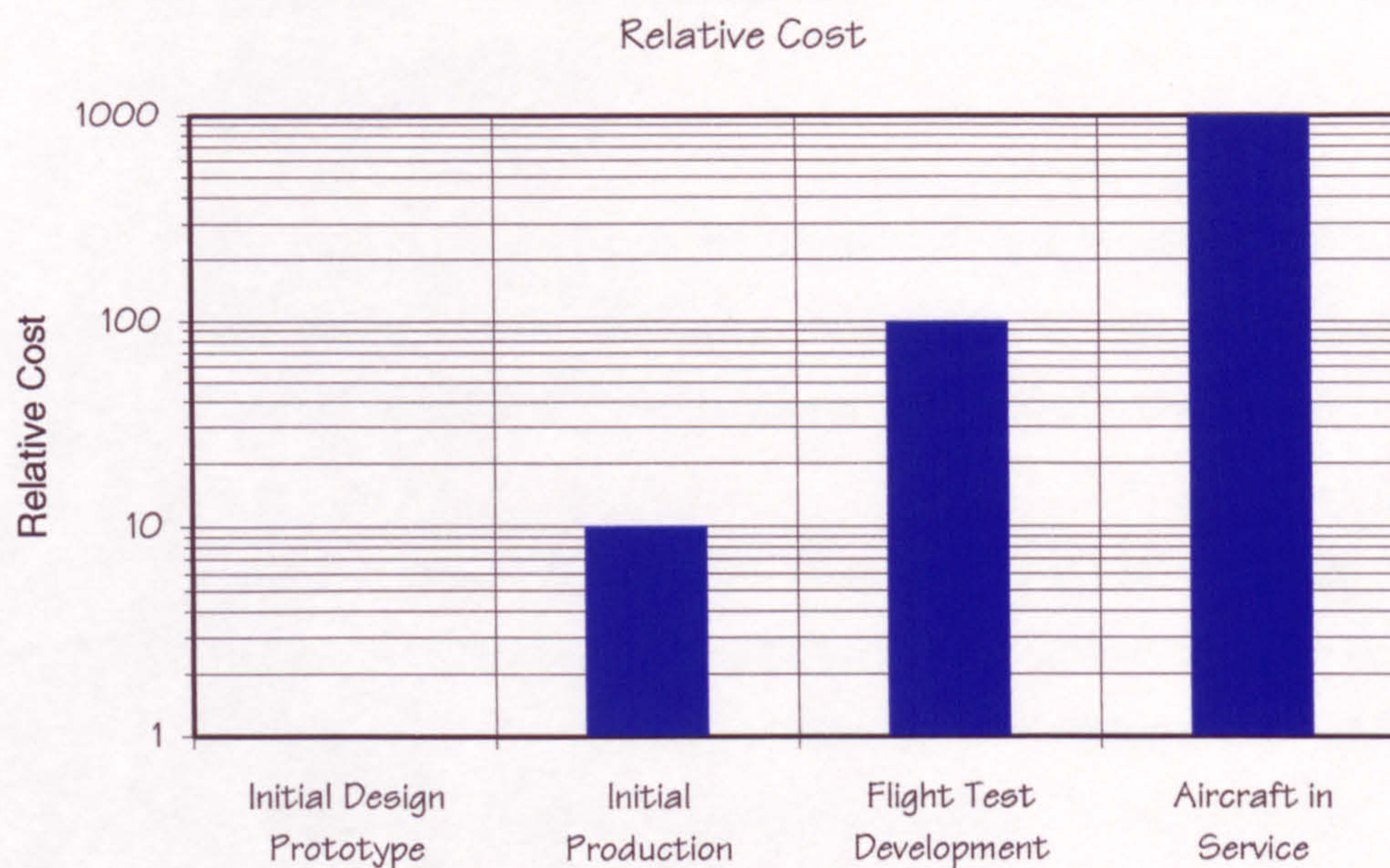


**Figure 1.2      Relative Cost**

Wing Design is a highly complex and important part of the development of an aeroplane configuration. It is a continually evolving design process that typically centres around a wind tunnel test programme, theoretical analysis and design, and includes compromises between many technical disciplines. The primary purposes of this design study are :

- To provide a design guide for the wing designer including techniques, requirements, criteria, constraints, and trade-offs, general technical considerations, tools, references and previous wing design experience.



- To provide a reference manual for the wing designer including a description of computational tools, computational aerodynamics and computational structural analysis.
- To present a suggested design procedure that will yield a good wing design, and that also will provide a point of departure to a more thorough study.

Also the objectives of this thesis are to study in the field of multi-disciplinary design, to develop a method to perform conceptual design of transport aircraft wings and to demonstrate that aerodynamics analysis using computational fluid dynamics (CFD) and structures analysis using the finite element method (FEM), can be coupled with the aircraft synthesis program in a seamless distributed computing environment.

Computational methods are significantly more advance compared with several years ago. The analytical tools provide significantly improved initial wing design. Although the analytical design is emphasised, the final wing will be based on additional wind tunnel tests since the analytical programs are adequate only at cruise conditions (Ref. 22). A suggested wing design procedure is presented to meet the design requirement. The wing design procedures is an iterative process between computational and wind tunnel test. The wing design process is iterated between analysis and experimental until an acceptable solution is reached within the limits of time and money.

In this thesis the procedure illustrated by Fig. 1.3 to 1.5, does not include the wind tunnel test. The first cut computational design of the wing is suggested in the thesis, and this should be tested in the wind tunnel as the next step. The suggested wing design process is shown in Fig. 1.6.

## 1.2 Description of the work

The work is done by studying the method to be taken at each step of the design process. This is initially a conceptual design, and the preliminary design is also considered in the form of pressure distribution calculations and detail design of the structural layout.

In Chapter 2 current computerised aircraft design programs are reviewed. In that chapter programming methods are also studied to get some practical knowledge of how to solve aircraft design problems. Various aircraft design disciplines are studied and analysed. The required input data and output are examined and the way to provide the data is thought. Semi-empirical methods, computational aerodynamics methods and computational structural methods are analysed.

The wing design process is studied thoroughly. Aerofoil selection and other wing geometry parameters are studied. Methods to calculate the wing geometry are studied and explained in Chapter 4.



The advance in computers enables computational aerodynamics to be a useful a tool. In Chapter 5 several computational aerodynamic programs are studied and explained. The decision to use a panel method is also explained in that chapter. Modelling of the aeroplane is very critical in order to get a good result; modelling technique is explained and described in that chapter. Lift coefficient and drag coefficient from computational aerodynamics are compared with the semi-empirical method. Spanload distribution results are used to increase the aerodynamic efficiency by varying the twist angle.

In Chapter 6 the structural layout of the aeroplane is described and several finite element programs are studied. The reason for selecting a particular computational structural analysis is given. A static aeroelasticity check is explained in that chapter and the structural optimisation method is explained. The result of the structural module is then calculated in the form of weight and compared with the semi empirical method. The modelling of the wing is also described in that chapter where the validity of the finite element model used for obtaining the weight estimates is assessed. Several methods of modelling the wing are studied thoroughly by using a finite element model employing different elements

The integration of the whole modules is very important in this multi-disciplinary design process. In chapter 7 the integration methodology used in this project is described. Design problem formulation and the characteristics of the integration method is explained in that chapter. Data

transfer between various modules are also important and explained in that chapter along with the static aeroelasticity analysis and twist optimisation study.

The ability of the program to detect when the static aeroelastic constraints have been violated, and the ability to provide the user with a solution to this problem is explained in detail in that chapter. This capability makes the program able to perform a limited automated design cycle.

At the end of the thesis several case studies are explained and discussion and conclusion given.

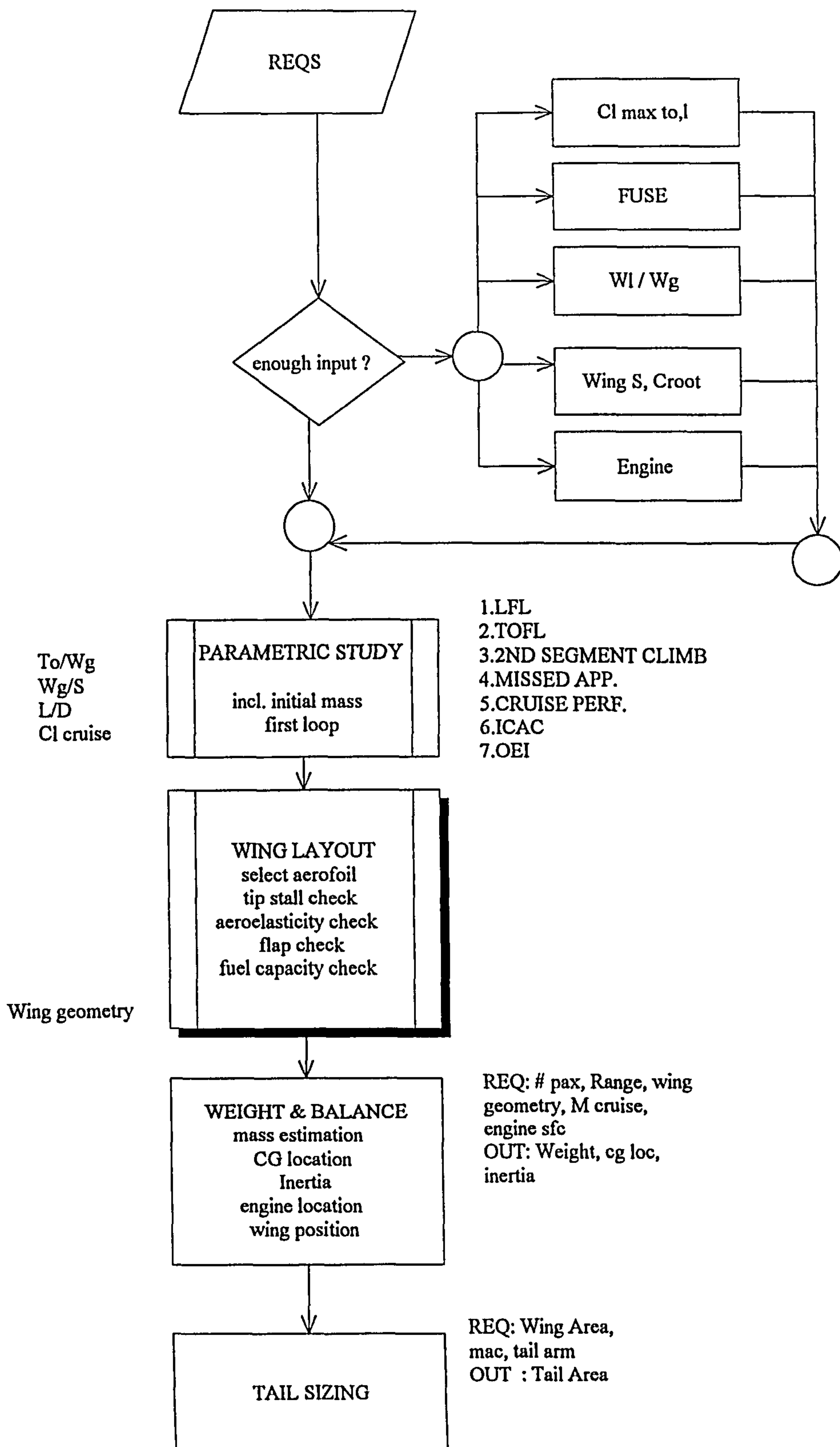


**Figure 1.3 Proposed Flowchart**

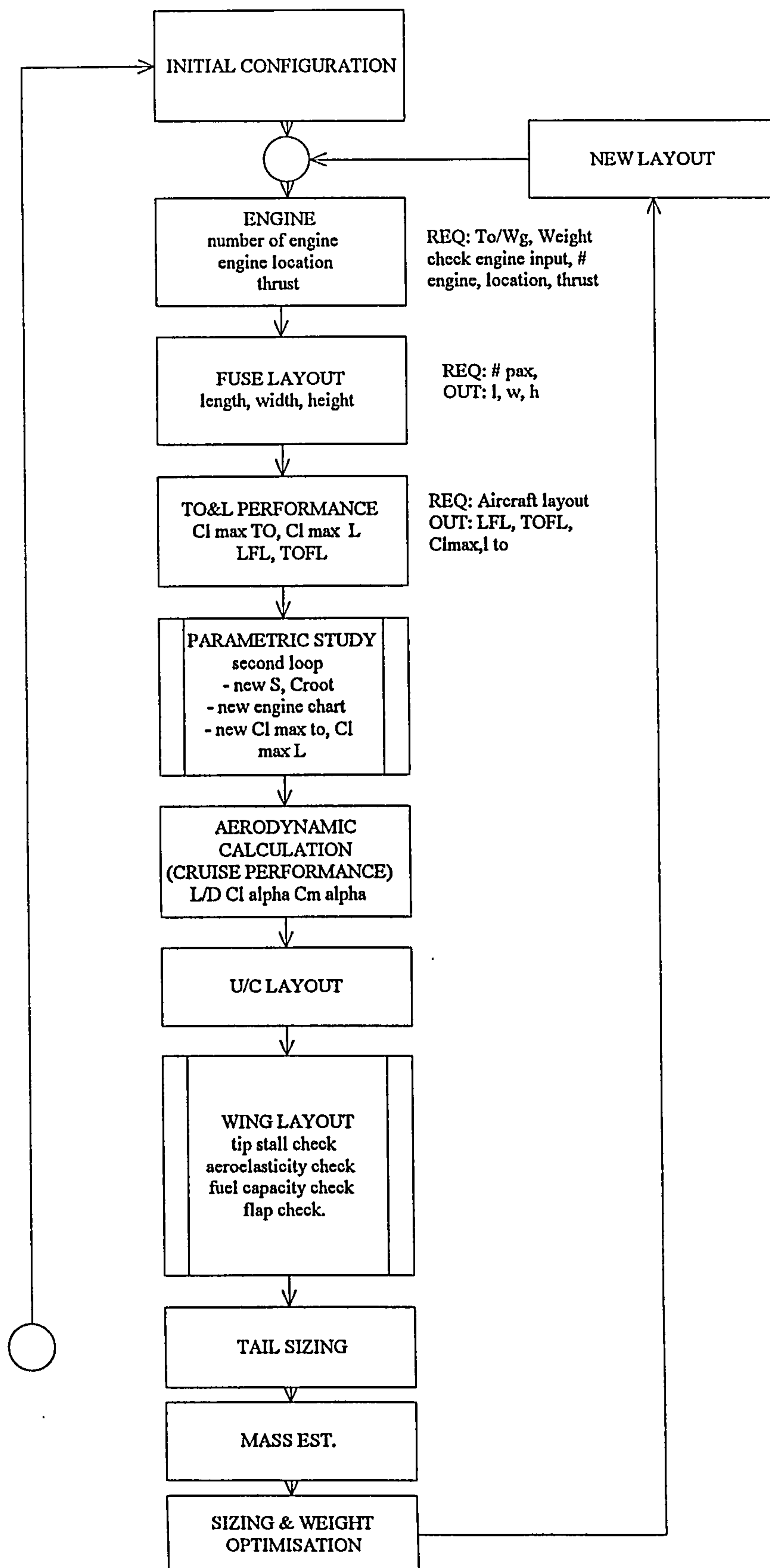


**Figure 1.4 Proposed Flowchart**

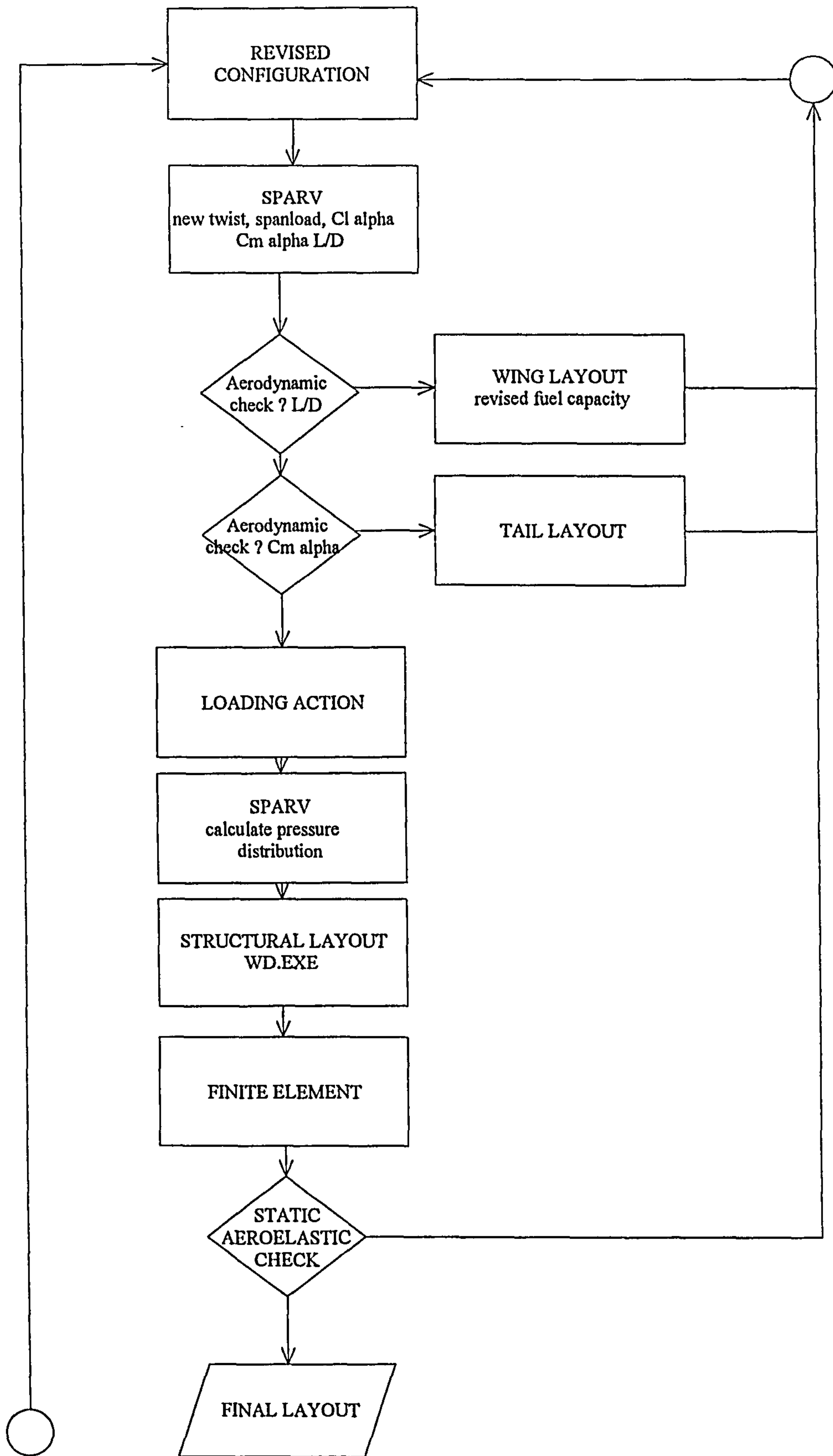


**Figure 1.5**      **Proposed Flowchart**



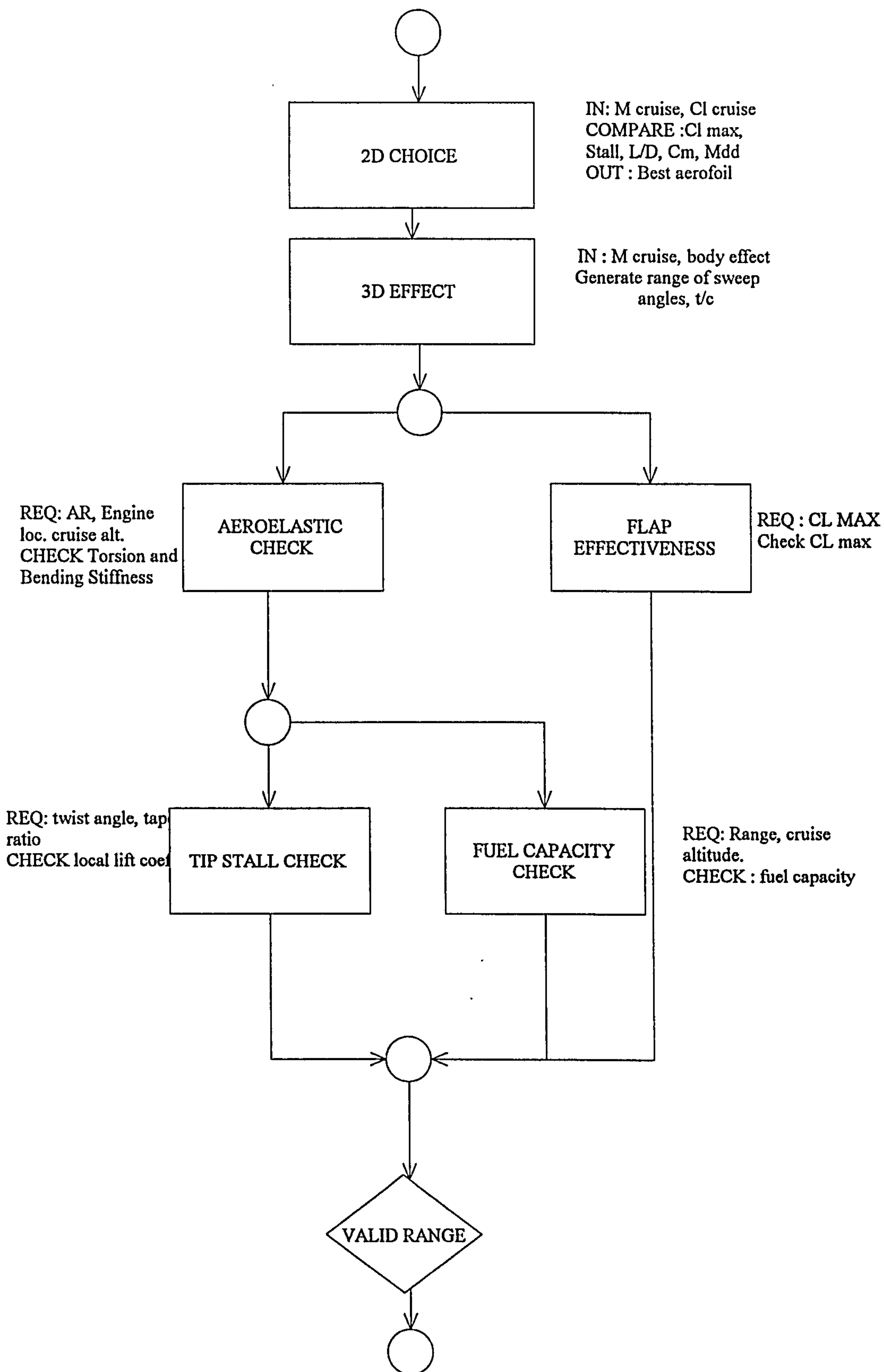


**Figure 1.6 Proposed Flowchart for WINGLAYOUT**

# *Chapter 2*

## 2. PAST COMPUTERISED AIRCRAFT DESIGN / LITERATURE STUDY

### 2.1 Introduction

Several computerised aircraft design processes have been found during the literature studies. Most of the design programs are aimed at designing the whole aircraft. Unlike this thesis, which will go through design process of the wing design by including the structural wing layout of the aircraft, most of the computerised aircraft design programs found do not include the structural layout of the wing.

The purpose of this chapter is to review the available computerised aircraft design programs and to extract the benefit from previous aircraft designs in order to develop a new and better wing design methodology.

Some of these investigations are reviewed briefly in this chapter.

### 2.2 ADROIT (Ref. 4)

ADROIT (Aircraft Design by Regulation of Independent Tasks) is intended to be an aircraft design program, but several modules that are intended to be included have not been finished, and the only complete module in the program is the wing design module. The program starts by selecting the best aerofoil in the database by comparing several criteria such as  $Cl_{MAX}$ ,  $C_M$  and  $M_{CRIT}$  of the aerofoils. The program uses stated relative importance of each criterion in order

to pick the best aerofoil. This method of comparing each criterion of the aerofoils by using given values of relative importance is considered a weakness of the method. The program will pick the same aerofoil no matter what kind of aircraft is to be designed. In the proposed method, the capability of the program to adjust the relative importance of each criteria in order to pick the suitable aerofoil section is included. In this case for an aircraft that does not need a high cruise mach number it might not pick an aerofoil section that has a high Mach critical number.

ADROIT studies a range of sweep angles and checks each sweep angle against several checking methods such as flap check, tip stall check, aeroelastic check, but makes no attempt to pick the wing sweep angle combinations. The proposed wing design program, developed from ADROIT, will use the same method of checking but will then be extended to be able to pick the suitable sweep angle of the aircraft. This is done by studying each sweep angle, and actually designs the whole aircraft based on that sweep angle. The proposed method for picking the sweep angle is described in chapter 4.

### 2.3 Pasaribu (Ref. 9)

This program, developed by Pasaribu (Ref. 9), uses a visual interface to communicate between the user and the program. This program was also found to have several independent modules that can be run by selecting the program that is needed to be executed from the menu given by the main program. It is found that each step of the aircraft design



process must be picked manually by the user. Wing layout is based only on the database. The method that is used to design the wing is by studying the wing loading and thrust loading parameters and studying the current aircraft on the database. Like other programs no structural wing layout is computed.

The program uses a very good GUI (Graphical User Interface), which is machine specific and not portable. Several problems are encountered when the computer is upgraded. The program will only run on a specific computer (SUN) with a specific operating system (SunView). Problems are encountered when the system is upgraded into a different operating system.

Learning from this experience, the proposed wing design program is intended to be a text only program. Because the output is intended only in text forms, several files are generated in an intermediate step in a form that can be easily plotted. Points are generated in the X and Y pairs that will make it easy to plot. Transferring this file to a spreadsheet program or other plotting program will enable it to be viewed graphically.

## 2.4 DESAID (Ref. 8)

DESAID (Development of an Expert System for Aircraft Initial Design) is the continuation of ADROIT. In this program parametric study, fuselage design, tail plane design, etc. are included in the program. But the choice of several variables such as wing twist angle, wing dihedral

angle, and taper ratio is not chosen. As a matter of fact wing planform, thickness-to-chord ratio, taper ratio, twist, and swept angle must be defined by the designer (Ref.8, p64). From the structural point of view the designer has to arrange the wing rib and spar locations of the wing manually.

The proposed program is intended to choose wing twist, sweep angle and structural layout automatically.

## 2.5 MVO (Ref. 7)

MVO (Multi Variate Optimisation) was developed by the Royal Aircraft Establishment in 1970. This program was originally a design synthesis for a high-subsonic speed transport aircraft in the preliminary stage of development which could be combined with an optimisation technique. The program was originally written for transport aircraft of conventional design with rear-fuselage mounted engines and with wings with moderate sweepback which was then a common configuration (Ref.7). Although the current MVO program is a lot more advanced than the original, the method that used is generally the same.

The wing design part in the MVO program is very rough. The program assumes that the wing planform of the aircraft is a trapezoidal shape (without a kink) and having constant thickness-to-chord ratio.

The MVO program is still under development, the newer version of MVO dated 1984 is capable of designing a high-

subsonic-speed transport aircraft with moderate sweepback on the wing and moderate to high aspect ratio. The engine can now be installed on the rear fuselage or/and on the wings and there is a facility to specify the degree of improvement in the in the technology of wing design over the 1970's standards. The wing planform is still assumed trapezoidal with constant thickness-to-chord ratio.

Learning from MVO, the proposed wing design program is studied by including the capability of using different thickness-to-chord throughout the wing. Kink of the wing is also assumed unavoidable in the real aircraft design problem, and the proposed program also has the capability of studying the kinked wing. Undercarriage design then plays an important role in the process.

## 2.6 ACSYNT (Ref. 27)

ACSYNT is an Aircraft Synthesis program. The aerodynamic prediction methodology in the program is considered to be the best empirical procedures currently available(Ref. 27).

This program is developed by NASA Ames Research Centre with an institute of groups consisting of eight US aerospace companies and is only available to the member of the institute.

Recently a standard sizing methodology has been initiated by aircraft concept designers and evaluators at the NASA AMES Research Centre. This effort is based on the NASA AMES



originated aircraft sizing and optimisation work which resulted in ACSYNT.

ACSYNT unlike similar programs in its class, remains with a conventional approach to the design process of the aeroplane. This approach requires a vast amount of computer memory and computing time since adequate resources are required to investigate the various concepts to be included in the system.

The newest version of this program also includes a Computer Aided Design package that uses graphical user interface and generates a 3-D surface model. The graphical user interface is claimed to follow international graphics and programming standards which make it machine and graphics device independent.

Learning from the ACSYNT experience which started from a text based program and led to a program with full graphical user interface, it is assumed that at a later time, a graphical user interface could be developed with the same technique that is used in ACSYNT which makes it machine independent. The programming technique for making a graphical user interface machine independent is considered out of the scope of this thesis.

In order to give a 3-D surface output, the proposed project will use a public domain Gnuplot which is available in many computer platforms.



## 2.7 GASP (Ref. 37)

GASP (General Aircraft Synthesis Program) is developed by NASA as a basic aircraft synthesis program which only uses semi-empirical methods to design an aircraft. This program is intended for conceptual design of general aircraft in the class of Cessna-150 aircraft (Ref. 37). The user of this program is required to give extensive input such as aspect ratio of wing, horizontal tail and vertical tail. Details such as wing sweep angle are also required as an input. On the other hand the program will give detail geometric results of the wing such as wing span, wing chords and wing mean aerodynamic chord.

Although this program is good for a basic calculation of aircraft design, the method that was used is very crude for today's technology as this program was developed in 1978.

## 2.8 NASA Langley Research Center

Several papers from NASA Langley Research Center have been found which relate to the multi-disciplinary optimisation of aircraft design. Although these works are on aircraft design, they concentrated on finding the method for solving large optimisation problems and concentrated on structural optimisation. Several techniques were studied in these papers in order to solve the optimisation process.

NASA Langley Research Center lead by Sobieszczanski-Sobieski worked on methodology for decomposing large, complex systems into a series of smaller sub-systems, using

sensitivity derivatives of the data exchanged among the sub-systems as the basis for total system optimisation (Ref. 74). These works have been expanded and used in many programmes.

One of the works concentrated to develop a computerised procedure to generate cross-sectional dimensions and fiber orientations for composite airframe structures. A methodology of its application to a wing structural synthesis has been established involving the selection of type of construction, material, and other design variables (Ref. 73).

NASA Langley team also worked on integrated aerodynamic-structural design of a transport wing which works by designing the wing for minimum weight subject to required range (Ref. 57). This work concentrated on reducing the cost of sensitivity calculation in the optimisation procedures.

The research believes that the idea of 'push button design' must be discarded in favour of a realistic recognition of the role of human mind as the leading force in the design process (Ref. 75). This research also outlines techniques to allow engineers to work concurrently on manageable tasks and communicating with each other by means of sensitivity data.

Unlike the work done at NASA Langley Research Centre, the subject of this thesis is not intended to use a complex optimisation method due to aim that the program will be

used is in the conceptual design phase and will not require a complex optimisation process. A limited automated design process is introduced in this thesis in order to achieved the target of an automated design cycle which does not require operator interference.

## 2.9 Other related research studies

Several structural - aerodynamic integration studies have been found. Most of these works are based on the ACSYNT module. Most of them use a very powerful computer system and although the aerodynamics module is integrated with the structural module, the study is based on a specific aircraft. A joined-wing aircraft is one example of the research, it is not based on general aircraft, but only designed for a specific joined-wing aircraft.

Other related work that has been found is work by Borland, Benson, et al. (Ref.30). This work is used in the detail design of the aircraft wing. The work is based on an existing twin-engined commercial transport. Several design objectives were explored, including minimum weight, minimum drag and maximised range. Although this work was on detail design step compared with the proposed work which starts from the conceptual design, the benefit of linking aerodynamic and structural computational analysis can be studied for the proposed work.

Other aircraft design programs were also found. Some authors of aircraft design text books also wrote aircraft design computer programs. Raymer (Ref.25) wrote RDS - a PC



based aircraft design, sizing and performance system. This is written primarily as an instructional aid and is a complement to the AIAA textbook. It features a 3-D CAD module for design layout, and has analysis modules for aerodynamics, weights, propulsion and cost. Although it is for general aircraft, the program is believed to be based on military aircraft. It is very rough and does not start from blank paper. The decision for important criteria such as wing sweep angle is left to the designer and by trial and error the designer can increase or decrease the sweep manually.

Roskam (Ref.10), the author of a series of books on airplane design, also wrote an aircraft design program. The program uses a Graphical User Interface and basically all the methods and steps are just as explained in his textbooks. The method is semi-empirical and does not use computational aerodynamics or computational structural analysis in the design process.



# *Chapter 3*

## 3. HIGH SUBSONIC AIRCRAFT DESIGN PROCESS

### 3.1 Introduction

In this chapter the process used in the program is explained. Although the proposed study is intended to concentrate on the wing design, it is impossible to eliminate other aspects of the aircraft design process.

The aircraft design process used in the program is divided into several modules which start from the parametric study of the aircraft. Although it is possible to run each module independently, the whole design process is completed by the program seamlessly by running all modules iteratively including the computational calculations.

The aim of this chapter is to give details on how each module works and how it is implemented in the program. Methods and the effect of the module in the design process are also explained in this chapter.

The detail of the wing design module is explained in the next chapter.

### 3.2 Parametric Study

The parametric study is a starting point for aircraft design. This study is intended to give an optimum point of wing loading ( $W/S$ ) vs. thrust loading ( $T_0/W$ ). This value is crucial and an accurate prediction of ( $W/S$ ) vs. ( $T_0/W$ ) is

needed in order to design a good wing. Several methods are studied and modified to meet the need. The parametric study is based on Ref.5 with some modification based on Ref. 6 and some semi-empirical data are updated to the current state of technology. A detailed method for the process can be found in Ref.5.

This parametric module is used in the wing design program very extensively. Each configuration has to be designed at the optimum  $(W/S)$  vs.  $(T_o/W)$ . This is one of the reasons why time has been spent to modify the parametric module in order to give good results. As can be seen in Fig. 3.5, the optimum point is picked based on the minimum weight of the combination between  $(W/S)$  and  $(T_o/W)$  that fulfil the constraints

Details and summary of the parametric study can be found in Appendix A. Reference 5 should be consulted if more detailed information is needed. In this appendix each criterion chosen and the constraints are explained.

For validation purposes, several high subsonic speed aircraft have been studied and tested using this method. From Ref. 70 which contains data from several sources such as manufacturer's catalogues and Flight International magazine, input data required for validation are collected. These aircraft are relatively new and cruise at high Mach number, with the exception of Fokker 100 and BAe 146 which cruise at  $M=0.70$  and  $0.65$  respectively. The TU 154 is also used as a comparison against western aircraft.



A comparison between the predicted wing loading and the actual value for the aircraft can be seen below (Fig. 3.1).

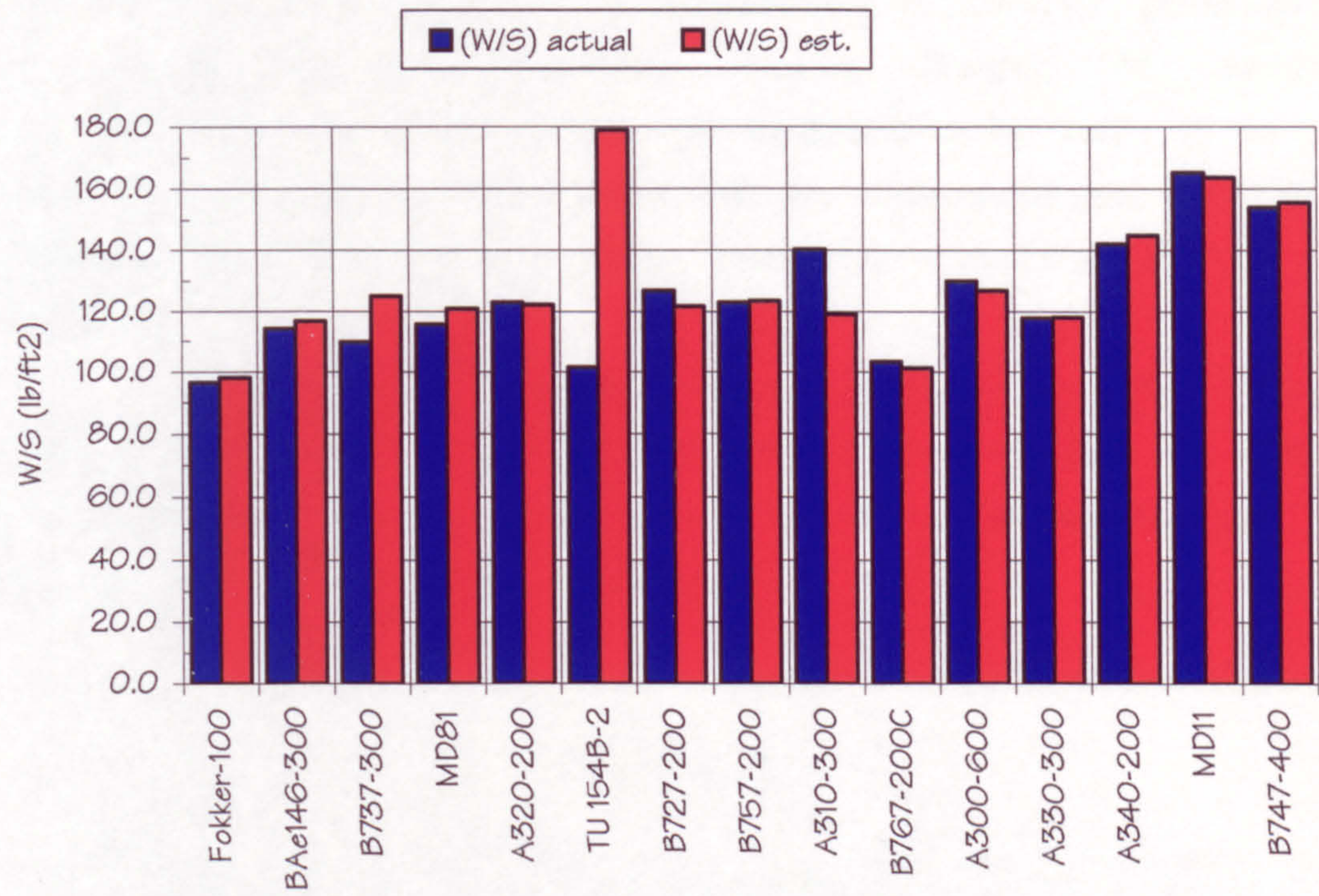


Figure 3.1 (W/S) Comparison

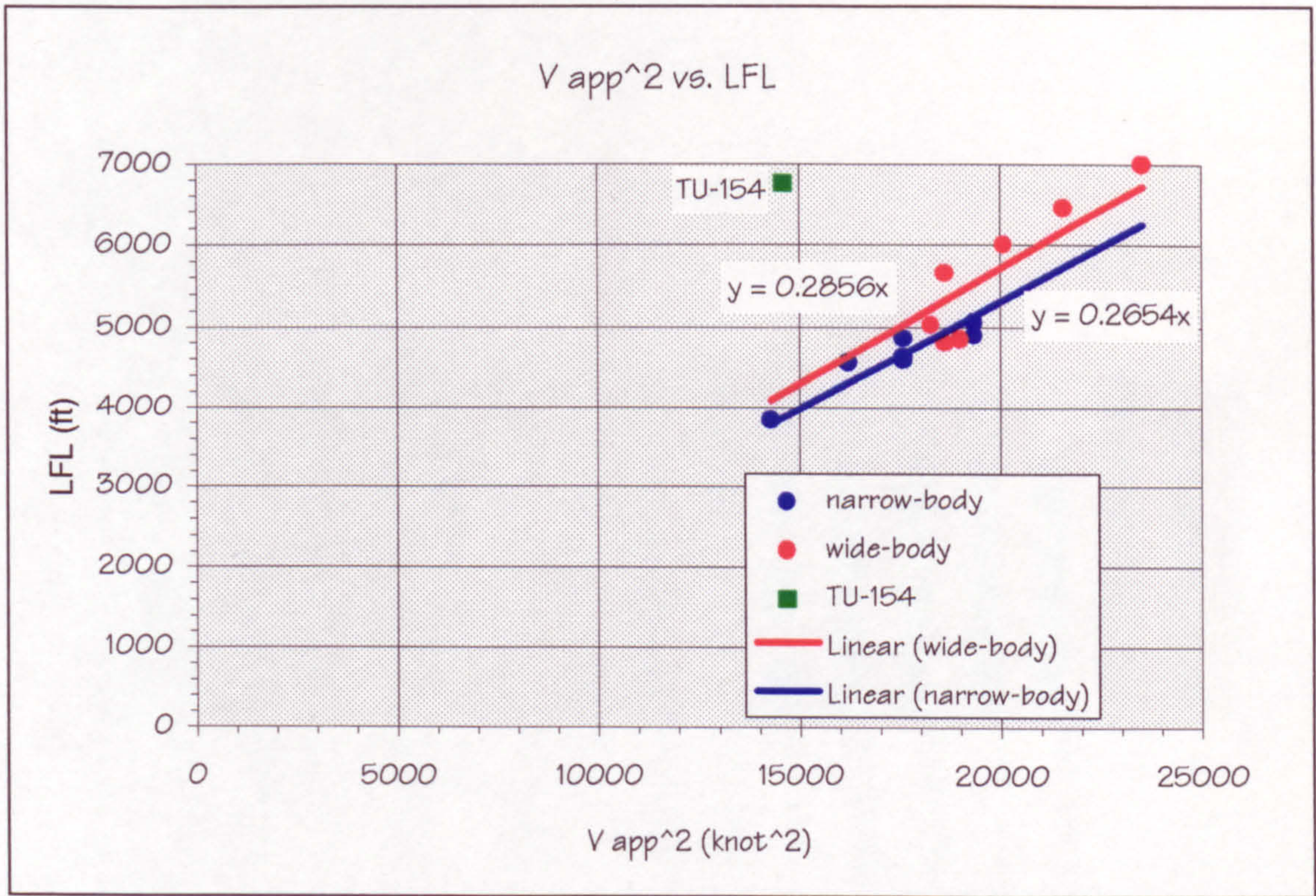
As can be seen from Fig. 3.1, the program predicts the wing loading very accurately except for the TU 154. On the TU 154 the module found that although the aircraft is capable of producing a  $C_{l_{MAX}}$  during landing of 2.8, its landing field length (LFL) requirement is rather high. Ref.14 stated that the field required is 6760 ft, almost as long as the Boeing 747 requires. It caused the program to predict a rather small wing area and thus high wing loading for the aircraft.

As suggested by Ref. 5, the program uses a linear equation for estimating the relation between  $V_{APP}^2$  vs. LFL. But after



studying data from current aircraft, it was decided to update the equation and to divide the equation into two separate conditions one for narrow body and the other for wide body aircraft. Ref. 5 suggested a higher prediction for estimating the landing field length of current aircraft. The equation that was suggested by Ref. 5 is  $LFL = 0.3 \times V_{APP}^2$  which was modified in the program to  $LFL = 0.2654 \times V_{APP}^2$  for narrow body and  $LFL = 0.2856 \times V_{APP}^2$  for wide body aircraft.

In Fig. 3.2 it is clearly seen that the data for TU 154 is not consistent with the linear relation between  $V_{APP}^2$  vs. LFL that was used in the program.



(source : Ref. 70)

Figure 3.2  $V_{APP}^2$  vs. LFL



The accuracy of the data from the Soviet aircraft is considered unknown and is only used throughout this thesis as a comparison, which does not effect the semi-empirical equation generated for the program.

The comparison between the program and the actual values of thrust loading ( $T_0/W$ ) also shows a very good accuracy. Again the prediction for the TU 154 is rather high. It is concluded that the data of both take-off field length (TOFL) and landing field length of the TU-154 can not be used and must be considered inaccurate. Fig. 3.3 clearly shown that the program can correctly predict the ( $T_0/W$ ) of the aircraft.

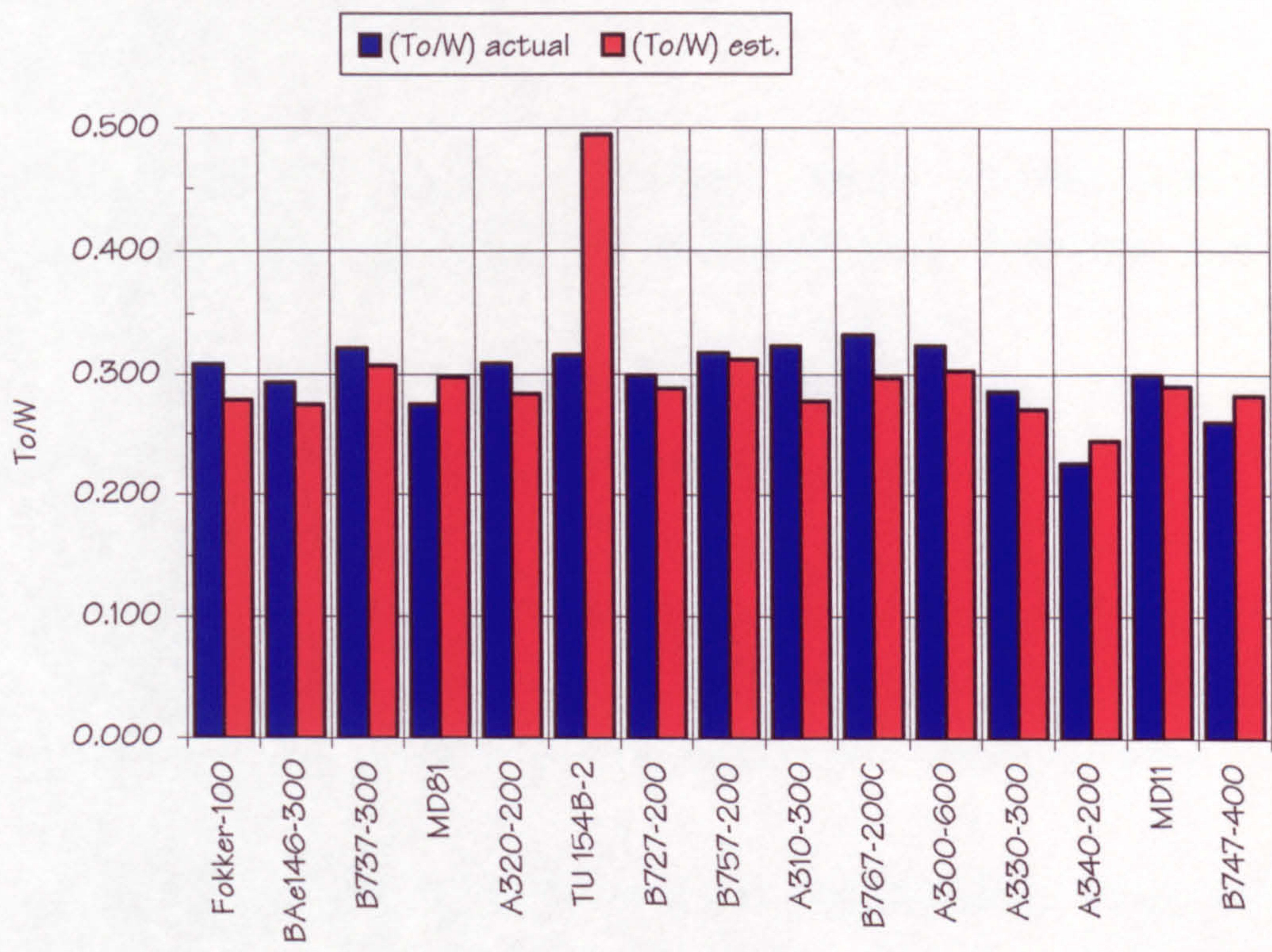


Figure 3.3 ( $T_0/W$ ) Comparison



Optimum thrust loading ( $T_0/W$ ) from this parametric module is used to calculate the thrust required for the aircraft and the optimum wing loading ( $W/S$ ) found is used in the next module to find the layout of the wing after the prediction of the weight of the aircraft.

### 3.3 Fuselage Design

The purpose of the fuselage in the aircraft is to serve several tasks, but the main task is as the load carrying part of the aircraft in the form of passenger and cargo. It also needs to react the loads such as shear forces, torsion and bending moments transmitted from the wing, tails and undercarriages.

Aerodynamically, the fuselage must have low drag characteristics and low interference drag with the wing and empennage.

Considerations in designing the fuselage are :

1. Simple structural layout to give the possibility of increasing the fuselage length and efficient structural layout to minimise the loss of space.
2. Fuselage should have a good aerodynamic drag and low interference drag to the wing and other parts of the aircraft.

3. The number of emergency exits and passenger doors needs to be fulfilled and determined by the number of passengers.

4. Sufficient levels of comfort to the passenger must be provided. This can be translated into the relation between seat abreast, seat pitch and aisle width.

Interference drag between fuselage and wing is assumed a detail design matter and is considered out of the scope of this thesis, although it does effect wing design.

The fuselage module in this program is studied for the purpose of giving good results when calculating the weight and the drag. The studies are based on a semi-empirical method. An option to by-pass the fuselage design is also provided in the program. This is in order to enable a more extensive fuselage design program to be used first and the results then inputted manually to the wing design program.

As intended, the required variable input of the program is the number of passengers. This variable is set constant through out the iteration thus assuming that the fuselage is constant also. The program will only compute the number of seat abreast, length, and width of the fuselage. Other details such as type of container to be used is not computed by the program as an assumption of circular cross-section is assumed. As mentioned earlier, a more extensive fuselage program can be used to provide fuselage details.



### 3.4 Wing Design

In the wing design module, geometric variables such as sweep angle  $\Lambda$ , taper ratio  $\lambda$ , wing area  $S$ , span  $b$ , aspect ratio  $AR$  and thickness ratio are computed. This computation is done iteratively and by using a gross optimisation technique. The weight of all possible solutions are calculated and the lightest solution is picked as the optimum configuration.

This wing design program, which is the main subject of the study, is explained in a more depth in the next chapter.

### 3.5 Engine Selection

Engine selection is very important in the aircraft synthesis. In real life one of the criterion to chose the number of engines used by the aircraft is the availability of an engine in the market. This criterion is difficult to model in the program as a huge database needs to be built. In this program the number engines selection is only based on the range required. With the arrival of big engines such as RR Trent and GE 90 for the Boeing 777 and Airbus 330, almost all ranges and size can be covered by only 2 engines.

The number of engines to be used in the program is decided to be either 2 or 4. The choice of three engines is concluded as inefficient as proved in the case of Tristar. It is believed that the engines that are available in the

market are in a very wide thrust range which can cover with just two engines what used to require three engines.

This number of engines criteria plays an important role in the parametric calculation as it sets the required climb gradient in the event of engine failure during take off, second segment climb, and missed approach conditions. More details on this condition can be found in Appendix A.

### 3.6 Weight and Balance

Weight and balance calculation is required to be calculated in order to give a good design for the tailplane. The tailplane sizes and weight are needed in the wing design process, because of the drag, weight and the trim drag of the tailplane.

The weight calculation is done in the program by using two types of estimation. In the beginning, a semi-empirical calculation based on Ref. 64 is used. This method gives a quick calculation needed in the initial stages. After the wing detail geometric is found, the computational analysis is performed and the new weight is used instead of the semi-empirical one.

Centre of Gravity calculation is also needs to be performed because the c.g. is needed in the process of locating the wing on the fuselage. The wing location is done by calculating the overall c.g. of the aircraft equal to 25 % MAC during OWE (Operating Empty Weight) condition (Ref. 2.). This process is done by dividing the weight into two



groups, fuselage and wing group. and putting the wing such that overall c.g. location is at 25% m.a.c.

The actual aircraft m.a.c. and c.g. range can be seen on Table 3.1.

Table 3.1 Aircraft m.a.c., lemac, and c.g. range

Aircraft	mac (in)	lemac (in)	cg range (% mac)
B737	136.5	534.6	10.0 - 33.0
B767	237.5	828.7	11.0 - 32.0
DC-10	295.8	1066.5	8.0 -18.0
B747	327.8	1168.0	13.0 - 33.0

(source : Ref. 65)

As can be seen from the table above, setting the c.g. of the aircraft on 25% m.a.c. on OWE condition is appropriate for this class of aircraft.

3.7 Undercarriage Design

In this project, the undercarriage criterion that needs to be considered is the layout of the undercarriage. In general the layout of undercarriage can be divided into three arrangements as follows :

- Nosewheel tricycle layout
- Tailwheel layout
- Bicycle layout.



Tailwheel layout is considered obsolete due to the fact that the take-off is difficult due to the increased drag of the fuselage attitude.

An example of bicycle layout is the Harrier Jump Jet, and this layout is usually used in the fighter aircraft and considered not appropriate for high subsonic transport aircraft.

In the nosewheel tricycle layout the arrangement that needs to be studied for this project is the location of the main undercarriage. The location of the main undercarriage on the wing is governed by several criteria such as :

- The main undercarriage should be mounted behind the c.g. but not too far to keep the nosewheel loads low. This criteria is known as the tip-up margin.
- The main undercarriage should clear the aft fuselage from touching the ground during take-off and landing. This angle of pitch during take-off and landing should be at least equal to the limits imposed by take-off and landing angle. Ref. 2. suggested an angle of 14 degrees.
- Stability during taxiing. This criterion requires the track of main undercarriage should be as wide as possible. However, it has to avoid nosing over during braking.



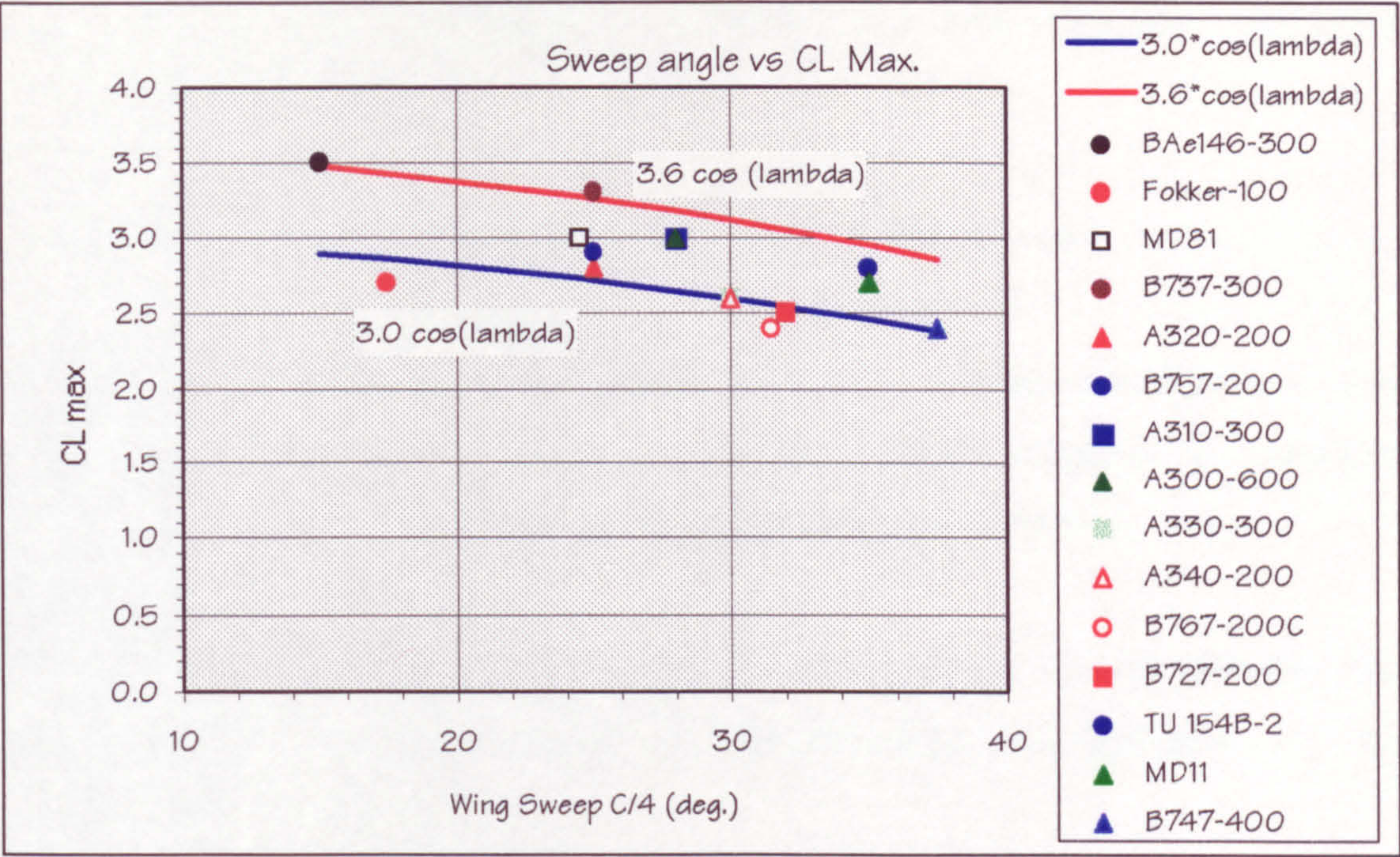
In this project the undercarriage has been studied thoroughly and is an important consideration especially when the kink location of the wing is governed by the undercarriage location.

### 3.8 Performance Analysis

Performance of the aircraft is studied by dividing it into two categories. Slow speed (take-off and landing) and high speed (Cruise). The flap /  $C_{L,MAX}$  requirement is very important in the wing design. Several studies of current aircraft reveal that a higher  $C_{L,MAX}$  on the swept wing can be achieved now compared with the previous method stated by Ref.2.

In this thesis the flap for each wing is considered to be producing the maximum lift coefficient based on the possible  $C_{L,MAX}$  achieved at a certain sweep angle. Ref. 2 suggested that the maximum lift that can be achieved at certain sweep angle  $\Lambda$  follows the equation of  $3.0 \times \cos(\Lambda)$  which is based on simple sweep theory. After comparing the equation with the current values of recent aircraft it is clearly seen that modern aircraft can achieve more than the values suggested (Fig. 3.4). It is decided that in the program the value of  $3.6 \times \cos(\Lambda)$  is used. This value should be achieved with conventional flap arrangements in today's aircraft. The equation still follows the simple sweep theory.





(source : Ref. 70)

**Figure 3.4      CL<sub>MAX</sub> vs. Sweep C/4**

Ref. 22, as can be seen in Figure 3.6, also suggested a higher value than that of Ref. 2. In this reference advanced leading edge and trailing edge flaps can achieve even higher than the 3.6 cos (Λ) line.

### 3.9 Tailplane Design

From studying current high subsonic transport aircraft, it is found that all of the tail layouts are a low tail arrangement. Because of this the tail layout used in the program is a low-tail layout only. Several tail layout are :



- High Tail. This is consist of a single fin with horizontal tailplane mounted on top of the vertical fin.

Some of the advantage of this layout are :

1. Moment arm from c.g. is longer compared with the low tail layout which means a smaller horizontal tailplane can be used.
2. The aft fuselage is easier to manufacture, due to the lack of horizontal tailplane on the fuselage.
3. Minimises the wing downwash effect from the wing.
4. Clear from engine exhausts.

The disadvantages of this high tail layout are :

1. The end plate effect can cause side loads on the fin due to rudder application or from the yaw induced rolling moments, increasing the torque reacted by the aft fuselage. This will require an increase in the stiffness of aft fuselage.



2. Deep stall problems can occur in some engine layouts, due to the wake caused by the aft-mounted engine.

3. The load from the horizontal tailplane causes an increase of stiffness on the vertical fin.

- Low Tail. This layout consists of a single vertical fin with the horizontal tailplane mounted on the fuselage.

The advantage of this Low Tail layout are :

1. Forces and moments can be easily reacted on the aft fuselage.
2. Access to the tailplane actuators is easier compared with the high tail layout.

The disadvantages are :

1. The need for the attachment between horizontal tailplane to the aft fuselage to be flat in order to be able to move the horizontal tailplane angle setting.
2. Lower aerodynamic efficiency due to the downwash and interference effect.



Other tail arrangements such as cross tail, twin vertical tail, and V tail are not appropriate for high subsonic aircraft and are only used in a special case condition such as the effect of the engine or propeller wash affecting the efficiency of the tail.

In this project tailplane design is studied in order to achieve an optimum wing and tailplane combination. The pitching moment of the wing is limited in order not to end up with a large horizontal tailplane. At this stage the tailplane is designed by using (V bar) method. Mitchell stability and control program (Ref. 47) is used as a means of checking.

### 3.10 Design Optimisation

The target of this program is to find the minimum weight configuration. This target is achieved by calculating all possible solutions that fulfil the criteria mentioned above. This calculation is done iteratively by using a crude method of optimisation by calculating all possible solution. More sophisticated optimisation could be used which will cut the time spent during initial design. But more sophisticated optimisation is considered difficult to implement due to the nature of how the program works. The internal call by the main program to the structural and aerodynamic computational package makes it difficult to perform. Studying the time required to run the whole program, it can be concluded that the benefit of using better optimisation method is minimal because most of the



time spent is on the computational package of NASTRAN and SPARV.



# PARAMETRIC STUDY OF AIRBUS 310-300 CF6-80C2-A2

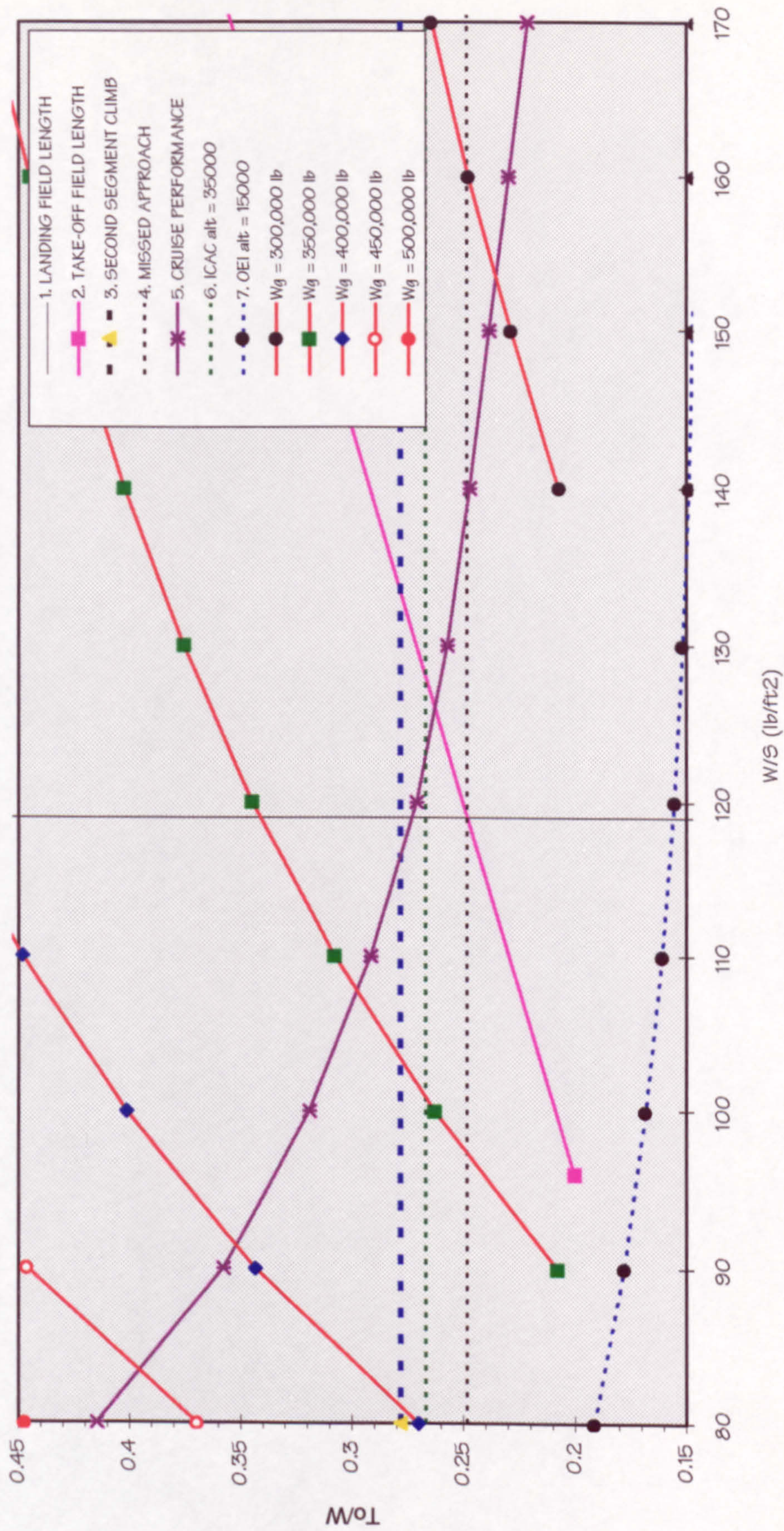


**Figure 3.5 Parametric Study**



# DEMONSTRATED $C_{L_{MAX}}$ LEVELS

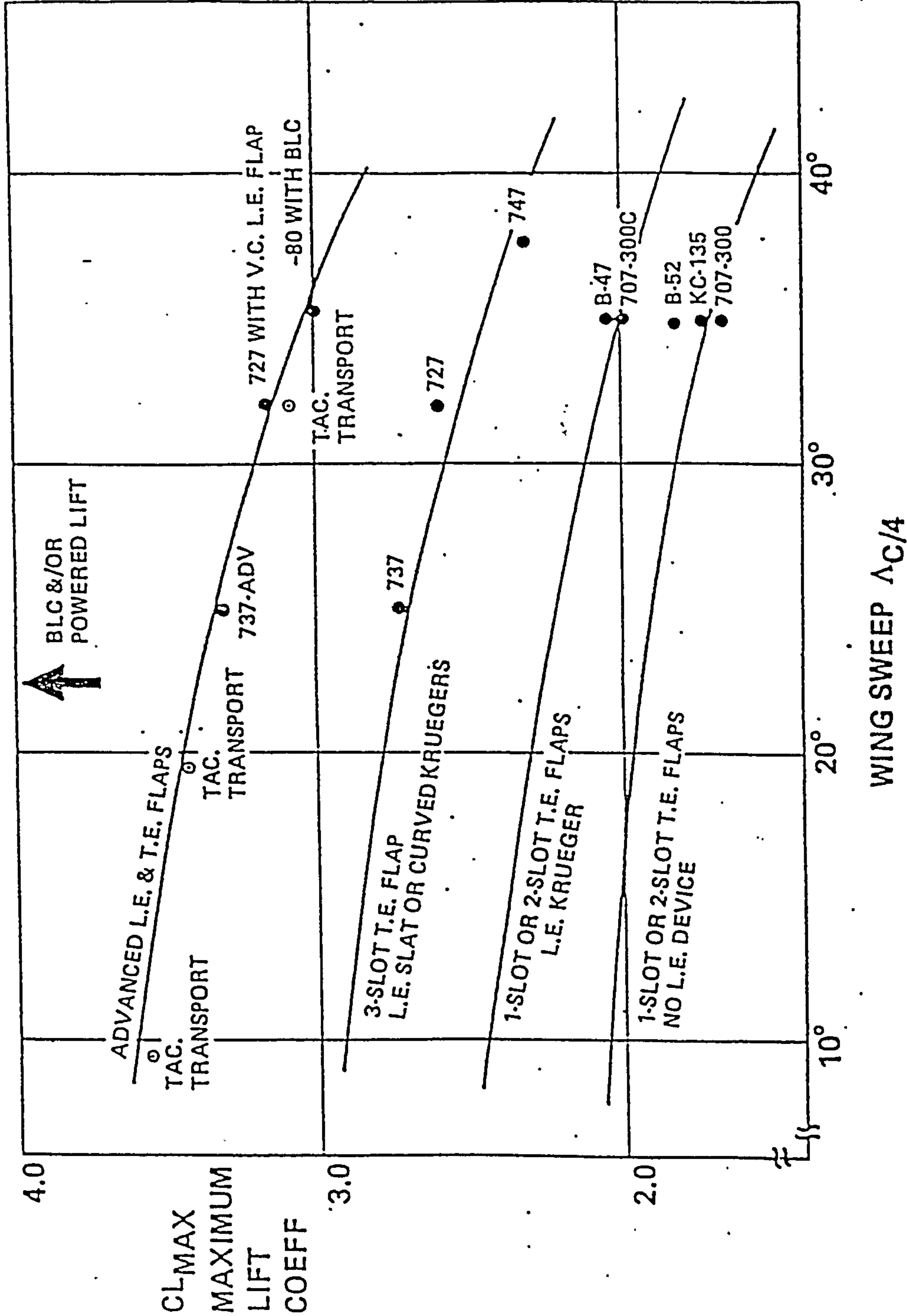


Figure 3.6      Demonstrated  $C_{L_{MAX}}$  levels



# *Chapter 4*



## 4. WING DESIGN PROCESS

### 4.1 Introduction

Wing Design is of key interest to the aerodynamicist because of its dominant influence on the aeroplane performance. Early transport wing design was based on previous experience and considerable wind tunnel testing. Computational aerodynamics is changing the design process so that more highly refined configurations are possible.

Wing design is a highly integrated process involving not only the aerodynamicist but also all other engineering disciplines, marketing, manufacturing, structure and design groups. Basic requirements that must be achieved for successful wing design include :

- The configuration must satisfy the performance goal in the design objectives and requirements while achieving good economy return.
- Flight characteristics, handling qualities, and aeroplane operation must be satisfactory and safe over the entire flight envelope for all aeroplane configurations (cruise, high speed, low speed, undercarriage position, etc.).



- Design of the structure must be possible within the defined external shape such that it meets the strength, torsion, fatigue, flutter, weight life-cycle, maintainability, accessibility and engine requirements and the development and manufacturing costs.
- Sufficient space must be provided for fuel for the design range, for the retraction of the undercarriage, and for the aeroplane systems (flaps, slats, ailerons, fuel, spoilers, etc.).

Meeting all of these requirements simultaneously is very difficult and most likely requires compromise for a satisfactory configuration.

Performance achieved will require interpretation of the requirements of payload, range, initial cruise altitude, landing field length, take-off field length , etc.

The aeroplane structural design will impact the wing design primarily in the influence of wing span limitations, weight, and undercarriage storage. Structural efficiency for minimum wing weight is defined not only by span and chord but also by spar depth. Requirements of fuel volume, flap and control systems, and actuator size may all influence the spar depth and thus the weight.

The importance of spar depth is mentioned by Ref. 34. Airbus Industrie use modern advanced sections for the A310,



A320 and A330/A340 and family resemblance of those wing sections can be clearly seen. The obvious difference is the A320 lower surface that needs to be modified in order to maintain rear spar depth on a much smaller aircraft (Table 4.1). Hydraulic pipes and actuators, electric cables and fittings, etc. do not scale directly with aircraft size and neither the size of the maintenance engineer's hand and access equipment. It can be seen in Table 4.1 that the A320 rear spar depth is typically the same as the larger A310.

**Table 4.1      Rear Spar Depth**

Aircraft	wing chord (mm)	rear spar depth (mm)
A300	5341	444
A310	4509	332
A320	3348	316
A330/A340	6984	438

wing section at 35% semi-span (source : Ref. 34)

In this chapter, the process of wing design in the WINGLAYOUT module is explained. The process includes the process in the 2D aerofoil selection and the 3D wing layout.

## 4.2 Aerofoil selection

Designing a special aerofoil section for the wing is considered as a detail design work and outside the scope of this thesis as the project is intended for conceptual / preliminary design. Because of this reason, the aerofoil section must be picked from the available aerofoil sections in the database. Method for selecting an aerofoil was







In the proposed method, the program calculates the relative importance of the criteria based on the DRO of the aircraft to be designed, i.e. the program checks whether  $M_{DD}$  is very important for the aircraft, or not, by analysing the required  $M_{CRUISE}$ . Detail explanation and example calculations can be seen in appendix B.

### 4.3 Wing Area

It is convenient to separate wing area and wing shape effect in the design process. Wing area and flaps are closely related to the aeroplane performance. Wing shape parameters such as sweep, taper, twist and aerofoil section will typically influence stall and mach number at which drag rise occur.

A plot of the aeroplane weight, wing area, and engine size that satisfies the field performance, cruise requirement, initial cruise altitude capability (ICAC), and cruise speed is used to investigate the required wing area. This plot represents a matrix of point design aeroplane solutions that meet the design requirements for a fixed aeroplane configuration. Wing, engine and empennage size and weight are scaled to meet the fixed payload (i.e. number of passenger) and range requirements. The Maximum Take Off Weight (MTOW) is shown in the plot of  $(T_0/W)$  vs.  $(W/S)$  as lines of constant values. The optimum point of  $(T_0/W)$  and  $(W/S)$  is picked based on the minimum weight criterion. (Figure 4.1).



The  $(T_o/W)$  vs.  $(W/S)$  plot is an optimisation plot that allows selection of wing area and engine thrust while minimising or constraining various parameters. Contours of constant MTOW are shown in the graph along with lines of constant Landing Field Length, Take-off Field Length, ICAC, etc.

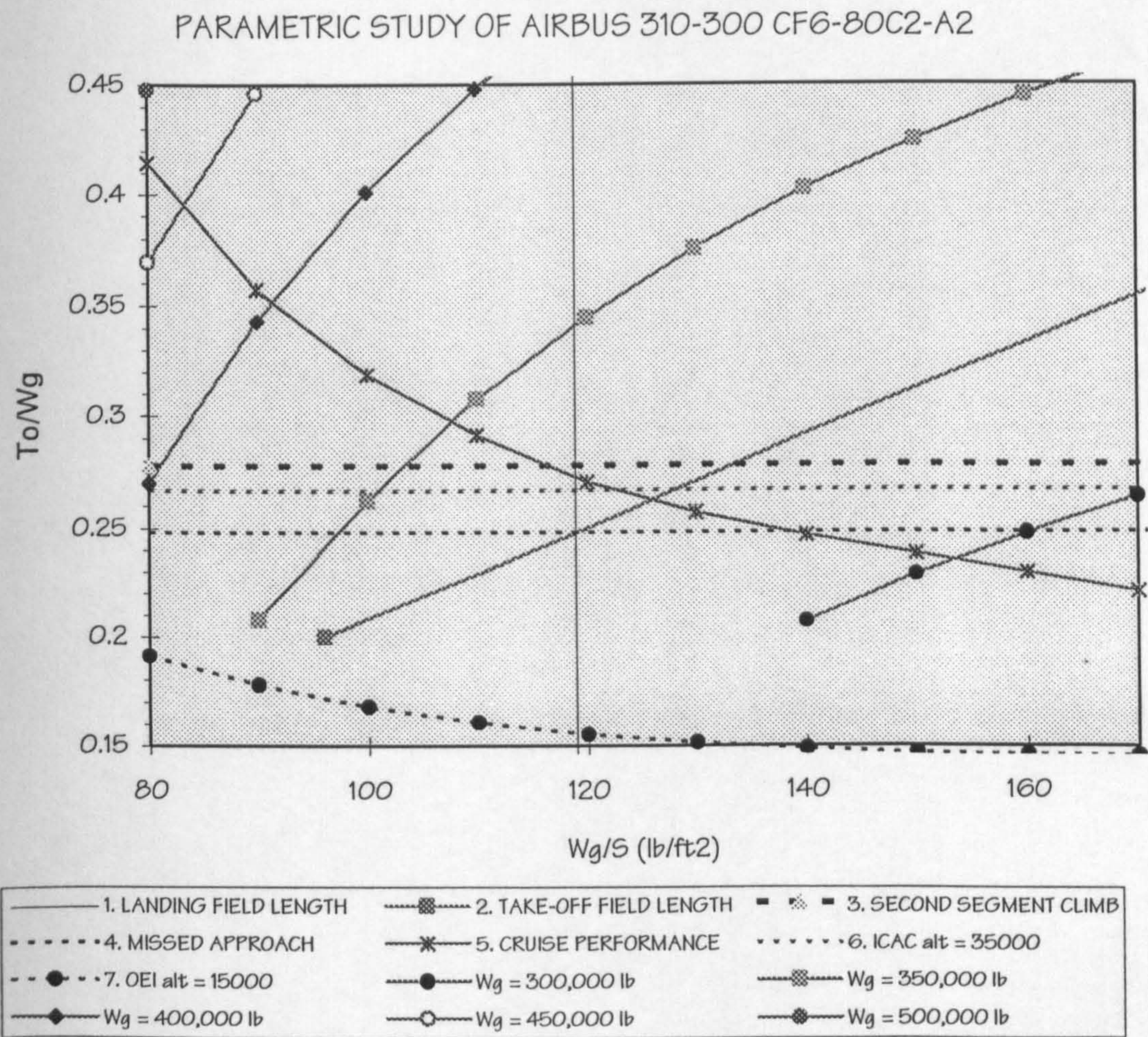


**Figure 4.1**  $(T_o/W)$  vs.  $(W/S)$

During the initial calculation, a number of variables are assigned an initial value. After the optimum  $(T_o/W)$  and  $(W/S)$  are found an initial weight estimation is performed. Knowing the weight and wing loading the initial wing area



can be found. Knowing the wing area, other wing variables can then be calculated, such as thickness-to-chord ratio, sweep angle, etc. The new values are then inputted into the parametric study to get the revised  $(T_o/W)$  and  $(W/S)$ . This looping is done until convergence is achieved.

#### 4.4 Thickness ratio, Sweep and Mach number trade-offs

Several sweep angles are studied and checked by various criteria such as Sweep effect (3D drag rise effect), aeroelastic check, local  $C_l$  (tip stall check), flap effectiveness check and finally fuel capacity check. Several combination of AR,  $t/c$  and Sweep angles that pass the checking are then compared. The lightest combination is picked.

When the thickness ratio, sweep angle, and wing geometry is known, the 3D wing model is constructed. The aerofoil is generated by using the best aerofoil previously computed, being the one chosen by modifying the relative importance of each category of the criteria. After the aerofoil is picked, the thickness ratio of the wing section is constructed. This is done by scaling the thickness ratio up or down according to the thickness ratio needed. The aerofoil section is scaled about the section chordline (Fig. 4.2). This is to achieve transonic similarity. Although the method is very rough, for a first cut try it is acceptable. The scaling of the aerofoil is assumed to not change the aerodynamic coefficients of the section. At



the next step of the design computational aerodynamics is used to verify this.

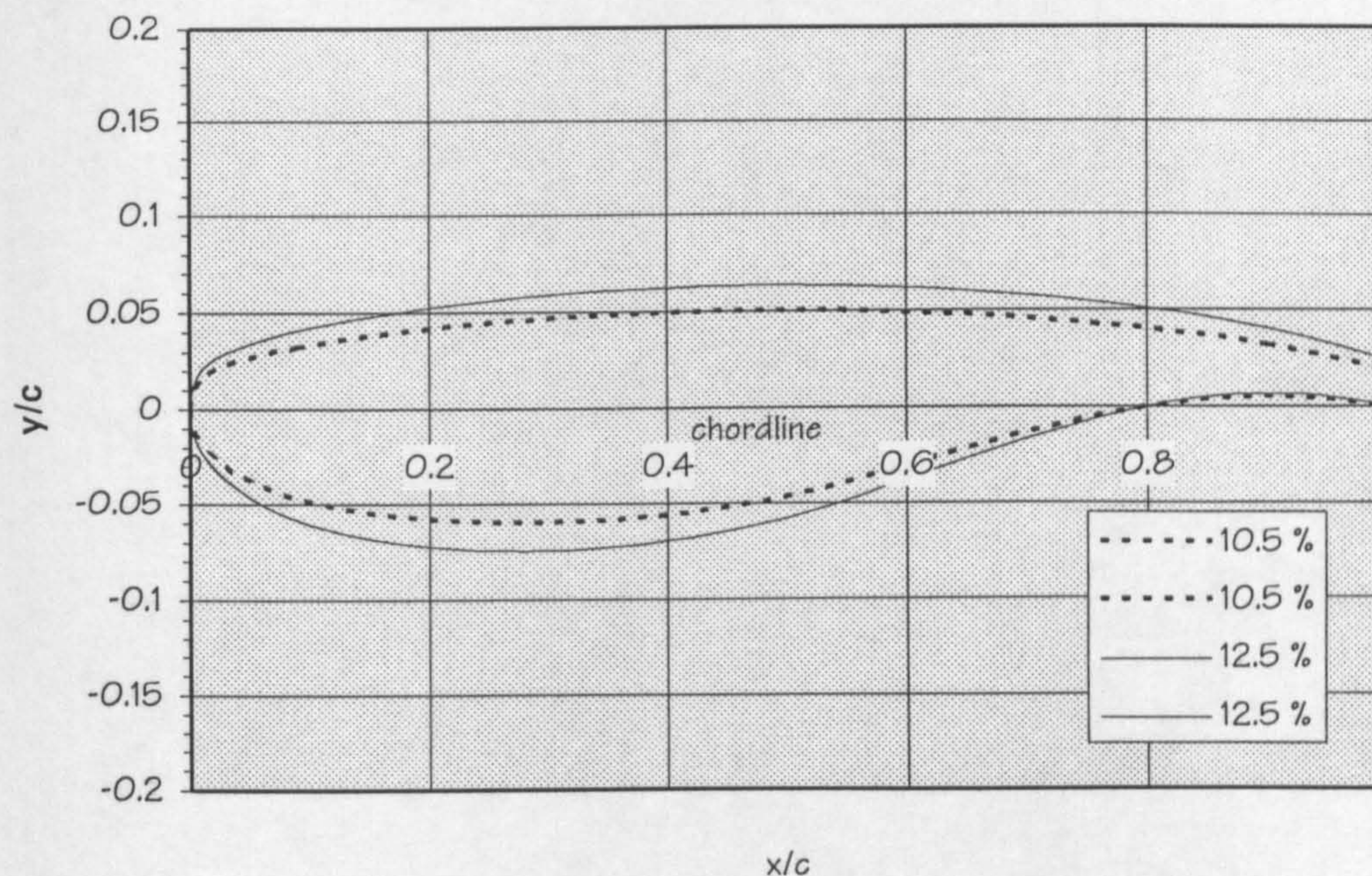


**Figure 4.2 Scale up of aerofoil section**

The primary function of wing sweep angle is to increase the Mach number capability of an unswept wing with the same aerofoil section. Swept wing aerodynamics are based on simple sweep theory. Simple sweep theory is based on the concept of an inviscid infinite yawed wing and does not account for the effects of a finite wing, taper, a body, or a boundary layer flow.

Wing sweep has several important aerodynamic effects which are listed below. The positive effects of increased sweep angle are :



- Increased sweep angle will increase the  $M_{DD}$  ( Mach Drag Divergence) Mach number at which drag rise occurs.
- Increased sweep angle will decrease the wing lift curve slope and therefore reduce the aeroplane response to gust inputs. This results in an improvement in passenger ride comfort.

The negative effect of increasing sweep angle are :

- Increased sweep angle will decrease the maximum lift coefficient. This effect is particularly important if the required landing field length is crucial.
- Increased sweep angle will introduce non-linear stability and control effects.
- Increased sweep angle will increase the structural wing weight.

It is suggested by Ref. 2, that wing sweepback should not be more than the minimum required. It suggested that even when a higher sweep angle is possible on a certain configuration, the minimum sweep angle should be picked. The best choice is the result of a trade-off between structural weight, maximum useable lift and high speed performance.



## 4.5 Wing Aspect Ratio and Span

With the wing area previously found and the sweep now selected, the wing span and AR can be picked based on trade studies. Consideration for the span include airport "gate" requirements for ground handling. Airline gate requirements are somewhat flexible and usually not a limiting factor unless a very large aircraft is designed.

A high AR is very desirable since it produce a higher L/D than at lower AR. Since  $M_{CRUISE}$  is an input required from the user, the only way to get the highest ML/D is by increasing L/D. This is achieved by using higher AR. The AR is checked with the semi-empirical method to make sure it passes the aeroelasticity check.

AR has a big effect on wing weight. High AR produces a heavier wing thus the advantage of higher L/D from high AR has to be compared to the weight increase caused by it. In very high AR, the weight increase outweighs the advantage of higher L/D.

Ref. 34 suggested limitations on maximum AR at particular sweep angle. The limits are :

Sweepback (deg)	24	28	32
Maximum AR	9.5	9.0	8.5

This suggests a linear relationship between sweep angle and AR (  $AR = -0.125 \times \Lambda + 12.5$  ). Based on these limits,



several current aircraft are found to be outside of the boundary such as the A330 and A340 (see Fig. 4.3).

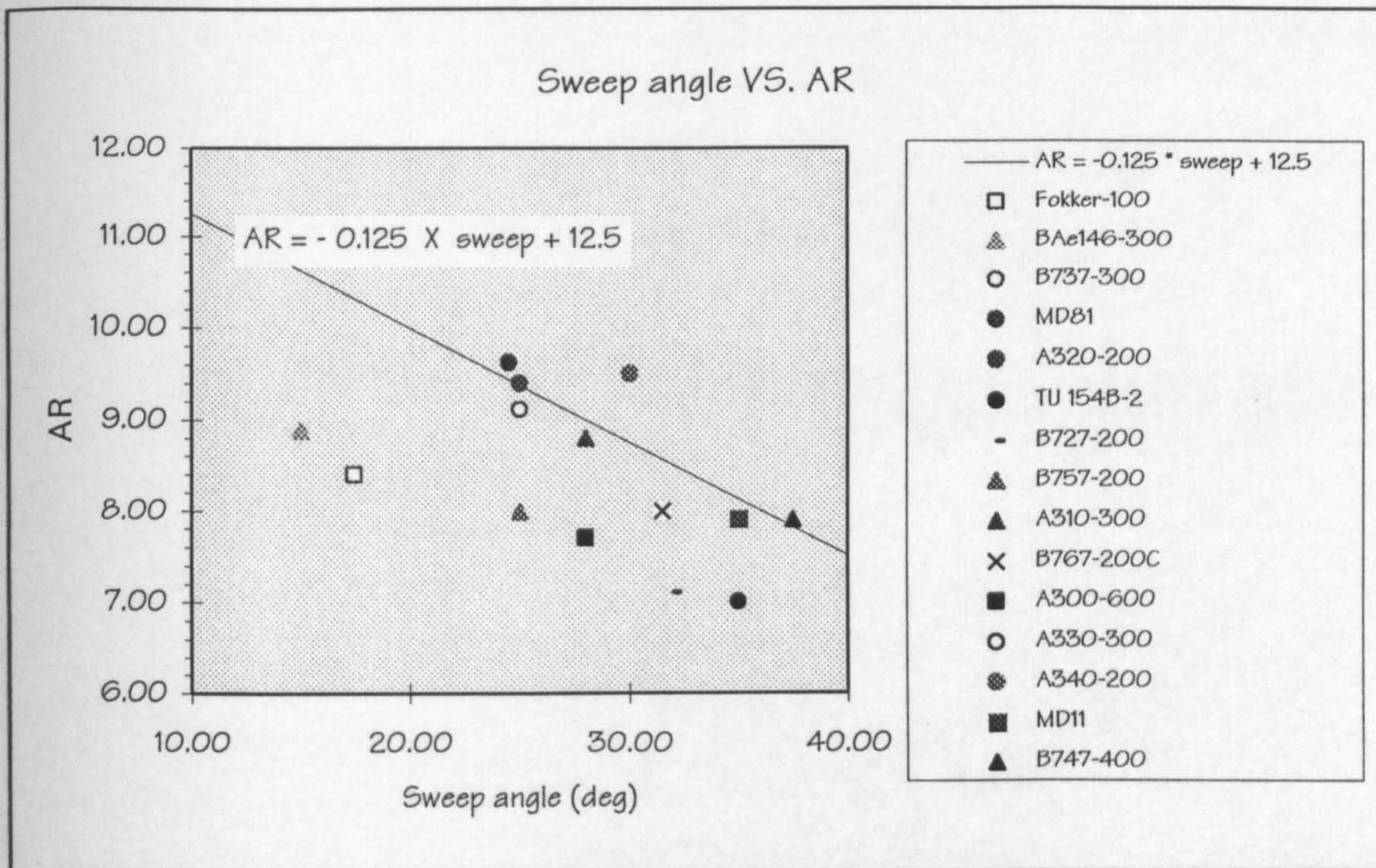


Figure 4.3 Sweep angle vs. AR

#### 4.6 Spanload and Taper Ratio

Choice of the wing spanload distribution is an important decision in the wing design process. Ideally an elliptic distribution is desirable at the cruise condition because of the implied minimum induced drag. However several factors make a slightly triangular distribution very desirable. An elliptic loading at cruise tends to overload the wing tip. This implies a more outboard centre of pressure associated with increased wing structural weight. More pressure load on the tip of the wing increasing the bending moment of the root section.



A constant section lift distribution is desired so the shock development and eventually the separation will occur uniformly. The actual distribution of section lift will be depend on upon the wing taper ratio.

Taper ratio has a major effect on the wing weight and therefore may be selected based on the wing trade off while the spanload is achieved by twisting the wing.

#### 4.7 Wing Incidence Angle

Wing incidence angle on the fuselage is chosen based on the average angle of attack of the wing required during cruise. In the program, this is calculated after determining the required lift coefficient to be produced by the whole aircraft and the wing body angle is set in order for the fuselage angle of attack to be equal to zero during cruise conditions.



# *Chapter 5*



## 5. COMPUTATIONAL AERODYNAMIC PROCESS

### 5.1 Introduction

In this chapter several computational aerodynamic programs are compared and studied. Panel modelling is also described and techniques required are also described briefly.

The module of computational aerodynamics is used in the program to generate the pressure on the wing surface which is used in the next module of computational structural analysis. Other purposes of this module is to check the drag and lift produced by the aircraft. This data is used to check the semi-empirical calculation undertaken in the beginning.

### 5.2 Computational Aerodynamics Program

Investigation of the available computational aerodynamics packages was done in the beginning of the work. There are several computational aerodynamics package available. Currently the College of Aeronautics and Cranfield University have 'SPARV' (Ref. 12) and 'PHOENICS'. Later 'EAGLE' computational program will become available. Study of the two programs SPARV and PHOENICS leads to the conclusion that SPARV is a more appropriate program to choose. PHOENICS is rather difficult to use and is not designed specifically for calculating the aerodynamics of aircraft. The lack of familiarity in using SPARV makes it



necessary to study modelling technique. In the next section several modelling tips when using SPARV are described.

The target computer of this study is a workstation such as Silicon Graphics or SUN microcomputer system. Due to that aim, a more time-consuming computational aerodynamics package, such as a program based on Navier-Stokes equation is considered not appropriate for this study.

The fundamental physical principles of all fluid dynamics is the conservation of mass, Newton's second law, and conservation of energy. From these principles the corresponding governing equation of fluid flow can be generated, these are continuity equation, momentum equation, and energy equation (Ref. 42). From these governing equations several equations can be generated. These are :

1. Navier-Stokes Equations
2. Euler Equations
3. Full Potential Equations
4. Laplaces Equations

These equations basically originated from Navier Stokes Equations and by omitting several terms several other equations can be generated. Omitting terms from the Navier Stokes means simplifying the equations and usually results in less time to solve. These equations can be seen in Fig. 5.1.



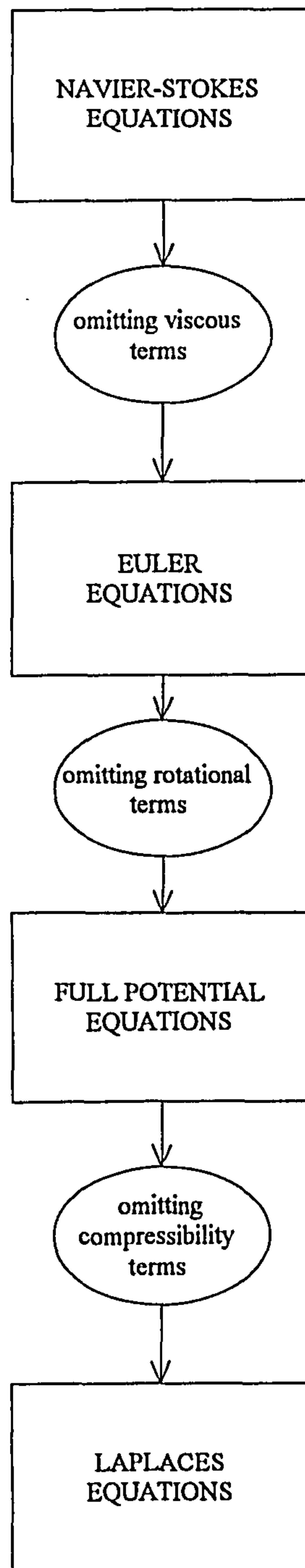


**Figure 5.1      Flow Equations**



### 5.2.1 Navier Stokes Equations

This is a condition where the phenomena of friction, thermal conduction and/or mass diffusion is included in the equation. Several computational aerodynamic program based on this equation are becoming available, although a high speed digital computer is needed to solve the equation. This equation is for an unsteady, three dimensional, compressible, and viscous flow.

### 5.2.2 Euler Equations

For an inviscid flow where the dissipative, transport phenomena of viscosity, mass diffusion, and thermal conductivity are neglected, the equation is called the Euler equation. These are the same equations as in Navier-Stokes except the terms involving friction and thermal conductivity are dropped. This becomes an equation for an unsteady, three dimensional, compressible, and inviscid flow.

### 5.2.3 Full Potential Equations

These equations are generated by omitting the rotational terms from the Euler equations.

### 5.2.4 Laplaces Equations

These equations are generated by omitting the compressibility terms from the Full Potential Equations.



### 5.3 Panel Method

From the equations explained in the previous section, several methods are used to solve these equations. One of the method is Panel Method which is a method to solve the Laplaces Equations.

SPARV program is based on Laplaces Equations and uses a Panel Method to solve those equations. SPARV is decided to be used in the program, although it is a simple computational aerodynamics program compared to Navier-Stokes or Euler based program, it is assumed that this module is suitable for the beginning of the aircraft design. Also if a more sophisticated program becomes available, the module can be exchanged for the new one. As mentioned before, by using several modules instead just one big program, the change of one module can be easily done.

### 5.4 Panel Method Modelling

The proposed method for wing design will require the use of computational aerodynamics in order to achieve a better wing design than is obtainable with other procedures. The purpose of using computational aerodynamics is for correcting the semi-empirical method used in the previous step and also to get pressure distribution over the wing. The spanload distribution of the wing can then be used to modify the twist distribution of the wing to get a higher efficiency.



In order to use the computational method the program needs to know data such as, wing geometry, airfoil geometry and fuselage geometry. This required input is generated in the module called winglayout. After running the WINGLAYOUT module, a subroutine called PRESPARV.EXE is used in order to generate the input data for SPARV.

PRESPARV has been checked and used. It will generate the input data required for SPARV by using an optimised panelling model that has been studied manually before. This modelling study included a time vs. error study. The number of panels is kept at a moderate value in order not waste the time of running the SPARV. Panel distributions such as the sine distribution, are also introduced to the model which keeps a much smaller panel at the region where the pressure gradient is high.

Because SPARV is intended to be used several times in the proposed wing design program, a study of the number of panels that will be used was undertaken by keeping the number of panels as low as possible. Fig. 5.2 and Fig. 5.3. have been generated with the same configuration of aircraft but with a different number of panels. The distorted spanload distribution of Fig. 5.3 is the result of decreasing the number of panels chordwise. Although the number of panels spanwise is kept the same, the effect of decreasing the number of panels chordwise is clearly seen in the spanload distribution. The same method of study was used for selecting the number of panel spanwise. It is found for a typical aircraft, the number of panel spanwise and chordwise should be around 25.



Study of the modelling of the trailing edge angle has also been performed. Closed trailing edge model (Fig. 5.7) and open trailing edge model (Fig. 5.5) were studied and the data then compared to the wing tunnel result. As can be seen in Fig. 5.4, the SPARV results match closely the wind tunnel result. But when the trailing edge is closed a jump in the pressure is found in the trailing edge. The trailing edge is closed by generating a point in the middle of the trailing edge gap (Fig. 5.6). Some computational aerodynamics programs will give a better result if the trailing edge is closed, however it is found that for SPARV the trailing edge is best kept open.

## 5.5 Aircraft Cruise Lift Coefficient Estimation

It is found that by running the model at various angles of attack, a lift curve slope can be estimated. This value is used in the second loop of the aircraft design to give a better result.

## 5.6 Validation

SPARV and PRESPARV have been successfully validated. Several limitations such as the high Mach number limitation has been investigated. The use of the viscous option in the SPARV has also been studied. Validation has been done against the wind tunnel data of a swept back aircraft (Ref. 29) which represents well a typical high subsonic aircraft.



CL\*C/LREF - VKI 3 - alpha = 5.8

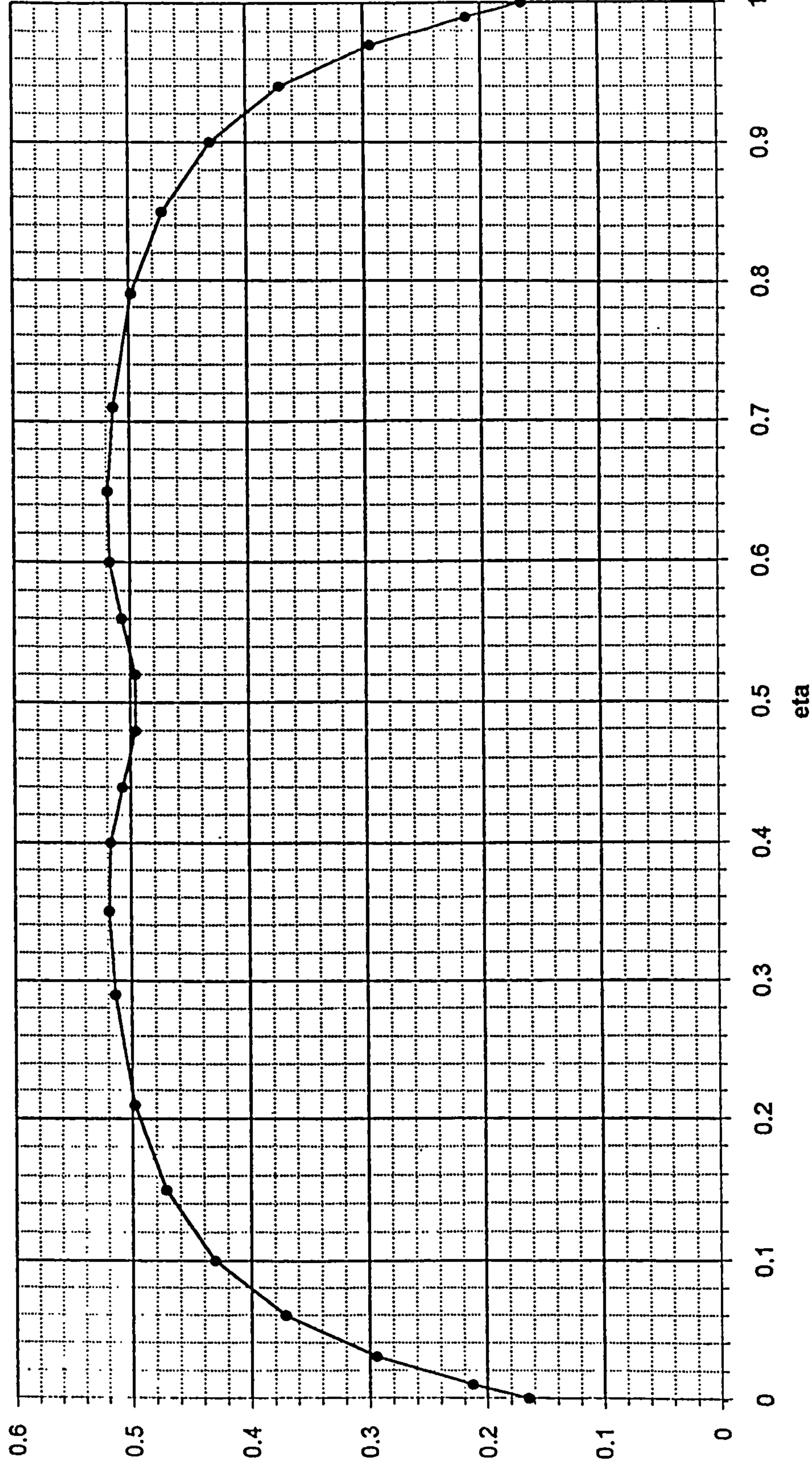


Figure 5.2 SPARV with 25 panels chordwise



CL\*C/LREF - VKI 4 - alpha = 5.8

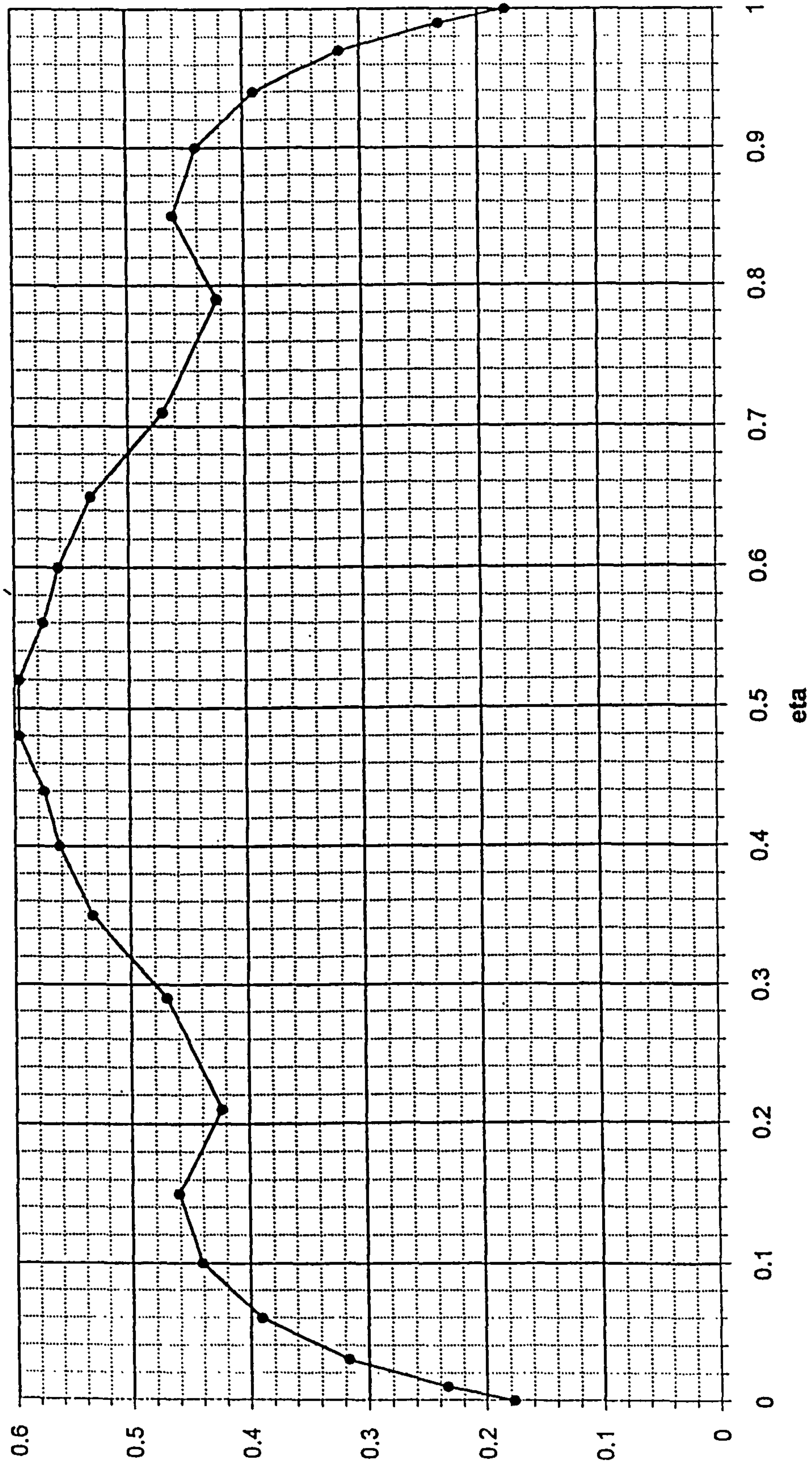


Figure 5.3 SPARV with 13 panels chordwise



RAE 9515 ( $\alpha=5.0$   $M=0.3$ )

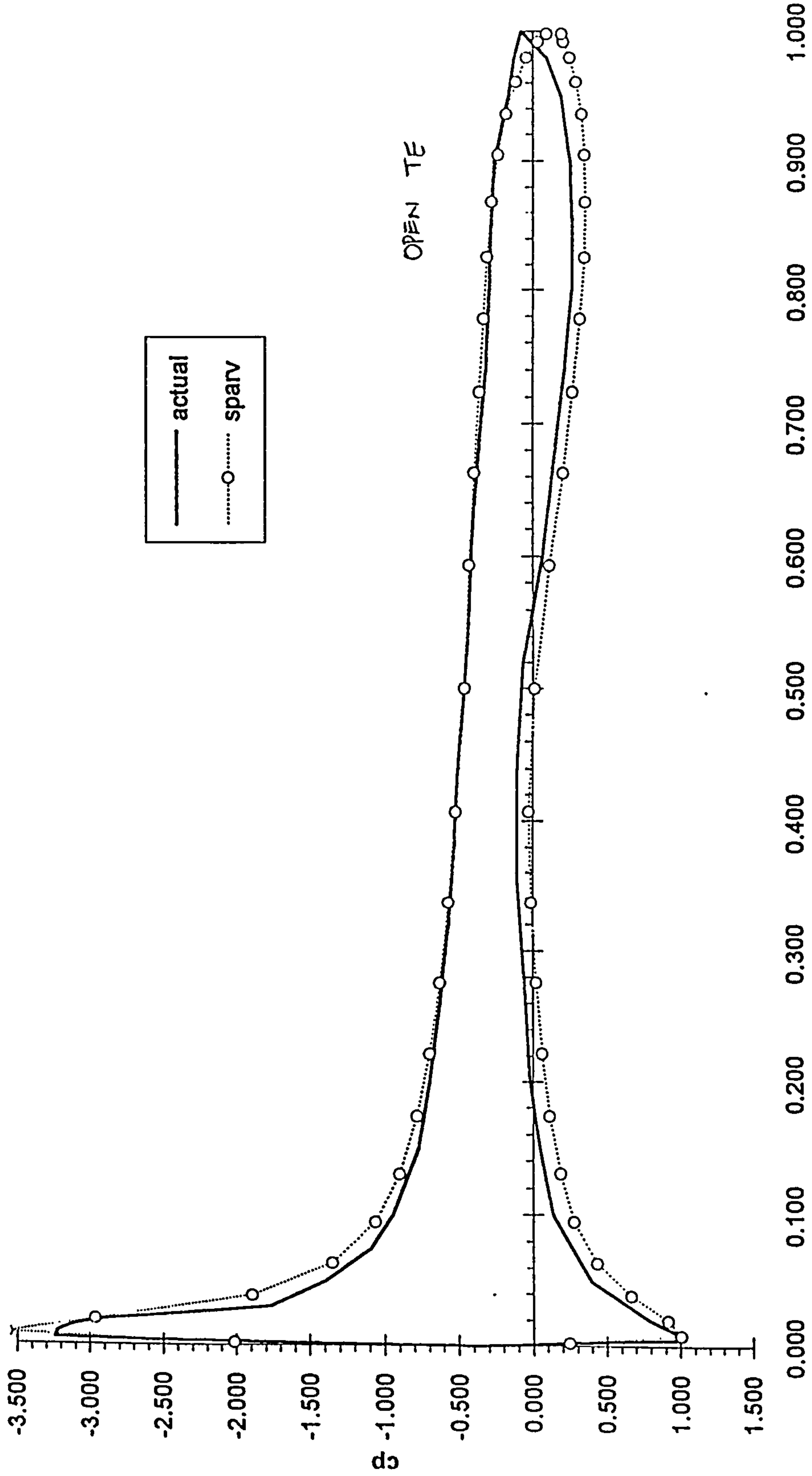


Figure 5.4 Pressure distribution comparison (Open Trailing Edge)



SPARV wing cross section model (open trailing edge)

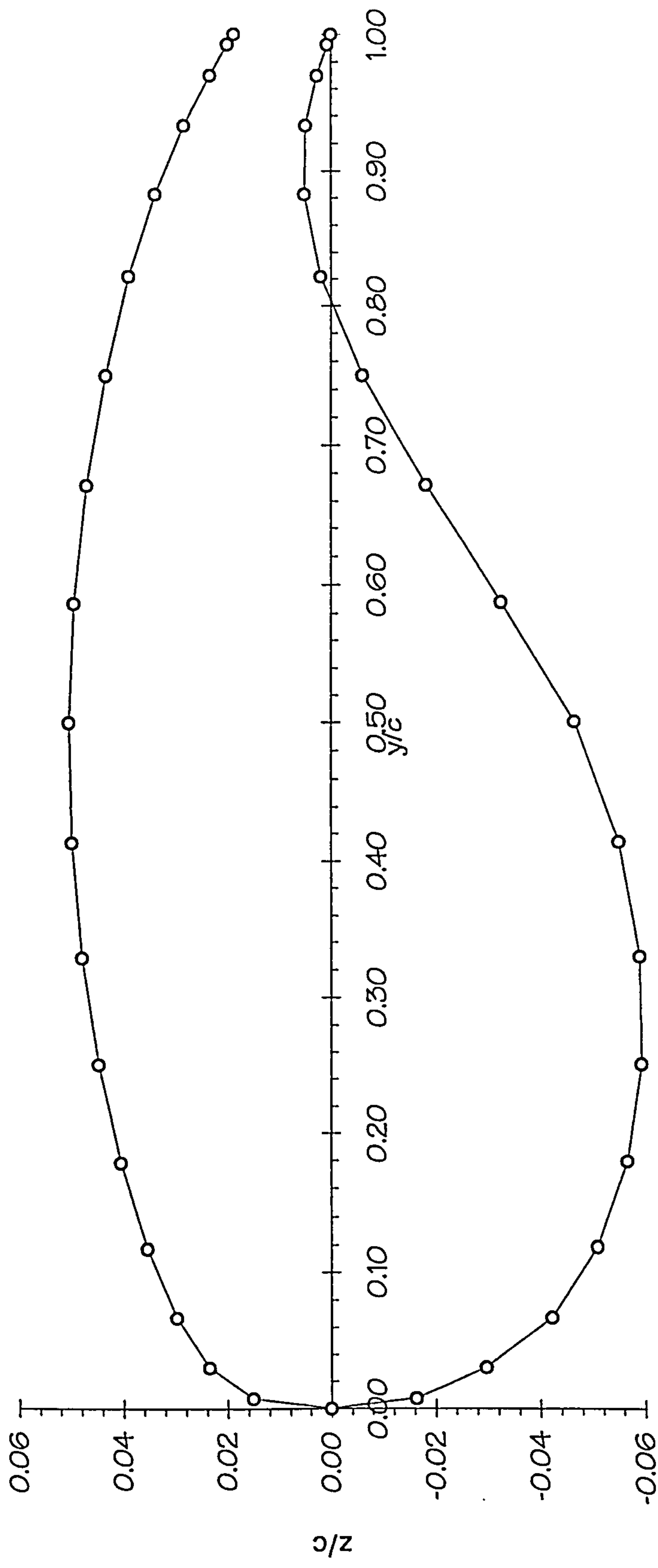


Figure 5.5 SPARV Wing Cross Section Model (Open Trailing Edge)



RAE 9515 ( $\alpha=5.0$   $M=0.3$ )

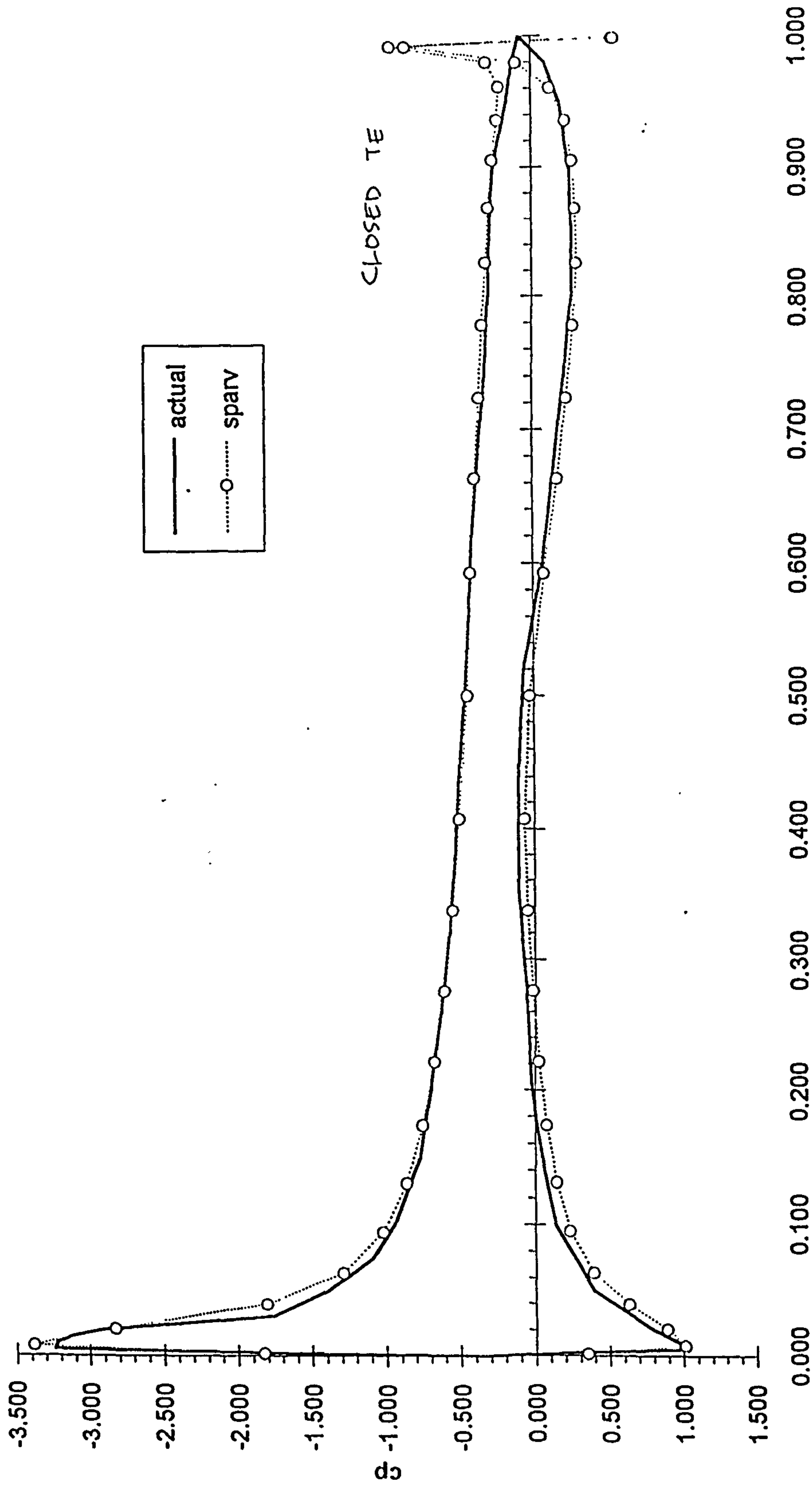


Figure 5.6 Pressure distribution comparison (Close Trailing Edge)



9515 - closed trailing edge

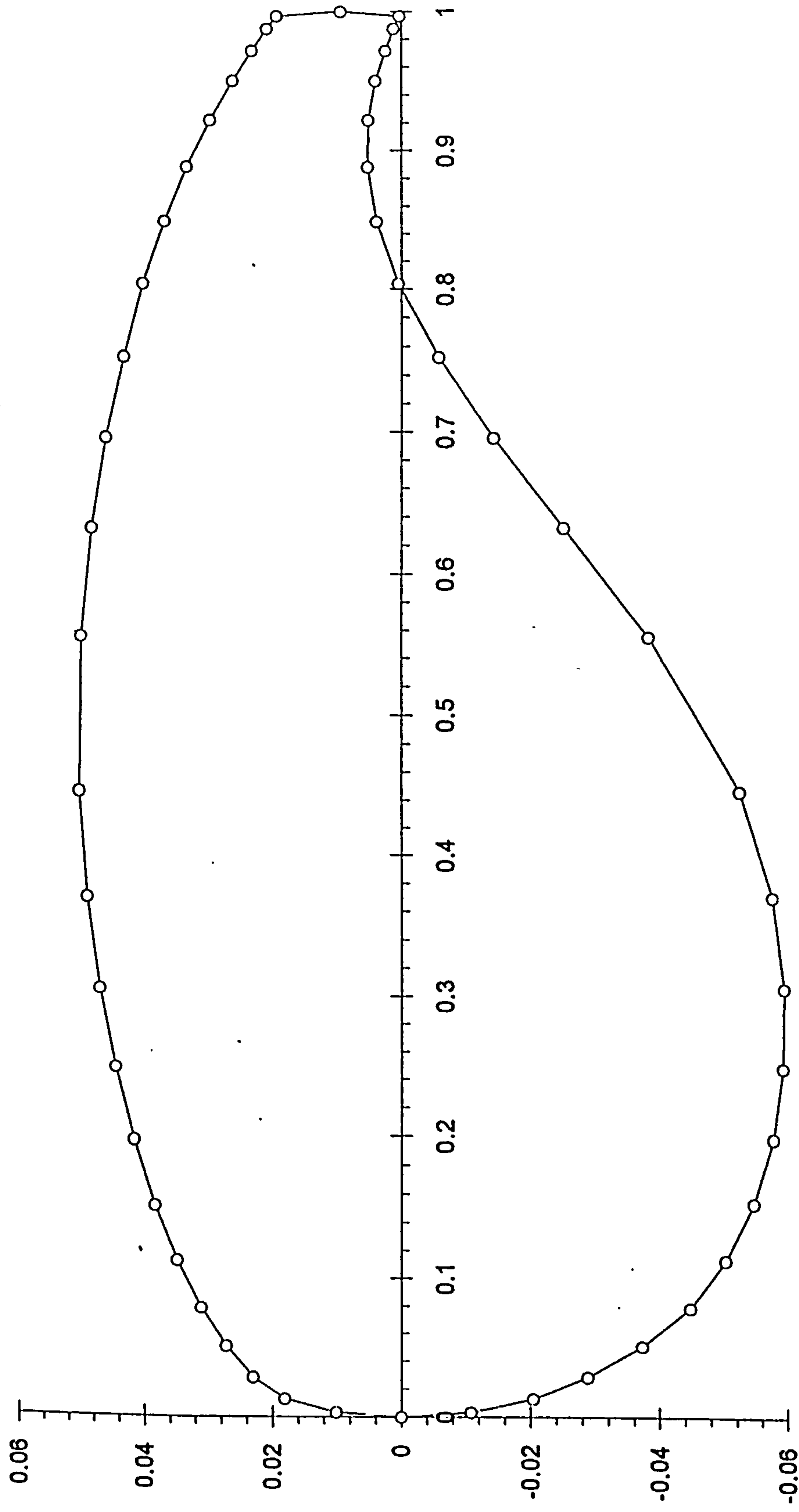


Figure 5.7 SPARV Wing Cross Section Model (Close Trailing Edge)



# *Chapter 6*



## 6. COMPUTATIONAL STRUCTURAL ANALYSIS PROCESS

### 6.1 Introduction

In this chapter the computational structural analysis is described. Computational analysis is done as part of the whole wing design study. This computational structural study is one part of the discipline in the iterative process to study the static aeroelastic effect. The static aeroelastic study, as mentioned earlier, consists of the iterative analysis of computational aerodynamics and computational structural design.

Wing geometry is determined during the aerodynamic analysis to satisfy the performance requirements and objectives in terms of lift, drag and moments. The wing structure is designed based on the loads at critical cases, i.e. condition in the flight envelope which gives the highest load on the structure. In general, the critical case occurs at symmetric case (normal gust case, + or -, or 2.5 g pull up manoeuvre case). As suggested by Ref. 30, the critical loads for high subsonic transport wing is during the +2.5 g pull up. Loads during the 2.5 g manoeuvre were approximated by factoring the cruise load (1 g) by the appropriate factor (2.5). All design load were then factored by a safety margin of 1.5 since the ultimate (failure) materials allowable were used.



In order to design the structure of the wing, one must consider the wing's structural role. The purpose of the wing structure are (Ref. 32) :

- Transmit the wing lift which balances the fuselage inertia loads to the root. This requires a spanwise beam.
- Collect chordwise airloads and loads from control surface and flap hinges and transfer them to the main spanwise structure. This has to be done by a series of chordwise beams and imposes a torque on the spanwise structure as well as shears.
- Transmit inertia loads from components such as powerplants and landing gears to the main structures.
- React landing loads at undercarriage attachments.
- Provide fuel tankage.
- Provide adequate torsional stiffness to the wing to satisfy aeroelastic requirements
- React the wing drag and thrust loads.

In order to design the structural layout of the wing, several positions of components and fuel need to be found first :



Engine position : For the 2 engined aircraft the engine position is located in the kink location of the wing. The engine on the wing will give inertia relief to the wing.

Undercarriage : The location of undercarriage is determined from other criteria. The wing mounted undercarriage will provide inertia relief.

Flaps and flight control : The position of flap and control surfaces need to be decided first. This location is needed in order to decide the rib locations.

Leading edge de-icing : The leading edge de-icing requirements will dictate the type of structure required for the forward part of the wing.

Wing fuel tanks : Integral tanks are common for this type of aircraft, therefore the wing must be leakproof. The problems occur at the end tanks, particularly at the corner where a 'suitcase corner' has to be placed. The other requirement is the access panel, where it is placed on the lower part of the wing and must be leakproof also.

## 6.2 Structural Layout

Structural layout of the wing is restricted by certain geometrical limitation e.g. :

Aileron : 25 to 30 % of chord, and  $\pm 35\%$  of span.

Flap : 25 to 30 % of chord, and  $\pm 65\%$  of span.

Leading Edge : 10 to 15 % of chord, most of span.



Leading edge : After studying the aircraft in this class, it is found that leading edge devices, consist of between 5 to 6 slats along the semi-span, and each slat being fixed to the front spar by 2 hinges arrangement.

Trailing edge : The trailing edge of the aircraft is divided into 65% of the semi-span for the flaps, and the 35% of the semi-span for aileron. These are usually fixed by 2 or 3 hinges.

#### 6.2.1 Chordwise location of spars

Generally there is no need for varying the chordwise location of front and rear spar along the span (Ref. 33). Usually the spar chordwise location at the tip is the same as in the chordwise location at the root.

Generally the front spar has to be as far forward as possible subject to :

- Wing depth being adequate to enable vertical shear loads to be reacted efficiently.
- There is adequate nose chord for the leading edge devices.

As mentioned before the typical location of the front spar is between 10% to 15% of local chord, but study on the AIRBUS aircraft have revealed that the front spar can go as far back as 20 % chordwise.



For the rear spar the location has to be as far aft as possible subject to :

Located in front of the trailing edge flap, control surfaces, spoilers, etc. and their operating mechanisms

The rear spar location is typically between 55% to 70% of the chord with around 60% being the most common.

Data from existing aircraft can be seen in Table 6.1 and Fig. 6.1.

Table 6.1 Spar location

	front spar	rear spar
A300	16.5 %	59.5 %
A310	19.2 %	64.2 %
A320	16.3 %	63.3 %
A330	14.4 %	66.4 %

wing section at 35 % semi-span (source : Ref. 34)

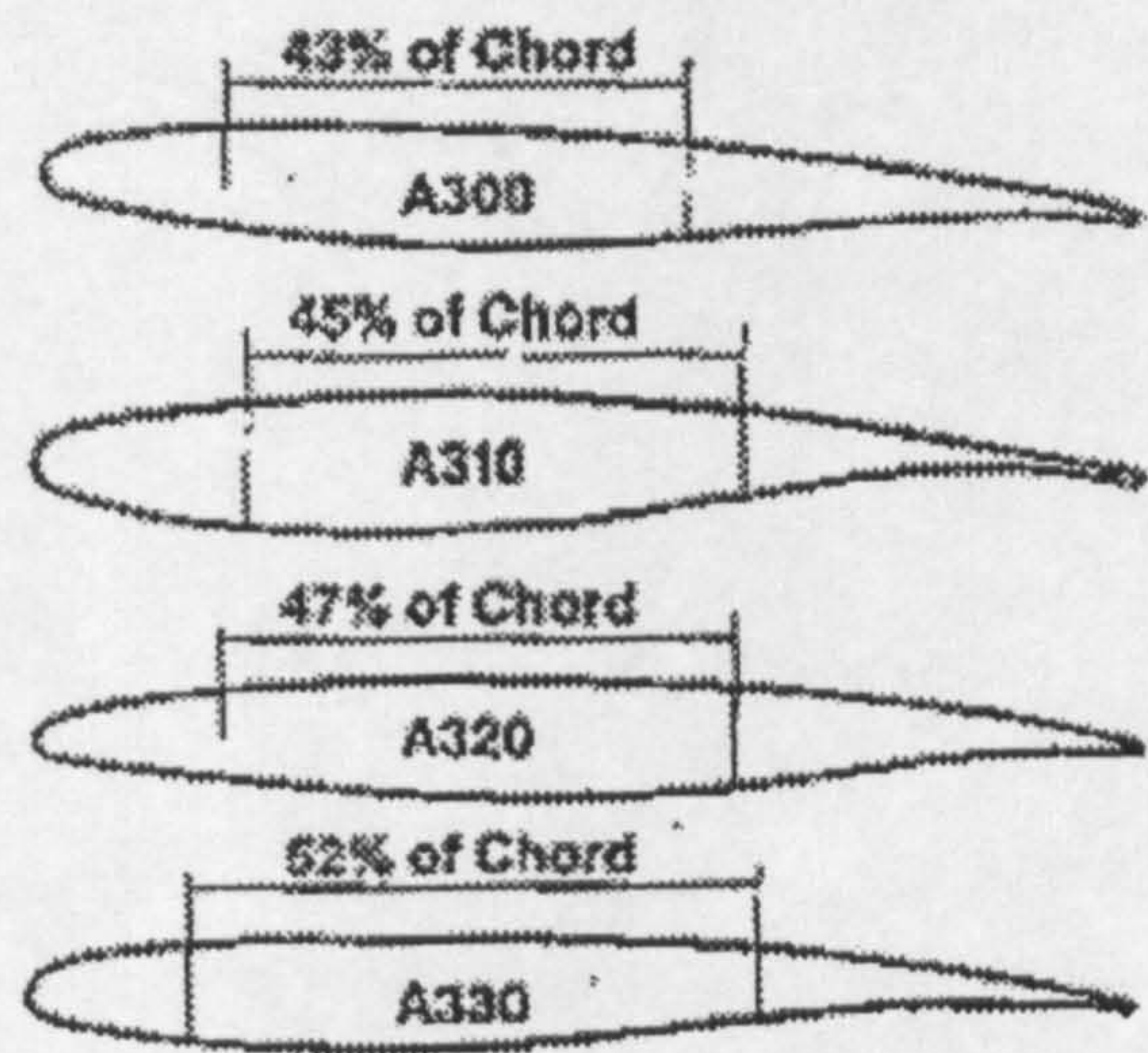


Figure 6.1 Airbus spar location



In this thesis the rear and front spar locations are calculated iteratively to give a space required for the fuel which also satisfies the constraints of the LE and TE devices.

### 6.2.2 Rib pitch

Several authors has derived the optimum rib pitch to give minimum weight. The general equation has the following appearance (Ref. 38) :

$$L_{opt} \propto t \left( \frac{E}{P} \right)^{1/3}$$

where :

$L_{opt}$

= Optimum rib pitch

$t$

= thickness

$E$

= Young's modulus of elasticity

$P$

= Panel load per unit chord

By using Ref. 38 derivation, this equation can be translated into :

$$L_{opt} = (1 - \eta)L_r \dots\dots\dots (6.1)$$

where :

$\eta$

= semi-span fraction

$L_r$

= Rib pitch at the root

This is not a realistic outcome, as the pitch become zero at the tip. It must be concluded that in practice the rib pitch is based on other considerations than weight minimisation.



Ideally the rib spacing should be determined to ensure adequate overall buckling support to the distributed flanges. This requirement may be considered to give a maximum pitch (Ref. 33). However, other considerations are likely to determine the actual rib locations. Such as :

- Hinges for control surfaces and attachment points to the flap slats, spoilers, etc.
- Attachment locations of powerplants, landing gear structures, etc.
- End of Integral tanks.

The location of the kink, flaps and ailerons of existing aircraft can be seen in the Table 6.2 below :

**Table 6.2 Kink, flap, and aileron location**

	kink location	end of flap	end of aileron
B-737-300	34 %	76 %	93 %
B-747-400	40 %	66 %	90 %
B-757-200	40 %	76 %	95 %
B-767-200	38 %	75 %	96 %
MD-80 series	32 %	64 %	84 %
MD-11	37 %	71 %	90 %
A-300-600	39 %	82 %	N/A
A-310	41 %	85 %	N/A
A-320	38 %	78 %	94 %
A-330/A340	30 %	66 %	96 %

percentage of semi-span (source : Ref. 14)



This is just to give a picture about the location of the flap and aileron hinges. These hinges are needed in order to decide the pitch layout of the ribs.

In this thesis the rib pitch at root is calculated by using the equation from Ref. 33 :

$$L_r = 0.3(3.3d)^{1/2} \dots\dots\dots (6.2)$$

where :     d = spar depth

at the other spanwise positions, the rib pitch is determined by equation (6.1) and hinges and attachment conditions.

6.2.3 Rib direction

For a high subsonic aircraft, it is considered that the wing is swept. This gives 3 choices of ribs direction. These ribs layouts are :

- 1. Parallel with the flight direction.
- 2. Perpendicular to the rear spar.
- 3. Perpendicular to the rear spar and gradually becoming parallel to the streamwise as it is closer to the fuselage.

1. Parallel with the flight direction.

This arrangement gives greater torsional stiffness, but the ribs are relatively heavier than the perpendicular



arrangement. It is also found that this arrangement produces a more complex connection between ribs and spars since they have to joint at an angle. In general the disadvantages outweigh the gains (Ref. 33).

## 2. Perpendicular to the rear spar.

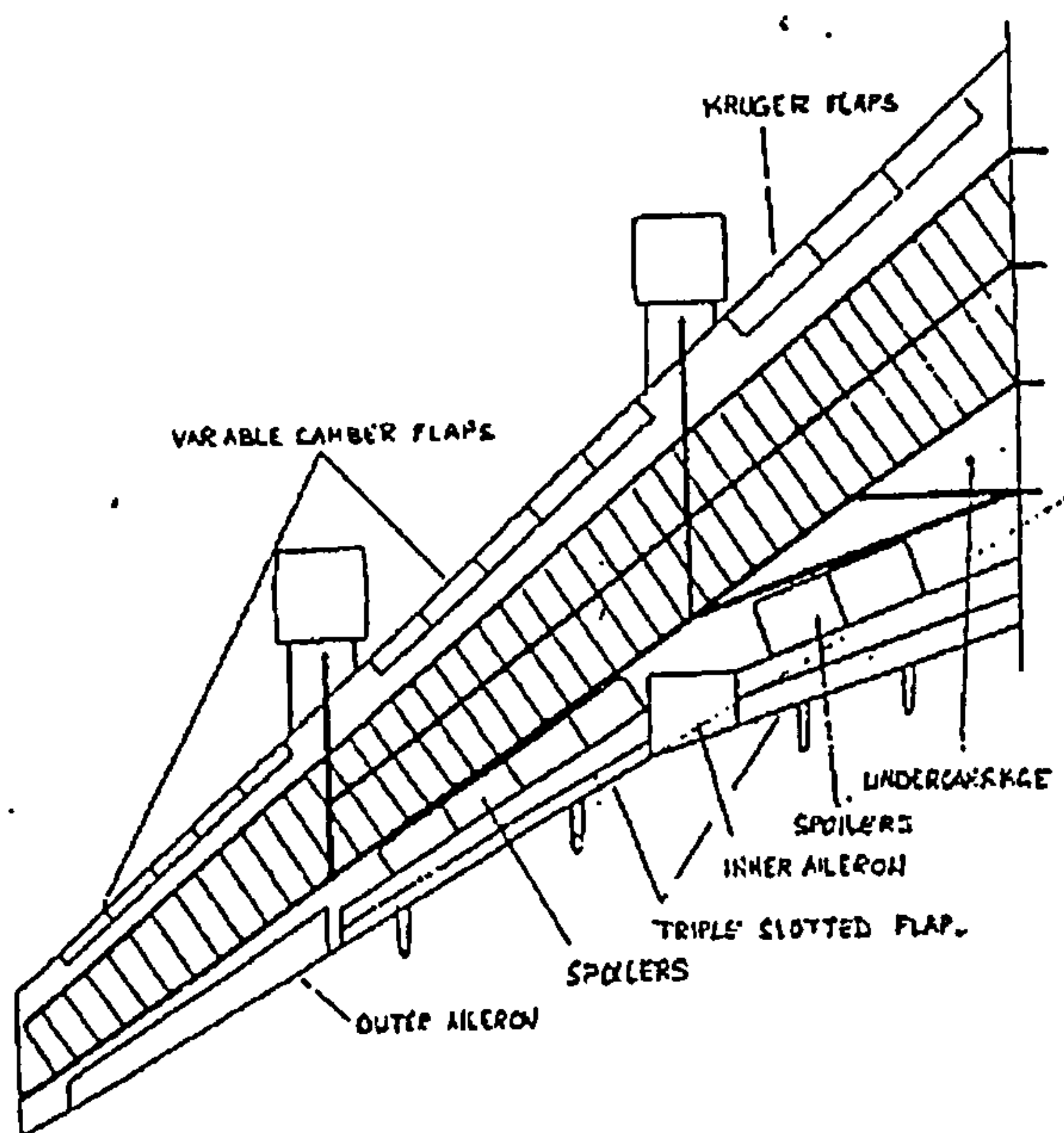


**Figure 6.2 B747 Rib Layout**

This arrangement is usually the most satisfactory in facilitating hinge pick-ups, etc. and usually is lighter than the previous arrangement. As can be seen of Fig. 6.2, for a swept wing aircraft, this configuration gives a "difficult triangle" in the root section of the wing, which requires a careful detail design.



3. Perpendicular to the rear spar and gradually become parallel to the streamwise.

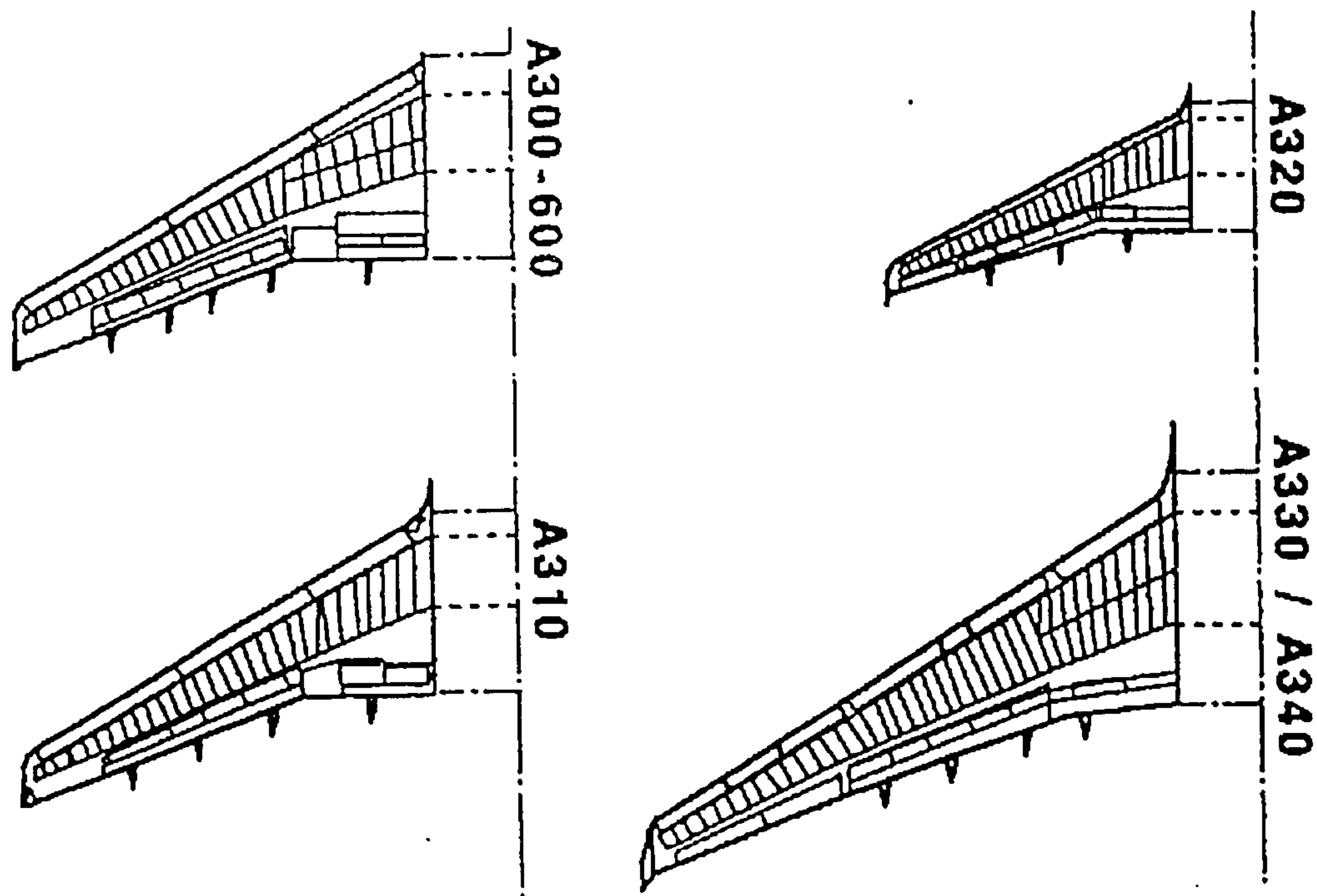


Figure 6.3 Airbus Rib Layout

This arrangement is believed to be the lightest solution of the wing structural layout. The difficult triangle in the root section is eliminated by gradually rotating the ribs to become parallel to the fuselage at the wing root. As can be seen on Fig. 6.3, this arrangement is used in all AIRBUS aircraft.

For choosing the rib layout of the wing, a study of existing aircraft was performed. It was found that BOEING has changed its wing structural layout from the 2nd choice (perpendicular) to the 3rd choice and back to the 2nd choice again. The latest BOEING aircraft, BOEING 777 has



the rib layout to be perpendicular to the rear spar (Fig. 6.4). This is due to the fact that the consideration of the ease of manufacturing and cost of maintenance is believed to be in favour of the 2nd choice.

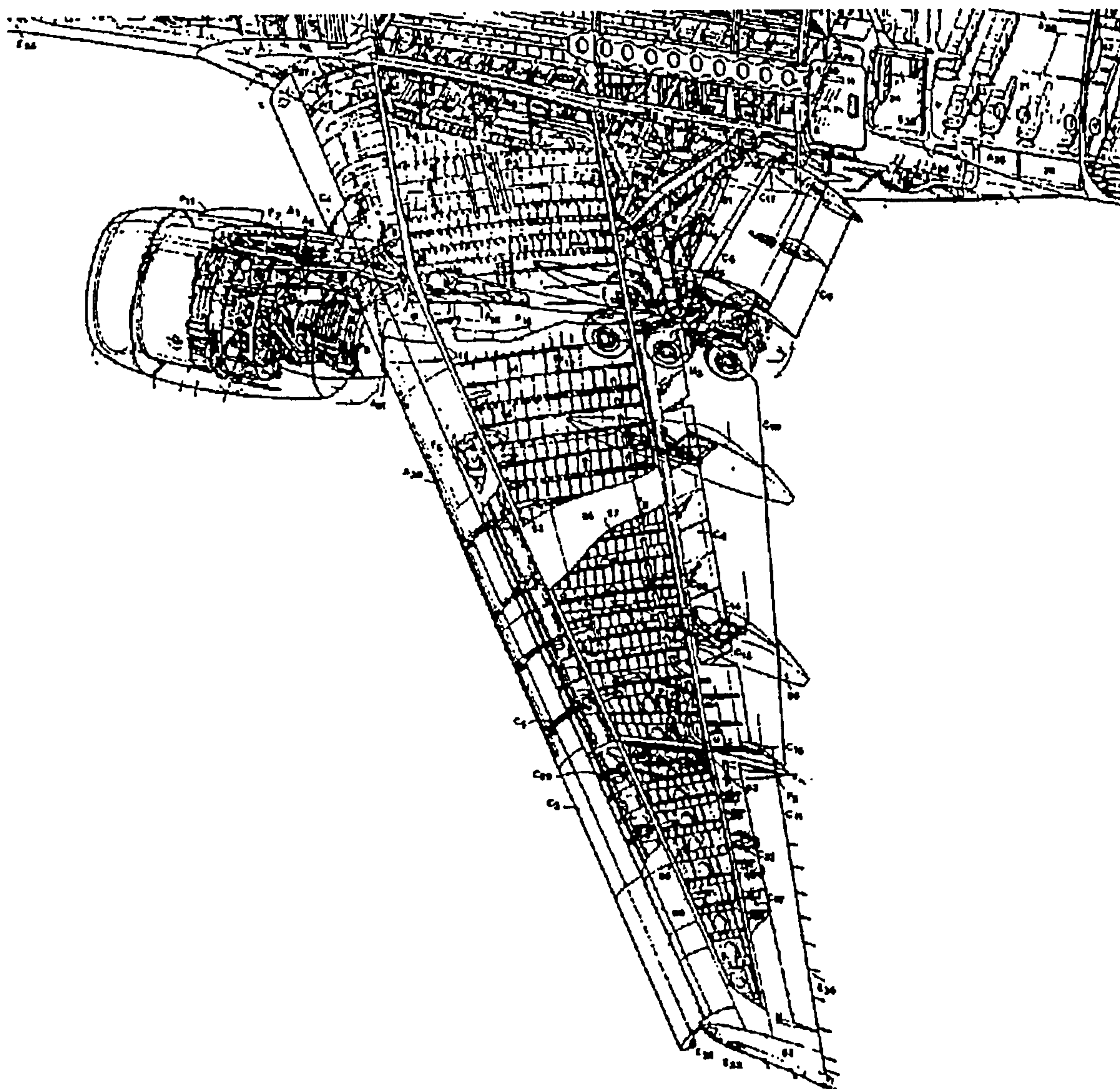


Figure 6.4 Boeing 777 cutaway



Data from existing aircraft can be seen in Table 6.3 below.

Table 6.3 Ribs Layout

ribs layout	
B-747	perpendicular to rear spar
B-767	perpendicular than become parallel
B-777	perpendicular to rear spar
DC 9-80	perpendicular than become parallel
DC 10-30	perpendicular to rear spar
A300-600	perpendicular than become parallel
A310	perpendicular than become parallel
A320	perpendicular than become parallel
A330/A340	perpendicular than become parallel

(source : Ref. 33,34,39)

Since ease of manufacturing and maintenance cost is considered to be out of the scope of this thesis, the BOEING decision is considered to be appropriate and was used in this thesis. The ribs layout is chosen to be perpendicular to the rear spar all the way from tip to root.

### 6.3 Finite Element Modelling

An aircraft wing is a very complex structure. It is very difficult to model it fully without sacrificing the time of computation. In most cases a careful simplifying is necessary in order to achieve an optimum condition between time and results. The simplification can be as far as modelling it with cantilever beam, or as detailed as a



model representative which including skin, ribs and stiffeners.

There are several structural computational programs available in the College of Aeronautics. They vary from a relative simple model such as STRUCT (Ref. 71), to a powerful Finite Element Program such as NASTRAN (Ref. 36). STRUCT can be used to model the wing with a limitation that it can not model the wing skin. In STRUCT pressure load has to be applied to the nodes. Since research will be done by analysing the pressure load of the wing, a detailed pressure load is required to achieve a good result. Pressure loads need to be applied to the skin itself rather than to the ribs and spars. STRUCT in this case cannot be used.

There are several other finite element programs also available that can tackle the anticipated problems above. IDEAS for example is an interesting package.

After studying several choices, the finite element calculations are done by using NASTRAN finite element program. This is for several reasons :

- Simple to run

Unlike other finite element programs, NASTRAN can be run by submitting "NASTRAN DATAFILE.DAT" from within another program. The ability to by-pass the Graphical Interface is a must in this research.



- Capable of performing optimisation

The Solution 200 in NASTRAN is used to design the component sizes of the wing structure. Rather than performing it manually, the ability of NASTRAN to perform optimisation will simplify the main program.

- Widely used

A fact that NASTRAN is well known and widely used is a benefit. Finding literature and validation data are relatively easy to perform.

Modelling of the wing structure is done by generating the grid points and choosing the elements to be used with other criteria such as material properties. The grid points are carefully generated by the PRENASTRAN module according to the layout of the aircraft. The points are extracted from the SPARV output. The number of panels spanwise is decided to be the same as the number of ribs.

Pressure load is extracted from the SPARV pressure distribution output which is extracted by the POSTSPARV / PRENASTRAN module.

### 6.3.1 NASTRAN Sol-200

NASTRAN Solution 200 is an option in MSC NASTRAN that is needed in order to perform an optimisation. The optimisation that was performed in this project is the ability to find the minimum thickness of a structure which satisfies several constraints. The requirement that was used is the maximum stress limit.



NASTRAN will iterate and find the solution which satisfies the requirements and achieve the target. The target can be minimum deflection or minimum weight. Each of these targets have been investigated and it was decided to use weight as the only target in this module. The deflection target was not found to be the governing criteria.

The structural optimisation capability of MSC NASTRAN is unique in that it can automatically modify the structural design and the associated analysis model to satisfy the criteria prescribed by the user (Ref. 36).

This is distinctly different from ordinary structural analysis capabilities in which structural responses are calculated for a given and fixed analysis model. The relation between analysis and optimisation may be visualises in the most simplest form from the Fig. 6.5 below.

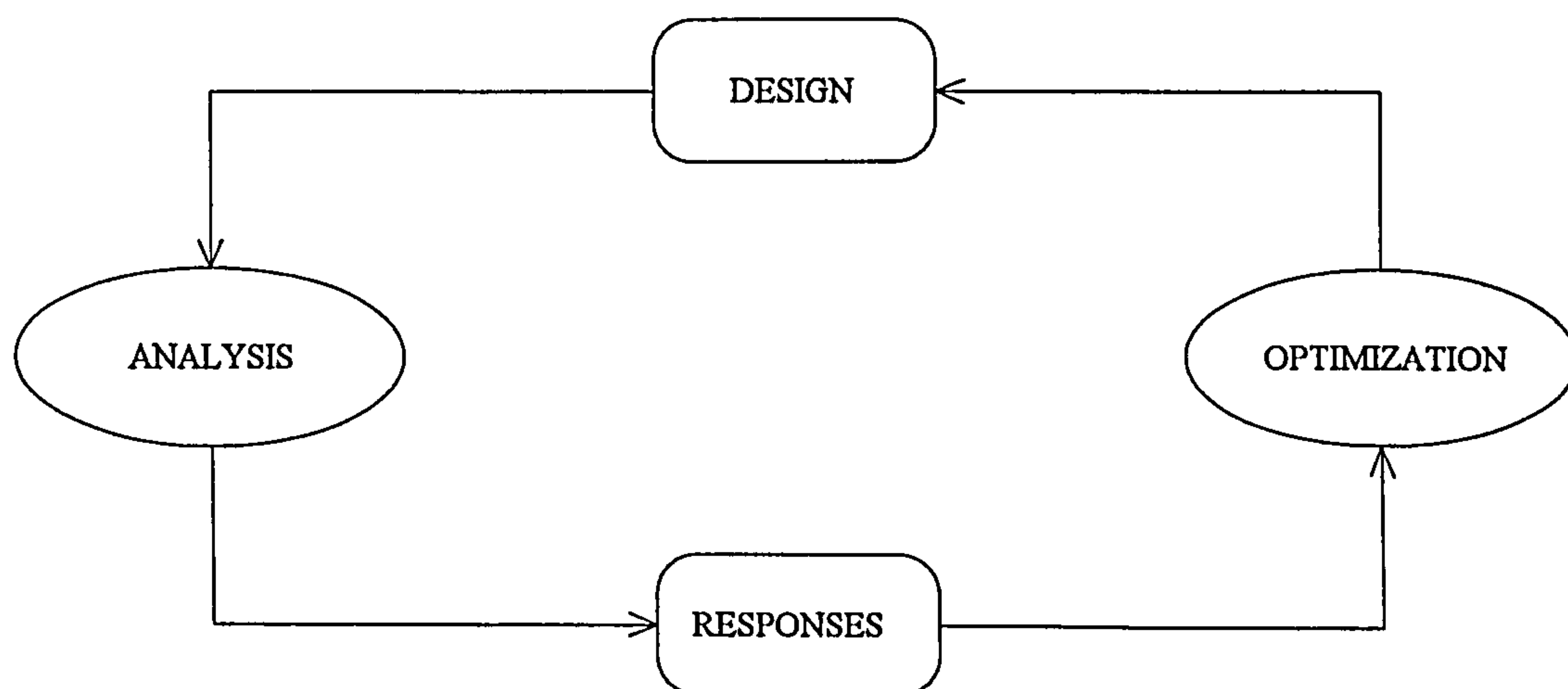


**Figure 6.5      Relation between Analysis and Optimisation**



Starting from the initial design that was generated by the PRENASTRAN module, an MSC NASTRAN SOL-200 is carried out. The analysis computes the various structural responses, such as stresses, displacements, etc., together with their sensitivities to the specified set of design model parameters. These response data are fed into the optimisation program to propose an improved design. Based on this new design, the analysis model is modified and new iteration cycle starts. These iterations are done until a specified time or until it converges.

### 6.3.2 Optimisation for minimum weight

The minimum weight is picked to be the target of the structural program. This is consistent with the previous target, since the parametric study target is minimum weight.

A design optimisation problem in NASTRAN must be formulated in the specific form as shown in the equation below :

Find  $x = (x_1, x_2, \dots, x_n)$  such that  $F(x)$  is minimise  
subject to :

$$G_j(x) \leq 0 \quad j = 1, 2, \dots, NCON$$

$$x_i^L \leq x_i \leq x_i^U \quad i = 1, 2, \dots, NDV$$

where  $x$  is a vector of the design variable,  $F(x)$  is a scalar function of the design variables called the objective function.  $G_j(x)$  ( $j=1,2,\dots,NCON$ ) are scalar functions of the design variables called constraint functions.  $F(x)$



and  $G_j(x)$  are usually implicit functions of  $x$  for structural optimisation. In other words they can only be evaluated by carrying out a finite element analysis on the analysis model corresponding to the set of design variable values stored in the  $x$  vector.  $x_i^L$  and  $x_i^U$  are the lower and upper bounds imposed on the individual design variables  $x_i$ .

For a wing design problem, the design aim can be described as determining the structural panel thickness distribution subject to the minimum gauge requirements. The total structural weight must be as small as possible, while maintaining a sufficient safety margin against the material yield and guarding against the local buckling. This problems can be written as :

Find panel thickness  $T = (t_1, t_2, \dots, t_n)$  so that total structural weight  $W(T)$  is minimised, subject to :

- Von Mises Stresses for all elements  $\leq$  Allowable stress
- Local buckling conditions are suppressed

$$t_i \geq t_{i \min} \quad t_{i \min} \text{ is the minimum gauge}$$

If all thicknesses  $t_1, t_2, \dots, t_n$  are given, then it is possible to compute the structural weight and the panel stresses by running MSC NASTRAN. The local buckling criteria are usually given by a simple analytical formula or design charts which can be interpreted numerically.



### 6.3.3 NASTRAN Finite Element Model

The NASTRAN model for this project consists of half wing of an aeroplane. It consists of upper and lower skin, front and rear spars and the complete ribs. Leading edge and trailing edge are excluded and the forces acting on them are distributed on the front and rear spars.

The wing is modelled by using quadrilateral elements. Skins are modelled with QUAD4 elements. For a difficult part such as the tip and the root section, a triangular element is needed, TRIA3 elements are used. The Pressure loads are automatically interpolated by the PRENASTRAN module and applied to the grid. A typical NASTRAN model can be seen in Fig. 6.10.

For all elements, PLATE elements are used. The decision to use plate elements was made at the beginning of the work. Suggestion for carrying a study for using membrane elements is also done later to study the validity of the weight estimation used in the program. Study on these elements (membrane and plate elements) is carried out and the weight outputs are compared. All of these models have the same loads and fixations. It is found that the different weights of the wing box are as follows :

$W_{\text{WING BOX}}$	=	10,004 lbs	for membrane elements
$W_{\text{WING BOX}}$	=	11,046 lbs	for plate elements



These results are based on all plate elements and all membrane elements. Only those two conditions were found to be working. Using plate elements for the spars and the ribs and membrane elements for the skins are found to be impossible due to the way pressure loading was put to the model. Major modification is needed in order to allow pressure loading to be put to the spars plate elements instead of the skin membrane elements which does not take perpendicular force.

Modelling the wing with all membrane elements in this condition gave an unusual result. As can be seen in the previous weight comparison, the all membrane elements gave heavier result. This is unexpected due to the use of optimiser where membrane thickness is expected to be thinner and thus lighter compared to the all plate elements due to the inability of membranes elements to take moments.

Studying the results from these two elements confirm that plate elements used since the beginning of the work is correct. Also it can be concluded that membrane elements are inadequate to be used in the modelling of the wing. This was shown by the reaction force at the wing root.

In order to study the effect of this different modelling method, Von Misses stresses of those modelling methods are plotted and compared (Fig. 6.6 and Fig. 6.7). Studying these plots, there is appear to be some peculiarity due to the way boundary condition is chosen. The low stresses on the centreline of the aircraft is due to the selection of fixation conditions at the side of the fuselage.



Study between these modelling techniques has also been done on the wing twist and wing deflection. As can be seen in Fig. 6.8 and Fig. 6.9, the differences are small. The twist and deflection of those models can be seen in Table 6.4.

**Table 6.4      All membrane vs. all plate study**

	twist at wing tip	tip deflection
membrane	2.62	4.1 ft
plate	2.57	4.1 ft





Figure 6.6 Von Mises stress of membrane elements



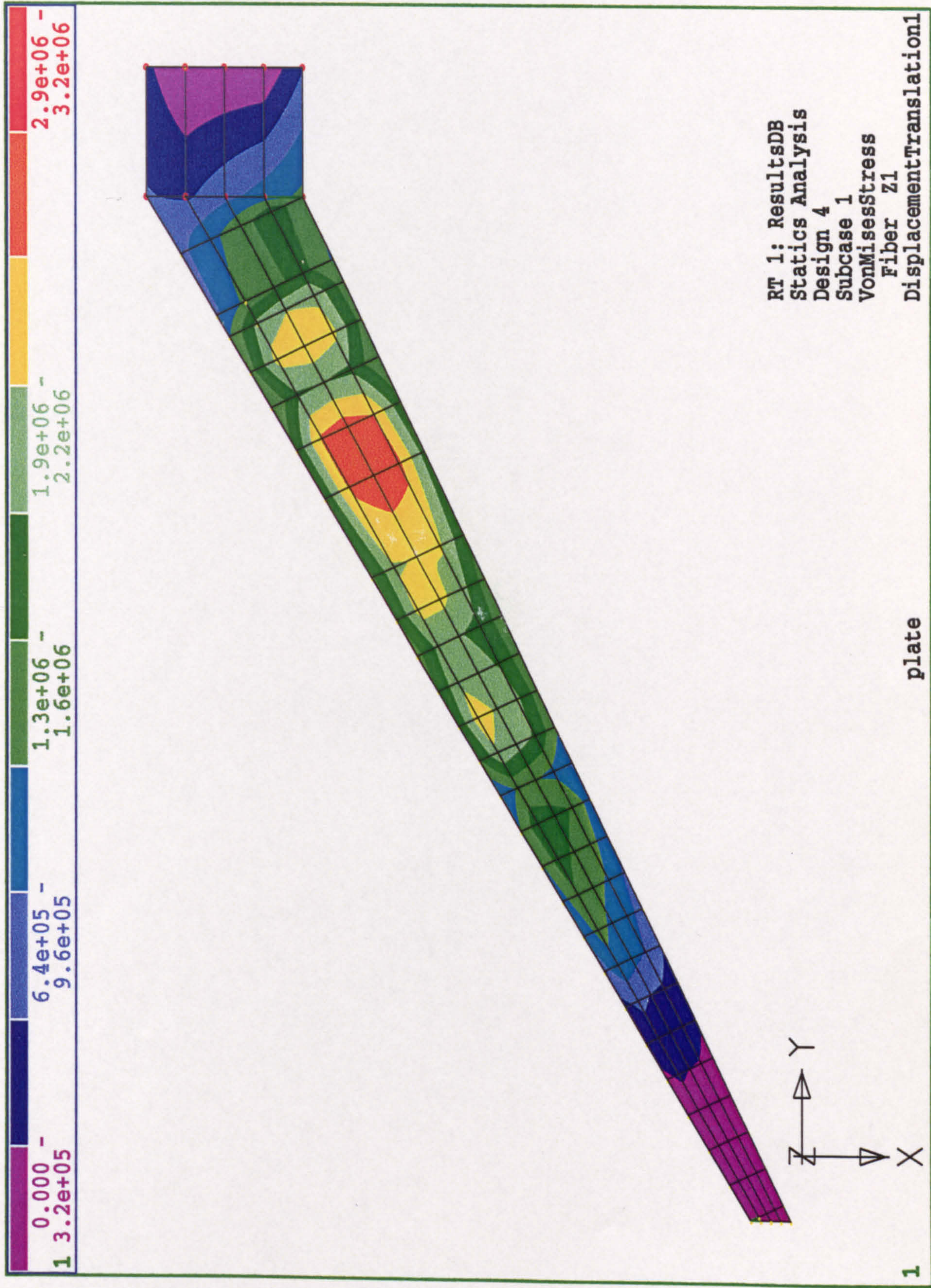


Figure 6.7 Von Misses stress of plate elements



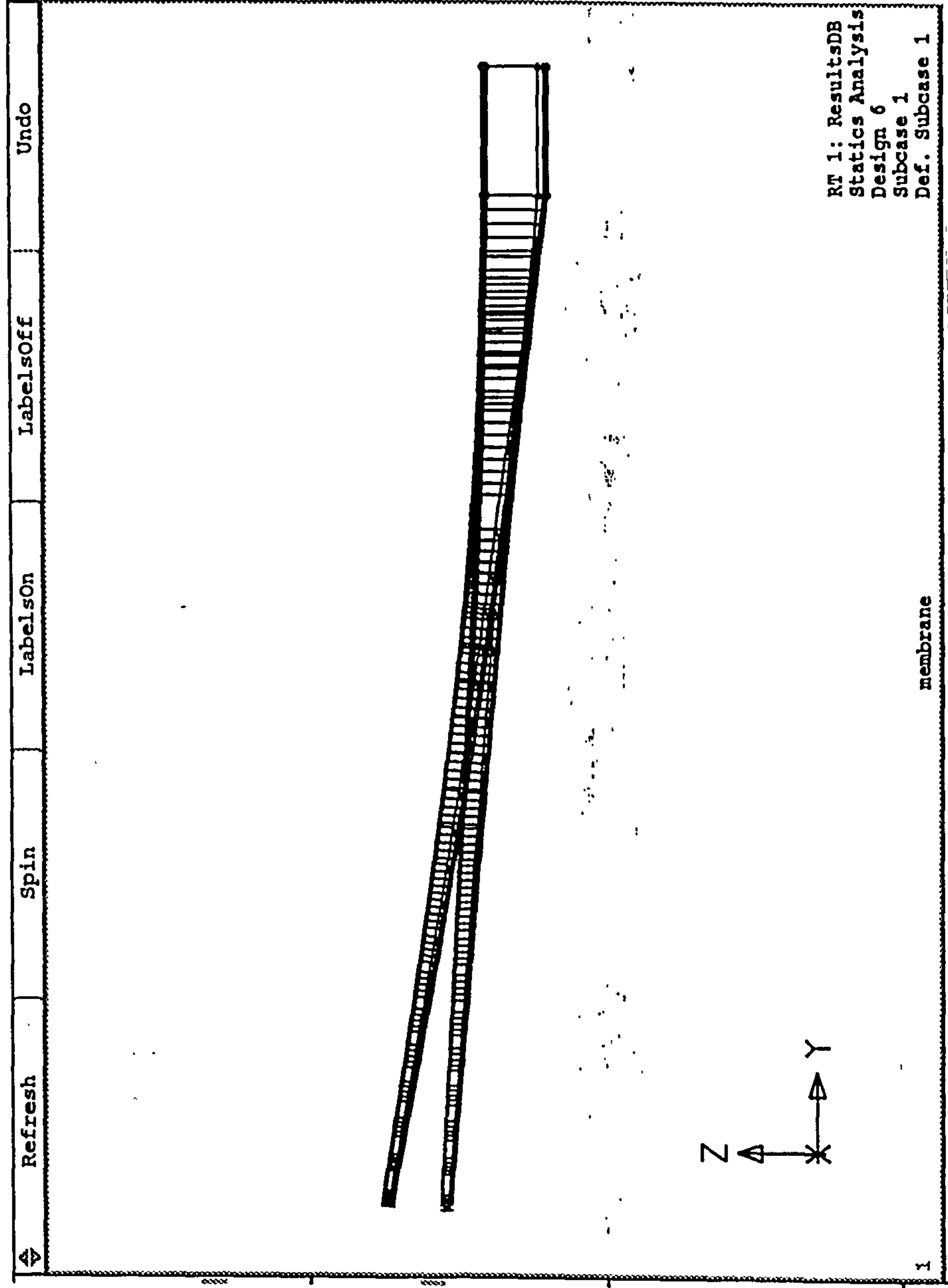


Figure 6.8 Tip deflection of membrane elements



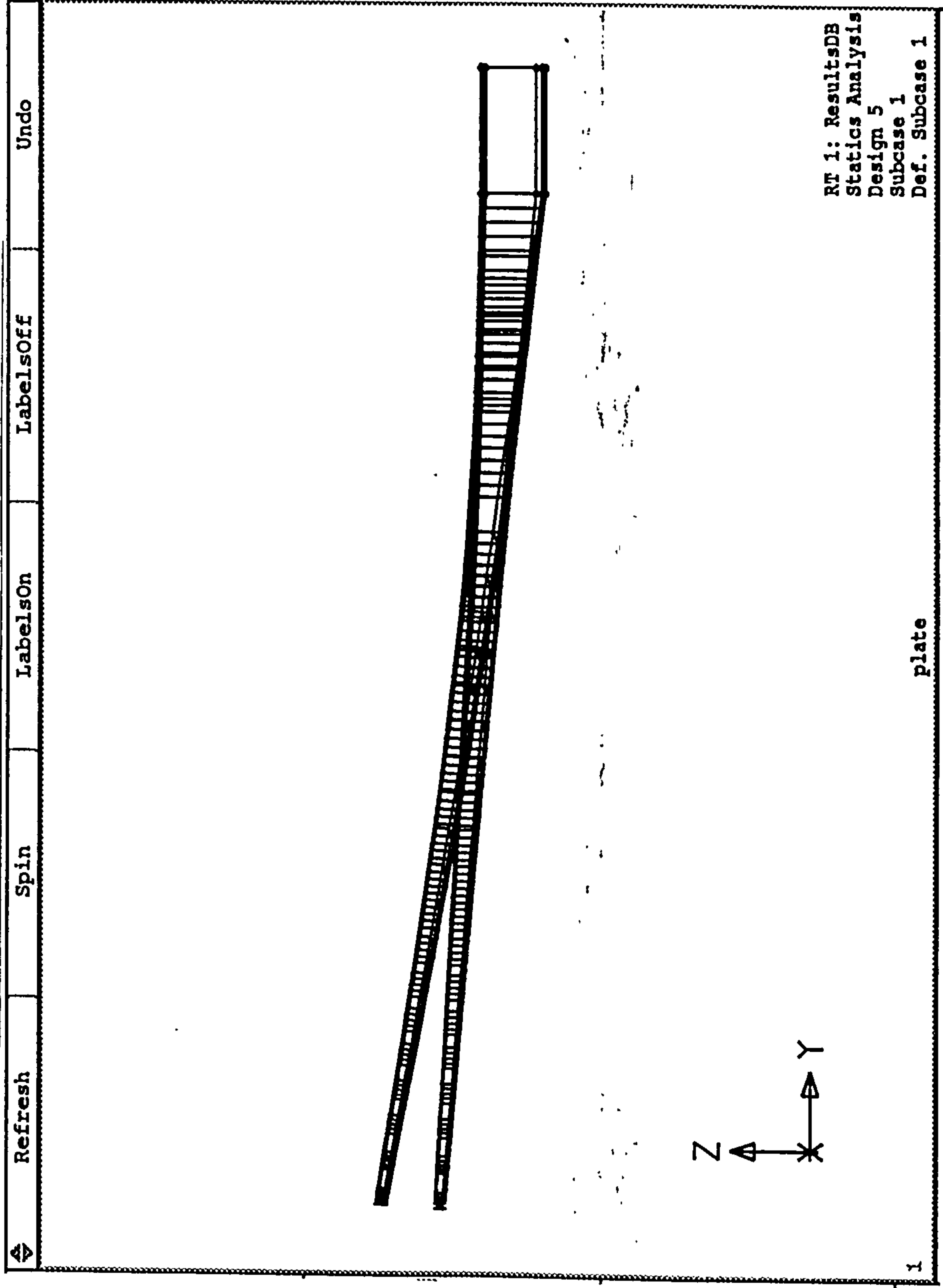


Figure 6.9 Tip deflection of plate elements



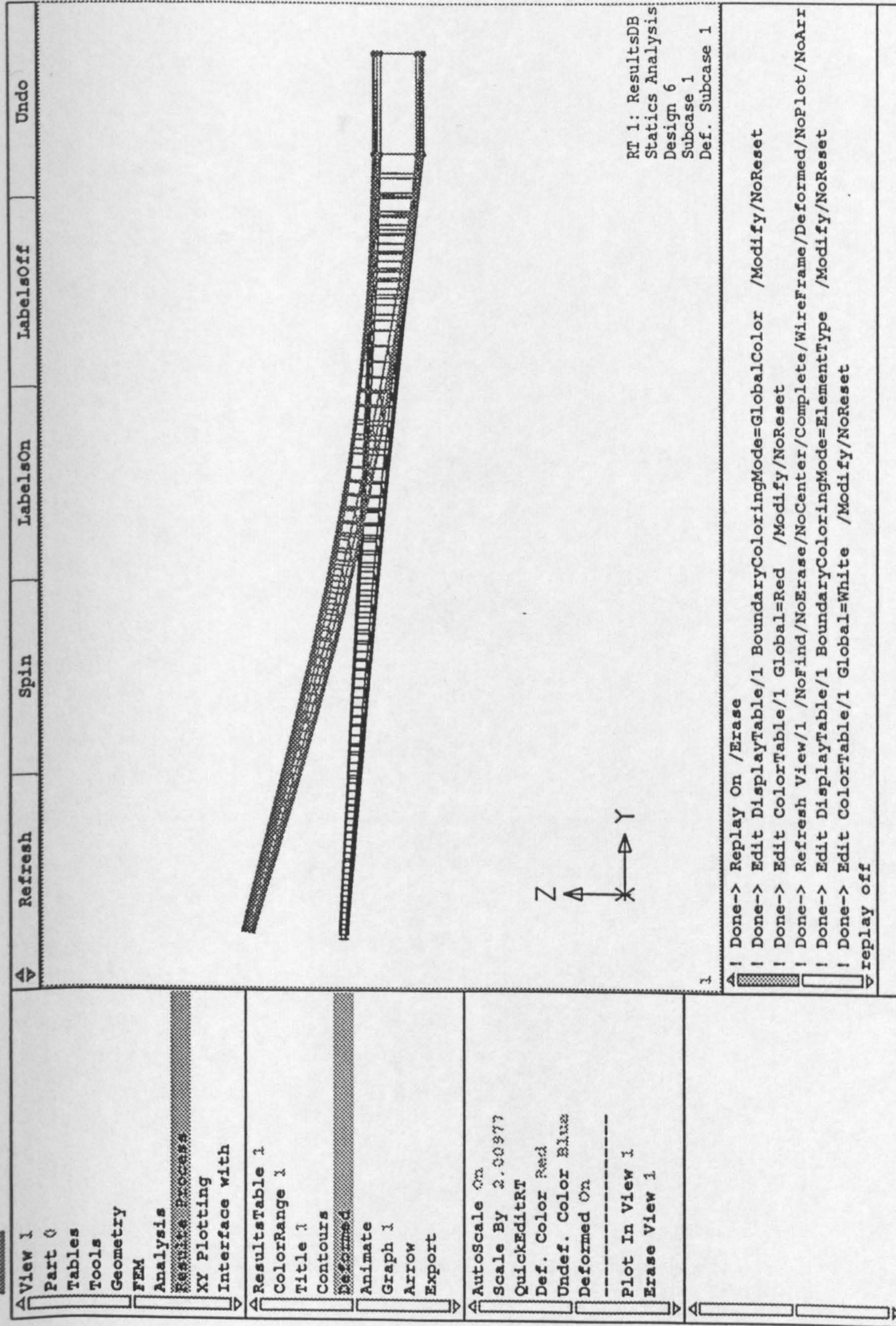


Figure 6.10 Example of NASTRAN model



## 6.4 Fatigue

The increasingly competitive nature of both the operational and manufacturing sides of the aviation business has had effect of making the designer more conscious of the economic characteristics to be built into the aircraft. Fatigue is an important factor in determining both the engineering quality of the product and its potential as a commercial proposition.

The implementation of fatigue criteria into the design will cause incremental manufacturing costs due to the increased weight, additional control of processes, and protective treatments required to ensure the guaranteed life upon which the purchaser insists (Ref. 40). But from the operational point of view, fatigue considerations give direct benefits on the reduction in the amount of maintenance and inspection, delaying of the fail safe repair threshold, and extension of the amortisation period. Benefits from implementation of fatigue consideration outweigh its disadvantages.

The effect of fatigue implications of design requirements in terms of structure weight can be summarised as follows: It is estimated that a structure weight saving of about 11 per cent could be achieved if fatigue were not a consideration. Since the calculation done in the program is only based on ultimate stresses without considering the fatigue case, it is necessary to increase the weight calculated by 11 % (Ref. 40).



The effects of fatigue on the structure weight can be described as follows: If an aircraft is designed without any consideration of airworthiness requirements or fatigue, but is merely capable of sustaining limit aerodynamic loads and also has the capability of carrying the payload a given distance in the necessary environment, this would require a structural weight of the order of 60 percent of the practical design weight. The static ultimate safety factor of 1.5 increases the weight to about 89 percent, the final 11 percent to reach the actual aircraft structural weight is that due to the fatigue life requirements.

The following figure shows the weight build-up plotted against the fatigue life of each stage.

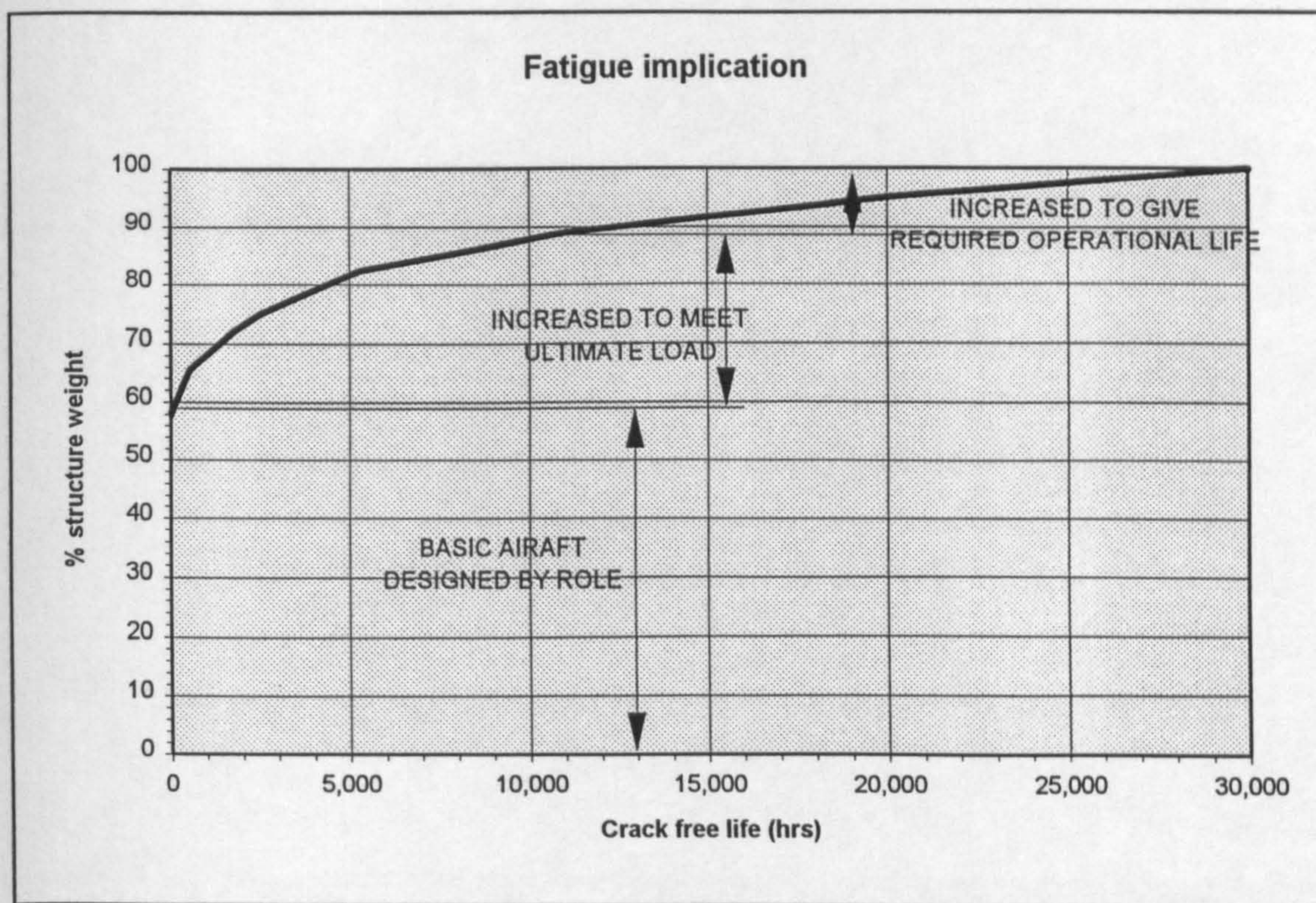


**Figure 6.11 Fatigue implication**



As can be seen from the Fig. 6.11 above, the target of 30,000 hours of crack free life will increase the structure weight by 11 % from a requirement to just meet the ultimate load. The sizing of the structural members of the wing in the iteration process that was used in the project do not include the consideration of fatigue, because of that, the actual total weight of the aircraft will be 11 % heavier than calculated. So, in the analysis process the weight of the wing is considered to be increased by 11 % from the weight calculated by the structure analysis program.

## 6.5 Design Results

As will be shown in Chapter 7, Fig. 7.4, the iterative method usually takes about 3 to 4 iterations to achieve convergence. The first iteration (rigid wing) can be seen to give a large deflection, and it subsequently converges in the next iterations.



# *Chapter 7*



## 7. PROGRAM INTEGRATION METHODOLOGY

### 7.1 Introduction

In this chapter the interface between the various disciplines is explained. A lot of work has been done to integrate the structure module with aerodynamics module. Other modules such as stability and control and the aircraft synthesis program are also explained.

### 7.2 Program Design Philosophy

The design philosophy is to demonstrate that aerodynamics analysis using computational fluid dynamics (CFD) and structures analysis using finite element method (FEM), can be coupled with the aircraft synthesis program in a seamless distributed computing environment. The philosophy used to seamlessly link computational programs such as NASTRAN, SPARV and other programs requires that an interface between the programs be created. It is also the aim to achieve portability.

The programs are designed in several modules where the main program is called INTEGRATE. This is basically the skeleton of the program which does the internal calling the other modules.



### 7.2.1 Portability

As was mentioned before, portability is one of the aims of the project. The meaning of portability is the ability to compile and run the program on more than one type of computer without modification. Based on several experiences from previous students, the Graphical User Interface (GUI) is avoided since it can cause problems for future developments when the target computer is updated.

The task of achieving portability imposed many restrictions on the achievement of user friendliness, as experienced by Murphy (Ref. 43) and Pasaribu (Ref. 9). Murphy dropped the initial aim of portability due to the limited technical capability of the finite element program (LUSAS) that he used.

### 7.2.2 The Target Computer

Although several modules can be compiled and run on a small computer, the target computer depends on the machine that will be needed to run the computational fluid dynamics and the finite element program. Almost every individual module has been tested and proved portable on several platforms, which makes it possible to run the program semi-automatically by running synthesis programs on a personal computer and transferring the data manually in order to run the computational fluid dynamics and the finite element program. The target computer has to fulfil several requirements.



- The target computer must be fast enough to finish running the whole program in a reasonable time. It is the target that this program should finish by 9.00 AM when submitted at 5.00 PM on the previous day.
- The computer must be extensively used in the aerospace industry.
- The computer must be extensively used by PT. IPTN, the sponsor of this project.

Based of the above requirements, it is considered that the SUN workstation can fulfil the requirements and was chosen to be the target computer.

### 7.2.3 The Programming Language

Aiming for portability and using the target computer defined above, effectively cut down the number of programming languages available. It is a fact that until now most engineering application programs are written in FORTRAN. But because of many subsets/version of FORTRAN, the degree of portability is found to be lower than expected.

Other 'new' computer languages are also found to be portable. Surprisingly, although it is relatively new, C++ language is found to be more portable than FORTRAN. It is also widely used, especially with computer programmers, because it can be linked with FORTRAN.



Because of the reasons above, most of the project is programmed using C++ language with some programs written with FORTRAN. This is due to the fact that FORTRAN has a lot of available subroutines.

### 7.3 Design Problem Formulation

The technique to solve the problems of Multi-Disciplinary Design which use available programs is the way to integrate the various modules. Unlike programming from scratch, difficulties are found in preparing the input data. This arises because each module has its own input set. Interfaces are needed in order for the modules to be able to be used seamlessly.

Working with several modules is found to have advantages and disadvantages. One of the disadvantages is that in order for the data from one module to be passed to the other module the data needs to be written to the disk. This slows down the program and requires a large disk space. Writing the data to the hard disk makes it easier to debug. But since NASTRAN and SPARV are only available in the executable forms, it is unavoidable to use the hard disk as a means to pass the data.

The problems of the whole project are tackled by dividing them into several major modules. These major modules are :



- INTEGRATE

This is the outer skeleton of the program. In this module the various modules such as NASTRAN and SPARV are called.

- AIRCRAFT SYNTHESIS

This is an aircraft synthesis program that was developed especially to tackle these problems and take advantage of the computational fluid dynamics and computational structural analysis programs.

- STABILITY & CONTROL

This is the stability and control program which works closely with the aircraft synthesis program.

- PRESPARV

This is the pre-processor of the computational fluid dynamics program of SPARV. It is uniquely programmed to cater for the requirements of SPARV and the main synthesis program.

- SPARV

This is the chosen computational fluid dynamics program.

- POSTSPARV

This module analyses the output result of the CFD program and extracts the data that is needed in order to continue to the next process.



- PRENASTRAN

The pre-processor of NASTRAN. Although NASTRAN has its own pre-processor program, the XL, it is necessary to develop a different pre-processor, since the NASTRAN input is heavily dependent on the results of SPARV.

- NASTRAN

This is the chosen computational structural analysis Program.

- POSTNASTRAN

This module analyses the results of NASTRAN, such as weight and deflection.

These modules are connected to one another by using an intermediate file. The relations can be seen on the next page, Fig. 7.1.



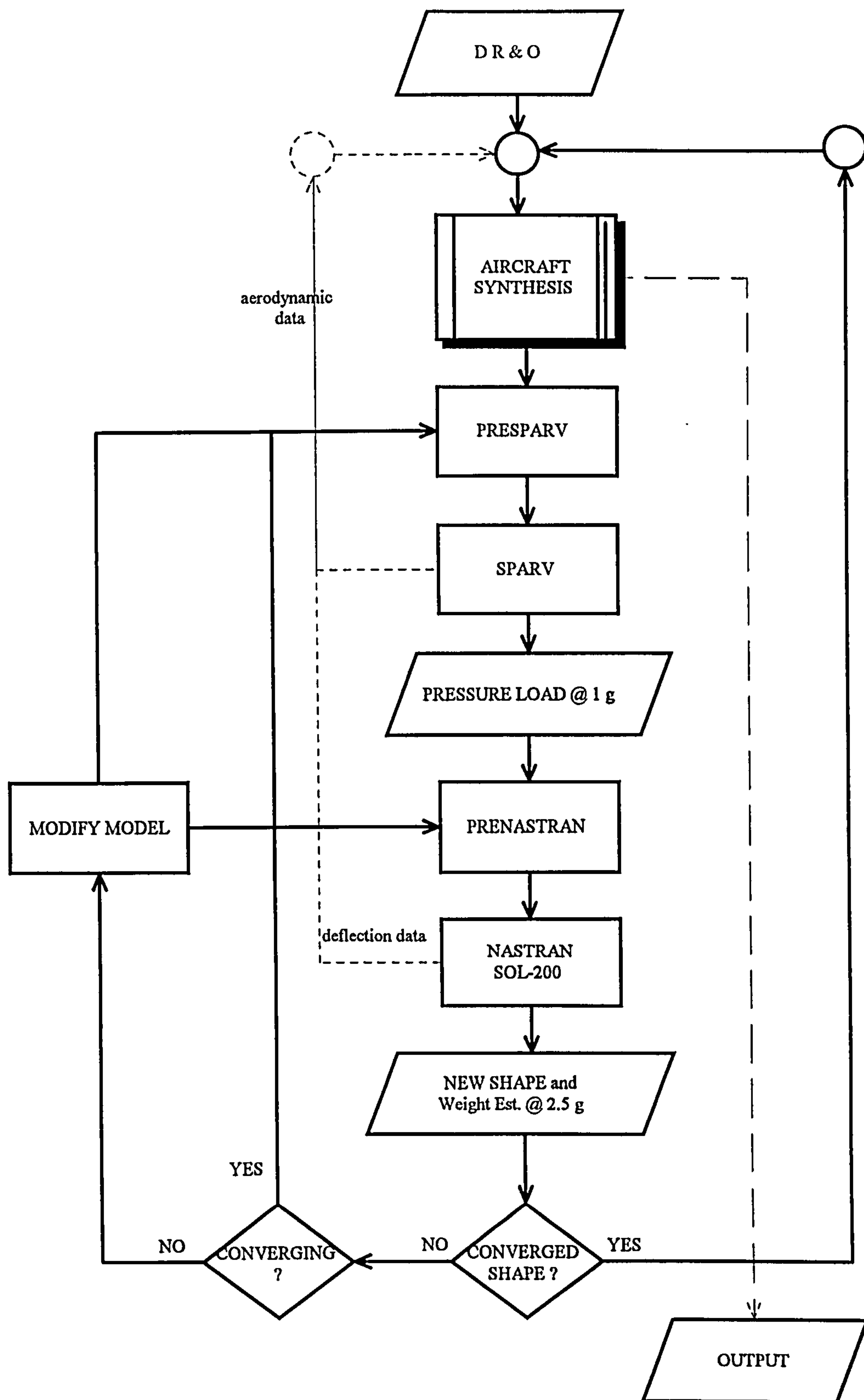


Figure 7.1 Flowchart of the main module



## 7.4 Characteristics of Integration Method

The integration method that was used was by writing the required input data of each module on the appropriate subdirectory and calling the modules one by one. These are done by using intermediate files.

For example in order to run the SPARV module the required input data of SPARV needs to be generated and this is done by the PRESPARV module. The PRESPARV module needs to extract the required information to generate SPARV input data from the results of the AIRCRAFT SYNTHESIS program.

Hard disk space is found to be one of the drawbacks of using this method of solution, especially when some of the computational programs required a huge 'scratch file'.

## 7.5 Data Transfer Techniques

As mentioned earlier, the use of several independent modules requires an intermediate file as a means of data transfer.

The major data transfer required are the airload pressure data from aerodynamics program to the structure and the deformation interface program to transfer the wing geometry deformation from structure to the aerodynamics program. Other transfer data required are considered minor as they only contains small amount of data such as the aerodynamics derivatives from the aerodynamics program.



### 7.5.1 Aircraft Synthesis Data

The program is designed to have an input file that is needed to run the aircraft synthesis module. This data basically contains the design requirements and objectives of the target aircraft. This aircraft synthesis program calls various other programs, such as the stability and control program. The module starts with a semi-empirical calculation but when more accurate data of the computational method is available it uses the improved aerodynamic and structural data.

To be clear, the flowchart of the aircraft synthesis program can be seen in Fig. 7.2.



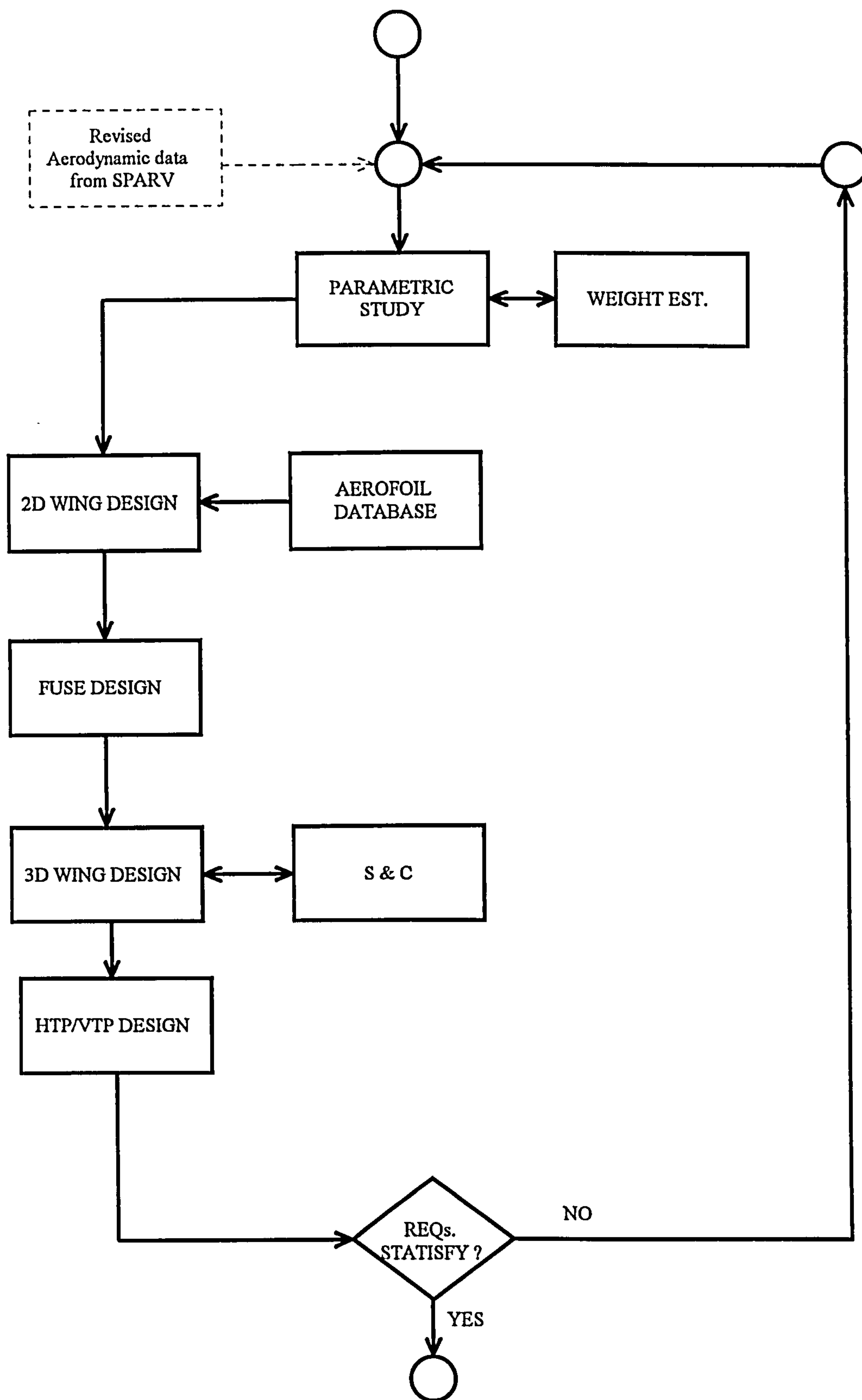


Figure 7.2 Flowchart of aircraft synthesis



### 7.5.2 Stability and Control Data

Stability and control is one of the modules that was used in the aircraft synthesis module. The package used for calculating the stability and control is based on the MITCHELL stability and control program (Ref. 47). This module is called from within the aircraft synthesis module internally by using 'system' call.

### 7.5.3 Pressure Load Data

The computational fluid dynamics program SPARV produces airloads in the form of pressures on each panel. The computational structure analysis program requires that this air pressure be applied to the membrane elements. Due to the different panel modelling between SPARV and NASTRAN, pressure loads from SPARV need to be interpolated in order to find the correct pressure in the grid point of NASTRAN. These pressure loads must be interpolated linearly or bilinearly into a concentrated load to be applied to the NASTRAN grid point.

The pressure point in NASTRAN needs to be applied on the element where the pressure is applied. This means that each grid point in the skin of the wing of the NASTRAN model needs to have a pressure definition. It is much simpler if the pressure can be applied on the skin itself (not on the grid point). But this is not allowed in NASTRAN. The only solution is to calculate the pressure at the nearest grid point. This has to be done by interpolating the pressure from SPARV. There are some disadvantages of using this



method. Pressure applied on the structure model may not be the actual pressure on the real aircraft, but because the number of panels on both NASTRAN and SPARV is considered rather high, the interpolation can be assumed to give an accurate result. Study of the number of panels, as can be seen from previous chapter, shows that this is so. The accuracy of the interpolation results depend on the number of meshes and the size of mesh of both programs.

This procedure is done automatically by using the PRENASTRAN module. POSTSPARV/PRENASTRAN converts the pressure information from SPARV results and interpolates them to find the correct pressure to be applied to the structure member.

#### 7.5.4 Deflection / Deformation Data

One of the modules that was used in the program is the POSTNASTRAN module. The main task of this module is to convert and analyse the results of NASTRAN and using PRESPARV generates the panel for the computational fluid dynamics SPARV. This module needs to interpolate the NASTRAN results. This is done by using linear or bilinear interpolation technique.

### **7.6 Interface Program**

The interface program is needed in order to run the whole program. The interface job basically is to convert the data from one module to the form that the next module can



understand. This is the only solution because SPARV and NASTRAN input formats cannot be changed.

#### 7.6.1 Pressure Load Interface

The interface between SPARV and NASTRAN is needed as a form of pressure load interface. This interface converts the output of SPARV to the form accepted by NASTRAN. This is done by interpolation. As can be seen from Fig. 7.3 below, the panels of NASTRAN and SPARV are not the same. The major difference is that the aerodynamic panels are streamwise and the structural panels are perpendicular to the rear spar.

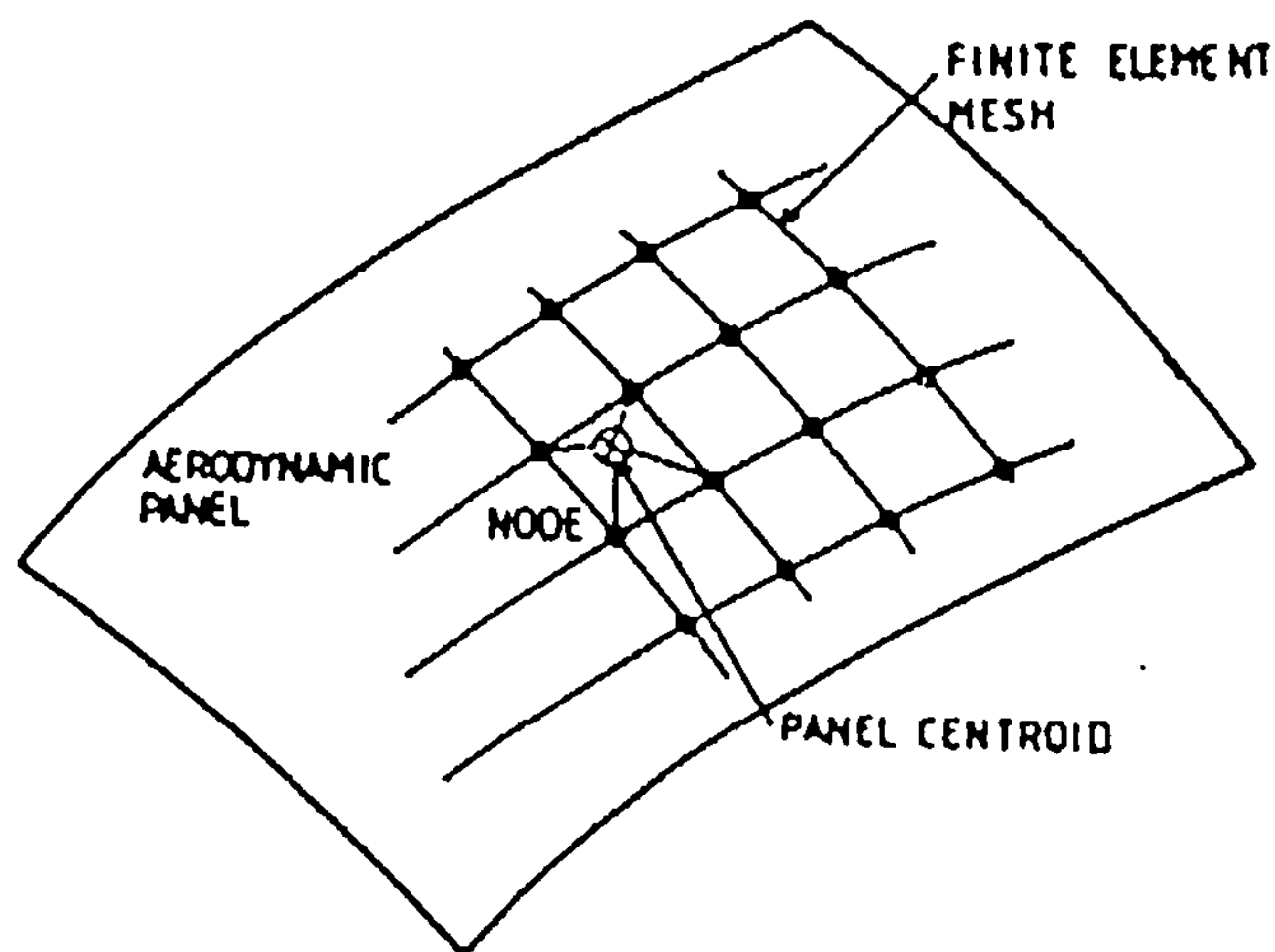


**Figure 7.3      Aerodynamic and Structural panel**

The aerodynamics program gives a pressure load at the middle of the panel. This pressure load along with 3 other pressure points needs to be interpolated to extract a pressure at one Structural point. This is done by using bilinear interpolation. The reason for using linear



interpolation is one of simplicity and due to the small panels used in the aerodynamics calculation, linear interpolation is assumed to be adequate. An example of both aerodynamic and structure panels used on the wing can be seen in Fig. 7.7.

#### 7.6.2 Deflection / Deformation Interface

The interface needed for the deflection is almost the same as the previous interpolation, the structure program gives a deflection at a structural point and the needs to be interpolated to give the deflection at a specific aerodynamic point.

This is done by using bilinear interpolation too. The number of panels used makes it unnecessary to use other form of interpolation.

### **7.7 Static Aeroelasticity Analysis**

Static aeroelastic effects happen when the aerodynamic forces of the wing deflect the flexible wing, which will changes the pressure load / forces of the wing until it comes to a steady state. The solution to this problem assumes that the system comes to a state of static (or quasi-static) equilibrium. Basically there are two methods of analysis for this problem of static aeroelasticity : direct solution and iterative solution.



### 7.7.1 Direct Solution

MSC NASTRAN Static Aeroelastic Analysis uses a direct method to determine the quasi-static condition. The structural load distribution on an elastic aeroplane in the trimmed flight condition is determined by solving the equation for static equilibrium (Ref.41).

Matrices of aerodynamic influence coefficients are computed from data describing the geometry of the aerodynamic finite elements. The choice of aerodynamic grid points for the aerodynamic model is independent of the location of the structural grid points. The analysis at subsonic speed utilises the Vortex-Lattice aerodynamic theory (i.e. the steady case of Doublet-Lattice Method).

The aerodynamic modelling in MSC NASTRAN is done by using Doublet-Lattice panels, which are idealised as planes parallel to the flow. This limitation of the inability to model the wing aerofoil is one of the reasons for not using this module. Instead the computational fluid dynamic program of SPARV is used together with the NASTRAN Computational Structural Analysis. This MSC NASTRAN aeroelastic module is compatible with the general structural capability, but it is not designed for use with other special capabilities such as structural optimisation.

### 7.7.2 Iterative Analysis

The iterative solution of static aeroelasticity is done by first calculating the pressure load from the assumed rigid



shape, then the pressure load is used in the structural analysis program to calculate first elastic shape. This elastic shape is then input to the aerodynamic program to extract the new pressure load. This pressure load is then input to the structure program and so on. This iteration is done until the shape and pressure load are consistent.

This iterative method of static aeroelasticity consumes much more time than the rigid analysis and time is a very important factor to be considered.

### 7.7.3 MODIFY module

The criterion of a converged wing used in the program is when the difference between the tip deflection of current iteration to the previous iteration is small. The program will compare the tip deflections and decide whether to run the next iteration or not. Studies have been performed and it is found that almost all the wings designed by the aircraft synthesis module will converge within four iterations.

Although during the case studies and program testing the wing which was designed by the aircraft synthesis module was always found to converge, it is believed that there is a possibility that the wing will not converge in the static aeroelastic study of the wing. In order to solve this problem a module to be able to modify the model is introduced. This module is called the MODIFY module. The relation between this module and the rest of the program can be seen in Fig. 7.1. This module is able to detect when



the static aeroelastic constraints have been violated and is able to provide the user with a solution to this problem.

Study has been performed in order to provide NASTRAN SOL-200 optimiser with a set of new constraints in order to achieve a converge wing. By limiting the maximum tip deflection of the wing, this new constraint will increase the bending stiffness and torsional stiffness of the wing.

Study also has been performed on how to detect the instability of the wing and how to limit the tip deflection and by how much.

In order to study this, two wings have been designed where one wing is a converged wing and the other is a diverged wing. Those two wings can be seen on Table 7.1.

**Table 7.1 Divergence study**

	WING A (CONVERGED)	WING B (DIVERGED)
sweep angle	30°	33°
AR	10.4	13.2
span	163 ft	178 ft
thickness	16.4 %	13.5 %
ratio at root		

WING A is generated by using the normal program and it was found that the wing deflection converged. On the other hand WING B is designed by relaxing several constraints in the aircraft synthesis module and forced to select a particular



sweep angle. It is found that in normal case for this type of aircraft (high subsonic aircraft), all wings are found to converge. The difficulties found when relaxing constraints in the aircraft synthesis module in order to achieved a diverged wing, proved that it is very unusual to find a diverged wing in this type of aircraft.

The results of static-aeroelastic study on WING A can be seen on Fig 7.4, and the summary of the results can be found in Table 7.2 below.

Table 7.2 Converged wing (WING A) study

iteration	twist at wing tip	tip deflection
1.	6.8°	7.6 ft
2.	-5.1°	-6.8 ft
3.	4.0°	5.2 ft
4.	3.9°	5.2 ft

As can be seen from Table 7.2, the wing is assumed converged at the fourth iteration because it fulfils the criteria set earlier regarding the tip deflection, the difference of less than 0.1 ft of the tip deflection and less than 0.1 degree of twist angle from the previous iteration are assumed converged.

Study on the diverged wing (WING B) can be seen on Fig. 7.5 and the summary can be seen from Table 7.3 below.



Table 7.3 Diverged Wing (WING B) study

iteration	twist at wing tip	tip deflection
1.	4.1°	6.9 ft
2.	-2.1°	-1.9 ft
3.	6.1°	10.3 ft
4.	-6.0°	-9.1 ft

As can be seen from Table 7.3, after the fourth iteration the wing is not yet converged thus it assumed diverged. The assumption is made at the fourth iteration because of the time elapsed constraint. The target of 16 hours elapsed time (from 5 PM to 9 AM) restricts the maximum number of iteration to four.

Analysing the results of both wings, it can be concluded that the maximum tip deflection and the wing tip twist angle cannot be used as a guidance whether the wing will converge or not. WING A, which has a tip deflection of 7.6 ft in the first iteration, is a converged wing, on the other hand WING B which has smaller tip deflection of 6.9 ft is a diverged wing. The comparison of the wing tip deflection is done by taking into consideration the span of the wing also.

The twist at the wing tip at the first iteration is also found not relate to the convergence of the converged wing. WING A has a twist of 6.8° and the diverged wing of WING B has a smaller twist angle of 4.1°.

As mentioned in Ref. 33, the criteria that effect the wing aeroelasticity are AR, thickness ratio, sweep angle, and



design diving speed. Because of that reason, knowing the tip deflection and twist of the wing on the first iteration can not predict whether the wing will converge or not. Another method has to be found in order to use the optimisation routine in NASTRAN to develop a converged wing.

In order to solve the problems mentioned earlier, a subroutine MODIFY.EXE is developed to analyse the static-aeroelastic iterations of the wing and to generate new constraints in the NASTRAN optimiser. This module is executed when wing convergence has not been achieved. The module starts by analysing the whole iterations process and after studying the tip deflection and wing twist, the module sets new constraints for the NASTRAN optimiser. This new set is a new limitation of the maximum the wing tip can be twisted and/or deflected. The methods used in the MODIFY module can be seen in the flowchart in Fig. 7.6.

Tip deflection limitation is set to the NASTRAN model in order to increase the stiffness of the wing and to achieve a converged wing. The tip limitation is searched manually. The first try is to set the maximum tip deflection to 0.618 of the maximum deflection. On the next run, the tip limit is set at  $0.618 \times \text{previous deflection}$  or the tip limit is increased by  $0.618 \times (0.382 \times \text{max. deflection})$ . This line search is done manually until a converged wing is achieved.

Study on a converged wing revealed that maximum tip deflection constraints in the NASTRAN SOL-200 model can be used to achieved a converged wing from an initially



diverged wing when there is no tip limit constraints. The study can be seen in Table 7.4 below.

Table 7.4 Results of tip limitation

No tip limitation

iteration	twist at wing tip	tip deflection	weight (lbs)
1.	5.7°	9.4 ft	10,510
2.	-11.9°	-18.6 ft	3,580
3.	7.5°	12.2 ft	24,410
4.	-7.1°	-10.7 ft	8,700

tip limit =  $0.618 * 9.4 \text{ ft} = 5.8 \text{ ft}$

iteration	twist at wing tip	tip deflection	weight (lbs)
1.	3.2°	5.7 ft	12,270
2.	2.5°	5.3 ft	12,840
3.	3.3°	5.7 ft	14,520
4.	1.1°	3.2 ft	12,140

tip limit =  $0.618 * 0.618 * 9.4 \text{ ft} = 3.6 \text{ ft}$

iteration	twist at wing tip	tip deflection	weight (lbs)
1.	2.1°	3.5 ft	18,520
2.	2.0°	3.5 ft	17,250
3.	2.1°	3.5 ft	18,950
4.	2.0°	3.5 ft	16,520

tip limit = 5.0 ft

iteration	twist at wing tip	tip deflection	weight (lbs)
1.	2.5°	4.9 ft	13,700
2.	2.6°	4.9 ft	13,370
3.	2.8°	4.9 ft	13,100
4.	2.0°	4.9 ft	12,180

As can be seen from Table 7.4 above, the wing is found converged at the tip limit set at  $0.618 * 0.618 * \text{maximum deflection}$  or 38% of the maximum deflection of the diverged wing. This methods of limiting the maximum tip deflection



is introduced in the MODIFY module and use to increased the stiffness of the diverged wing in order to find a solution of a converged wing.

Study also has been done to put a deflection limit at the engine location. It is found that limiting the deflection limit at the engine location gives similar results with setting up the limitation on tip deflection. Due to the larger deflection on the tip deflection, it is easier to work on maximum tip deflection.

Study has also been done on limiting the twist at the wing tip. This is done by setting a different deflection limit on front spar and rear spar of the wing. But this is not pure torsional limit on the wing but actually both bending and torsional limit. The inability of NASTRAN SOL-200 to optimise based on torsional limit only makes it impossible to study of just limiting the wing twist only. It is believed that in other structural optimisation packages the ability to work on torsional limit only is available and a similar method explained before on the bending limit can be applied.

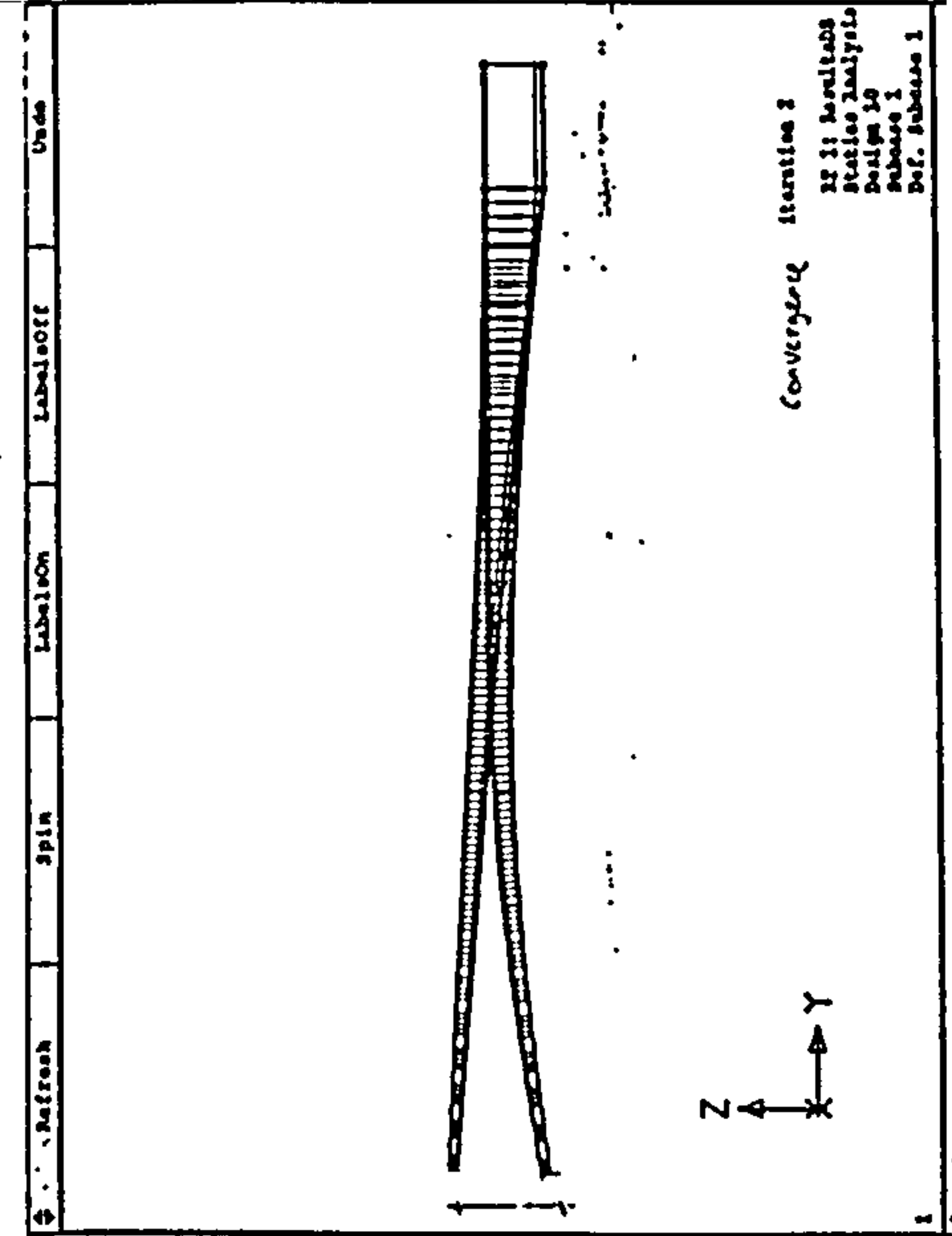
the MODIFY module works by setting new displacement constraints in the DRESP1 (response ID) and DCONSTR (constraint) card of NASTRAN optimiser. As can be seen in Table 7.5, the new constraints are ID 21 and ID 22 (DZ1 and DZ2). These constraints are given to the node 1 and 38 which in this example data are the tip front and rear spar.



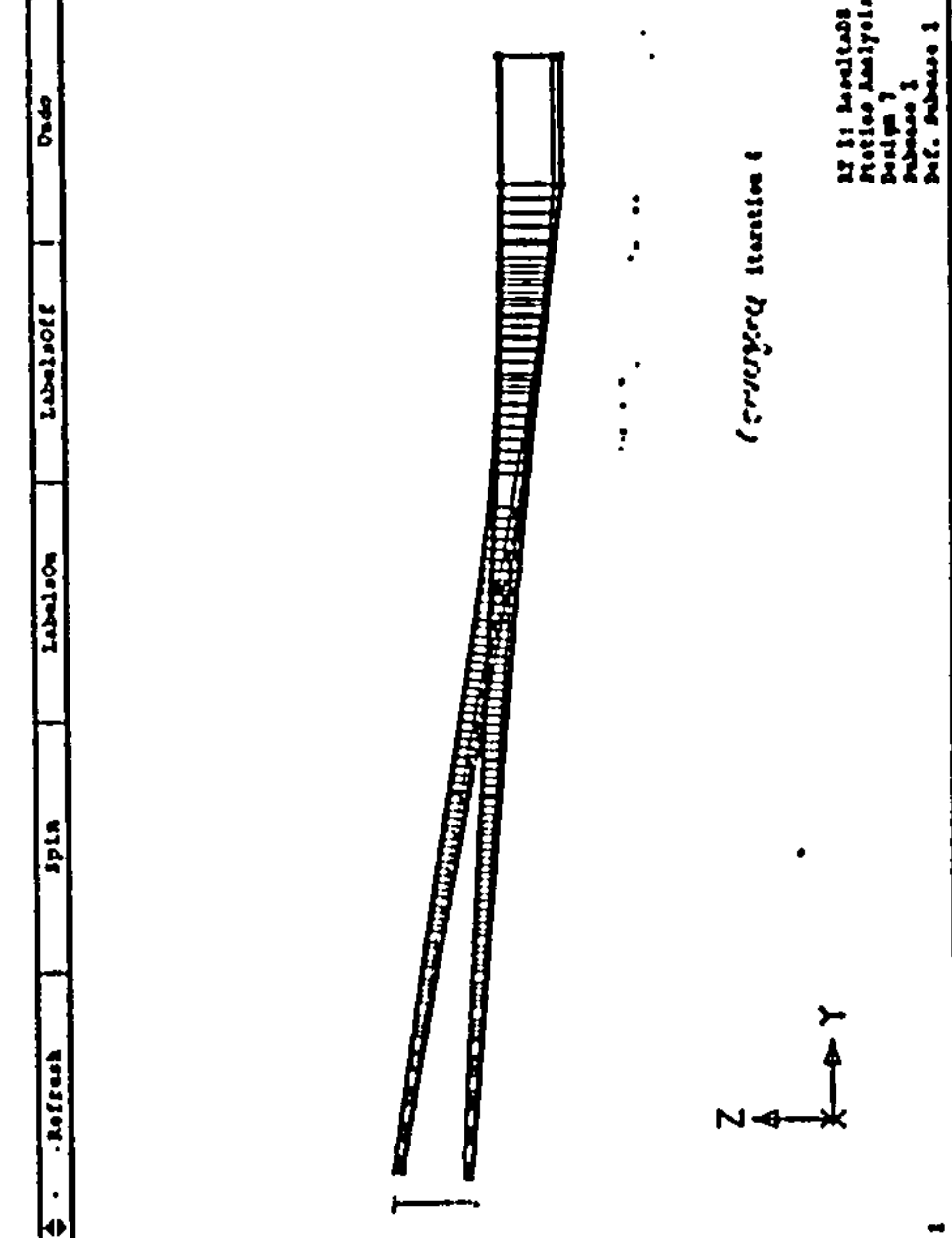
Table 7.5 Displacement Constraint

```
$ STRUCTURAL RESPONSE IDENTIFICATION
$23456781234567812345678123456781234567812345678123456781234
$
DRESP1 20      W      WEIGHT
DRESP1 21      DZ1     DISP              1              1
DRESP1 22      DZ2     DISP              2             38
DRESP1 23      S1      STRESS  PSHELL     2              1
DRESP1 24      S1      STRESS  PSHELL     2              2
DRESP1 25      S1      STRESS  PSHELL     2              3
$
$ CONSTRAINTS
$
$2345678123456781234567812345678123456
$
DCONSTR 21      ALL      -7.0    7.0
DCONSTR 22      ALL      -6.5    6.5
DCONSTR 23      ALL      -15000. 20000.0
DCONSTR 24      ALL      -15000. 20000.0
DCONSTR 25      ALL      -15000. 20000.0
```

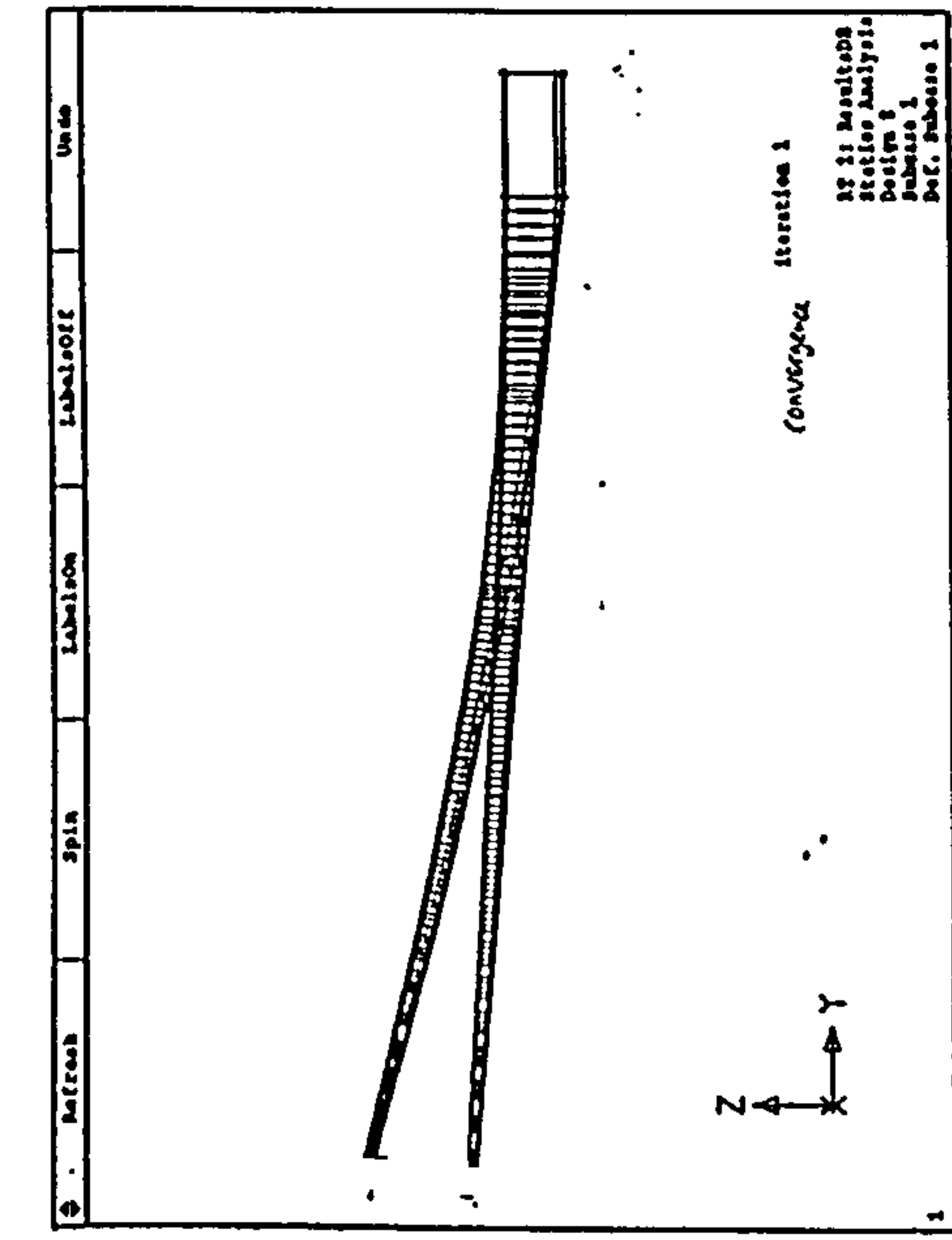




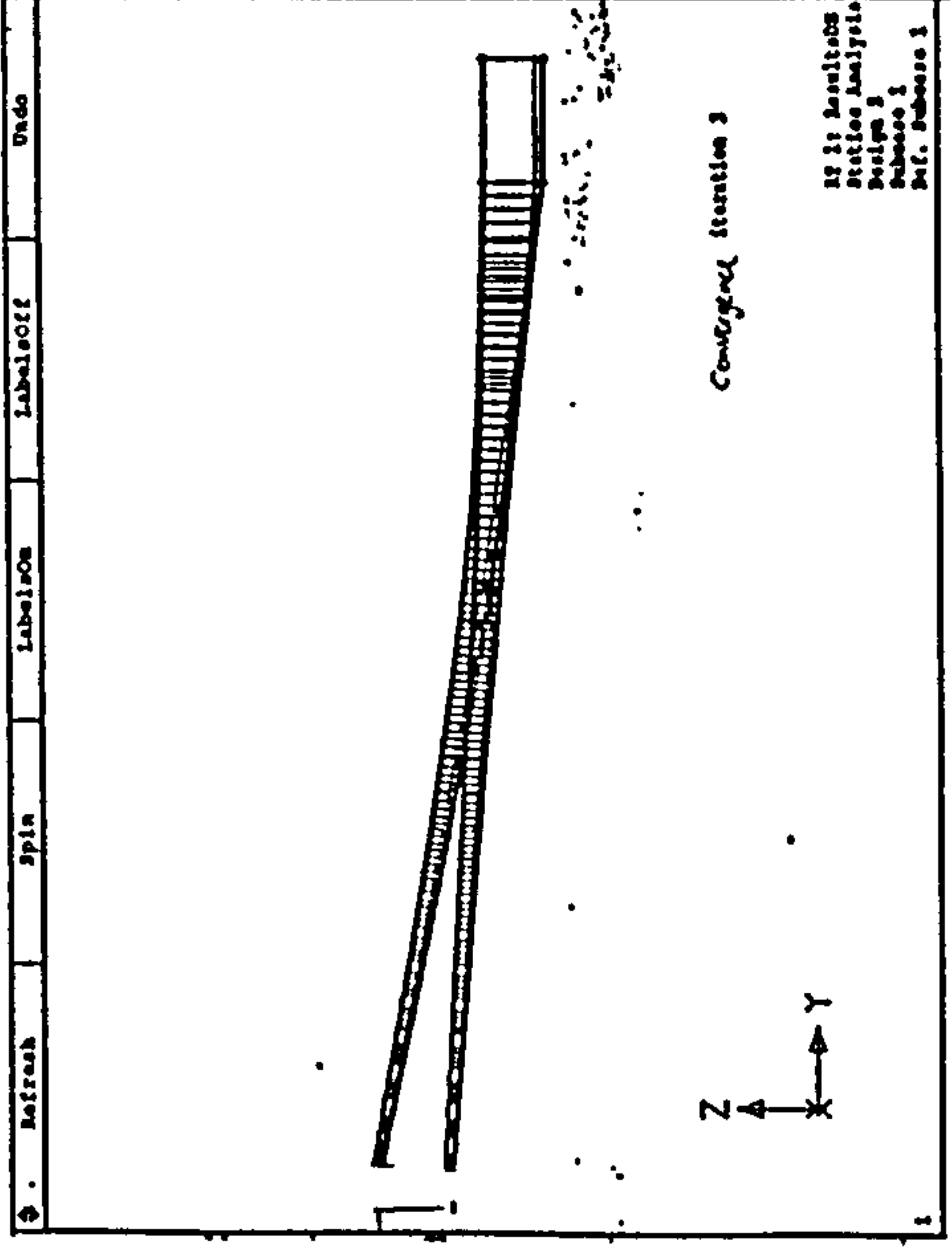
iteration 1



iteration 2



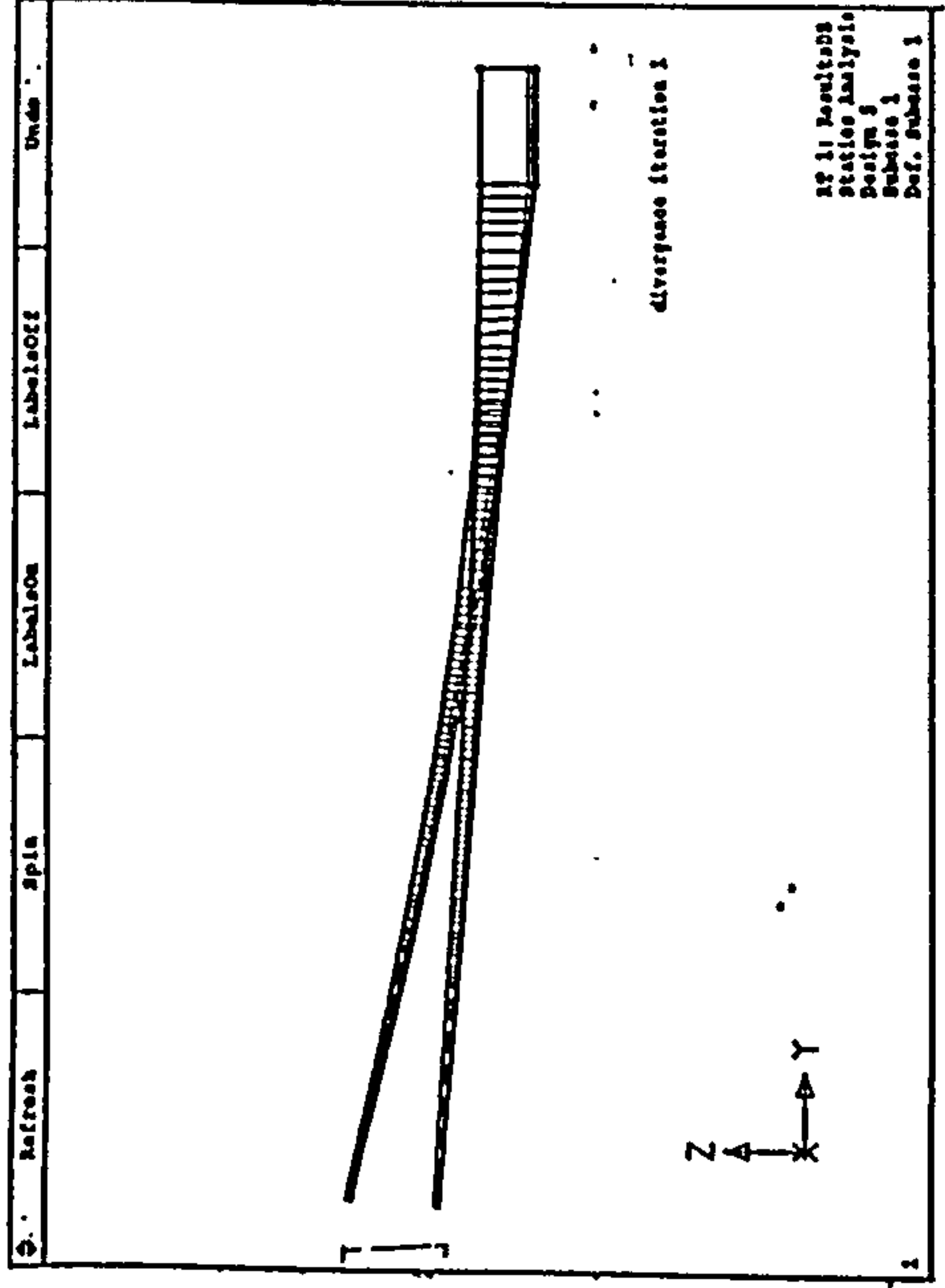
iteration 3



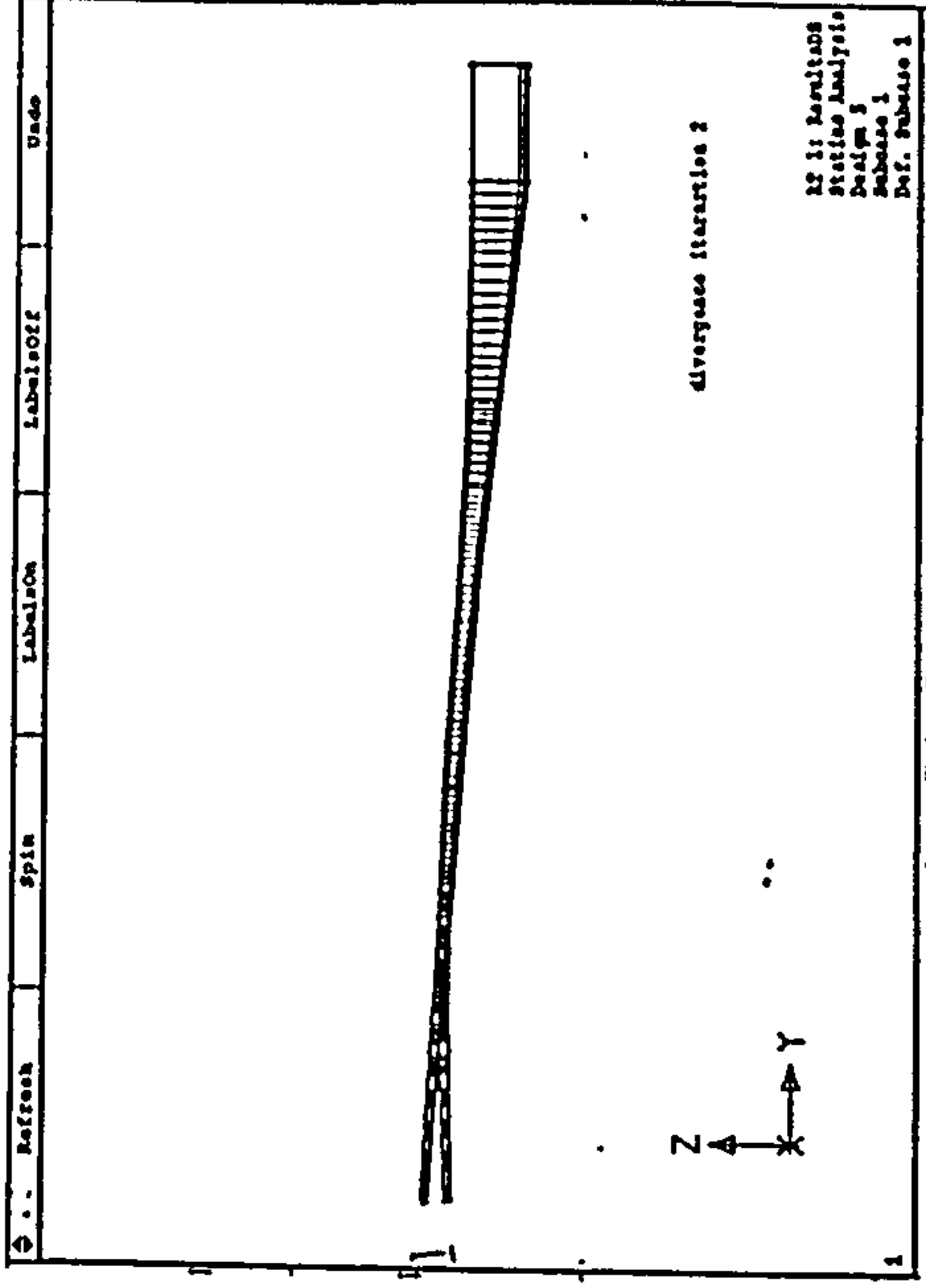
iteration 4

Figure 7.4 Converged wing (WING A)

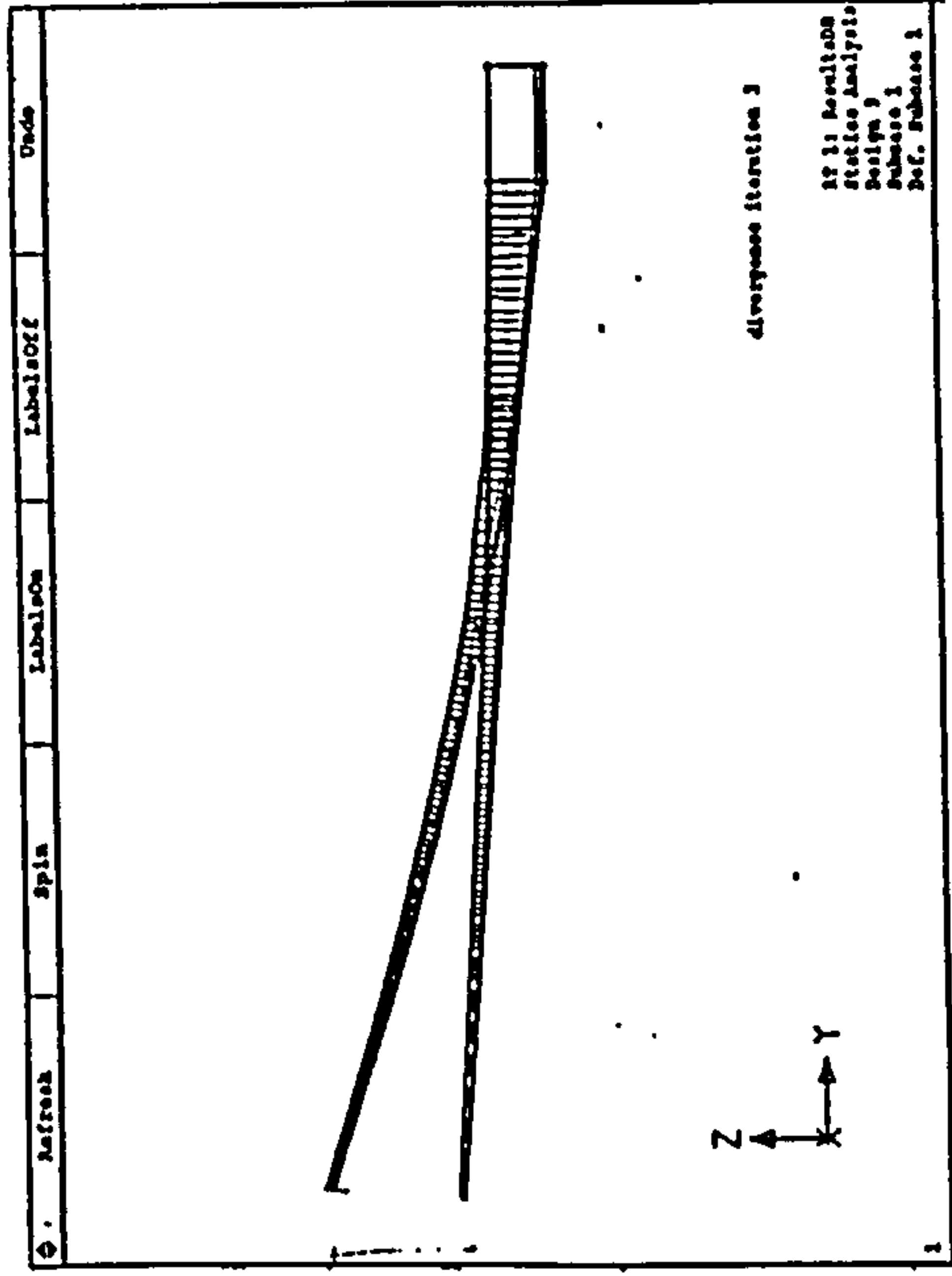




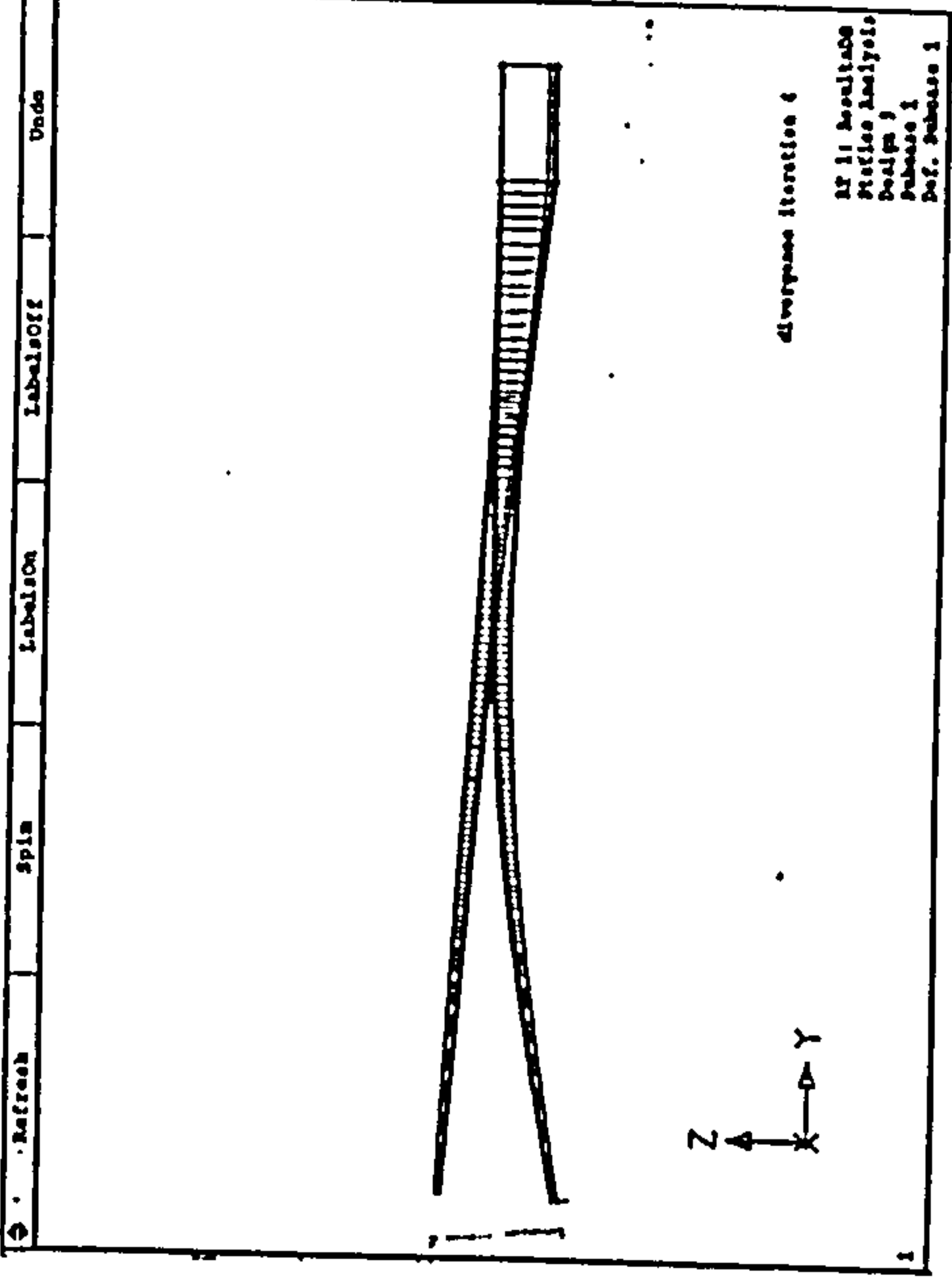
iteration 1



iteration 2



iteration 3



iteration 4

Figure 7.5 Diverged wing (WING B) study



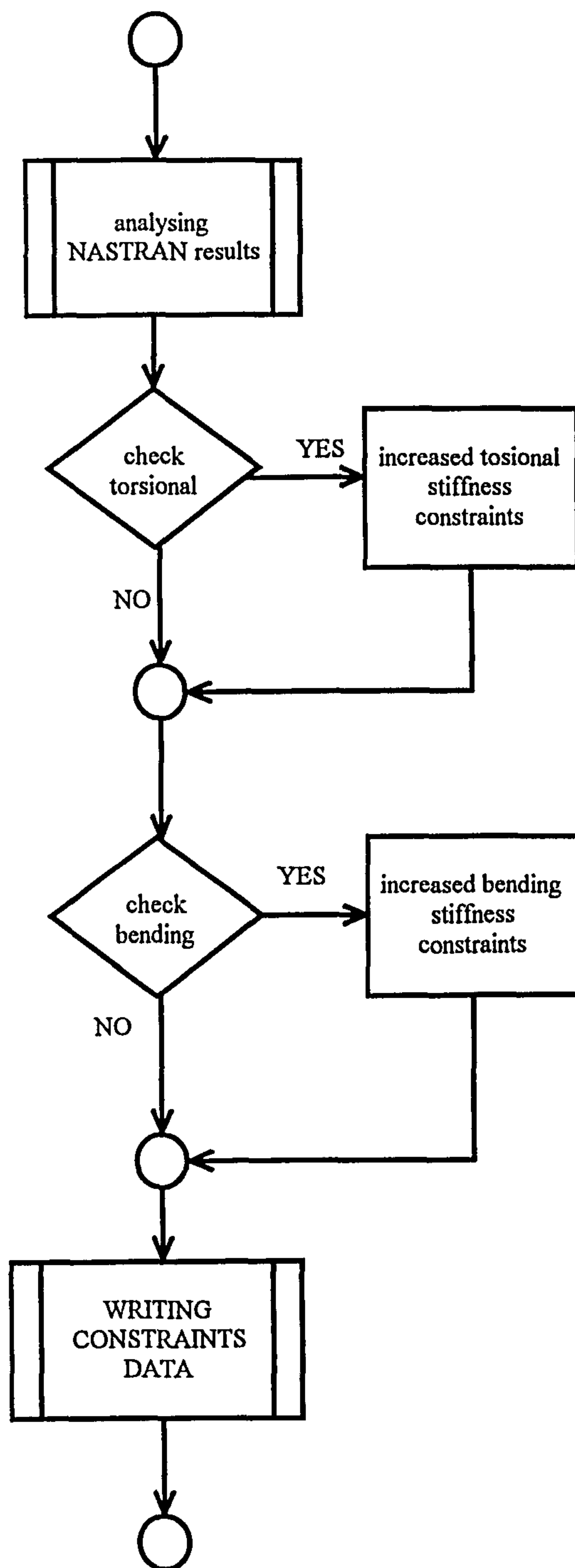


Figure 7.6 Flowchart of MODIFY module



## 7.8 Convergence and Optimality

After studying the effect of flexibility on the iteration process of static aeroelasticity, it is found that 4 iterations give a convergence result. Although a pre-set difference value of deflection is assumed to be more correct, the iteration is set to 4 in order to decrease the number of iterations and the time consumed.

As can be seen from Fig. 7.8, 4 iteration is assumed enough and acceptable for this project.



# aerodynamic and finite element panel

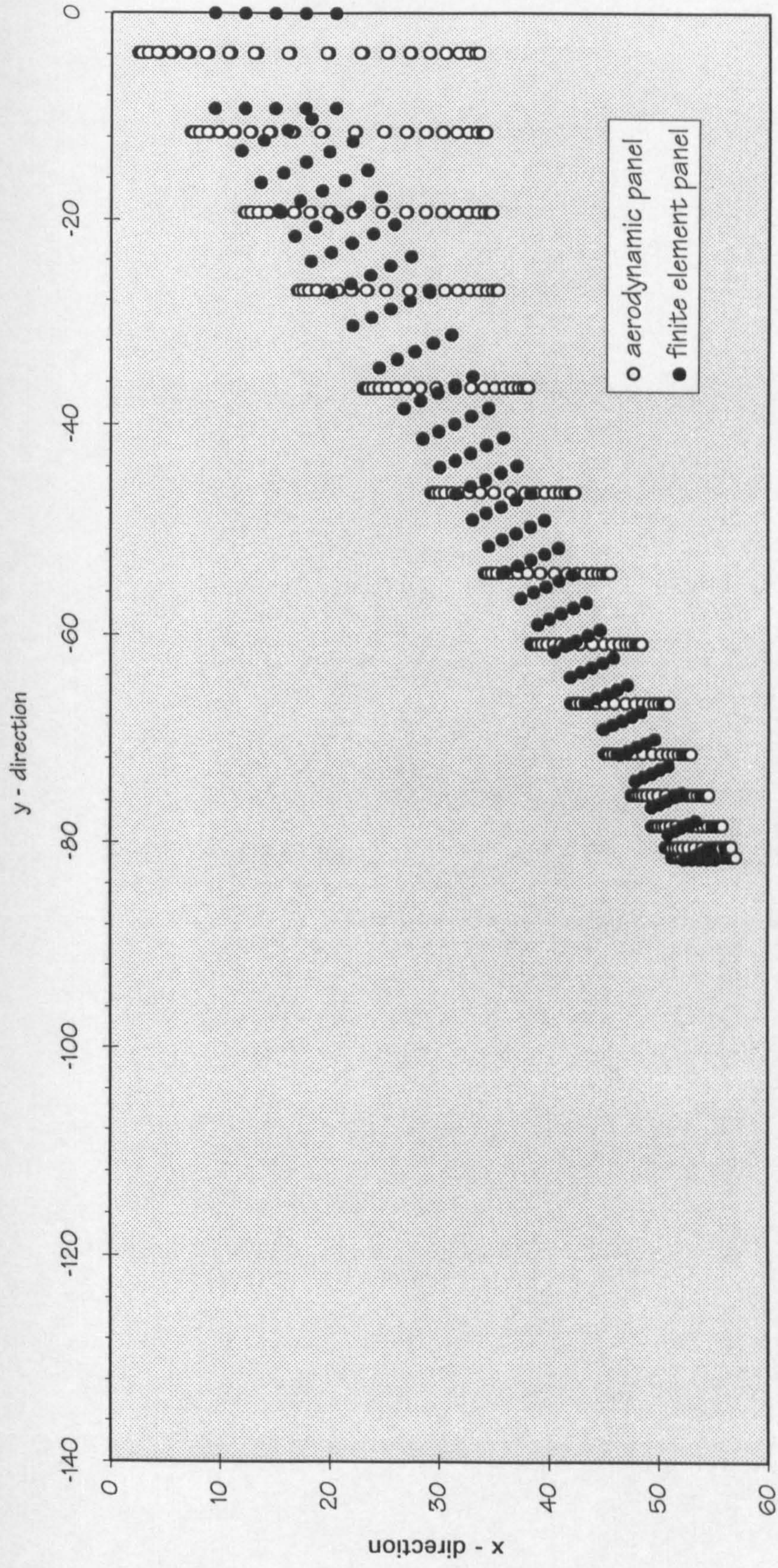


Figure 7.7 aerodynamic and finite element panel



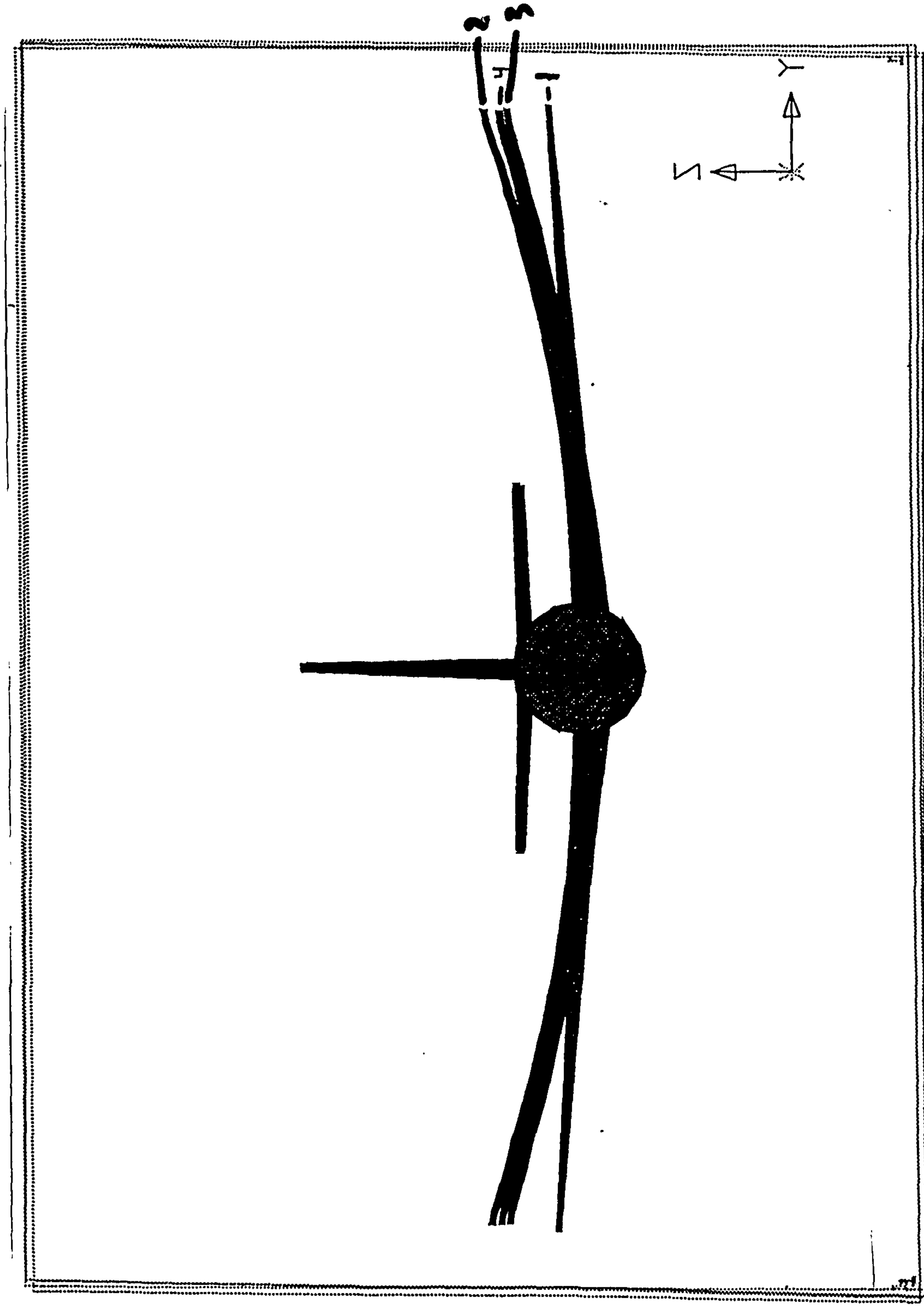


Figure 7.8 Wing Convergence



## 7.9 Twist Optimisation

One of the benefit of calculating the spanload distribution is that the wing twist to achieve a near elliptic pressure distribution in order to reduce lift dependent drag, can be evaluated.

On the next page, the effect of original twist and the final twist is compared, Fig. 7.9.



# Non-Dim. - Spanwise Distribution

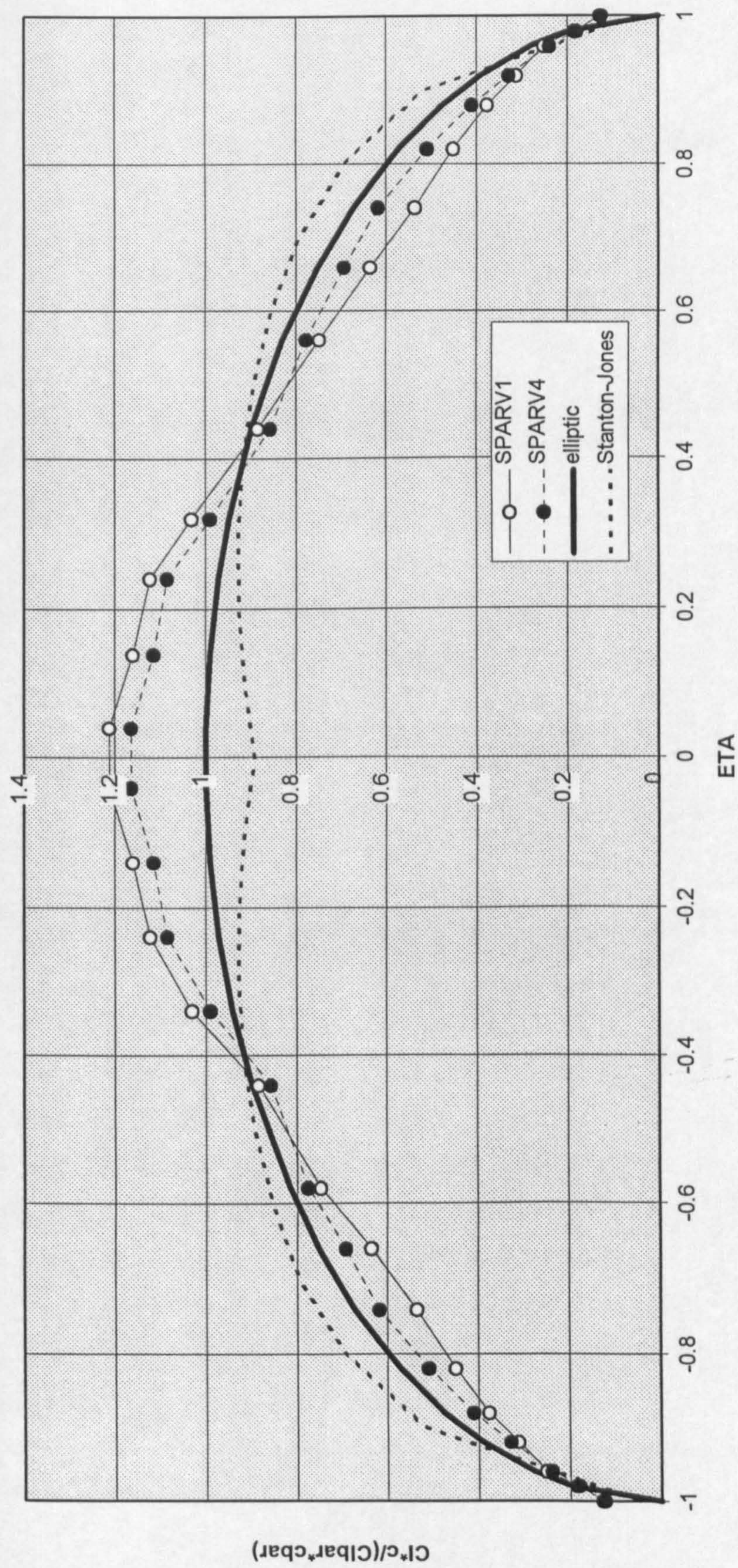


Figure 7.9 Twist Optimisation



# *Chapter 8*



## 8. CASE STUDIES

### 8.1 Introduction

In this chapter case studies undertaken by using of the program are presented. Validation is based on an older aircraft, this is due to the fact that for new aircraft sufficient data is very difficult to gather. In this chapter an example case is also presented. This is the case where the program starts from the beginning, which is the aircraft synthesis module. Several 'stand-alone' program results are also presented.

### 8.2 Validation (VC-10)

The validation is basically to test the static aeroelasticity module which is the module of aerodynamics and the structure. The Aircraft Synthesis module in this case is by-passed. The wing is modelled based on the actual aircraft. Sweep angle and kink location were not decided by the program but manually inputted. The structural model is based on the exact aircraft also. The VC-10 was chosen to be the validation target. This aircraft represents the intended target aircraft of a high subsonic aircraft. Weight data of this aircraft is available which makes it easier to compare.



### 8.2.1 SPARV Model

The SPARV model of the VC-10 is explained in this section. Modelling is done by running the PRESPARV module. The input file is created manually. During a normal mode the input file of PRESPARV module is created by the aircraft synthesis module. As can be seen at the next page, the VC-10 aircraft is modelled by assuming a round fuselage.

The number of panels spanwise and chordwise of the wing was decided earlier when studying the sensitivities studies. The number of panels is set to a fixed number based on the result of that study. This assumption works fine with the VC-10 model, but it was found later that the number of panels needed to model the aircraft wing accurately varies with the size of the wing. It was found later that for bigger aircraft (i.e. bigger wing), a more dense panel geometry is required, thus increasing the time consumed to run the program.

The aerodynamic calculation of the VC-10 aircraft is done in order to extract the pressure load. The actual pressure load distribution of the aircraft is needed in order to make a comparison, but it was found that this data is unavailable. Thus validation of the pressure load distribution can not be done. The validation is done in the structural module.

The aerodynamic panel of the VC-10 can be seen on Fig 8.1 and Fig. 8.2.



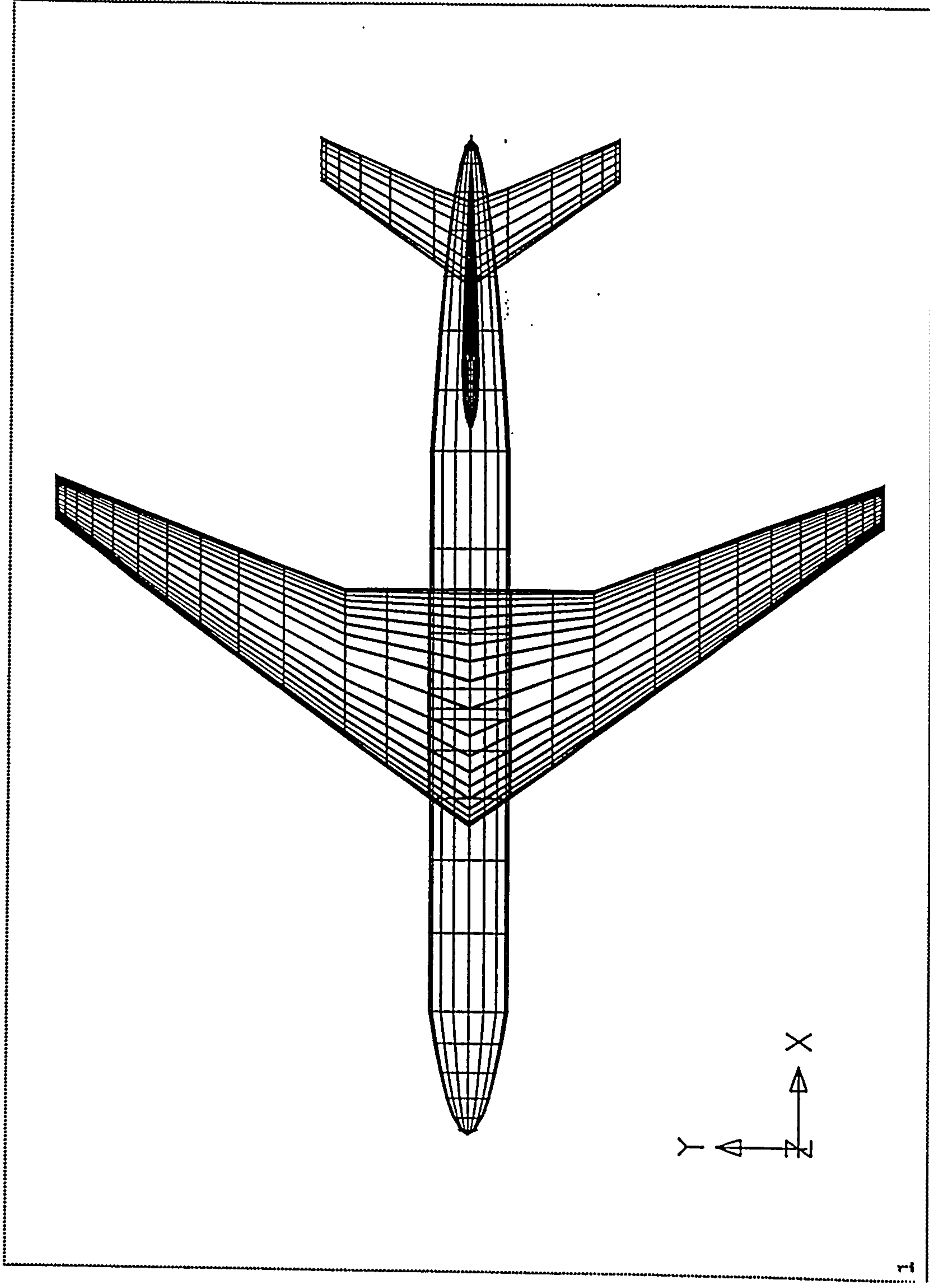


**Figure 8.1 VC-10 Aerodynamics panel TOP VIEW**



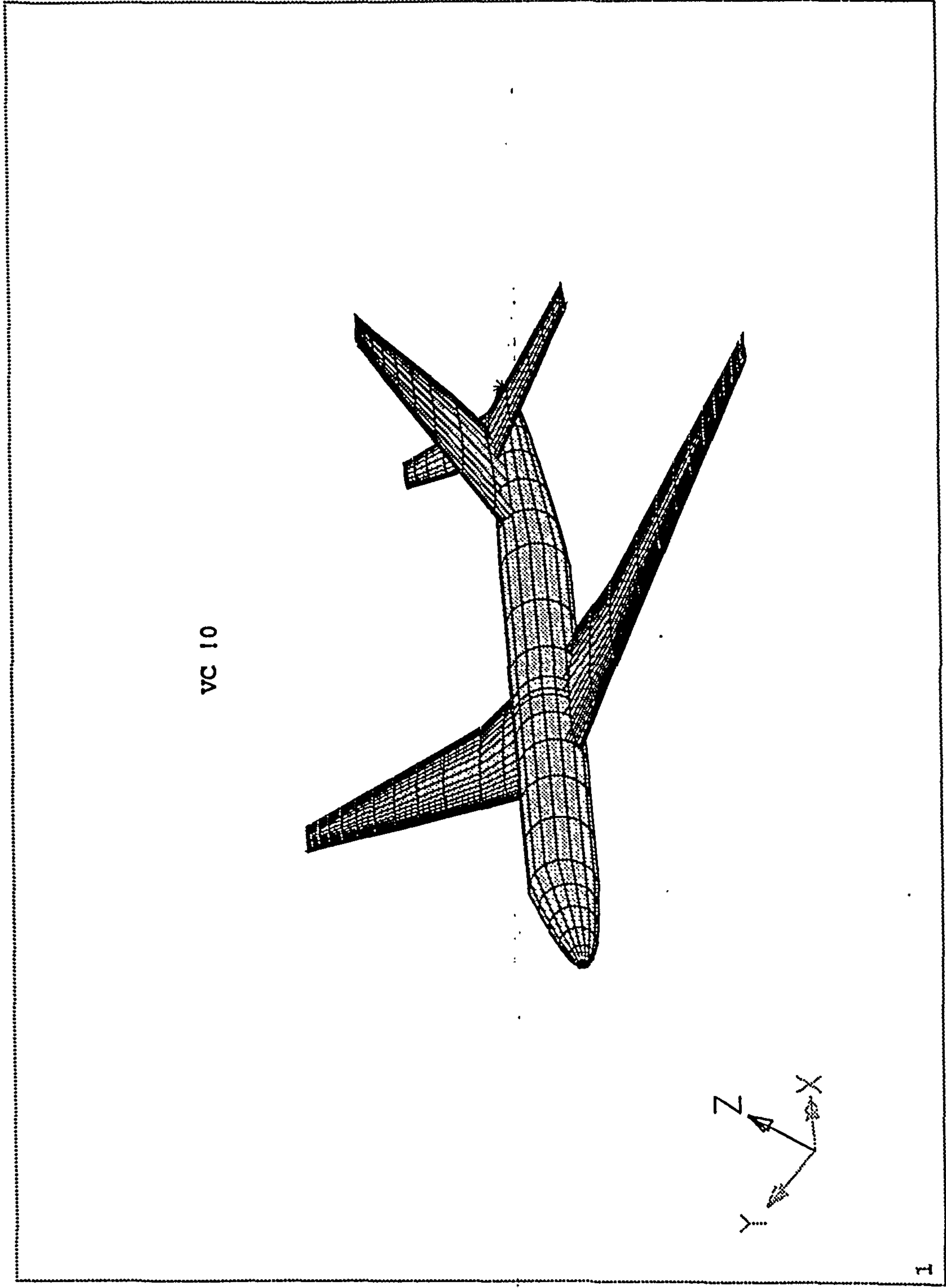
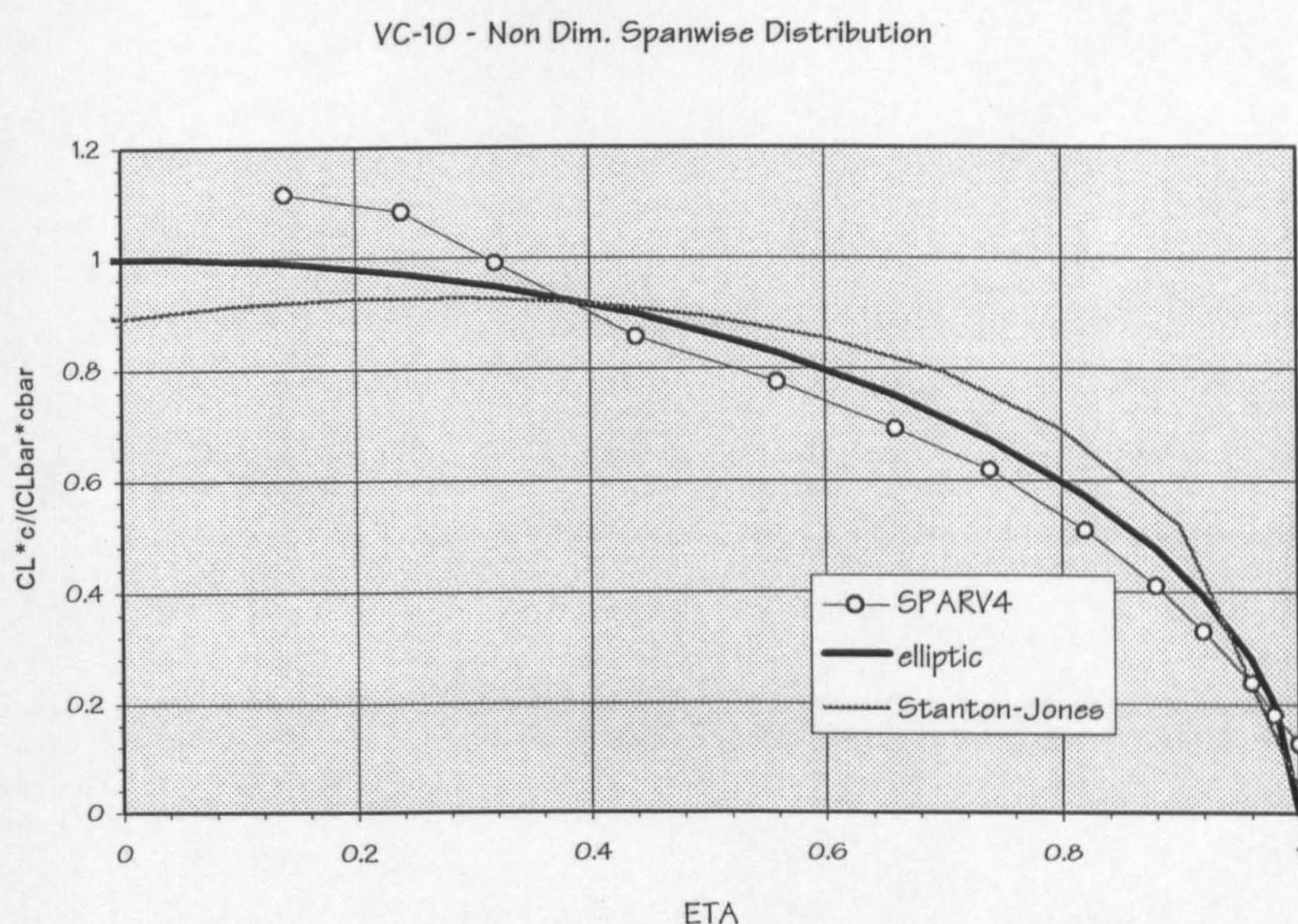


Figure 8.2 VC-10 Aerodynamics panel 3-VIEW



As can be seen from the figure 8.3 below, the SPARV calculation gives different results to the Stanton-Jones method (Ref. 33). In this figure both calculations are compared to the elliptic distribution. It is assumed that the results of SPARV is better due to the fact that Stanton-Jones method is unable to calculate the effect of twist and kink of the wing.



**Figure 8.3** VC-10 Spanwise Distribution

The pressure load from the last iteration in the static aeroelastic module (SPARV iteration 4) is given to the structural module and used as the final airload. This load is used in the structure module to predict the deflection and weight of the wing.



8.2.2 NASTRAN Model

The NASTRAN model of the VC-10 aircraft is done by executing the PRENASTRAN program. The input file required by PRENASTRAN program is done manually, in a normal case it is created by the aircraft synthesis program. The model is created by carefully generating the rib layout and spar layout as close as possible as the actual aircraft.

The SOLUTION-200 package of NASTRAN as mentioned earlier, is capable of finding the optimum thickness of each member and is also capable of calculating the weight. A typical iteration number to find the minimum weight of a member is about seven but sometimes it can go as high as fifteen. Due to the constraint of time required to calculate, it was decided to fix the maximum number of iteration to ten. Usually if the iteration goes more than ten it means there is an error in the modelling of the wing.

A typical iterations in the SOL-200 are as follows ; Table 8.1 :-

Table 8.1 SOL-200 Design Variable History

DESIGN VARIABLE HISTORY (ft unit)									
: DV. ID. :	INITIAL :	1 :	2 :	3 :	4 :	5 :	6 :		
1 :	0.3000E-02 :	0.1703E-01 :	0.3690E-01 :	0.5000E-01 :	0.5000E-01 :	0.5000E-01 :	0.5000E-01 :		
2 :	0.3000E-02 :	0.1850E-01 :	0.3739E-01 :	0.5000E-01 :	0.4998E-01 :	0.4998E-01 :	0.4998E-01 :		
4 :	0.7000E-02 :	0.2437E-01 :	0.3424E-01 :	0.3043E-01 :	0.3094E-01 :	0.3072E-01 :	0.3072E-01 :		
5 :	0.1700E-01 :	0.5000E-01 :	0.5000E-01 :	0.4928E-01 :	0.4928E-01 :	0.4928E-01 :	0.4928E-01 :		
6 :	0.1700E-01 :	0.2872E-01 :	0.4545E-01 :	0.5000E-01 :	0.4989E-01 :	0.4989E-01 :	0.4989E-01 :		
7 :	0.1900E-01 :	0.1891E-01 :	0.1889E-01 :	0.1881E-01 :	0.1879E-01 :	0.1856E-01 :	0.1856E-01 :		
8 :	0.1900E-01 :	0.1892E-01 :	0.1890E-01 :	0.1883E-01 :	0.1881E-01 :	0.1850E-01 :	0.1850E-01 :		
9 :	0.1900E-01 :	0.1890E-01 :	0.1888E-01 :	0.1879E-01 :	0.1877E-01 :	0.1850E-01 :	0.1850E-01 :		
10 :	0.1900E-01 :	0.1902E-01 :	0.1899E-01 :	0.1889E-01 :	0.1886E-01 :	0.1840E-01 :	0.1840E-01 :		
11 :	0.1900E-01 :	0.1942E-01 :	0.1939E-01 :	0.1926E-01 :	0.1923E-01 :	0.1879E-01 :	0.1879E-01 :		
12 :	0.1900E-01 :	0.1968E-01 :	0.1964E-01 :	0.1949E-01 :	0.1946E-01 :	0.1880E-01 :	0.1880E-01 :		
13 :	0.1900E-01 :	0.2022E-01 :	0.2018E-01 :	0.2000E-01 :	0.1989E-01 :	0.1924E-01 :	0.1924E-01 :		
14 :	0.1900E-01 :	0.2090E-01 :	0.2085E-01 :	0.2065E-01 :	0.2060E-01 :	0.1972E-01 :	0.1972E-01 :		
15 :	0.1900E-01 :	0.2158E-01 :	0.2152E-01 :	0.2129E-01 :	0.2125E-01 :	0.2037E-01 :	0.2037E-01 :		
16 :	0.1900E-01 :	0.2240E-01 :	0.2233E-01 :	0.2208E-01 :	0.2201E-01 :	0.2089E-01 :	0.2089E-01 :		
17 :	0.1900E-01 :	0.2336E-01 :	0.2329E-01 :	0.2300E-01 :	0.2294E-01 :	0.2170E-01 :	0.2170E-01 :		
18 :	0.1900E-01 :	0.2436E-01 :	0.2428E-01 :	0.2395E-01 :	0.2388E-01 :	0.2245E-01 :	0.2245E-01 :		



19	:	0.1900E-01	:	0.2531E-01	:	0.2523E-01	:	0.2487E-01	:	0.2481E-01	:	0.2331E-01	:	0.2331E-01	:
20	:	0.1900E-01	:	0.2634E-01	:	0.2636E-01	:	0.2596E-01	:	0.2591E-01	:	0.2423E-01	:	0.2423E-01	:
21	:	0.1900E-01	:	0.2801E-01	:	0.2826E-01	:	0.2783E-01	:	0.2772E-01	:	0.2591E-01	:	0.2591E-01	:
22	:	0.1900E-01	:	0.3194E-01	:	0.3350E-01	:	0.3298E-01	:	0.3225E-01	:	0.2978E-01	:	0.2978E-01	:
23	:	0.1900E-01	:	0.4045E-01	:	0.4474E-01	:	0.4401E-01	:	0.4340E-01	:	0.4027E-01	:	0.4027E-01	:
24	:	0.1900E-01	:	0.2568E-01	:	0.2662E-01	:	0.2513E-01	:	0.2825E-01	:	0.1617E-01	:	0.1617E-01	:
25	:	0.1900E-01	:	0.2742E-01	:	0.2853E-01	:	0.2992E-01	:	0.3327E-01	:	0.4846E-01	:	0.4846E-01	:
26	:	0.1900E-01	:	0.3472E-01	:	0.2617E-01	:	0.2564E-01	:	0.2901E-01	:	0.3857E-01	:	0.3857E-01	:
27	:	0.1900E-01	:	0.2164E-01	:	0.2026E-01	:	0.1828E-01	:	0.2069E-01	:	0.2546E-01	:	0.2546E-01	:
28	:	0.1900E-01	:	0.3358E-01	:	0.3757E-01	:	0.3579E-01	:	0.3943E-01	:	0.5000E-01	:	0.5000E-01	:
29	:	0.1900E-01	:	0.2892E-01	:	0.2909E-01	:	0.2789E-01	:	0.2815E-01	:	0.2265E-01	:	0.2265E-01	:
30	:	0.1900E-01	:	0.1262E-01	:	0.7425E-02	:	0.6672E-02	:	0.6515E-02	:	0.8603E-02	:	0.8603E-02	:
31	:	0.1900E-01	:	0.1787E-01	:	0.2574E-01	:	0.2443E-01	:	0.2388E-01	:	0.2915E-01	:	0.2915E-01	:
32	:	0.1900E-01	:	0.2624E-01	:	0.2638E-01	:	0.2517E-01	:	0.2542E-01	:	0.2268E-01	:	0.2268E-01	:
33	:	0.1900E-01	:	0.2423E-01	:	0.1996E-01	:	0.1862E-01	:	0.1832E-01	:	0.2251E-01	:	0.2251E-01	:
34	:	0.1900E-01	:	0.5000E-01	:	0.4983E-01	:	0.4762E-01	:	0.5000E-01	:	0.4860E-01	:	0.4860E-01	:
35	:	0.1900E-01	:	0.1653E-01	:	0.1599E-01	:	0.1378E-01	:	0.1334E-01	:	0.3812E-02	:	0.3812E-02	:
3	:	0.3000E-02	:	0.1703E-01	:	0.3690E-01	:	0.5000E-01	:	0.5000E-01	:	0.5000E-01	:	0.5000E-01	:

Design Variables (first column) in this case is a thickness of the member (rib, spar, skin, etc.). These can be distinguished as :

- |        |         |   |                                  |
|--------|---------|---|----------------------------------|
| DV. ID | 1       | = | Upper wing skin                  |
|        | 2       | = | Lower wing skin                  |
|        | 3       | = | Upper wing skin (at root)        |
|        | 4       | = | Lower wing skin (at root)        |
|        | 5       | = | Front Spar                       |
|        | 6       | = | Rear Spar                        |
|        | 7 to 35 | = | Ribs, 7 is at tip and 35 at root |

As can be seen from the table above most members are set initially to almost the same value. The initial value can be distinguished as spars, skins, and ribs. To give the consistency in the units used, these values are in feet instead of the usual inches of the structure calculation.

It is clearly seen above that in this case after 5 iterations the thickness converged. Although the thickness of each member is not needed in this project, it is used as a means of checking that the skin thickness is reasonable. The results that are needed from this calculation is the



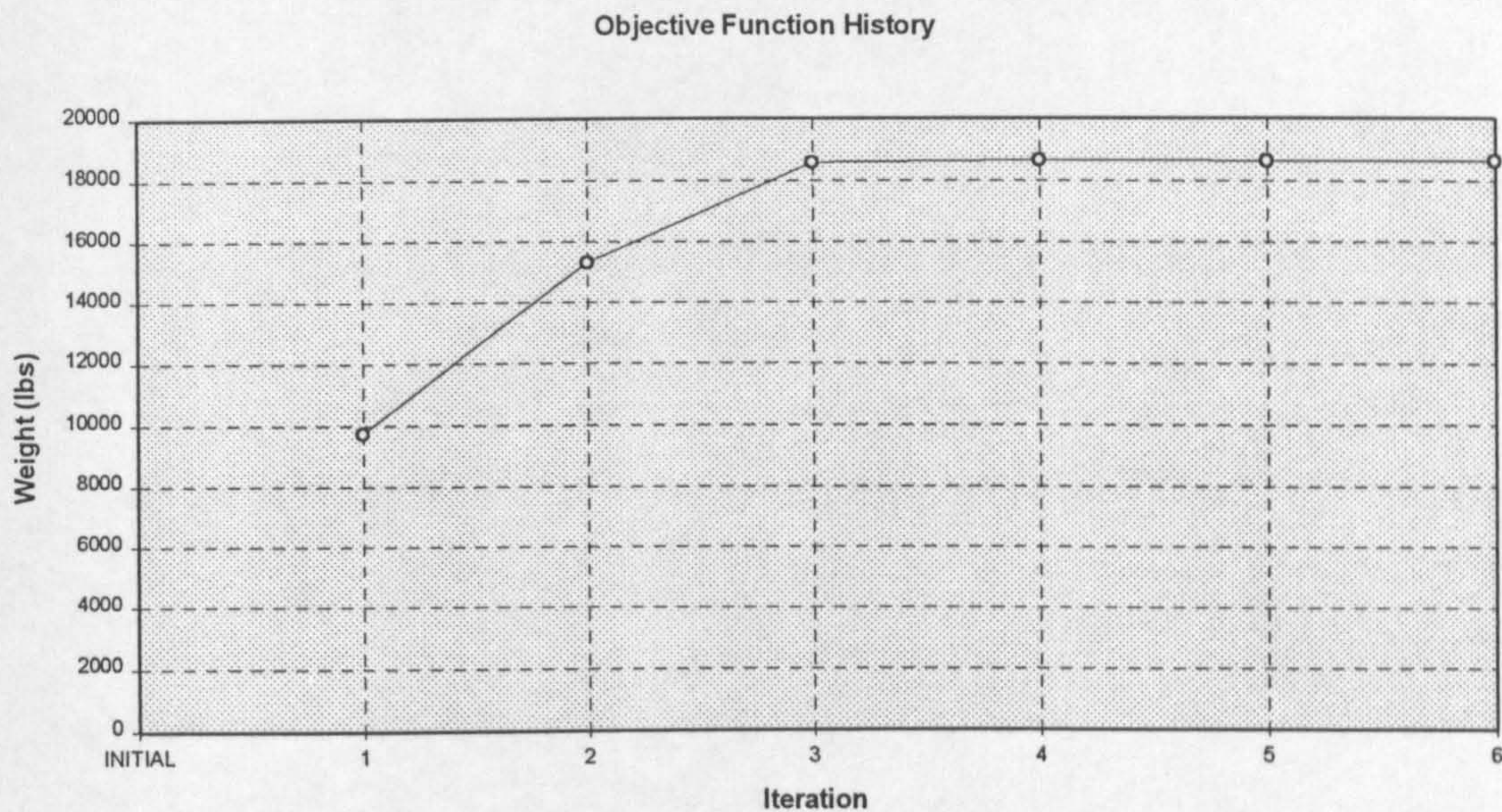
weight. The weight of the wing is calculate by the program and is also based on the optimum thickness of the member. The weight of the aircraft wing based on these iteration can be seen below, Table 8.2.

Table 8.2 SOL-200 Objective Function History

OBJECTIVE FUNCTION HISTORY (lb unit)			
ITERATION NUMBER	OPTIMAL WITH RESPECT TO APPROXIMATION	EXACT EVALUATION BY COMPLETE ANALYSIS	FRACTIONAL ERROR OF APPROXIMATION
INITIAL		0.355017E+04	
1	0.971921E+04	0.971922E+04	-0.904298E-06
2	0.153239E+05	0.153239E+05	0.254912E-06
3	0.185750E+05	0.185750E+05	-0.210296E-06
4	0.186511E+05	0.186511E+05	0.000000E+00
5	0.186383E+05	0.186383E+05	0.209582E-06
6	0.186383E+05	0.186383E+05	0.000000E+00

From Table 8.2, the objective function (weight) of the optimised wing can be seen on the third column. These numbers are for the wing box only and did not include the consideration of fatigue. As can be seen from the Figure 8.4 , after the third iteration the weight starts to converge.





**Figure 8.4 SOL-200 Objective Function History**

To find the weight of the whole wing, the wing box weight has to be transferred into a wing weight. Ref. 58 quotes that for this type of aircraft the weight of the whole wing can be calculated from the known wing box weight. The equation is as follows :

$$W_{\text{WING}} = W_{\text{WING BOX}} + (F \times \text{MTOW})$$

where :  $W_{\text{WING}}$  = wing weight

$W_{\text{WING BOX}}$  = wing box weight.

$F$  = 0.0415 for wing with 2 engines.

= 0.0405 for wing with no engine.

MTOW = Maximum Take-Off Weight.



By using this equation, the weight of the wing can be calculated as :

$$\begin{aligned}W_{\text{WING}} &= 18638 + 314000(0.0405) \\ &= 31355 \text{ lbs. (no fatigue consideration)}\end{aligned}$$

The result found above is without fatigue considerations. As mentioned earlier, fatigue considerations are assumed to increase the structural weight by 11 % (Ref. 40).

For the actual aircraft the actual wing weight is found to be 34632 lbs (Ref. 54). This reference also mentions the weight of sealing, bolts and rivets to be 370 lbs or about 1 %. The weight of the calculated aircraft build up can be seen as follows :

$$\begin{aligned}W_{\text{WING}} &= 31355 \text{ lbs. (no fatigue consideration)} \\ &= 33219 \text{ lbs. (with fatigue)} \\ &= 33551 \text{ lbs. (+ bolts, rivets, etc.)}\end{aligned}$$

$$\text{actual } W_{\text{WING}} = 34632 \text{ lbs.}$$

The difference is -3.1 %. This differences is assumed to be very good.

The detail of the layout of the structural panels can be seen on Fig. 8.5.



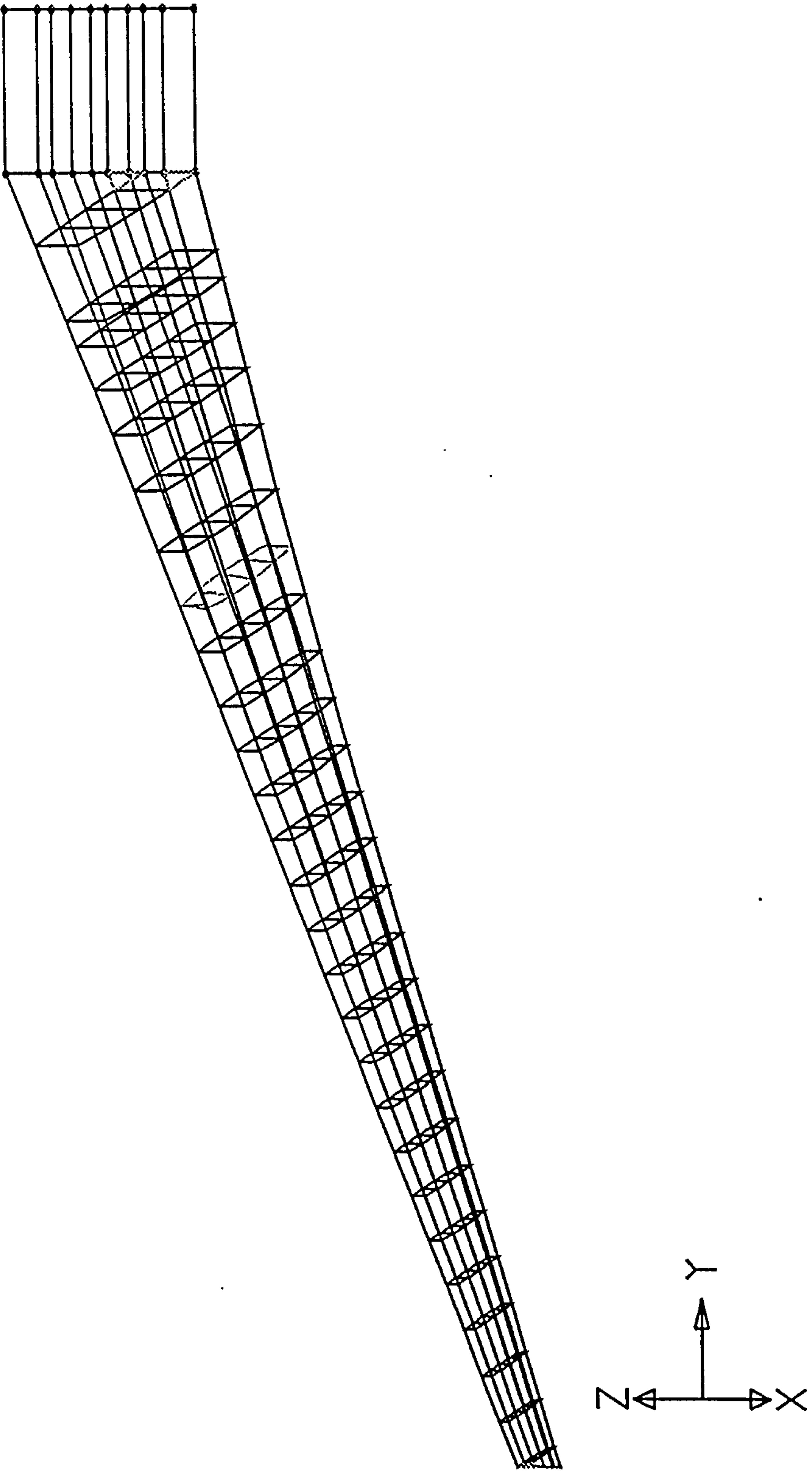


Figure 8.5 VC-10 Structural panel



### 8.3 Interface Program Results

The results of the calculation in this section can be divided into two categories, the pressure load results and the structural results. The aerodynamic results can not be checked with the actual results because the data is unavailable. But, since weight is assumed to be the main target, the end results that needs to be compared is the structural wing weight.

#### 8.3.1 Pressure Loads

As explained before, the pressure is just an intermediate result as a way to visualise the pressure load gathered from the computational fluid dynamics results. This pressure load is used as an input in the next module of computational structure analysis.

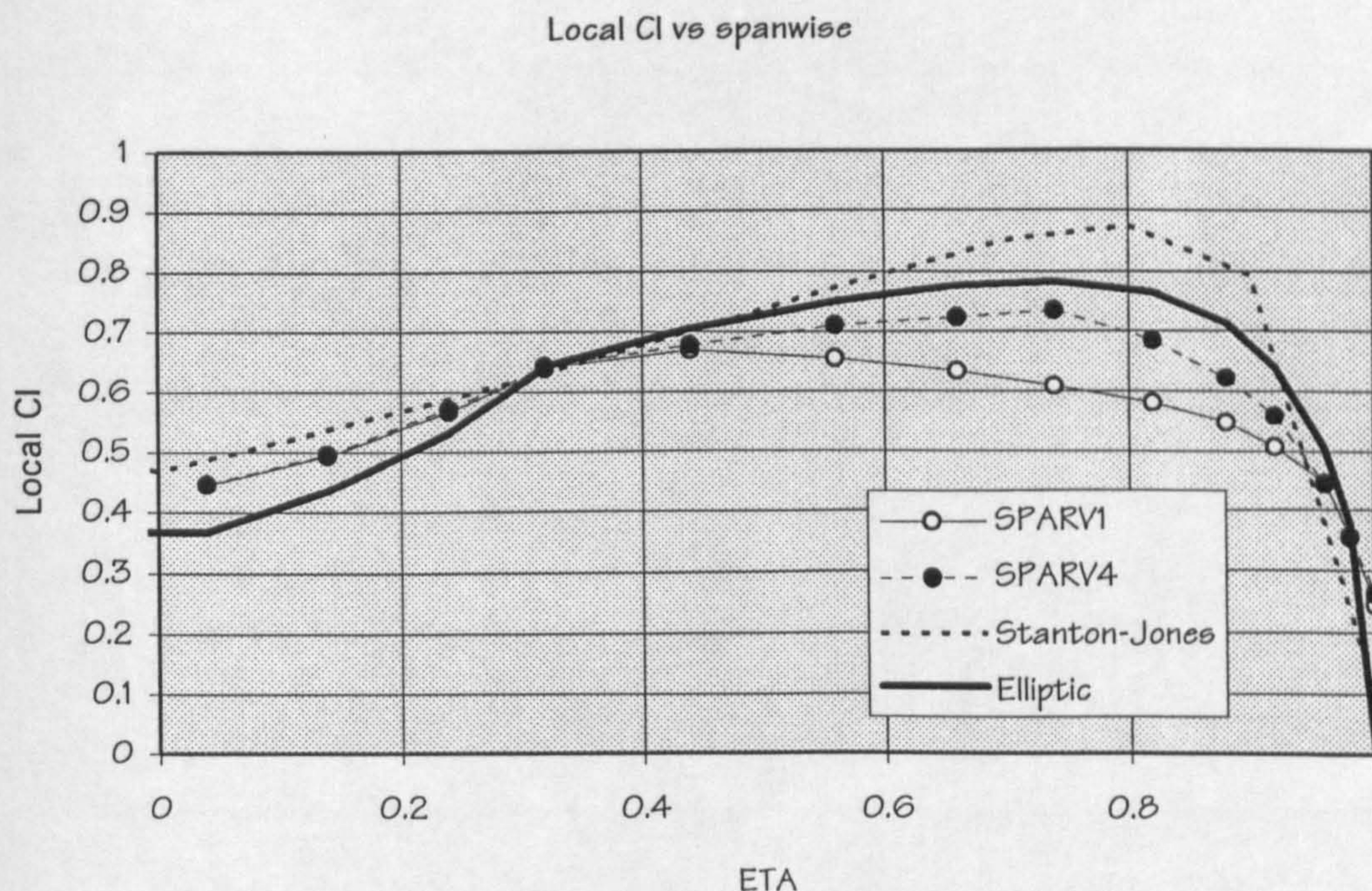
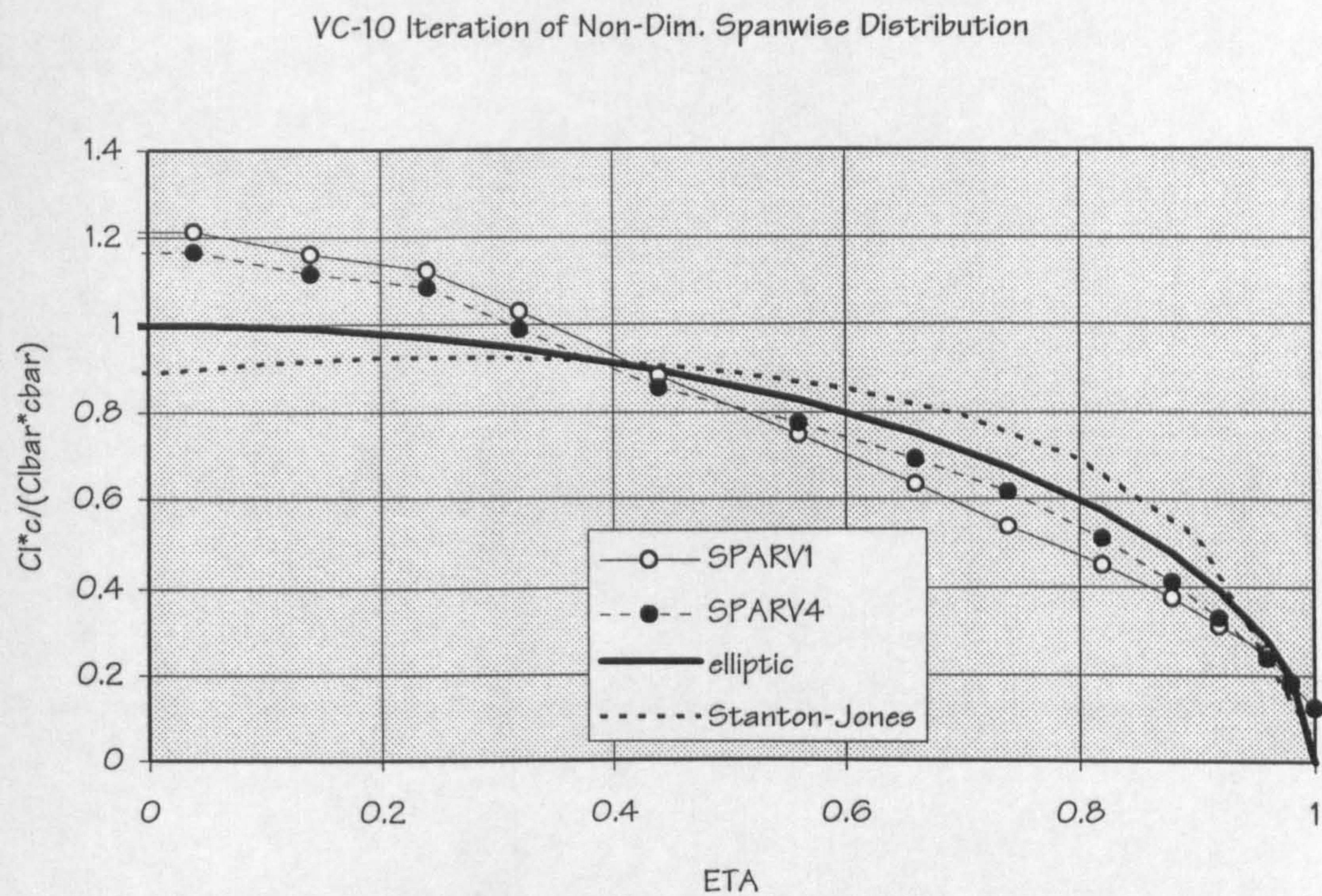


Figure 8.6 Spanwise Lift Coefficient of VC-10



As can be seen from Figure 8.6, there is some difference in the pressure load between first iteration of the SPARV (SPARV1) to the last iteration (SPARV4). But because this is happening at the tip which has relatively smaller loads, the total difference is rather small. To be more clear, a non-dimensional plot can be seen at the next figure (Fig.8.7).



**Figure 8.7** VC-10 Iteration of Spanwise Distribution

The actual results extracted from SPARV is the coefficient of pressure. This coefficient of pressure needs to be multiplied by the dynamic pressure and the load factor to get the final pressure to be used in the NASTRAN. As mention before the load factor used is 3.75 which comes from maximum manoeuvre load factor of 2.5 times the safety



factor of 1.5. The Dynamic Pressure used is a function of cruise altitude and cruise mach number.

A typical chordwise pressure distribution can be seen in the next figure (Fig. 8.8).

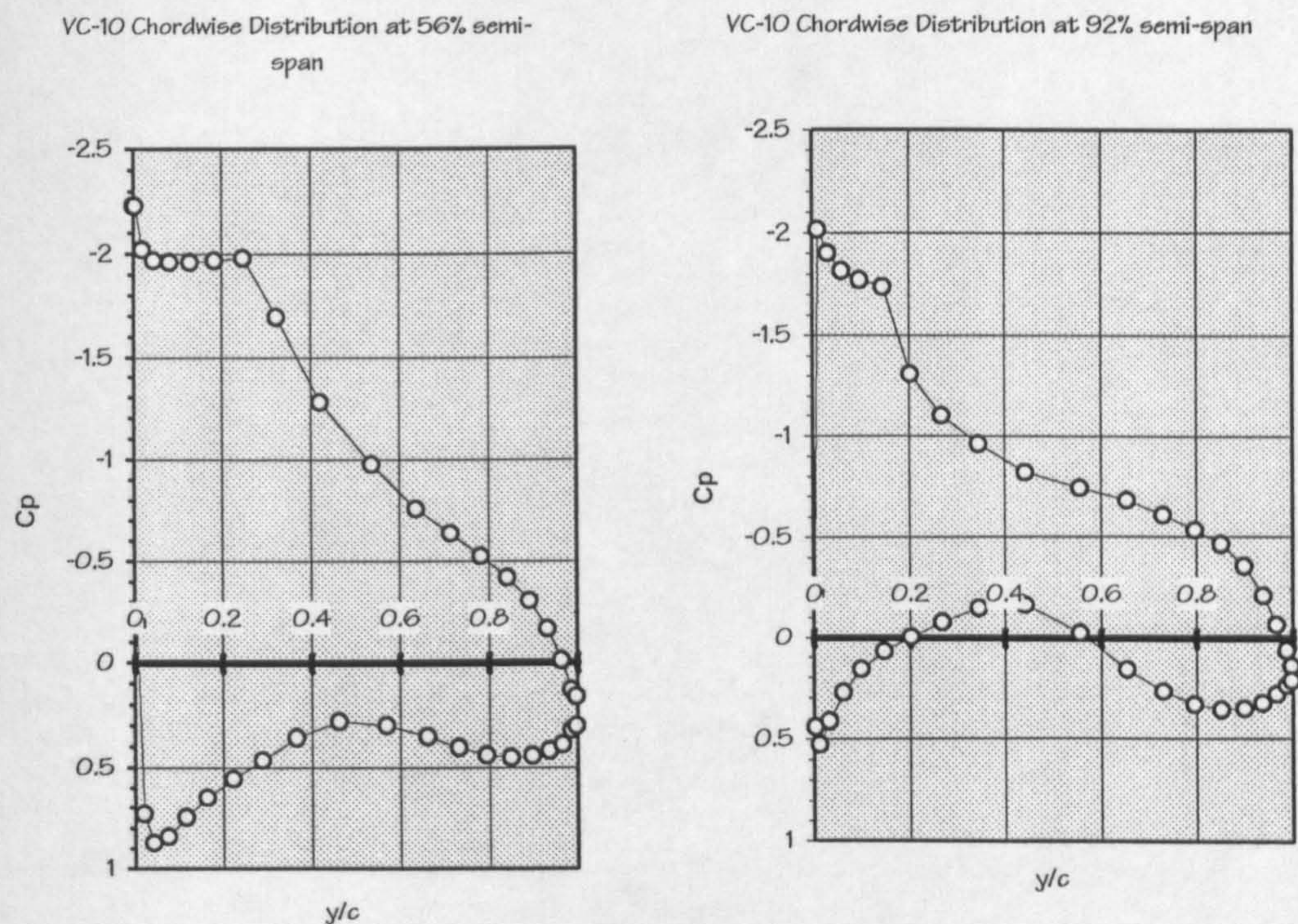


**Figure 8.8** VC-10 Chordwise Distribution

These pressure coefficients after multiplying by the correct factor are inputted to the NASTRAN in the form of pressure load (PLOAD4). Because the structural model is only the wing box, only pressure loads between the front spar and rear spar are actually used. The load from the leading edge to the front spar is inputted to the NASTRAN in the form of FORCE. This is done in the PRESPARV module



by multiplying the pressure with the corresponding panel area.

### 8.3.2 Structure Deflection

The structural deflection of the wing is used only for checking. In the beginning of the project, deflection was used as one of the constraints but after studying the effects, it was decided to use only maximum stress as a constraint. Difficulties were found to set a criteria to set the maximum wing tip deflection. It is also found that usually tip deflection is not used in the structural design consideration.

The tip deflection of the VC-10 can be seen on the next table (Table 8.3).

**Table 8.3 VC-10 Tip Deflection**

Iteration	Deflection (ft)
1	0.0 ft
2	8.4 ft
3	6.2 ft
4	7.3 ft

It is clearly seen that the wing calculation is converging. As can be seen from this table, the wing is not fully converged yet but due to the time constraint, it is decided that the 4th iteration is assumed to be sufficiently converged.



## 8.4 Static Aeroelastic Iteration Results

In this section, the static aeroelastic result is analysed. As mentioned in section 8.3.2, after four iterations the wing deflection is converging but not fully converged as yet. A study was done to find the number of iterations actually for the wing deflection to converge. A difference of 0.1 ft is set as a criteria for converged condition. It is found that the wing will fully converge after 7 iterations. The final result is not far from the 4th iteration thus iteration is set to the maximum number of four.

The results of each iteration can be seen on Fig. 7.5 on previous chapter. This figure is generated from several tip deflection plots (Fig. 8.9).



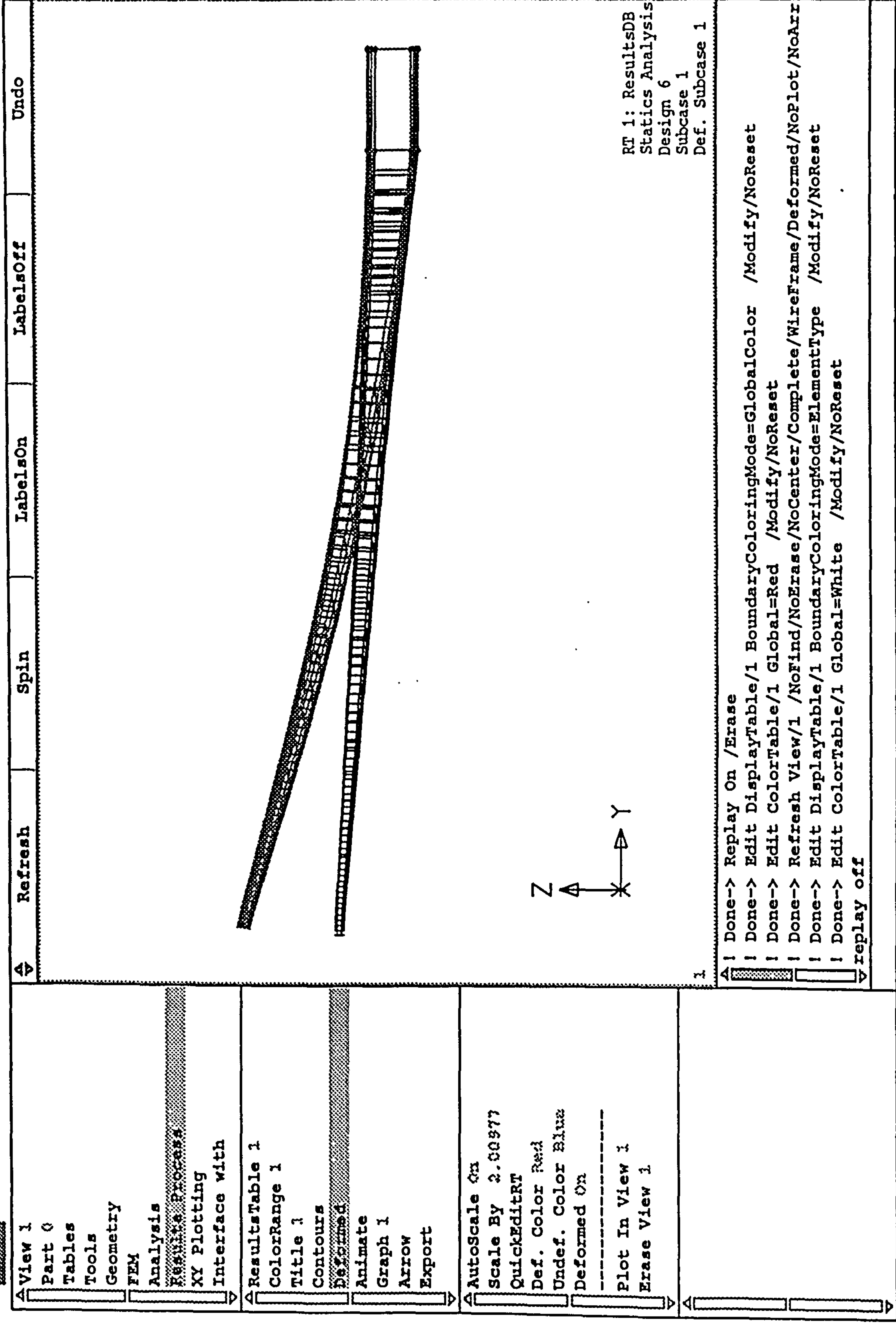


Figure 8.9 Tip Deflection



## 8.5 Divergence Test

This test was done in the earlier time when studying how to model the wing. The wing analysis is found to diverge when not modelled correctly. The error was found when modelling the finite element program NASTRAN. The element to be used was found to be critical to give a correct result. The model of the wing was compared with the actual aircraft.

As can be seen on Fig. 8.9, the wing analysis is clearly converging.

## 8.6 Test Case Results

This test case is just an example of the whole program. The program starts from the aircraft synthesis module and continues to the next module as explained before.

The program starts by running the aircraft synthesis module. This aircraft synthesis makes an internal call to run various other module such as parametric study, stability and control, and wing layout and empennage module. The details of the input and output files of these program can be found next.

### 8.6.1 Parametric Study

This module is called first, in the aircraft synthesis program. An input file required for this module basically is the Design, Requirement and Objective of the aircraft.



The sample input of the parametric module can be seen below.

PARM.DAT:

```
AIRBUS 310-300 CF6-80C2-A2
3.0      Cl_max_l
2.4      Cl_max_to
0.82     Wl/W
0.99     percent_LDmax
4850.0   LFL(ft)_or_Vapp(knots)
7500.0   TOFL(ft)
2        n_engine
5.05     BPR_(By_Pass_Ratio)
2357.0   S(ft2)
18.5     fuse_diam(ft)
148.1    fuse_length(ft)
0.8      M_cruise
28.1     C_root(ft)
37000.0  cruise_alt(ft)
1        num_AR
8.8      first_AR
1.0      delta_AR
10       num_W/S
80.0     first_W/S(lb/ft^2)
10.0     delta_W/S(lb/ft^2)
1        num_ICAC_altitude
35000.0  first_ICAC_altitude(ft)
2000.0   delta_ICAC_altitude(ft)
3.0      fuel_burnt_during_climb_(%_TOW)
300.0    Rate_of_Climb(ft/min)
1        num_OEI_altitude
15000.0  first_OEI_altitude(ft)
1000.0   delta_OEI_altitude(ft)
0.55     Mach_OEI
280      num_pax
5200.0   Range(n.miles)
0.84     M_max
1        engine_on_wing_?
1        fuel_on_CW_Tank_?
0.650    sfc_(lb/hr/lb)
0.333    taper
28.0     lambda
18.0     t_per_c_root
```

Apart from the Design Requirement and Objectives, several other initial values are also given. Initial values such as wing area, root chord are given. This is done in order to cut the number of iteration done internally in the module when these data are not given. The module will give the exact results with or without initial data (inputted as 0.0)



## output of parametric study

```
*****
*
*          PARAMETRIC
*    program for initial parametric study
*
*          developed based on
*
* [1] Loftin, L. K., Subsonic Aircraft: Matching of
*      Size to Performance
* [2] Raymer, D. P., Aircraft Design: A Conceptual
*      Approach
* [3] Corning, G., Supersonic and Subsonic CTOL
*      and VTOL Airplane Design
* [4] Simpkin, P., Preliminary Design of Subsonic
*      Civil Aircraft
*
*
*          by
*
*          Demil Y. Djafri
*          July 1994
*
*****
```

AIRBUS 310-300 CF6-80C2-A2

### FIRST LOOP OF PARAMETRIC STUDY

```
cruise_alt = 37000.000 ft
temperature = 390.000 R
speed_of_sound = 967.955 ft/s
V_cruise = 458.801 knots
```

#### 1. LANDING FIELD LENGTH

W/S = 118.991

```
V_approach = 127.148
Cl_app      = 1.775
Wl_per_S    = 97.572
```

#### 2. TAKE-OFF FIELD LENGTH

W/S	To / W
80.000	0.167
90.000	0.187
100.000	0.208
110.000	0.229
120.000	0.250
130.000	0.271
140.000	0.292
150.000	0.312
160.000	0.333
170.000	0.354

slope\_TOP = 480.000

#### 3. SECOND SEGMENT CLIMB

AR        To/W



8.800 0.278

Cl\_2 = 1.667

4. MISSED APPROACH

AR To/W  
8.800 0.248

5. CRUISE PERFORMANCE

AR L/D max Cl,m Cdo\_ref  
8.800 18.466 0.636 0.017

temp\_cruise = 390.000 R  
temp\_35 = 393.960 R

rho\_cruise = 0.676 x 10^-3 slug/ft^3  
rho\_35 = 0.739 x 10^-3 slug/ft^3

V\_cruise = 458.801 knots  
V\_cruise\_35 = 422.066 knots

L\_bar = 0.728

Cl\_bar max. = 1.000

REYNOLD'S NUMBER CORRECTION

AR L/D Cl,max Cd\_o  
8.800 17.983 0.636 0.018

Cl\_bar = 0.868

CRUISING AT 0.990 L/D MAX.

AR L/D Cl,max Cd\_o  
8.800 17.803 0.552 0.018

AR	L/D	Cl	Cl*M2	W/S	altitude
8.800	17.803	0.552	0.353	80.000	43978.703
8.800	17.803	0.552	0.353	90.000	41528.992
8.800	17.803	0.552	0.353	100.000	39337.652
8.800	17.803	0.552	0.353	110.000	37355.340
8.800	17.803	0.552	0.353	120.000	35602.273
8.800	17.803	0.552	0.353	130.000	33913.281
8.800	17.803	0.552	0.353	140.000	32326.393
8.800	17.803	0.552	0.353	150.000	30828.762
8.800	17.803	0.552	0.353	160.000	29409.889
8.800	17.803	0.552	0.353	170.000	28061.082

AR	L/D	Tc/To	To/W	W/S	altitude
8.800	17.803	0.135	0.415	80.000	43978.703
8.800	17.803	0.157	0.358	90.000	41528.992
8.800	17.803	0.176	0.319	100.000	39337.652
8.800	17.803	0.193	0.291	110.000	37355.340
8.800	17.803	0.207	0.271	120.000	35602.273
8.800	17.803	0.219	0.257	130.000	33913.281
8.800	17.803	0.227	0.247	140.000	32326.393
8.800	17.803	0.236	0.238	150.000	30828.762
8.800	17.803	0.245	0.230	160.000	29409.889
8.800	17.803	0.254	0.221	170.000	28061.082

6. INITIAL CRUISE ALTITUDE CAPABILITY

L\_per\_D = 17.803  
Weight = 280461.031 lbf



S wing = 2357.000 ft^2  
 Cl\_cruise = 0.552  
 prcnt\_init\_cruise = 0.970  
 Rate of Climb = 300.000 ft/min  
  
 ICAC at 35000.000 ft  
  
 speed\_of\_sound at 35000.000 ft = 972.856 ft/s  
 V\_cruise\_ICAC = 778.285 ft/s  
 V\_cruise\_ICAC = 46697.105 ft/min  
 Tc / To at 35000.000 ft = 0.213

AR	W/S	To/W	S	weight	Cd	Cl	D	T/W
8.800	80.000	0.267	5055.880	404470.375	0.034	0.350	0.728	0.267
8.800	90.000	0.267	4166.667	375000.094	0.034	0.394	0.728	0.267
8.800	100.000	0.267	3555.974	355597.438	0.035	0.438	0.728	0.267
8.800	110.000	0.267	3107.202	341792.188	0.035	0.482	0.728	0.267
8.800	120.000	0.267	2762.064	331447.688	0.035	0.526	0.728	0.267
8.800	130.000	0.267	2487.683	323398.781	0.036	0.570	0.728	0.267
8.800	140.000	0.267	2263.955	316953.750	0.036	0.613	0.728	0.267
8.800	150.000	0.267	2077.845	311676.813	0.036	0.657	0.728	0.267
8.800	160.000	0.267	1920.473	307275.750	0.037	0.701	0.728	0.267
8.800	170.000	0.267	1785.587	303549.813	0.037	0.745	0.728	0.267

7. ONE ENGINE INOPERATIVE CEILING

OEI Altitude = 15000.000 ft

AR	Cl OEI	Cl_bar	L/D	Altitude	W/S	To/W
8.800	0.316	0.462	13.081	15000.000	80.000	0.191
8.800	0.356	0.520	14.060	15000.000	90.000	0.178
8.800	0.395	0.578	14.879	15000.000	100.000	0.168
8.800	0.435	0.635	15.551	15000.000	110.000	0.161
8.800	0.474	0.693	16.085	15000.000	120.000	0.155
8.800	0.514	0.751	16.496	15000.000	130.000	0.152
8.800	0.553	0.809	16.798	15000.000	140.000	0.149
8.800	0.593	0.866	17.003	15000.000	150.000	0.147
8.800	0.632	0.924	17.125	15000.000	160.000	0.146
8.800	0.672	0.982	17.176	15000.000	170.000	0.146

POSSIBLE OPTIMUM POINT

W/S	To/W	Weight (lbf)	VALID ?
118.991	0.248	323621.188	0
118.991	0.278	331706.500	1
118.991	0.248	323750.313	0
118.991	0.273	330242.031	0
118.991	0.267	328649.438	0
118.991	0.078	284976.031	0
133.558	0.278	320349.063	0
119.231	0.248	323542.313	0
125.997	0.262	321698.125	0
128.139	0.267	321246.688	0
0.000	0.000	0.000	0
0.000	0.000	0.000	0
116.388	0.278	334201.000	1
0.000	0.000	0.000	0
0.000	0.000	0.000	0
138.537	0.248	310081.813	0
0.000	0.000	0.000	0
0.000	0.000	0.000	0
122.765	0.267	325399.094	0
0.000	0.000	0.000	0



0.000 0.000 0.000 0

```
*****
To / W optimum = 0.278
W / S optimum  = 118.991
Weight         = 331706.500 lbf
*****
```

This module gives values ( $T_o/W$ ) and ( $W/S$ ) for the different performance requirements. Optimum values of these parameters can be determined, see below. In the whole process of this project, this parametric module is called many times, thus making it impossible to check the intermediate results of each of the parametric studies done. Because of this a 'stand alone' program was built to check the results of the parametric study.

This stand alone PARAMETRIC program can be run alone and automatically called a graphics program to show the results in graphics. A 'gnuplot' program is called from the PARAMETRIC program to show the results. Two PARAMETRIC program build in two different operating systems, SUN and WINDOWS 3.1. An example results of the PARAMETRIC program can be seen below (Figure 8.10).



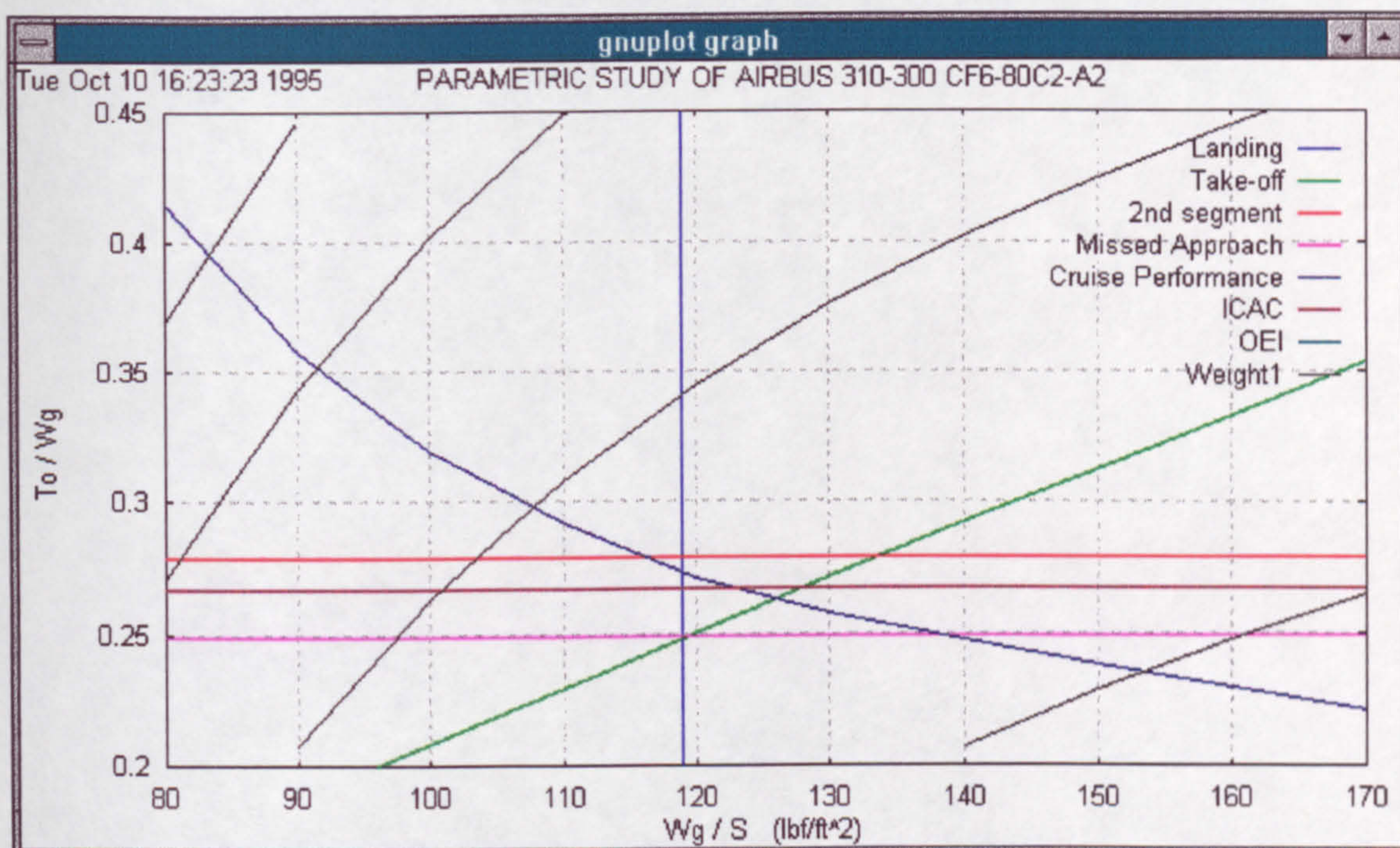


**Figure 8.10 Gnuplot Results of Parametric Study**

This picture of the Gnuplot graph of PARAMETRIC results shows the line of several constraints such as landing, take-off etc. Also overlaid in the chart are the constant weight lines. This is used by the program to pick the optimum combination of ( $T_0/W$ ) and ( $W/S$ ) which gives minimum weight.

### 8.6.2 Stability and Control

The stability and control program is used in the aircraft synthesis program to design the empennage and to set the wing on the fuselage. This program is called several times from the aircraft synthesis program. This program is based on the MITCHELL stability and control program (Ref. 47).



An example of the results of the MITCHELL program can be seen below.

STABILITY WITH CONTROLS FIXED AND RESPONSE TO CONTROLS FOR A RIGID AIRCRAFT  
(METRIC UNITS)

DESCRIPTION : AIRBUS 300-B2  
CASE 1 OF 1

PRINCIPAL GEOMETRIC PARAMETERS

WING SPAN = 49.8      OVERALL LENGTH = 54.5      FUSELAGE LENGTH = 53.5

===== WING =====  
AREA = 297.5      ASPECT RATIO = 8.33      TAPER RATIO = 0.173      1/4C SWEEP = 28.4  
SMC = 5.98      MAC = 6.97      L.E. OF MAC FROM APEX DATUM = 5.96

=====TAILPLANE=====  
AREA = 56.4      ASPECT RATIO = 4.55      TAPER RATIO = 0.500      1/4C SWEEP = 36.9  
ARM = 27.2      HEIGHT = 1.46      VOLUME = 0.865

=====FIN=====  
AREA(GROSS) = 101.4      AREA(NET) = 62.3      ASPECT RATIO (GROSS) = 2.124      1/4C SWEEP = 38.2  
ARM = 22.4      HEIGHT TO CP = 6.5      VOLUME = 0.153

CONFIGURATION DATA INSERTED  
WING AND FLAPS  
ALPHA 0(3-D) = -2.0 DEGREES      DCL-FLAP (2-D) = 0.000      CLMAX (3-D) = 1.400  
CM0 = 0.0700      CDO A/C = 0.2000      TAILPLANE SETTING = -3.0 DEGREES

FLIGHT CONDITIONS  
MASS = 136987.2      HEIGHT = 10668.0      SPEED = 234.3      MACH NO = 0.790  
CG FROM DATUM = 5.35      CG POSITION = -8.74% MAC      CG ABOVE DATUM = -1.34  
INCIDENCE (ALPHA) = 2.6      CL = 0.433

--- deleted ---

LONGITUDINAL MODES, STICK FIXED

ROOTS OF	REAL PART	IMAG. PART
MODE 1	-0.8735	2.4864
MODE 2	-0.8735	-2.4864
MODE 3	-0.0200	0.0538
MODE 4	-0.0200	-0.0538

VECTORS	REAL PART	IMAG.PART	AMPLITUDE	PHASE
MODE 2				
U	0.0004	0.0005	0.0006	-50.39
W	-0.0076	0.0758	0.0761	-95.76
Q	0.9944	0.0000	0.9944	0.00
THETA	-0.0242	0.0688	0.0729	-109.36
MODE 4				
U	-0.2048	-0.5337	0.5717	110.99



W	0.0022	0.0048	0.0053	-65.74
Q	-0.0814	-0.2189	0.2336	110.39
THETA	0.7865	0.0000	0.7865	0.00

# STABILITY PARAMETERS

MODE 2 IS OSCILLATORY

FREQUENCY= 0.3957HZ (= 2.486RAD/S)      PERIOD= 2.527SEC.

UNDAMPED FREQ.= 2.635RAD/S

DAMPING-- ANGLE=19.36DEG.      RATIO(ZETA)= 0.331

TIME TO HALF-AMP= 0.794SEC.      CYCLES TO HALF-AMP= 0.314

LOG.DEC.= 2.207

MODE 4 IS OSCILLATORY

FREQUENCY= 0.0086HZ (= 0.054RAD/S)      PERIOD=116.869SEC.

UNDAMPED FREQ.= 0.057RAD/S

DAMPING-- ANGLE=20.39DEG.      RATIO(ZETA)= 0.348

TIME TO HALF-AMP= 34.686SEC.      CYCLES TO HALF-AMP= 0.297

LOG.DEC.= 2.335

NORMAL ACCELERATION NZ/ALPHA = 0.259 G/DEGREE

# LATERAL MODES, STICK FIXED

ROOTS OF	REAL PART	IMAG. PART
MODE 1	0.0000	0.0000
MODE 2	-1.6891	0.0000
MODE 3	0.0057	0.0000
MODE 4	-0.2002	1.9303
MODE 5	-0.2002	-1.9303

VECTORS	REAL PART	IMAG.PART	AMPLITUDE	PHASE
---------	-----------	-----------	-----------	-------

MODE 1 HAS ONLY CONSTANT TERMS

# MODE 2

V	0.0021
P	0.9935
R	-0.0071
PHI	-0.1136
PSI	0.0008

# MODE 3

V	0.0006
P	0.0040
R	0.0292
PHI	0.1366
PSI	0.9902

# MODE 5

V	-0.0440	0.0357	0.0567	-140.95
P	0.8237	0.0000	0.8237	0.00
R	-0.3793	-0.4059	0.5555	133.06
PHI	-0.0085	0.0815	0.0820	-95.92
PSI	0.0441	-0.0334	0.0553	37.14

# STABILITY PARAMETERS

MODE 1 IS NEUTRALLY STABLE

MODE 2 IS EXPONENTIAL      TIME CONSTANT= 0.592 SEC.

MODE 3 IS EXPONENTIAL      TIME CONSTANT= -175.293 SEC.

MODE 5 IS OSCILLATORY

FREQUENCY= 0.3072HZ (= 1.930RAD/S)      PERIOD= 3.255SEC.



```

UNDAMPED FREQ.= 1.941RAD/S
DAMPING-- ANGLE= 5.92DEG.    RATIO(ZETA)= 0.103
TIME TO HALF-AMP= 3.463SEC.    CYCLES TO HALF-AMP= 1.064
LOG.DEC.= 0.652

```

### 8.6.3 Aircraft Synthesis

The aircraft synthesis program designs the whole aircraft by calling other modules internally, this module gives an input file that is required by PRESPARV and PRENASTRAN in order to model the aircraft. Data such as spar location, ribs layout, kink location, etc. are given in the form of an input file. An example of this file is as follows :

```

AIRBUS 300-B2    lambda = 31
21              sparv_NX
29              sparv_NY
5               nas_NX
26              nas_NY
20              eng_loc
16              spar_percent[1]
28.3            spar_percent[2]
40.5            spar_percent[3]
52.8            spar_percent[4]
65              spar_percent[5]
33.816          Croot_st
21.325          Cb
16.1146         C_kink
5.69377         Ctip
163.755         span
37.8            kink_percent(%)
18.5            fuse_diam(ft)
202.982         dynamic_pressure
10452.3         eng_weight_lb_each
3.75            maximum_g_accltion
0.0             deltay[1]
2.5             deltay[2]
5.0             deltay[3]
7.5             deltay[4]
10.0            deltay[5]
12.5            deltay[6]
15.0            deltay[7]
17.5            deltay[8]
20.0            deltay[9]
22.5            deltay[10]
25.0            deltay[11]
27.5            deltay[12]
30.0            deltay[13]
32.5            deltay[14]
35.0            deltay[15]
37.5            deltay[16]
40.0            deltay[17]
42.5            deltay[18]
45.5            deltay[19]
0.0             deltay[20]eng

```



0.0	deltay[21]
57.5	deltay[22]
60.0	deltay[23]
62.5	deltay[24]
64.0	deltay[25]
0.0	deltay[26]

#### 8.6.4 Aerodynamic

This module is responsible for calculating the pressure load on the wing. Panels are generated by PRESERV module. In the whole process, because of the target of a seamless coupling between the programs, the modelling of the aircraft is difficult to check. Because of that, a stand alone program of PRESERV was built. Just like the stand alone program of PARAMETRIC, this program calls internally a graphics program of Gnuplot. This is used to picture the model of the aircraft. Two stand alone program of PRESERV are built for both SUN and WINDOWS 3.1. This also demonstrates that the target of portability has been achieved.

The results of the PRESERV modelling can be seen from Gnuplot graph below (Fig. 8.11).



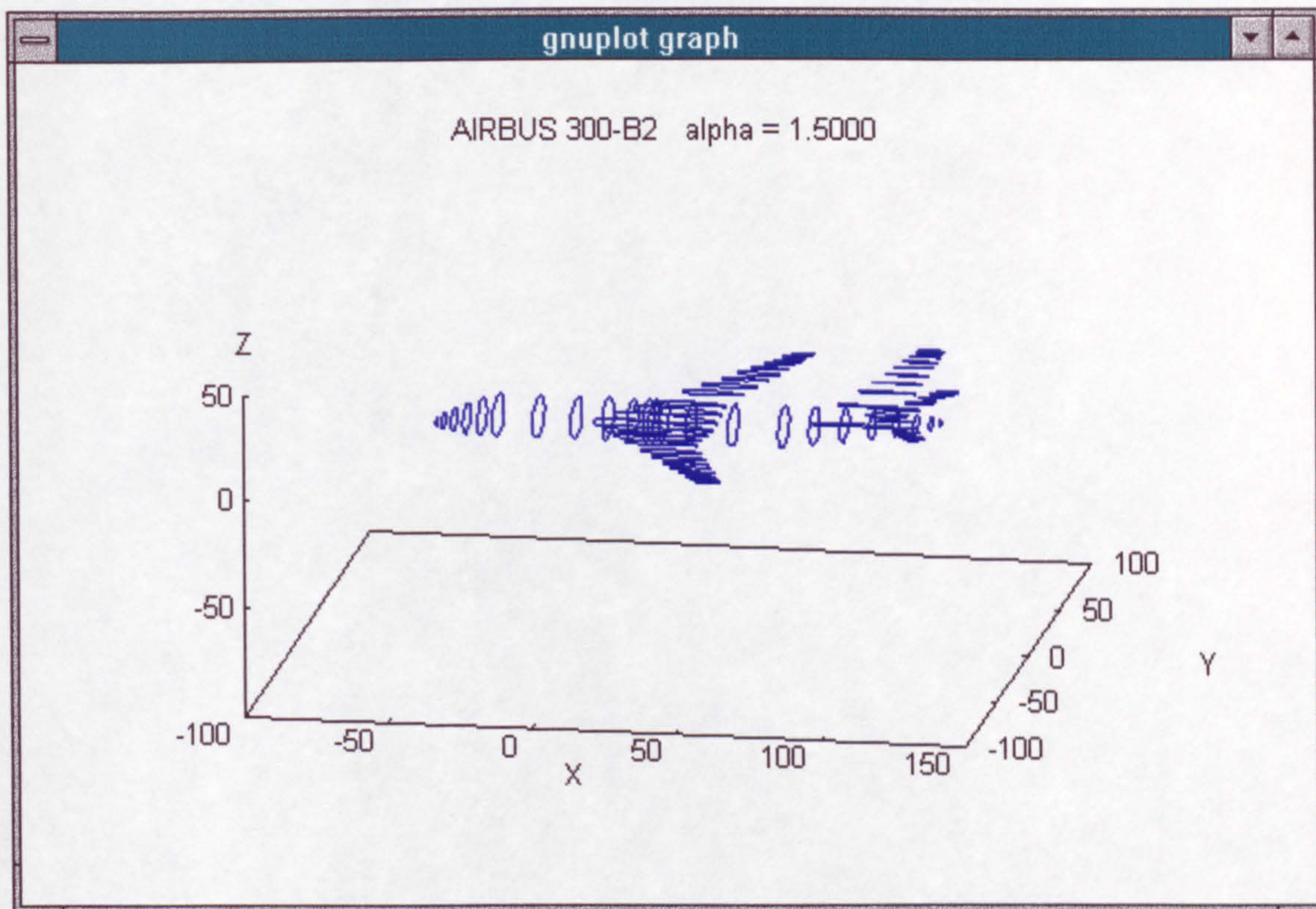


**Figure 8.11** Gnuplot result of PRESPARV

#### 8.6.5 Structure

The structural module is done by using PRENASTRAN module. The result of this module is checked by using XL pre-processor. The results of the modelling can be seen at the next page, Fig. 8.12.



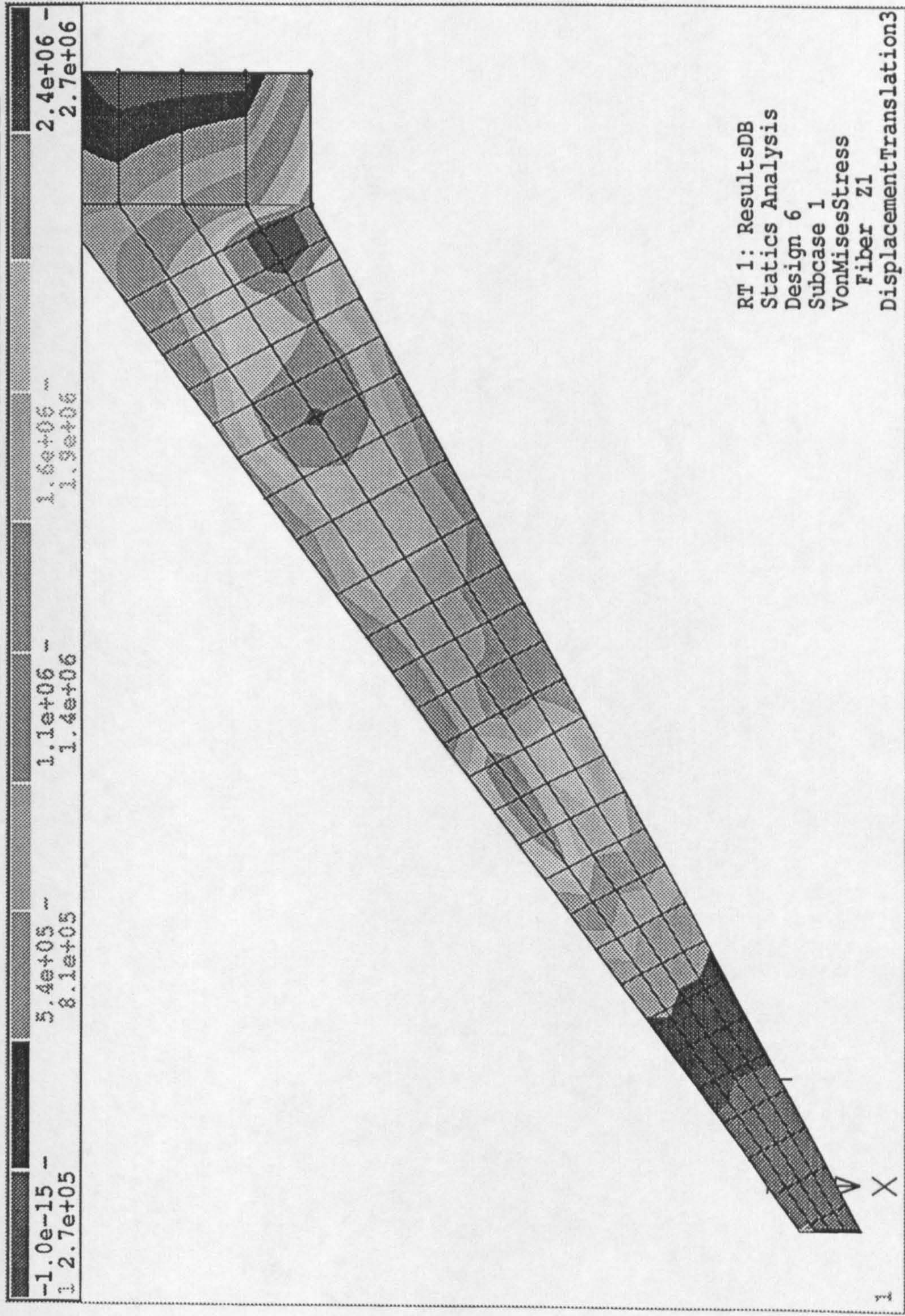
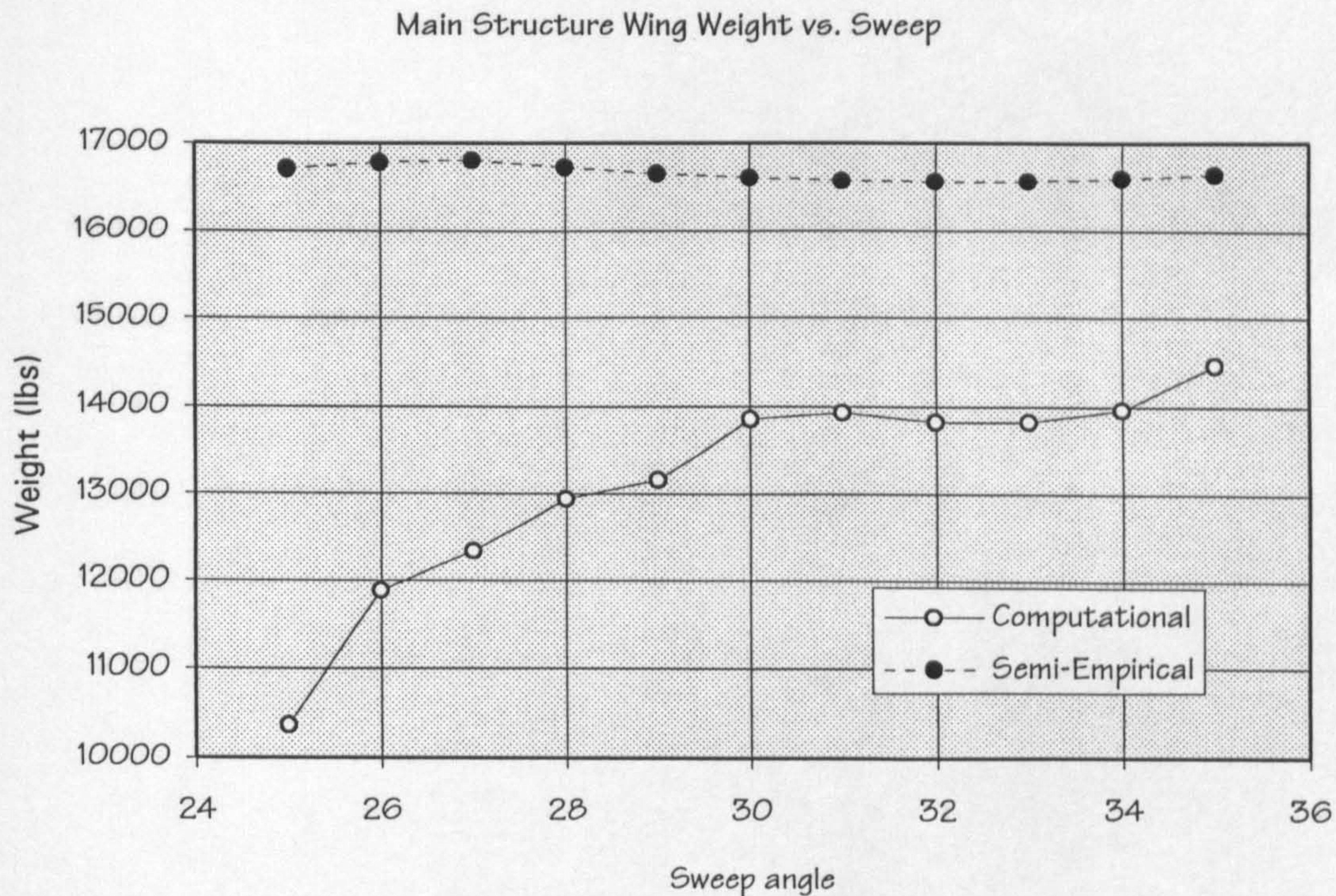


Figure 8.12 XL-pre processor



#### 8.6.6 Comparison with semi-empirical method

In order to give more confidence to the result of the program, a study of the difference between the results obtained from the program and the semi-empirical method was performed. As can be seen on Fig. 8.13, the results from the program (labelled Computational) gives the same tendency for sweep angle higher than 30 deg. This calculation was done by manually setting a particular sweep angle to be calculated by the program. In the actual case a lower sweep angle might not pass the  $M_{CRUISE}$  requirement but it was performed here to give an idea on the weight of the aircraft if the effect of drag rise is ignored. In the actual case, a sweep angle of 32 deg was picked to be the best angle.



**Figure 8.13** Computational vs. Semi-Empirical Method



# *Chapter 9*



## 9. DISCUSSION

The methods used and results achieved are discussed in the relevant parts of the work. The following discussion is therefore limited to an overview of the work.

A methodology for designing high subsonic wings for transport aircraft has been developed. This methodology includes the computational methods in addition to the semi-empirical method. It has demonstrated that computational methods can be linked with semi-empirical methods in a seamless distributed computing environment.

A wing parametric analysis module has been developed which has shown adequate accuracy for the prediction of the wing loading and thrust loading of an aircraft. Although the target is minimum weight, it can be easily changed to other criteria such as direct operating cost. A method for automatically selecting the optimum point in the parametric study has been developed.

The optimisation method in the whole process needs more investigation. Although most of the time was spent in the computational analysis, a better optimisation technique is needed when the initial design stages require more time.

Panel modelling of the computational modules has been studied and modelling techniques have been developed. It is found that the techniques are unique for each computational programs used. Because the computational methods are



treated as black boxes, changing the computational package will probably require different modelling techniques.

The inclusion of computational structural analysis module in the program has been achieved and the benefit of using this has been shown in the form of weight estimation.

The possibilities of running each module manually was developed in order to give the user a way to check how the program is running. By-passing some modules is also possible. This is done when some aircraft geometry is already known.

The aim of portability has been achieved by using portable computer languages and the exclusion of a machine-dependent graphics interface. Graphical output is done by using the GnuPlot program that is available in several computer platforms.

A target of 5PM to 9AM elapsed time for each run has been achieved. However this target is barely achieved on SUN Microsystems. Independent sensitivity studies must be performed first to check the accuracy of the computational modules since the accuracy is a function of number of panels or meshes used in the model. It is set such that the number of panels that the program uses will be enough to accommodate aircraft up to the size of MD-11. For bigger aircraft, more dense panels are needed and the time required is longer than the target.



The ability to modify the original finite element model is introduced in the program. This ability is used when the convergence in the static aeroelasticity study of the wing is not achieved. This is done by introducing a new set of constraints to the finite element model. By setting new constraints, bending and torsional stiffness of the wing are increased and convergence wing is achieved. This capability makes the program able to achieved a limited automated design cycle.

A case study has shown a very good accuracy and shows that the program is working. A limitation was found for designing aircraft with  $M_{CRUISE}$  higher than 0.84. But this limitation comes from the SPARV aerodynamic package rather than the limitation of the program.



# *Chapter 10*



## 10. CONCLUSION

A seamless computing environment for designing high subsonic wings for transport aircraft has been developed. This system uses multi-disciplinary tools to design wings for transport aircraft operating at high subsonic speed.

Computational fluid dynamic and finite element method programs have been coupled with the main aircraft synthesis program. Information from both the computational packages is used in the aircraft synthesis module in addition to the semi-empirical one.

The integration between various modules is carried out by using external files. This is unavoidable since to pass information from the two programs internally requires the linking of the two programs. In the case of NASTRAN and SPARV where the source code is unavailable, the only solution is to use intermediate external files. Although this research work is done on a single computer, by using external files the method permits the sharing of information between applications operating in potentially different environments.

The use of intermediate files gives the possibility of developing independent module that can be executed manually to check the design procedures. This modularity of design allows new programs to be introduced and old ones to be removed without disturbing the whole design program.



The target elapsed time required to run the program is appropriate for designing an aircraft up to the size of MD-11. But as computers become faster everyday, the time required will not be a problem for things to come, even with more powerful computational packages. This will lead to more research on this kind of aircraft design methodology.

The ability to modify a diverged wing in order to make it converge has been achieved. This is done by setting a new set of constraints to the finite element model. NASTRAN SOL-200 optimiser is found to be able to perform the tasks. Setting new constraints can only be achieved by limiting torsion and bending of the wing or limiting the bending only. Limiting the twist (torsion) of the wing only cannot be performed using NASTRAN optimiser.

The computational model has been validated by application to the known wing design and the whole program applied to a test case.

#### Recommendations for further works

- A more powerful CFD code (Euler or Navier-Stokes) is needed in order to get the benefit at higher Mach number.



- Optimisation of the wing spanload distribution can be achieved by modifying the aerofoil section using a more powerful a CFD package, in addition to changing the twist angle.
- The program should be extended to cover a wider range of wing structure design cases.
- Study on limiting the twist of the wing in order to achieved a converged wing should be performed using other structural optimiser programs. NASTRAN finite element program is found unable to do the task.



# *References*



## REFERENCES

1. Raymer, D. P. Aircraft Design : A Conceptual Approach. AIAA Education Series. Washington DC, AIAA 1989.
2. Torenbeek, E. Synthesis of Subsonic Airplane Design. Delft University Press. 1987.
3. Corning, G. Supersonic and Subsonic CTOL and VTOL Airplane Design. University of Maryland, 1982.
4. Alsina, J. Development of an Aircraft Design Expert System. College of Aeronautics, CIT, PhD Thesis 1988.
5. Loftin, L.K. Subsonic Aircraft Evolution and the Matching of Size to Performance, NASA RP 1060, 1980.
6. Simpkin, P. Preliminary Design of Subsonic Civil Aircraft, Cranfield College of Aeronautics. 1993.
7. Collingbourne, J. Multivariate Optimization Applied to the Initial Design of Transport Aircraft. RAE TR 84044, 1984.
8. Nam, S-H. DESAID - The Development of an Expert System for Aircraft Initial Design - CIT, PhD Thesis 1991.
9. Pasaribu, H. An Approach to Configuration Design Synthesis of Subsonic Transport Aircraft Using Artificial Intelligence Techniques, CIT, PhD Thesis 1991.
10. Roskam, J. Airplane Design, University of Kansas. 1989.



11. Nicolai, L. M.            Fundamental of Aircraft Design,  
Dayton, Ohio, 1976.
  
12. Petrie, J. A. H.        SPARV Manual, British Aerospace,  
PLC, 1987.
  
13. Sliwa, S. M.            OPDOT: A Computer program for the  
Optimum Preliminary Design of a  
Transport Airplane. NASA TM 81857,  
1980.
  
14. Lambert, L. (ed)        Jane's All the World's Aircraft.  
Jane's Information Group, 1994.
  
15. Currey, N. S.            Landing Gear Design Handbook,  
Lockheed - Georgia Company, 1982.
  
16. Fulker, J. L.            Aerodynamic Data for 3  
Supercritical Airfoils, RAE 9515,  
9530, 9550. RAE Report No. 3820.  
1975.
  
17. Kuchemann, D.          The Aerodynamic Design of  
Aircraft. Pergamon Press. 1978.
  
18. McRae, D. M.            The Aerodynamic Development of the  
Wing of the A300. Journal of RAeS,  
July 1973.
  
19. Anon.                    The Jet Engines. The Technical  
Publications Department, Rolls  
Royce plc, 1986.
  
20. Stinton, D.             The Design of the Aeroplane, BPS  
1983.
  
21. Jupp, J.                 Wings of Success. Aerospace, June  
1993.
  
22. Gillette, W.,  
    McIntosh, W.            Aircraft Configuration Synthesis.  
Part II: Aerodynamics, BOEING  
Seattle WA. 1979.



23. Kroo, I.                      An Interactive System for Aircraft Design and Optimization. AIAA 92-1190.
  
24. Mason, W. H.                Applied Computational Aerodynamics Case Studies. AIAA 92-2661. 1992.
  
25. Raymer, D. P.                RDS: A PC-based Aircraft Design, Sizing, and Performance System. AIAA 92-4226. 1992.
  
26. Malone, B.,  
Mason, W.                      Multi-disciplinary Optimization in Aircraft Design Using Analytical Technology Models. AIAA 91-3187. 1991.
  
27. Mason, W.,  
Arledge, T. K.                ACSYNT Aerodynamic Estimation - An Examination and Validation for Use in Conceptual Design. AIAA 93-0973. 1993.
  
28. Roskam, J.                    Rapid Sizing Method for Airplanes. Journal of Aircraft, July 1986.
  
29. Petrie, J. A. H.              The Prediction of Aircraft Stability and Control Derivatives by a Subsonic Panel Method. BAe Note YAD 3386, 1980.
  
30. Borland, C. J.,  
Benton, J. R.,  
et al.                          Multi-disciplinary Design Optimization of Commercial Aircraft - An Exploratory Study. AIAA 1994.
  
31. Anon.                        BAC Technical Manual - Reliability handbook, British Aircraft Corporation. 1965.
  
32. Anon.                        Wing Design - Structural Configuration of Transport and Combat Aircraft. Cranfield College of Aeronautics. DES 8854, 1988.



33. Anon. Introduction to Aircraft Structural Layout - Part 2. Cranfield College of Aeronautics. DAeT 9109, 1991.
34. Jupp, J. A. Wings for Airbus - Examples of Integrated Design. ECATA (European Consortium of Advance Training in Aeronautics) Cranfield University, December 1994.
35. Niu, M. C. Y. Airframe Structural Design, Conmilit Press Ltd. 1988.
36. Miura, H. MSC/NASTRAN Handbook for Structural Optimization, MSC Corporation, 1988.
37. Anon. GASP - General Aviation Synthesis Program. NASA CR 152302, 1978.
38. Torenbeek, E. Development and Application of a Comprehensive, Design-Sensitive Weight Prediction Method for Wing Structures of Transport Category Aircraft. Delft Report LR-693, September 1992.
39. Green, G.,  
Swanborough, G.,  
Mowinski, J. Modern Commercial Aircraft. Salamander Books Ltd. 1987.
40. McElhinney, D. M. Designing to Combat Fatigue - Observations on design methods adopted to combat fatigue and its effects on the economics of civil transport, Aircraft Engineering, October 1967.
41. Rodden, W. P.  
(ed.) MSC/NASTRAN Handbook for Aeroelastic Analysis, MSC Corporation, 1987.



42. Anderson. Jr., J. Computational Fluid Dynamics - The Basics with Applications, McGraw-Hill, 1995.
43. Murphy, N. A. D. Analytical Wing Weight Prediction Estimation Using Computer Based Design Techniques, Cranfield College of Aeronautics, PhD Thesis 1987.
44. Hollowell, S., Beeman II, E., Hiyama, R. Conceptual Design Optimization Study. NASA CR 4298, 1990.
45. Torenbeek, E. Optimum Wing Area, Aspect Ratio and Cruise Altitude for Long Range Transport Aircraft. Delft Report LR-775, 1994
46. Triplett, W. Aeroelastic Tailoring of a Forward Swept Wing Comparison with Three Equivalent Aft Swept Wings. AIAA 80-0794, 1980.
47. Mitchell, C. G. B. A Computer Programme to Predict the Stability and Control Characteristics of Subsonic Aircraft. RAE TR 73079, 1973.
48. Wedderspoon, J. R. The High Lift Development of the A320 Aircraft. ICAS 86-2.3.2, 1986.
49. Marx, W. J., Mavris, D., Schrage, D. Integrating Design and Manufacturing for a High Speed Civil Transport Wing. ICAS 94-10.8.4, 1994.
50. Barnum, J., Bathras, C., et al. Advanced Transport Design Using Multi-disciplinary Design Optimisation. AIAA 91-3082, 1991.
51. Ozimek, J. 767-X Airplane Development Status. AIAA 90-3218, 1990.



52. Truckenbrodt, E. How to Improve the Performance of Transport Aircraft by Variation of Wing Aspect Ratio and Twist. ICAS 80-0.1, 1980.
53. Zoontjes, R.,  
Rothwell, A. Wing Design: Program for the Structural Design of a Wing Cross-section. TU Delft Report LR-627, 1990.
54. Anon. VC-10 Series Weight Analysis. British Aircraft Corporation, Weybridge Division, 1967.
55. van Dalen, F.,  
Bil, C.,  
Rothwell, A.,  
Arendsen, P. Finite-Element Based Preliminary Design Procedures for Wing Structures. ICAS 94-9.6.2., 1994.
56. Gallman, J. W. Structural and Aerodynamic Optimization of Joined-Wing Aircraft. PhD Thesis, Stanford University, 1992.
57. Grossman, B.,  
Haftka, R. T.,  
Kao, P-J.,  
Polen, D. M.,  
Rais-Rohani, M.,  
Sobieszczanski-  
Sobieski, J. Integrated Aerodynamic-Structural Design of a Transport Wing. AIAA 89-2129, 1989.
58. Howe, D. Aircraft Wing Estimation. Cranfield College of Aeronautics, 1995.
59. Anon. Example of Preliminary Procedure for a Transport Aircraft Design. DES 8438, Cranfield Institute of Technology, 1984.
60. Anon. Jet Transport Performance Method. D6-1420, BOEING Flight Operations Engineering, 1989,



61. Murthy, S.,  
Paynter, G. Numerical Methods for Engine-Airframe Integration. AIAA Volume 102 Progress in Astronautics and Aeronautics. 1984.
62. Currey, N. Aircraft Landing Gear Design: Principles and Practices. AIAA Education Series, Washington DC, 1988. (See Ref. 15).
63. Anon. A Brief Summary of Aerodynamic Data of Modern Low-Speed, Medium-Speed and High-Speed Airfoil Sections for Application in Subsonic Airplanes Operating at subcritical or supercritical Flight Speeds. Delft Technical University, Volgno 1937, 1986.
64. Anon. Aircraft Mass Prediction - Structural Components. DAeT 9317, Cranfield College of Aeronautics, 1993.
65. Chai, S.,  
Crisafulli, P.,  
Mason, W. Aircraft Centre of Gravity Estimation in Conceptual / Preliminary Design. AIAA 95-3882, Washington DC, 1995.
66. Ashill, P. Modern Wing Aerodynamic Design. DRA Bedford, 1995.
67. Heyma, P. ADAS Implementation of a Panel Method for the Prediction of Aerodynamic Loads. Delft University of Technology, LR-723, 1993
68. Anon. Introduction to Transonic Flow. Cranfield College of Aeronautics Short Course, 1993.
69. Anon. Market Study of Commercial Airplane. Boeing Commercial Aircraft Company, 1988.



70. Anon. Aircraft Leading Data Tables. Cranfield College of Aeronautics, 1995.
71. Anon. Computer Structural Analysis. DES 8818, Cranfield College of Aeronautics, 1988.
72. Coen, G.,  
Sobieszczanski-  
Sobieski, J.,  
Dollyhigh, S. M. Preliminary Results from the High Speed Airframe Integration Research Project. AIAA 92-1004, Washington D.C., 1992.
73. Sobieszczanski-  
Sobieski, J., An Integrated Computer Procedures for Sizing Composite Airframe Structures. NASA TP 1300, 1979.
74. Logan, T.,  
Sobieszczanski-  
Sobieski, J.,  
Abdi, F., Optimization of Aircraft Configurations in a Multi-disciplinary Environment. ICAS 90.2.3.2., Sweden 1990.
75. Sobieszczanski-  
Sobieski, J. Multidisciplinary Design Optimization. AGARD-LS-186, May 1992.



# *Appendix A*



## A. PARAMETRIC STUDY

### A.1 Introduction

In this appendix the details of the parametric module used in the program are explained. As mentioned in Chapter 3, the basic module is based on work by Loftin (Ref. 5) and with some modification on the semi-empirical data based on current aircraft.

Work has been done on how to select the optimum point by calculating the weight for each of all possible results. More criteria are added to the original work of Loftin such as the ICAC (Initial Cruise Altitude Capability) and the OEI (One Engine Inoperative) criteria.

An example of the input and output files of the module, with the explanation is also included in this appendix.

### A.2 Parametric Study Criteria

In order to find the optimum ( $W/S$ ) and ( $T_o/W$ ), several criteria have to be fulfilled in order to achieve the Design Objectives and Requirements. These Criteria are :

- Landing Field Length
- Take Off Field Length
- Second Segment Climb
- Missed Approach
- Cruise Performance



- ICAC (Initial Cruise Altitude Capability)
- OEI (One Engine Inoperative) Ceiling

### A.2.1 Landing Field Length

The Landing Field Length (LFL) criteria effects the (W/S) because (W/S) is a function of  $V_A$  and  $C_{L,A}$ . By knowing the LFL,  $V_A$  can be calculated based on the empirical data. The value is calculated as below :

$$\frac{W_G}{S} = \frac{W_L}{S} \times \frac{W_G}{W_L}$$

$$\text{where } \frac{W_L}{S} = \left( \frac{V_A}{17.15} \right)^2 \times \sigma \times C_{L,A}$$

$$C_{L,A} = \left( \frac{C_{L,MAX L}}{1.3^2} \right)$$

$$\text{for wide body aircraft } V_A = \sqrt{\frac{LFL}{0.3}}$$

$$\text{for narrow body aircraft } V_A = \sqrt{\frac{LFL}{0.265}}$$

### A.2.2 Take Off Field Length

The FAR Take Off Field Length (TOFL) often called the FAR balanced field length, contains certain safety features to account for engine failure situations. Briefly, if an engine fails during take off roll at decision speed  $V_1$ , the sum of the distance required to accelerate to  $V_1$  and then decelerate to stop is the same as the total distance for the case in which the take off is continued following engine failure at  $V_1$ .



In order to achieve TOFL that fulfils this criteria, there is a certain relationship between  $(W/S)$  and  $(T_o/W)$  that can be generated.

$$\frac{W_g/S}{T_o/W_g} = TOP \times \sigma \times C_{L,T}$$

where  $TOP = \text{Take Off Parameter} = \frac{W_g/S}{\sigma C_{L,T}(T_o/W_g)}$

TOP is calculated from the empirical data of current aircraft from the linear relationship between TOP and FAR take off field length. It is found that  $TOP = \frac{TOFL}{37.5}$ .

By knowing the target of TOFL and the maximum lift coefficient during take off, the slope of  $(W/S)$  and  $(T_o/W)$  can be found.

### A.2.3 Second Segment Climb Gradient

This is an FAR criterion where in the event of engine failure the aircraft must be able to sustain a certain climb with flap in the take off setting and undercarriage retracted.



These required climb gradients are :

Table A.1      Climb gradient requirement

number of engine	climb gradient required
2	2.4 %
3	2.7 %
4	3.0 %

This criterion effecting the  $(T_o/W)$  of the aircraft and depends on the number of engines, aspect ratio, and climb lift coefficient  $C_{L,2}$ .

where  $C_{L,2} = \frac{C_{L,T}}{1.2^2}$

Empirical data on the relationship between AR, number of engine and  $C_{L,2}$  is available and can be found in Ref. 5.

#### A.2.4 Missed Approach

This criterion is in relation to the landing manoeuvre. This is the situation when the aircraft aborts a landing attempt. Power is applied and the aircraft climbs for another landing attempt. The aircraft is in the approach condition with flaps, slats, and undercarriage down.

A simple relation during climb can be found as:

$$T = D + W \sin \gamma$$



where         $T$         = Thrust  
                   $D$         = Drag  
                   $W$         = Weight  
                   $\gamma$         = flight path angle.

for small flight path angle,  $\sin \gamma$  is equal to  $\gamma$  which can be expressed in gradient.

In order for the climb gradient criteria to be satisfied with one engine inoperative, the  $(T_o/W)$  of the aircraft can be generated as :

$$\frac{T_o}{W_L} = \left( \frac{N}{N - 1} \right) \left( \frac{1}{L/D} \right) + \gamma$$

where         $N$         = Number of Engine

The value of the required climb gradient  $\gamma$  is the same as in the previous section as mentioned in Table A.1.

This calculation is done iteratively as the lift and drag can only be calculated if the whole aircraft geometry is known.

#### **A.2.5 Cruise Performance**

This is the case for optimising the engine with the airframe to permit the achievement of a required range at a given cruise Mach number for a minimum amount of fuel.



This criterion is basically generated from the Breguet Range equation :

$$R = \frac{V(L/D)}{c} \log_e \frac{1}{1 - (W_f/W_g)}$$

where

R	= Range (n. miles)
V	= speed (knots)
L/D	= aircraft lift-drag ratio
c	= engine specific fuel consumption (lb/lb/hr)
$W_g$	= Aircraft gross weight (lb)
$W_f$	= Aircraft fuel weight (lb)

Various empirical relations are used to calculate this criteria such as the relationship between engine by-pass ratio, Mach number, and altitude to the Thrust ratio ( $T_c/T_o$ ).

Just like the previous criteria, L and D of the aircraft can only be calculated when the aircraft geometry is known, thus this calculation needs to be done iteratively in order to generate the relation between ( $T_o/W$ ) and ( $W/S$ ).

An assumption is made as to whether the aircraft actually cruises at maximum (L/D). It is suggested by Ref. 59 that cruising at maximum (L/D) would be too optimistic and a value of 97% of (L/D) is suggested to be used.



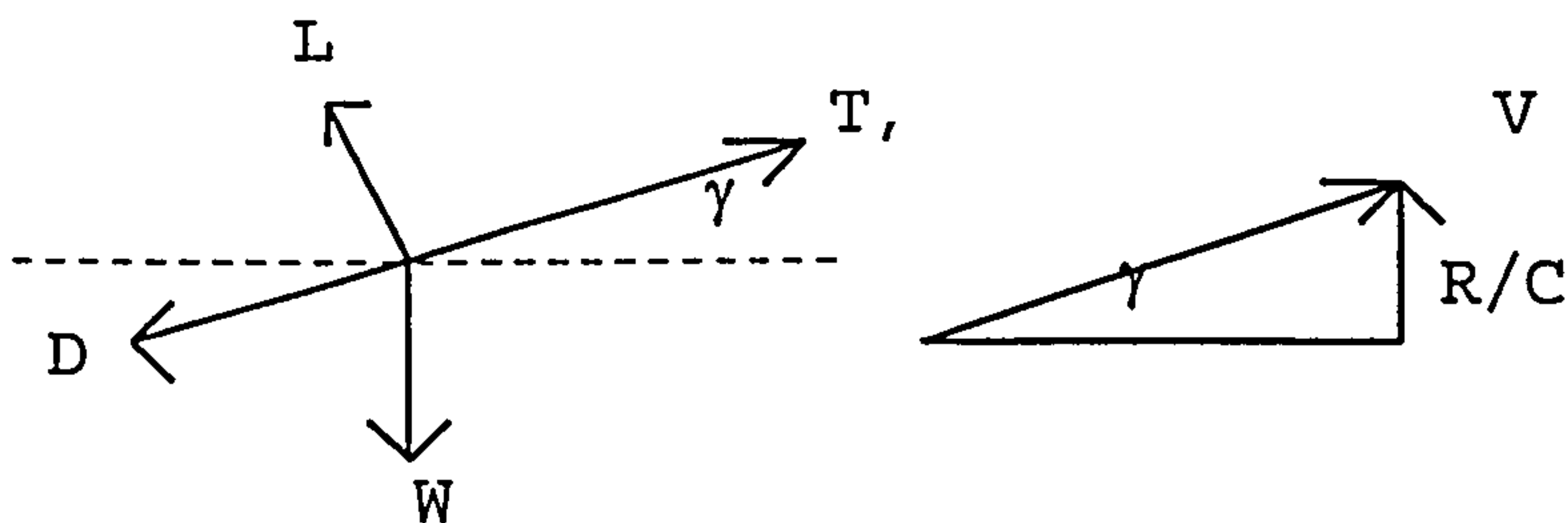
A.2.6 Initial Cruise Altitude Capability (ICAC)

Initial Cruise Altitude Capability (ICAC) is defined as the ability to sustain a certain rate of climb at the top of climb altitude (Ref. 6). The engine is at maximum climb rating and the aircraft at the cruise Mach number. Ref. 6 suggests the ability to climb at the climb rate of 300 fpm to be used for a high subsonic transport aircraft and the initial altitude is at least 2,000 ft above the optimum cruise line.

From the climb equation :

$T = D + W \sin \gamma \dots\dots\dots (A.1)$

- where        T        = Maximum Climb Thrust
- D        = Drag at  $M_{CRUISE}$  and 0.98 TOW
- W        = 0.98 Take Off Weight



from the diagram above, it can be seen that :

$\sin \gamma = \frac{(R / C)}{V} \dots\dots\dots (A.2)$

- where        R/C = Rate of Climb
- V     = True Air Speed



from these equations, the relationship between  $(T_o/W)$  and  $(W/S)$  can be generated and iterative process need to be done to calculate the drag.

Combining equation. A.1 and A.2 the equation of  $(T/W)$  can be generated as follows:

$$\begin{aligned}
 T &= D + W \frac{(R / C)}{V} \quad , \text{dividing with } W \\
 \frac{T}{W} &= \frac{D}{W} + \frac{(R / C)}{V} \dots\dots\dots (A.3)
 \end{aligned}$$

This equation does not give the function between  $(T_o/W)$  vs.  $(W/S)$  directly, can be calculated iteratively to give the relation between those two variables because drag is a function of wing area  $S$ .

**A.2.7 One Engine Inoperative (OEI) Ceiling**

This is a case wit an engine failure and the aircraft is still capable of achieving a certain altitude. Ref. 6 suggests a typical ceiling of 16,000 ft. This criteria is calculated from the equation :

$$\begin{aligned}
 T_c &= D \quad \text{by dividing by Weight} \\
 T_c/W &= 1/(L/D)
 \end{aligned}$$

where  $T_c$  = thrust at required altitude.  
 $W$  = weight after engine failure



This is calculated iteratively to find the relation between  $(W/S)$  and  $(T_o/W)$  since engine thrust at sea level  $T_o$  depends  $T_c/T_o$  which depends on altitude.  $(W/S)$  in this case can be generated from the variable  $(L/D)$  where during cruise condition  $W = L$ , and drag is a function of wing area  $S$ .

### A.3 Method for finding optimum point

From these criteria mentioned in previous section, the optimum point for  $(W/S)$  and  $(T_o/Wg)$  needs to be found. As a rule of thumb the aircraft needs to maximise wing loading  $(Wg/S)$  and minimise thrust loading  $(T_o/Wg)$ . But it is rather difficult in reality where there are several possibilities for optimum points. In real life the optimum point is needed to be found based on other criteria such as weight. The point picked as an optimum point is the condition where the combination of  $(T_o/W)$  and  $(W/S)$  gives the minimum weight for the aircraft.

For this reason, the equal weight lines need to be generated and overlaid on the  $(T_o/W)$  vs.  $(W/S)$  plot. As can be seen from the graph below (Fig. A.1), it is clearly seen that the optimum point picked is the minimum weight for the aircraft.



# PARAMETRIC STUDY OF AIRBUS 310-300 CF6-80C2-A2

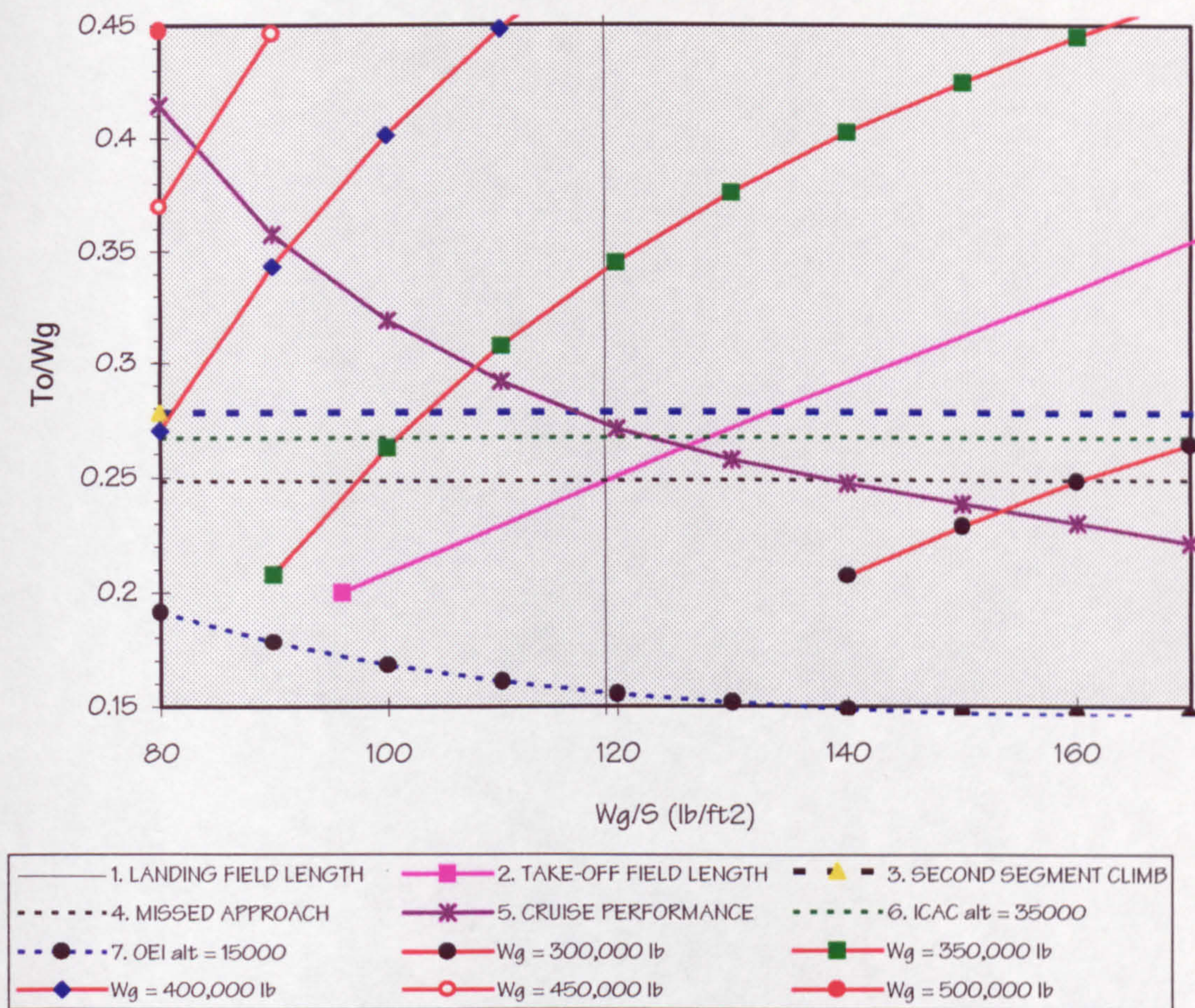


Figure A.1 Parametric Study

## A.4 Parametric Study Input File

The aircraft design process starts with the Design Requirements of the aircraft. Together with the program's own input requirements these data have to be inputted into the input file. An example of input file can be seen below :



Table A.2 Parametric Study Example Input File

BOEING 767-200C CF6-80C2-B2A	
2.4	Cl_max_l
2.2	Cl_max_to
0.863	Wl/Wg
0.99	percent_LDmax
4800.0	LFL(ft)_or_Vapp(knots)
5800.0	TOFL(ft)
2	n_engine
6.0	BPR_(By_Pass_Ratio)
3050.5	S(ft2)
16.5	fuse_diam(ft)
155.0	fuse_length(ft)
0.8	M_cruise
34.1	C_root(ft)
39000.0	cruise_alt(ft)
1	num_AR
8.0	first_AR
2.0	delta_AR
5	num_Wg/S
80.0	first_Wg/S(lb/ft^2)
10.0	delta_Wg/S(lb/ft^2)
1	num_ICAC_altitude
40000.0	first_ICAC_altitude(ft)
2000.0	delta_ICAC_altitude(ft)
3.0	fuel_burnt_during_climb_(%_TOW)
300.0	Rate_of_Climb(ft/min)
1	num_OEI_altitude
15000.0	first_OEI_altitude(ft)
1000.0	delta_OEI_altitude(ft)
0.55	Mach_OEI
290	num_pax
6120.0	Range(n.miles)
0.85	M_max
1	engine_on_wing_?
1	fuel_on_CW_Tank_?
0.0	sfc_(lb/hr/lb)
0.267	taper
28.0	lambda
18.0	t_per_c_root



Table A.3 Input Variables for Parametric Study

BOEING 767-200C CF6-80C2-B2A	Title of the project
Cl_max_l	Cl_max on landing (optional)
Cl_max_to	Cl_max on take-off (optional)
Wl/Wg	ratio of landing and gross weight (optional)
percent_LDmax	cruise at what percentage of L/D max.
LFL(ft)_or_Vapp(knots)	Landing Field Length or approach speed at standard ISA.
TOFL(ft)	Take Off Field Length required.
n_engine	number of engine (optional)
BPR_(By_Pass_Ratio)	engine By-Pass Ratio
S(ft2)	Wing Area (optional)
fuse_diam(ft)	Fuselage diameter (optional)
fuse_length(ft)	Fuselage length (optional)
M_cruise	Cruise Mach number
C_root(ft)	Chord length at wing root (optional)
cruise_alt(ft)	cruise altitude
num_AR	number of Aspect Ratio to be studied
first_AR	first AR
delta_AR	difference to the next AR
num_Wg/S	number of Wing Loading to be studied
first_Wg/S(lb/ft^2)	first Wg/S
delta_Wg/S(lb/ft^2)	difference to the next Wg/S
num_ICAC_altitude	number of Initial Cruise Altitude Capability to be studied
first_ICAC_altitude(ft)	first ICAC
delta_ICAC_altitude(ft)	difference to the next ICAC
fuel_burnt_during_climb_(%_TOW)	percentage of fuel burnt during climb
Rate_of_Climb(ft/min)	Rate of Climb
num_OEI_altitude	number of One Engine Inoperative to be studied
first_OEI_altitude(ft)	first OEI
delta_OEI_altitude(ft)	difference to the next OEI
Mach_OEI	Mach number with one engine inoperative
num_pax	number of Passenger
Range(n.miles)	Range
M_max	Maximum mach number
engine_on_wing_?	1 = engine on wing
fuel_on_CW_Tank_?	1 = fuel on Central Wing
sfc_(lb/hr/lb)	specific fuel consumption
taper	taper ratio
lambda	initial sweep angle of the wing
t_per_c_root	initial thickness ratio at root chord

Note :  
variable with (optional) mark is an option.  
0.0 should be inputted if the variable need to be calculated by the program.



A.5 Parametric Study Output File

Table A.4 Parametric Study Example Output File

```
*****
*
*          PARAMETRIC
*    program for initial parametric study
*
*          developed based on
*
*    [1] Loftin, L. K., Subsonic Aircraft: Matching of
*          Size to Performance
*    [2] Raymer, D. P., Aircraft Design: A Conceptual
*          Approach
*    [3] Corning, G., Supersonic and Subsonic CTOL
*          and VTOL Airplane Design
*    [4] Simpkin, P., Preliminary Design of Subsonic
*          Civil Aircraft
*
*
*          by
*
*          Demil Y. Djafri
*          July 1994
*
*****
```

AIRBUS 310-300 CF6-80C2-A2

FIRST LOOP OF PARAMETRIC STUDY

```
cruise_alt = 37000.000 ft
temperature = 390.000 R
speed_of_sound = 967.955 ft/s
V_cruise = 458.801 knots
```

1. LANDING FIELD LENGTH

```
Wg/S = 118.991

V_approach = 127.148
Cl_app      = 1.775
Wl_per_s    = 97.572
```

2. TAKE-OFF FIELD LENGTH

```
Wg/S    To / Wg
80.000  0.167
90.000  0.187
100.000 0.208
110.000 0.229
120.000 0.250
130.000 0.271
140.000 0.292
150.000 0.312
160.000 0.333
170.000 0.354

slope_TOP = 480.000
```

3. SECOND SEGMENT CLIMB

```
AR      To/Wg
8.800   0.278
```



Cl\_2 = 1.667

4. MISSED APPROACH

AR	To/Wg
8.800	0.248

5. CRUISE PERFORMANCE

AR	L/D max Cl,m	Cdo_ref
8.800	18.466 0.636	0.017

temp_cruise	= 390.000 R
temp_35	= 393.960 R

rho_cruise	= 0.676 x 10^-3 slug/ft^3
rho_35	= 0.739 x 10^-3 slug/ft^3

V_cruise	= 458.801 knots
V_cruise_35	= 422.066 knots

L\_bar = 0.728

Cl\_bar max. = 1.000

REYNOLD'S NUMBER CORRECTION

AR	L/D	Cl,max	Cd_o
8.800	17.983	0.636	0.018

Cl\_bar = 0.868

CRUISING AT 0.990 L/D MAX.

AR	L/D	Cl,max	Cd_o
8.800	17.803	0.552	0.018

AR	L/D	Cl	Cl*M2	Wg/S	altitude
8.800	17.803	0.552	0.353	80.000	43978.703
8.800	17.803	0.552	0.353	90.000	41528.992
8.800	17.803	0.552	0.353	100.000	39337.652
8.800	17.803	0.552	0.353	110.000	37355.340
8.800	17.803	0.552	0.353	120.000	35602.273
8.800	17.803	0.552	0.353	130.000	33913.281
8.800	17.803	0.552	0.353	140.000	32326.393
8.800	17.803	0.552	0.353	150.000	30828.762
8.800	17.803	0.552	0.353	160.000	29409.889
8.800	17.803	0.552	0.353	170.000	28061.082

AR	L/D	Tc/To	To/Wg	Wg/S	altitude
8.800	17.803	0.135	0.415	80.000	43978.703
8.800	17.803	0.157	0.358	90.000	41528.992
8.800	17.803	0.176	0.319	100.000	39337.652
8.800	17.803	0.193	0.291	110.000	37355.340
8.800	17.803	0.207	0.271	120.000	35602.273
8.800	17.803	0.219	0.257	130.000	33913.281
8.800	17.803	0.227	0.247	140.000	32326.393
8.800	17.803	0.236	0.238	150.000	30828.762
8.800	17.803	0.245	0.230	160.000	29409.889
8.800	17.803	0.254	0.221	170.000	28061.082

6. INITIAL CRUISE ALTITUDE CAPABILITY

L_per_D	= 17.803	
Weight	= 280461.031	lbf
S wing	= 2357.000	ft^2



Cl\_cruise = 0.552  
 prcnt\_init\_cruise = 0.970  
 Rate of Climb = 300.000 ft/min

ICAC at 35000.000 ft

speed\_of\_sound at 35000.000 ft = 972.856 ft/s  
 V\_cruise\_ICAC = 778.285 ft/s  
 V\_cruise\_ICAC = 46697.105 ft/min  
 Tc / To at 35000.000 ft = 0.213

AR	Wg/S	To/Wg	S	weight	Cd	Cl	D	T/W
8.800	80.000	0.267	5055.880	404470.375	0.034	0.350	0.728	0.267
8.800	90.000	0.267	4166.667	375000.094	0.034	0.394	0.728	0.267
8.800	100.000	0.267	3555.974	355597.438	0.035	0.438	0.728	0.267
8.800	110.000	0.267	3107.202	341792.188	0.035	0.482	0.728	0.267
8.800	120.000	0.267	2762.064	331447.688	0.035	0.526	0.728	0.267
8.800	130.000	0.267	2487.683	323398.781	0.036	0.570	0.728	0.267
8.800	140.000	0.267	2263.955	316953.750	0.036	0.613	0.728	0.267
8.800	150.000	0.267	2077.845	311676.813	0.036	0.657	0.728	0.267
8.800	160.000	0.267	1920.473	307275.750	0.037	0.701	0.728	0.267
8.800	170.000	0.267	1785.587	303549.813	0.037	0.745	0.728	0.267

## 7. ONE ENGINE INOPERATIVE CEILING

OEI Altitude = 15000.000 ft

AR	Cl OEI	Cl_bar	L/D	Altitude	Wg/S	To/Wg
8.800	0.316	0.462	13.081	15000.000	80.000	0.191
8.800	0.356	0.520	14.060	15000.000	90.000	0.178
8.800	0.395	0.578	14.879	15000.000	100.000	0.168
8.800	0.435	0.635	15.551	15000.000	110.000	0.161
8.800	0.474	0.693	16.085	15000.000	120.000	0.155
8.800	0.514	0.751	16.496	15000.000	130.000	0.152
8.800	0.553	0.809	16.798	15000.000	140.000	0.149
8.800	0.593	0.866	17.003	15000.000	150.000	0.147
8.800	0.632	0.924	17.125	15000.000	160.000	0.146
8.800	0.672	0.982	17.176	15000.000	170.000	0.146

## POSSIBLE OPTIMUM POINT

Wg/S	To/Wg	Weight (lbf)	
118.991	0.248	323621.188	0
118.991	0.278	331706.500	1
118.991	0.248	323750.313	0
118.991	0.273	330242.031	0
118.991	0.267	328649.438	0
118.991	0.078	284976.031	0
133.558	0.278	320349.063	0
119.231	0.248	323542.313	0
125.997	0.262	321698.125	0
128.139	0.267	321246.688	0
0.000	0.000	0.000	0
0.000	0.000	0.000	0
116.388	0.278	334201.000	1
0.000	0.000	0.000	0
0.000	0.000	0.000	0
138.537	0.248	310081.813	0
0.000	0.000	0.000	0
0.000	0.000	0.000	0
122.765	0.267	325399.094	0
0.000	0.000	0.000	0
0.000	0.000	0.000	0



# POSSIBLE OPTIMUM POINT

Wg/S	To/Wg	Weight (lbf)	VALID ?
118.991	0.248	323621.188	0
118.991	0.278	331706.500	1
118.991	0.248	323750.313	0
118.991	0.273	330242.031	0
118.991	0.267	328649.438	0
118.991	0.078	284976.031	0
133.558	0.278	320349.063	0
119.231	0.248	323542.313	0
125.997	0.262	321698.125	0
128.139	0.267	321246.688	0
0.000	0.000	0.000	0
0.000	0.000	0.000	0
116.388	0.278	334201.000	1
0.000	0.000	0.000	0
0.000	0.000	0.000	0
138.537	0.248	310081.813	0
0.000	0.000	0.000	0
0.000	0.000	0.000	0
122.765	0.267	325399.094	0
0.000	0.000	0.000	0
0.000	0.000	0.000	0

## INPUT DATA or UPDATED INPUT DATA ARE :

title	=	AIRBUS 310-300 CF6-80C2-A2
Cl_max_l	=	3.000
Cl_max_to	=	2.400
Wl_per_Wg	=	0.820
percent_LDmax	=	0.990
LFL	=	4850.000 ft
TOFL	=	7500.000 ft
n_engine	=	2
BPR	=	5.050
S	=	2650.579 ft^2
fuse_diam	=	18.500 ft
fuse_length	=	148.100 ft
M_cruise	=	0.800
C_root	=	28.100 ft
V_cruise	=	458.801 knots (function of M_cruise and cruise_alt)
cruise_alt	=	37000.000 ft
num_AR	=	1
first_AR	=	8.800
delta_AR	=	1.000
num_Wg_per_S	=	10
first_Wg_per_S	=	80.000
delta_Wg_per_S	=	10.000
num_ICAC_altitude	=	1
first_ICAC_altitude	=	35000.000
delta_ICAC_altitude	=	2000.000
prcnt_fuel_burned	=	3.000
Rate of Climb	=	300.000
num_OEI	=	1
first_OEI	=	15000.000
delta_OEI	=	1000.000
Mach_OEI	=	0.550
num_pax	=	280.000
Range	=	5200.000
M_max	=	0.840



ENGINE_WING	= 1
Fuel_on_CW	= 1
sfc	= 0.650
taper	= 0.333
lambda	= 28.000
t_per_c_mass	= 18.000



Weight Lines :

To/Wg \ Wg/S	80.000	90.000	100.000	110.000	120.000	130.000	140.000	150.000	160.000	170.000
0.200	371374.313	347432.281	331309.313	319676.563	310872.875	303973.875	298420.031	293857.750	290030.688	286783.969
0.250	391064.500	363937.344	345907.594	333005.375	323298.219	315723.219	309645.281	304657.750	300492.844	296963.500
0.300	413259.219	382254.469	361950.906	347562.500	336806.719	328452.219	321773.281	316309.500	311756.656	307905.250
0.350	438527.250	402707.625	379704.688	363534.406	351553.281	342296.469	334925.344	328915.906	323919.188	319701.719
0.400	467650.906	425752.969	399396.563	381150.063	367725.406	357413.781	349241.188	342605.094	337095.219	332459.125
0.450	501729.000	451963.844	421483.250	400695.531	385549.469	373997.188	364886.500	357513.063	351423.344	346302.000
0.500	542348.938	482120.813	446432.781	422529.469	405310.875	392281.469	382066.250	373835.500	367080.750	361379.500

\*\*\*\*\*  
To / Wg optimum = 0.278  
Wg / S optimum = 118.991  
Weight = 331706.500 lbf  
\*\*\*\*\*



## A.6 PARAMETRIC stand alone program

As mentioned earlier, a stand alone program which links to the 'GnuPlot' program was developed in order to give a tool to check the procedures used in the wing parametric program. This program can be run manually and can plot the results on screen instantaneously so the operator can check the results.



# *Appendix B*



## B. WING LAYOUT CALCULATIONS

### B.1 Introduction

In this appendix the method used in the wing layout module is explained. An example of the required input files for the wing layout modules, and an example of the output file are also given in this appendix.

The method used is explained in chapter 3 and the detail on the wing design method used is shown in chapter 4.

### B.2 Wing Layout input files

Because this module runs other modules such as the Mitchell stability and control program, the required input files are for both Mitchell and winglayout modules.

The required input files are :

- aerofoil.dat
- aerofoil\_file, ".DAT"
- relative.dat
- parmtric.dat
- fuse.dat        ----- for mitchell and presparv
- vtp.dat        ----- for mitchell
- htp.dat        ----- for mitchell
- engine.dat     ----- for mitchell
- line12.dat     ----- for mitchell
- line13.dat     ----- for mitchell



- line14.dat ----- for mitchell
- line16.dat ----- for mitchell

Example of each input file are as follows :

Table B.1      Example of AEROFOIL.DAT

4 number_of_aerofoil
rae9515
rae9530
rae9550
nacasc2

This is to give the number of aerofoil to be used and the file name of each aerofoil data.



Table B.2            Example of RAE9515.DAT

RAE9515					
1.030	Clmax_low_speed				
0.9530	Cl_at_1_deg_after_stall/Cl_stall				
Cd_at_given_Cl_Cruise_and_M_cruise					
M\Cl	0.3	0.4	0.5	0.6	0.7
0.5	0.0105	0.0111	0.0114	0.0144	0.0158
0.6	0.0106	0.0118	0.0132	0.0152	0.0166
0.7	0.0110	0.0120	0.0136	0.0164	0.0178
0.8	0.0136	0.0136	0.0138	0.0172	0.0184
0.9	0.0253	0.0290	0.0252	0.0305	0.0319
Cm_at_given_Cl_Cruise_and_M_cruise					
M\Cl	0.3	0.4	0.5	0.6	0.7
0.5	-0.080	-0.080	-0.080	-0.080	-0.080
0.6	-0.086	-0.084	-0.084	-0.082	-0.081
0.7	-0.094	-0.094	-0.090	-0.090	-0.088
0.8	-0.116	-0.115	-0.116	-0.136	-0.160
0.9	-0.136	-0.135	-0.136	-0.150	-0.180
Mdd	Cl_cruise				
0.80	0.3				
0.81	0.4				
0.80	0.5				
0.79	0.6				
0.77	0.7				
0.5793	fuel_capacity				
0.88	Cl_stall_highspeed				

The purpose of this file is to give aerofoil characteristics, such as lift coefficient, drag coefficient, etc.



**Table B.3            Example of RELATIVE.DAT**

Category	rel imp	rel_diff
cl_max	10	0.2
stall	10	0.1
cd_min	15	0.0050
cm	10	0.05
Mdd	30	0.1
Fuel	10	0.0333

This file gives the sensitivity of each criteria for selecting the best aerofoil section.

**Table B.4            Example of FUSE.DAT**

17	fuse_NX_A300
25	fuse_NY
65.8	B1 (fuse_paralel_aft_datum)
32.9	B2 (fuse_paralel_fwd_datum)
120.7	B3 (fuse_length_aft_datum)
54.9	B4 (fuse_length_fwd_datum)
18.5	B5 (fuse_height)
18.5	B6 (fuse_width)
2.2	B7 (wing_apex_below_datum)
28.4	B8 (main_u/c_aft_datum)
0.0	B9 (body_incidence_on_ground)
6	seat_abreast

This file is an optional, if not given, the program will generate by using an internal fuselage program.



Table B.5 Example of VTP.DAT

rae101c.dat	aerofoil_file
13	VTP_NX_number_of_point_in_x
11	VTP_NY_number_of_point_in_y_(must_be_odd)
70.3	V1_distance_aft_datum_ALL_IN_FEET
30.7	V2_chord_root
8.8	V3_chord_tip
43.0	V4_Sweep_LE
37.3	V5_height(semi_span)
0.0	V6_HTP_height
0.1	V7_(t/c_ave)
2.2	V8_body_height_at_0.25c
8.6	V9_Croot_HL
2.46	V10_Ctip_HL
11.0	V11_rudder_i/b
36.2	V12_rudder_o/b
25.0	V13_rudder_limit
0.0	V14_Croot_tab
0.0	V15_Ctip_tab
0.0	V16_lower_tab
0.0	V17_upper_tab
1.0	V18_gear_ratio(1)
10.0	t_per_c_tip
10.0	t_per_c_kink
10.0	t_per_c_root
24.2	chord_kink
41.0	25%_sweep
37.8	kink_percent
4.53	above_datum_ft



**Table B.6**      **Example of HTP.DAT**

rae101c.dat	aerofoil_fileA300
11	HTP_NX_number_of_point_in_x
13	HTP_NY_number_of_point_in_y_(must_be_odd)
94.4	H1_apex_aft_datum
15.4	H2_chord_root
7.7	H3_chord_tip
39.5	H4_sweep_LE
26.3	H5_semispan
3.85	H6_root_chord_HL
1.925	H7_tip_chord_HL
5.26	H8_semispan_to_i/b
25.5	H9_semispan_to_o/b
0.10	H10_(t/caverage)
-3	H11_incidence
-25.0	H12_elevator_up_limit
10.0	H13_elevator_down_limit
-10.0	H14_HTP_up_limit
5.0	H15_HTP_down_limit
0.0	H16_Croot_tab
0.0	H17_Ctip_tab
0.0	H18_lower_tab
0.0	H19_upper_tab
1	H20_gear_ratio(1)
10.0	t_per_c_tip
10.0	t_per_c_kink
10.0	t_per_c_root
13.12	chord_kink
33.0	25%_sweep
0.0	twist_angle
25.0	kink_percent
9.9	above_datum_ft
2.0	htp_dihedral



Table B.7    Example of ENGINE.DAT

28.6	E1_distance_from_CL_A300
5.6	E2_CG_aft_datum
8.8	E3_Thrustline_below_datum
19667	E4_thrust_of_one_engine_sea_level_lb
0.0	E5_(lb)_at_speed_V(ft/s)
0.0	E6_T=E4+E5*V+E6V**2
8.8	E7_distance_of_nose_nacelle_to_LE
6.6	E8_nacelle_diameter.
1	E9_=1_if_wing_mounted

B.3 Wing Layout output file

The example of the output file from WINGLAOUT.EXE are as follows :

Table B.8    Wing Layout Example Output File

```
BOEING 757-200 PW 2037

SWEEP (3D) EFFECT
Sweep  t/c eff t/c root t/c eff Simp  t/c rt Simp Cl_cr M_cr
15.0000 10.0304 10.4872          11.6337 12.1635 0.4638  0.8000
20.0000 10.1745 10.6379          13.0425 13.6365 0.5122  0.8000
25.0000 10.3608 10.8327          14.4561 15.1144 0.5603  0.8000
30.0000 10.5903 11.0726          16.0650 16.7967 0.5968  0.8000
35.0000 10.8641 11.3589          18.0527 18.8749 0.6107  0.8000
40.0000 11.1840 11.6933          20.1166 21.0328 0.6201  0.8000
45.0000 11.5522 12.0784          22.2618 23.2757 0.6247  0.8000

MDive = 0.9100
cruise_alt = 39000.0000 ft
speed_of_sound = 967.9545 ft/s
VDive = 521.5446 knots

AEROELASTIC CHECK
Sweep  t/c eff t/c rt  AR_tor  AR_ben  AR_combined
15.0000 11.6337 12.1635 6.5838  8.9179  6.5838
20.0000 13.0425 13.6365 7.8098  9.4490  7.8098
25.0000 14.4561 15.1144 9.1769  9.8788  9.1769
30.0000 16.0650 16.7967 10.8886 10.2824 10.2824
35.0000 18.0527 18.8749 13.2016 10.7092 10.7092
40.0000 20.1166 21.0328 15.9484 11.0076 11.0076
45.0000 22.2618 23.2757 19.2563 11.1648 11.1648
```



LOCAL CL CHECK

Sweep \ eta	0.0	0.1	0.2	0.3	0.4	0.5	0.6	0.7	0.8	0.9	1.0	max CLy VALID ?	Cl cr
15.0000	0.4102	0.4432	0.4773	0.5128	0.5495	0.5869	0.6235	0.6547	0.6679	0.6173	0.0002	0.6679	1 0.4639
20.0000	0.4417	0.4798	0.5196	0.5613	0.6050	0.6503	0.6957	0.7371	0.7580	0.7054	0.0206	0.7580	1 0.5122
25.0000	0.4662	0.5106	0.5572	0.6067	0.6591	0.7145	0.7718	0.8274	0.8598	0.8072	0.0530	0.8598	1 0.5603
30.0000	0.4749	0.5255	0.5792	0.6367	0.6985	0.7650	0.8358	0.9083	0.9550	0.9052	0.0954	0.9550	0 0.5968
35.0000	0.4639	0.5192	0.5782	0.6420	0.7113	0.7870	0.8694	0.9570	1.0172	0.9726	0.1373	1.0172	0 0.6107
40.0000	0.4458	0.5059	0.5705	0.6409	0.7182	0.8038	0.8988	1.0031	1.0785	1.0405	0.1848	1.0785	0 0.6201
45.0000	0.4206	0.4855	0.5559	0.6331	0.7189	0.8150	0.9236	1.0461	1.1381	1.1080	0.2374	1.1381	0 0.6247

FLAP EFFECTIVENESS

Sweep	CLmax_flap	CLmax, l VALID ?
15.0000	3.4773	2.9000 1
20.0000	3.3829	2.9000 1
25.0000	3.2627	2.9000 1
30.0000	3.1177	2.9000 1
35.0000	2.9489	2.9000 1
40.0000	2.7578	2.9000 0
45.0000	2.5456	2.9000 0

FUEL CAPACITY CHECK

Sweep	t/c eff	AR	Weight_lbm	To/Wg	Wg/s	Cl_cr	Cb	FS	RS	span
15.0000	11.6337	6.5838	240094.5469	0.3362	123.6494	0.4639	28.5210	17.1060	6.2053	113.0660
20.0000	13.0425	7.8098	226272.2656	0.3131	123.6494	0.5122	24.6210	21.6268	13.1688	119.5470
25.0000	14.4561	9.1769	217774.7969	0.3131	123.6494	0.5603	21.3171	26.2326	19.8227	127.1323
30.0000	16.0650	10.2824	212241.9531	0.3131	123.6494	0.5968	18.8430	30.9524	26.0044	132.8554
35.0000	18.0527	10.7092	209877.4531	0.3131	123.6494	0.6107	17.4060	35.7758	31.7458	134.8231
40.0000	20.1166	11.0076	208586.6250	0.3131	123.6494	0.6201	16.0720	40.6201	37.4034	136.2674
45.0000	22.2618	11.1648	208366.1250	0.3131	123.6494	0.6247	14.8009	45.4837	42.9808	137.1646

Sweep	t/c eff	AR	Weight(lb)	Wing Weight(lb)	Fuel Req.(lb)	Fuel cap (lb)	Fuel cap w/CW	Wing Area(ft2)
15.0000	11.6337	6.5838	240094.5469	18285.9785	85003.8281	74903.9766	100309.5078	1941.7230 1
20.0000	13.0425	7.8098	226272.2656	17748.0430	75797.8203	66659.9063	87885.3281	1829.9370 1
25.0000	14.4561	9.1769	217774.7969	17875.8145	68817.3594	59353.4805	76989.0156	1761.2220 1
30.0000	16.0650	10.2824	212241.9531	18054.5605	64177.7148	54136.6758	69449.7734	1716.5750 1
35.0000	18.0527	10.7092	209877.4531	18066.8730	62263.3906	52767.0781	67450.3672	1697.3470 1
40.0000	20.1166	11.0076	208586.6250	18351.8887	60938.8242	50729.7500	64679.8164	1686.9091 1
45.0000	22.2618	11.1648	208366.1250	18937.5234	60175.5078	47958.7773	61051.0508	1685.1310 1

The lightest = 3

SWEEP (3D) EFFECT



Sweep	t/c	eff	t/c	root	t/c	eff	Simp	t/c	rt	Simp	Cl_cr	M_cr
20.0000	10.1745	10.6379			13.0425	13.6365	0.5122			0.8000		
21.0000	10.2084	10.6733			13.3261	13.9330	0.5218			0.8000		
22.0000	10.2439	10.7105			13.6100	14.2298	0.5313			0.8000		
23.0000	10.2812	10.7494			13.8923	14.5250	0.5410			0.8000		
24.0000	10.3202	10.7902			14.1749	14.8205	0.5506			0.8000		
25.0000	10.3608	10.8327			14.4561	15.1144	0.5603			0.8000		
26.0000	10.4032	10.8770			14.7365	15.4076	0.5700			0.8000		
27.0000	10.4474	10.9232			15.0162	15.7001	0.5798			0.8000		
28.0000	10.4933	10.9712			15.2953	15.9919	0.5897			0.8000		
29.0000	10.5409	11.0210			15.6755	16.3894	0.5935			0.8000		
30.0000	10.5903	11.0726			16.0650	16.7967	0.5968			0.8000		

MDive = 0.9100  
cruise\_alt = 39000.0000 ft  
speed\_of\_sound = 967.9545 ft/s  
VDive = 521.5446 knots

AEROELASTIC CHECK									
Sweep	t/c	eff	t/c	rt	AR_tor	AR_ben	AR_combined		
20.0000	13.0425	13.6365	7.8098		9.4490		7.8098		
21.0000	13.3261	13.9330	8.0721		9.5439		8.0721		
22.0000	13.6100	14.2298	8.3403		9.6346		8.3403		
23.0000	13.8923	14.5250	8.6131		9.7204		8.6131		
24.0000	14.1749	14.8205	8.8924		9.8021		8.8924		
25.0000	14.4561	15.1144	9.1769		9.8788		9.1769		
26.0000	14.7365	15.4076	9.4674		9.9508		9.4674		
27.0000	15.0162	15.7001	9.7643		10.0180		9.7643		
28.0000	15.2953	15.9919	10.0678		10.0805		10.0678		
29.0000	15.6755	16.3894	10.4688		10.1823		10.1823		
30.0000	16.0650	16.7967	10.8886		10.2824		10.2824		

LOCAL CL CHECK															
Sweep \ eta	0.0	0.1	0.2	0.3	0.4	0.5	0.6	0.7	0.8	0.9	1.0	max CLy	VALID	? Cl	cr
20.0000	0.4417	0.4798	0.5196	0.5613	0.6050	0.6503	0.6957	0.7371	0.7580	0.7054	0.0206	0.7580	1		0.5122
21.0000	0.4472	0.4864	0.5275	0.5706	0.6158	0.6629	0.7105	0.7543	0.7772	0.7244	0.0260	0.7772	1		0.5217
22.0000	0.4523	0.4928	0.5352	0.5797	0.6266	0.6756	0.7254	0.7719	0.7969	0.7440	0.0319	0.7969	1		0.5313
23.0000	0.4573	0.4990	0.5427	0.5888	0.6375	0.6885	0.7406	0.7900	0.8172	0.7643	0.0383	0.8172	1		0.5409
24.0000	0.4619	0.5049	0.5501	0.5978	0.6483	0.7014	0.7561	0.8084	0.8381	0.7853	0.0454	0.8381	1		0.5506
25.0000	0.4662	0.5106	0.5572	0.6067	0.6591	0.7145	0.7718	0.8274	0.8598	0.8072	0.0530	0.8598	1		0.5603
26.0000	0.4702	0.5160	0.5642	0.6154	0.6699	0.7277	0.7879	0.8470	0.8822	0.8299	0.0613	0.8822	0		0.5700
27.0000	0.4738	0.5211	0.5710	0.6241	0.6807	0.7410	0.8042	0.8670	0.9054	0.8534	0.0704	0.9054	0		0.5798
28.0000	0.4771	0.5259	0.5775	0.6326	0.6915	0.7544	0.8209	0.8877	0.9294	0.8780	0.0802	0.9294	0		0.5897



29.0000		0.4762	0.5260	0.5787	0.6349	0.6953	0.7601	0.8287	0.8984	0.9426	0.8919	0.0878	0.9426	0	0.5935
30.0000		0.4749	0.5255	0.5792	0.6367	0.6985	0.7650	0.8358	0.9083	0.9550	0.9052	0.0954	0.9550	0	0.5968

FLAP EFFECTIVENESS

Sweep	CLmax_flap	CLmax,l VALID ?
20.0000	3.3829	2.9000 1
21.0000	3.3609	2.9000 1
22.0000	3.3379	2.9000 1
23.0000	3.3138	2.9000 1
24.0000	3.2888	2.9000 1
25.0000	3.2627	2.9000 1
26.0000	3.2357	2.9000 1
27.0000	3.2076	2.9000 1
28.0000	3.1786	2.9000 1
29.0000	3.1486	2.9000 1
30.0000	3.1177	2.9000 1

FUEL CAPACITY CHECK

Sweep	t/c eff	AR	Weight_lbm	To/Wg	Wg/s	CL_cr	Cb	FS	RS	span
20.0000	13.0425	7.8098	226272.1406	0.3131	123.6494	0.5122	24.6210	21.6268	13.1688	119.5469
21.0000	13.3261	8.0721	224421.5156	0.3131	123.6494	0.5217	23.9323	22.5416	14.5238	121.0397
22.0000	13.6100	8.3403	222651.1094	0.3131	123.6494	0.5313	23.2581	23.4596	15.8669	122.5479
23.0000	13.8923	8.6131	220955.8438	0.3131	123.6494	0.5409	22.5993	24.3810	17.1970	124.0613
24.0000	14.1749	8.8924	219333.0938	0.3131	123.6494	0.5506	21.9521	25.3053	18.5159	125.5934
25.0000	14.4561	9.1769	217774.7969	0.3131	123.6494	0.5603	21.3171	26.2326	19.8227	127.1323
26.0000	14.7365	9.4674	216290.7188	0.3131	123.6494	0.5700	20.6928	27.1627	21.1184	128.6879
27.0000	15.0162	9.7643	214866.0156	0.3131	123.6494	0.5798	20.0772	28.0954	22.4032	130.2587
28.0000	15.2953	10.0678	213500.7813	0.3131	123.6494	0.5897	19.4693	29.0308	23.6776	131.8469
29.0000	15.6755	10.1823	212824.3906	0.3131	123.6494	0.5935	19.1454	29.9905	24.8453	132.3846
30.0000	16.0650	10.2824	212241.9531	0.3131	123.6494	0.5968	18.8430	30.9524	26.0044	132.8554

Sweep	t/c eff	AR	Weight(lb)	Wing Weight(lb)	Fuel Req.(lb)	Fuel cap (lb)	Fuel cap w/CW	Wing Area(ft2)
20.0000	13.0425	7.8098	226272.1406	17748.0410	75797.6875	66659.8672	87885.2891	1829.9370 1
21.0000	13.3261	8.0721	224421.5156	17747.5176	74305.3281	65259.2734	85749.8281	1814.9709 1
22.0000	13.6100	8.3403	222651.1094	17760.3770	72864.4141	63831.1797	83595.7109	1800.6591 1
23.0000	13.8923	8.6131	220955.8438	17785.8965	71471.8438	62371.5938	81419.4141	1786.9480 1
24.0000	14.1749	8.8924	219333.0938	17824.7441	70124.4688	60880.8711	79218.9453	1773.8300 1
25.0000	14.4561	9.1769	217774.7969	17875.8145	68817.3594	59353.4805	76989.0156	1761.2220 1
26.0000	14.7365	9.4674	216290.7188	17940.9316	67556.2031	57794.1641	74734.1328	1749.2140 1
27.0000	15.0162	9.7643	214866.0156	18018.9863	66330.0234	56196.5117	72446.2813	1737.6920 1
28.0000	15.2953	10.0678	213500.7813	18110.4043	65138.5547	54560.4453	70125.1094	1726.6520 1
29.0000	15.6755	10.1823	212824.3906	18079.4082	64624.5547	54317.6797	69742.9141	1721.1830 1
30.0000	16.0650	10.2824	212241.9531	18054.5605	64177.7148	54136.6758	69449.7734	1716.5750 1



The lightest = 6

BOEING 757-200 PW 2037

Sweep	= 25.0000
AR	= 9.1769
Span	= 127.1323
Wing Area	= 1761.2220
C root	= 26.9930
C b	= 21.3171
C kink	= 15.7107
C tip	= 4.4979
taper	= 0.2110
t/c eff	= 14.4561
t/c root	= 15.1144
t/c kink	= 13.8549
t/c tip	= 11.3358
Cl cruise	= 0.5603
M cruise	= 0.8000
L/D cruise	= 18.0859
Wg / S	= 123.6494
To / Wg	= 0.3131
Weight	= 217774.7969



# *Appendix C*



## C. SPARV PRE AND POST PROCESSORS

### C.1 Introduction

Since the program requires to use SPARV computational aerodynamic in the iteration, the pre and post processors of SPARV needs to be developed. SPARV in the College of Aeronautics lacks both pre and post processor. In the past, UNIGRAPHICS CAD program was used to generate the co-ordinate points of the model and the input file was then prepared manually. Post processor of SPARV was done in a similar way also, the SPARV results were transferred into a UNIGRAPHICS file and plotted using UNIGRAPHICS display.

The process of using the UNIGRAPHICS CAD program to generate the co-ordinate points of the aircraft is considered inappropriate as this task cannot be done in a seamless way, because it requires operator input. A pre-processor of SPARV (PRESPARV) has to be developed which has the task of generating the input file which is unique for this project only.

Post-processor of SPARV (POSTSPARV) is developed which has the task of extracting the pressure distribution from SPARV and transferring it to the form of NASTRAN input file.

This appendix explains how the pre and post processor for SPARV work and shows an example input and output file.



## C.2 PRESPARV input file

In order to run PRESPARV, the aircraft geometric need to be defined first. The required input file basically gives the geometry of the wing, HTP, VTP, and fuselage.

The required input files are :

- fuse.dat
- vtp.dat
- htp.dat
- wing.dat (generated by WINGLAYOUT.EXE)

Fuselage, vtp, and htp can be prepared manually or can be generated by the program.

An example of the input file can be found in the previous appendix.

## C.3 PRESPARV output file

The output of the PRESPARV is an input file for the SPARV module. This file is generated from the known aerofoil section, wing geometry, fuselage geometry, etc. Example output of the PRESPARV module can be seen in Table C.1. The method of generating the point is explained below.



### C.3.1 Wing points generation

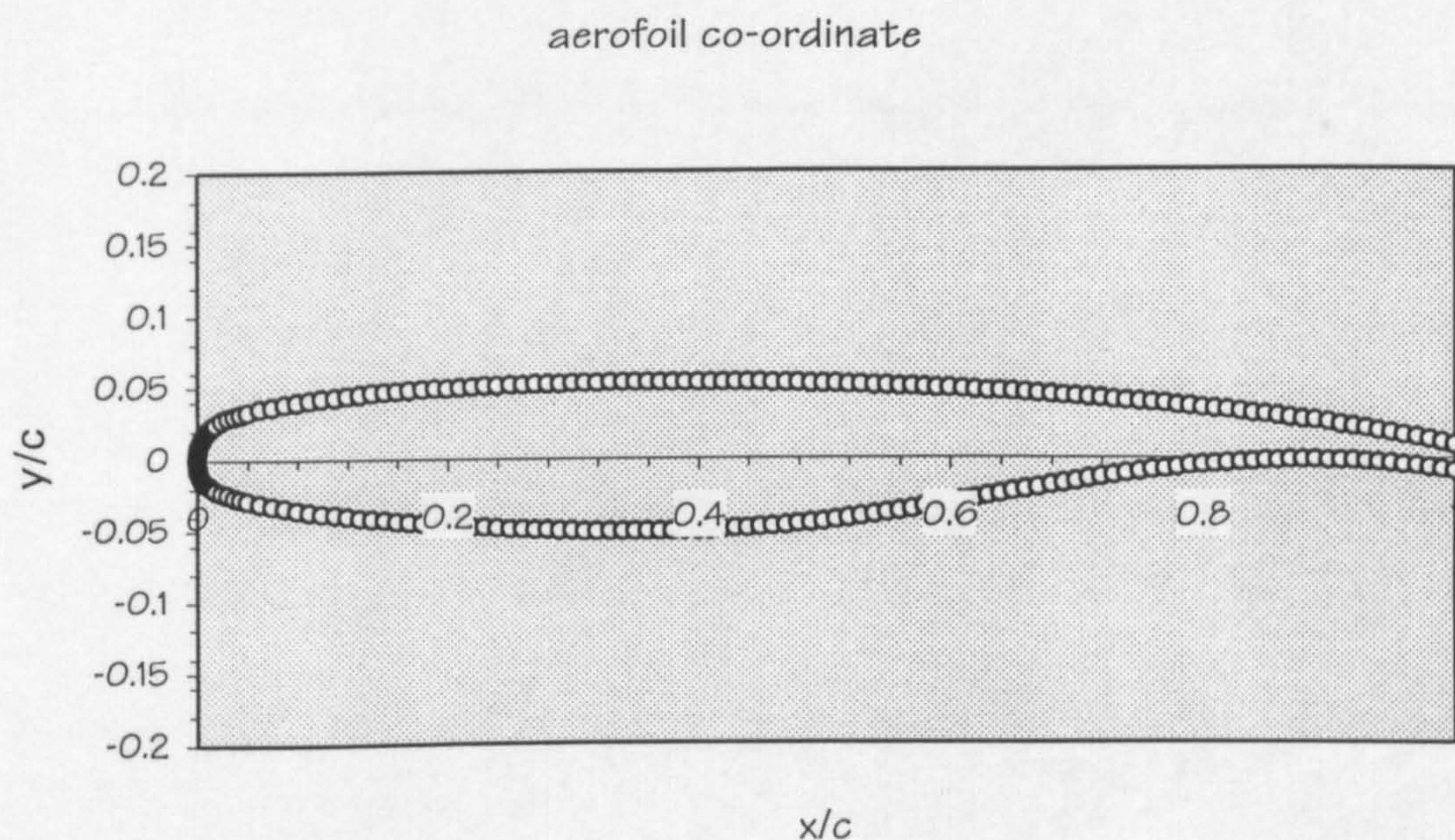


**Figure C.1**      **Original aerofoil co-ordinate**

The wing points generation is done in several steps. The first step is to generate the co-ordinate of the aerofoil. This is done by interpolating the co-ordinate from the known aerofoil co-ordinate found in aerofoil database. These points are based on a unit length chord. After generating the unit length co-ordinate, the co-ordinate has to be scaled up or down according to the required chord length. Then the thickness ratio of the aerofoil needs to be changed according to the actual thickness ratio. From these co-ordinates, the points are translated in the x direction to the required sweep angle. Dihedral angle effect of the wing is put to the co-ordinate by translating the points in the z direction. Finally the wing points are rotated to the required twist angle.



These steps can be summarised as follows :

1. Aerofoil points generation
2. Thickness ratio effect
3. Taper effect
4. Sweep effect
5. Dihedral effect
6. Twist Effect

#### C.3.1.1 Aerofoil points generation

The wing points are generated after the aerofoil to be used has been chosen. The co-ordinates of the aerofoil are stored in the aerofoil database and based on a unit chord length (Fig. C.1). The points to be used in the SPARV panel need to be generated according to the number of panel needed in the model. The panel is generated by using a sine distribution (see Fig. C.2). The sine distribution of the panel is generated by projecting an equal angle of a semi-circle to the aerofoil.

The sine distribution means that the leading and trailing edges of the aerofoil will have smaller panels compared with the middle section. The purpose is to give more panels where the gradient of pressure is high. As can be seen in Fig. C.3, the typical model has more dense panels on the leading edge and trailing edge.



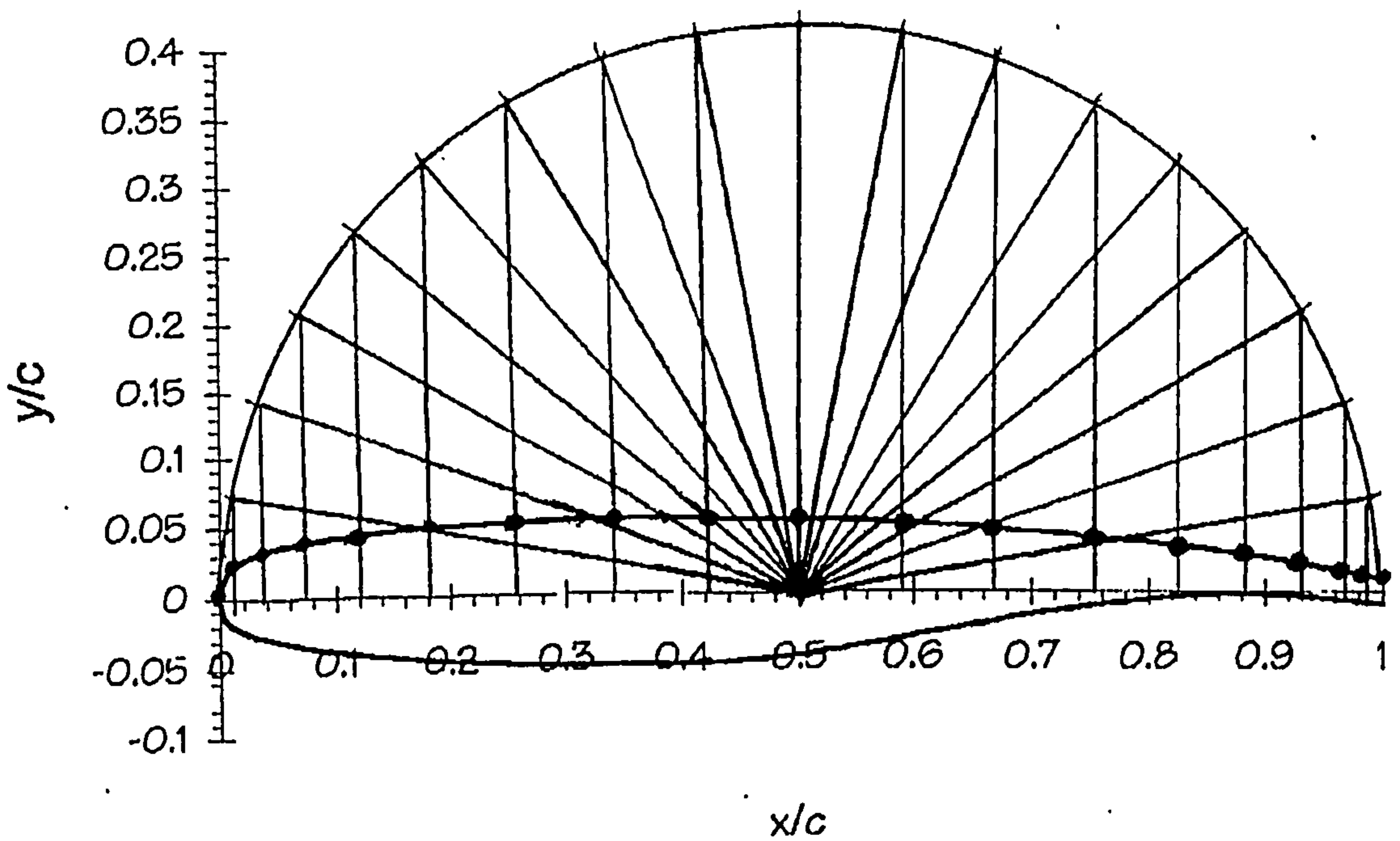


Figure C.2 Sine distribution

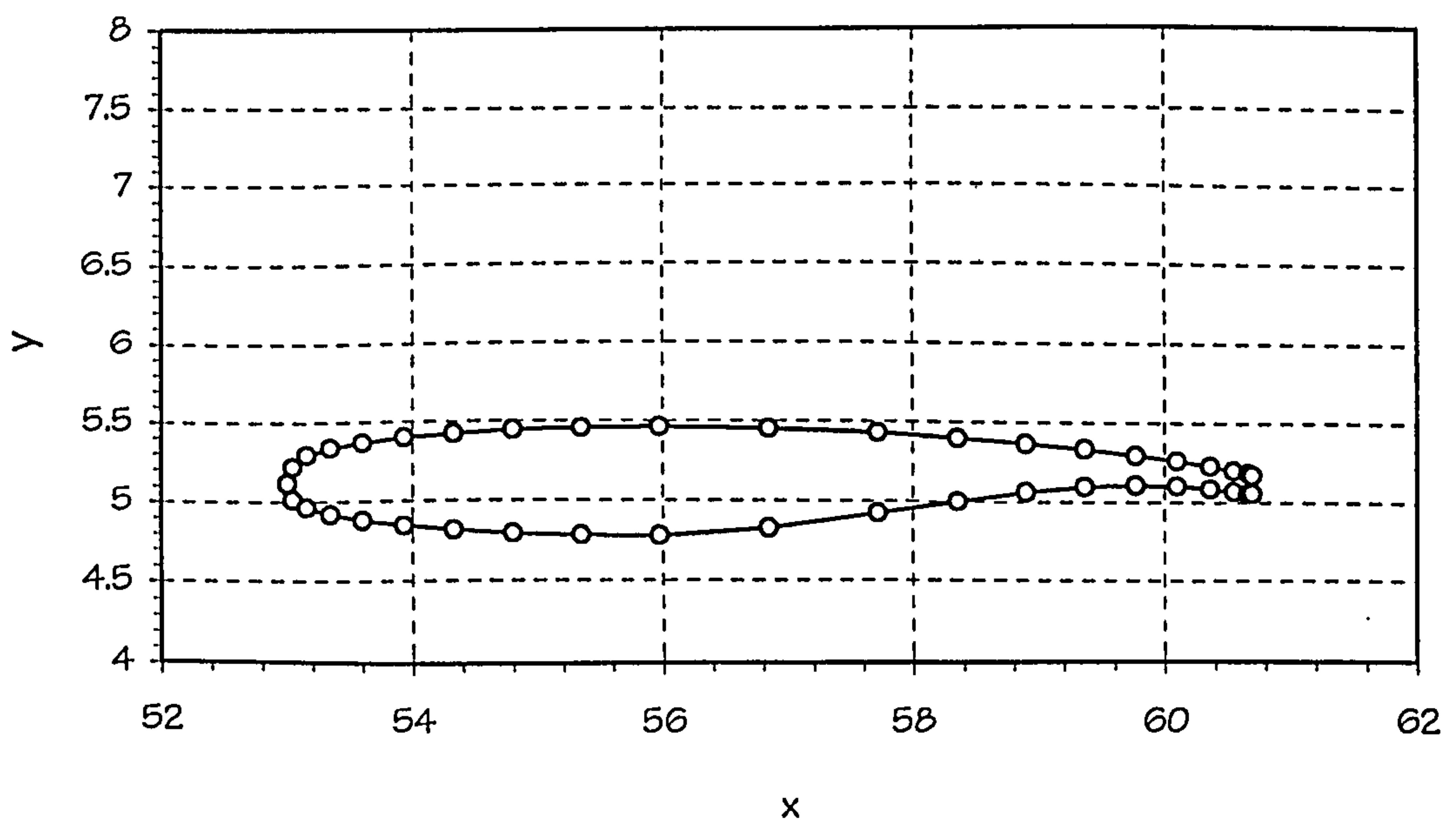


Figure C.3 Aerofoil co-ordinate point



C.3.1.2 Thickness ratio effect

The thickness ratio effect of the aerofoil is generated by scaling up or down the aerofoil in the z direction. This is done by scaling up the thickness from upper/lower surface to the chordline according to the required thickness ratio (Fig. C.4).

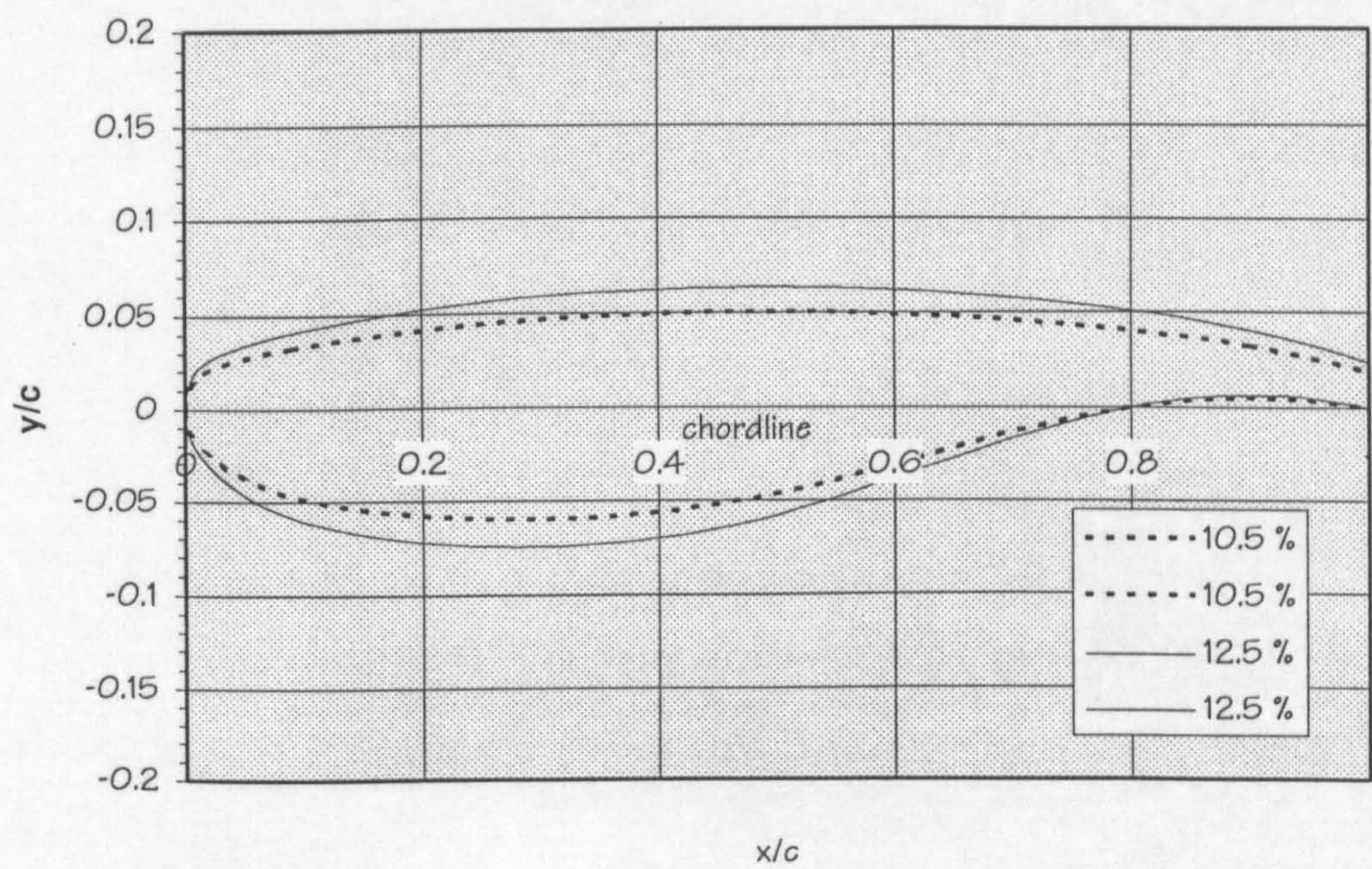


Figure C.4 Thickness ratio effect

C.3.1.3 Taper ratio effect

By knowing the taper ratio, the required chord at each spanwise station is known. The aerofoil point at each station is scaled up or down according to the required chord length.



C.3.1.4 Sweep effect

From knowing the sweep angle, the aerofoil points are translated in the x direction. The distance it needs to be translated depends on the spanwise location. At the root no translation is needed and at the tip maximum translation is required (Fig. C.5).

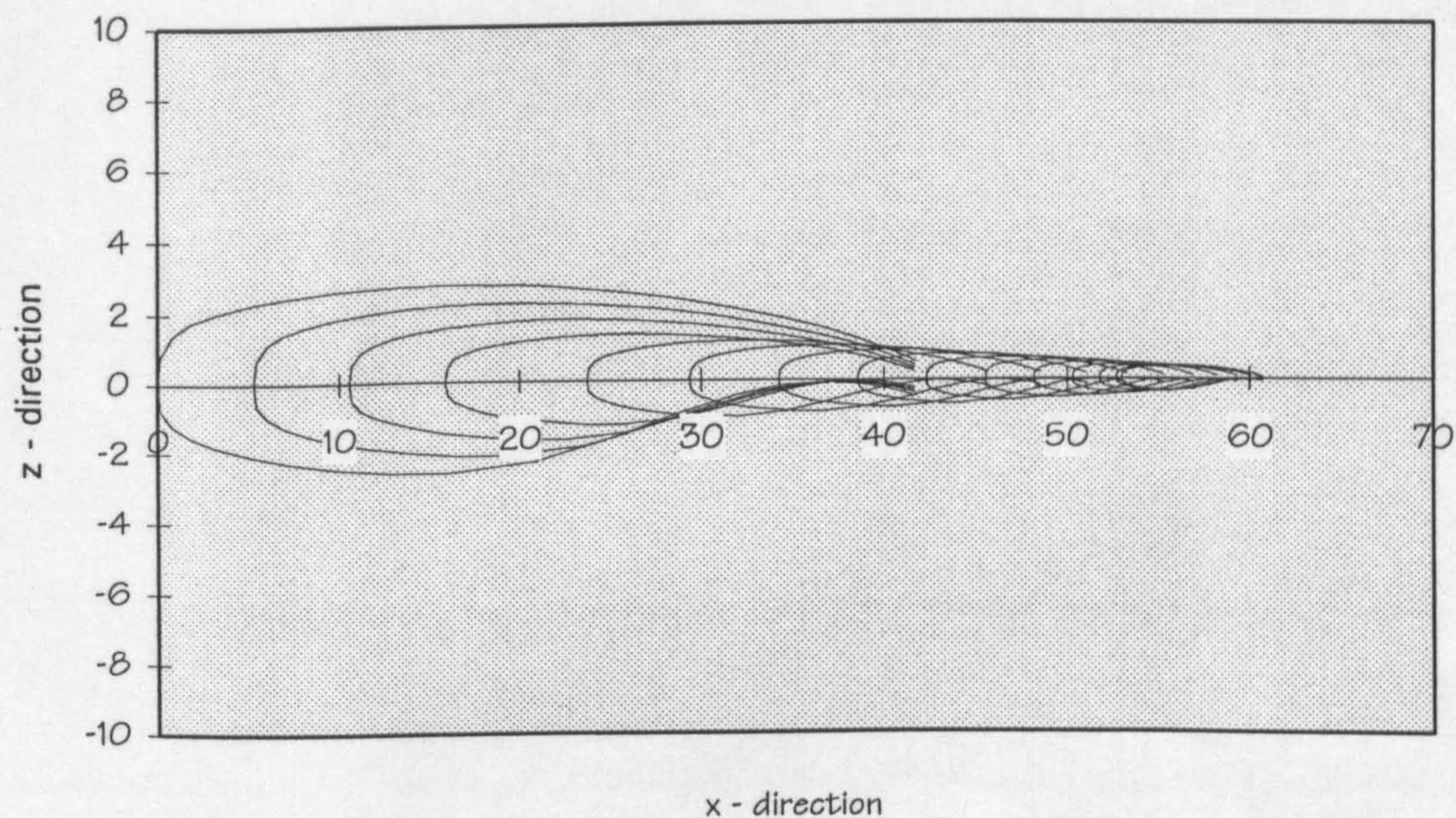


**Figure C.5      Sweep effect - twist=0,    dihedral=0**

C.3.1.5 Dihedral effect

Each point on the wing is then translated in the direction according to the required distance set by the dihedral angle (Fig. C.6).



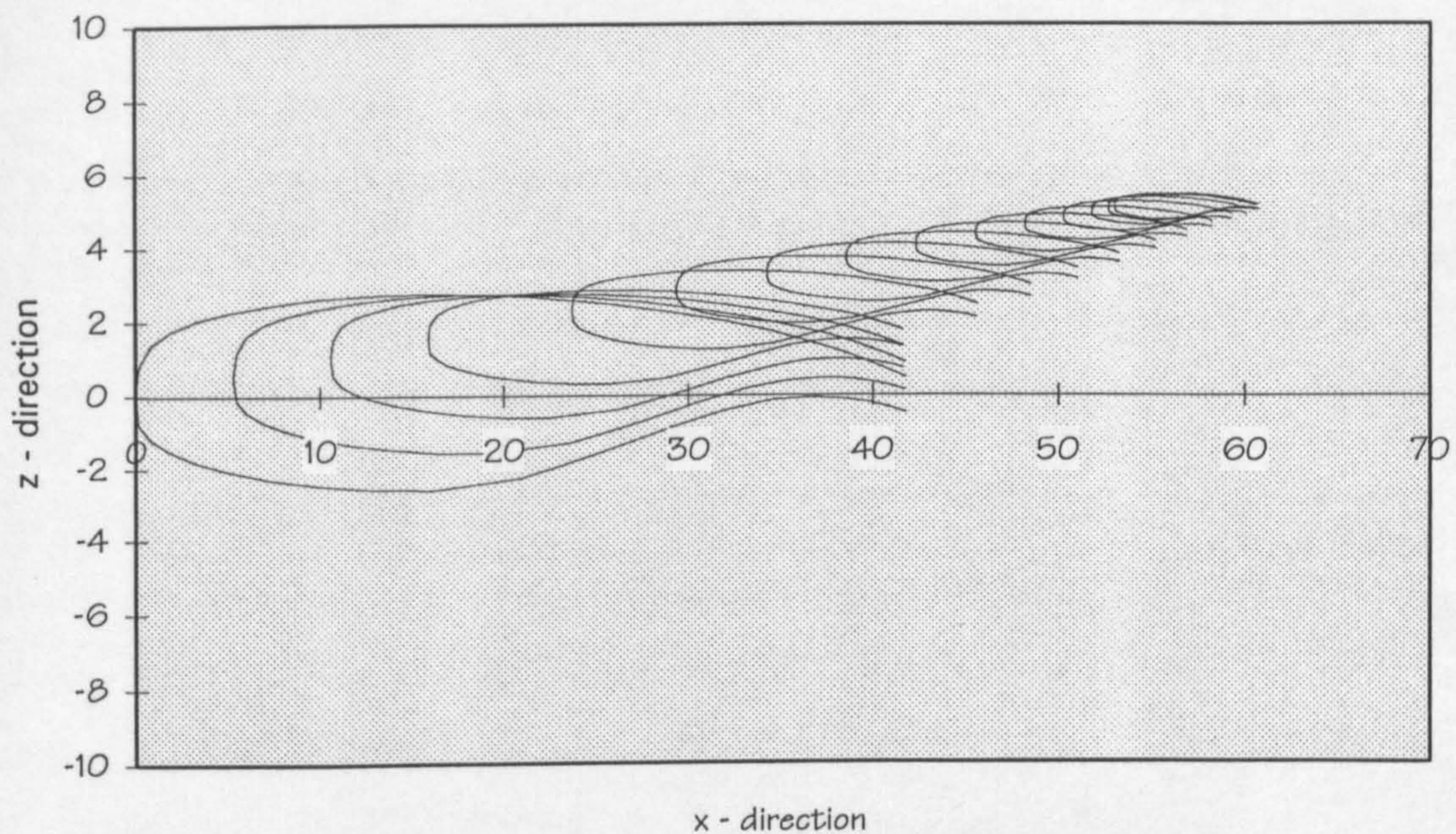


**Figure C.6** Dihedral effect - twist=0, dihedral=4

#### C.3.1.6 Twist effect

Finally, the wing is twisted at each spanwise station according the twist angle of the wing (Fig. C.7).

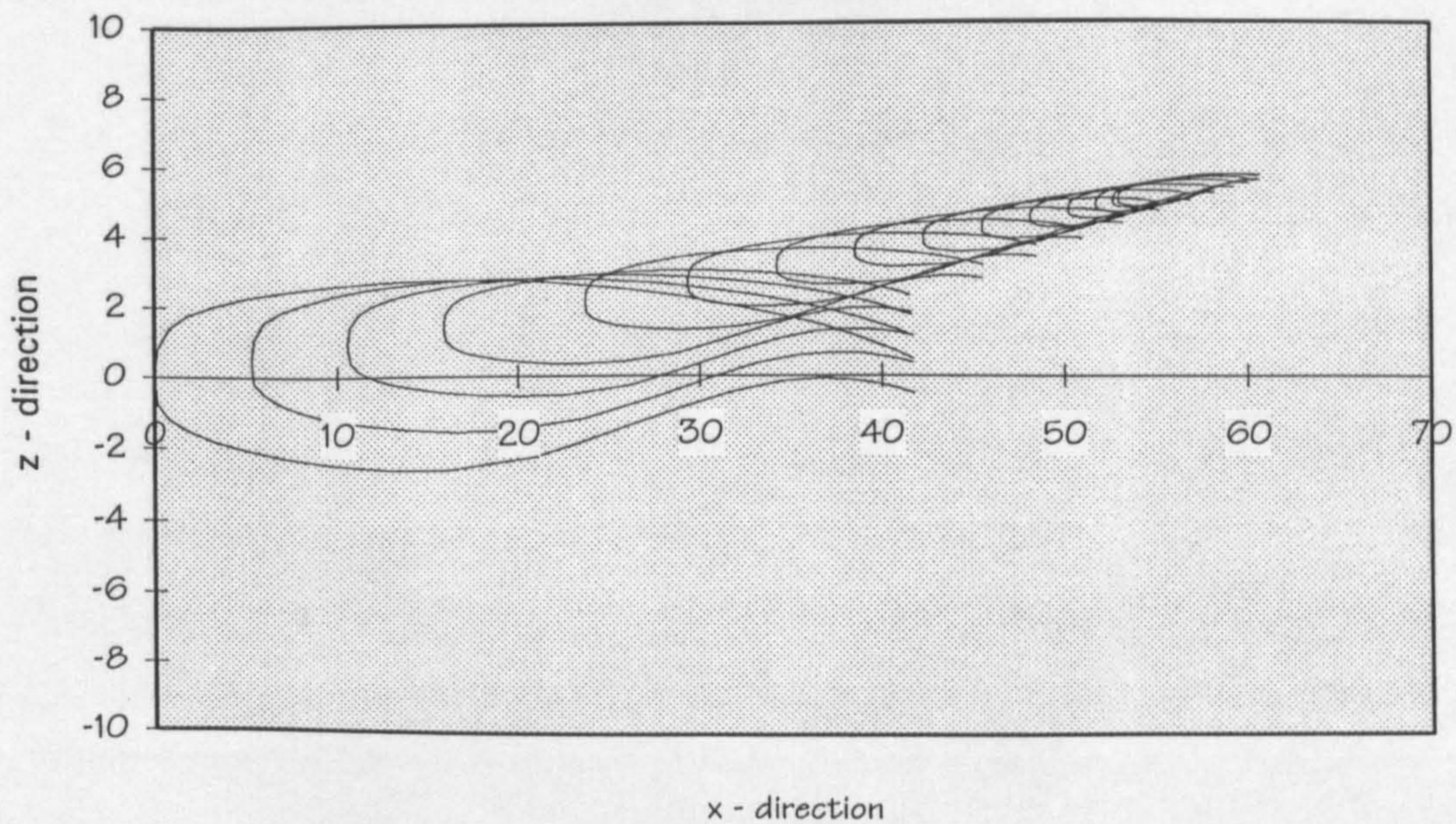


**Figure C.7** Twist angle effect - twist=5, dihedral=4



C.3.2 Fuselage points generation

Fuselage points are generated by using two sine distributions, the nose, middle fuselage, and tail are modelled with more panels. This is due to the bigger pressure gradients in these areas (Fig. C.8).

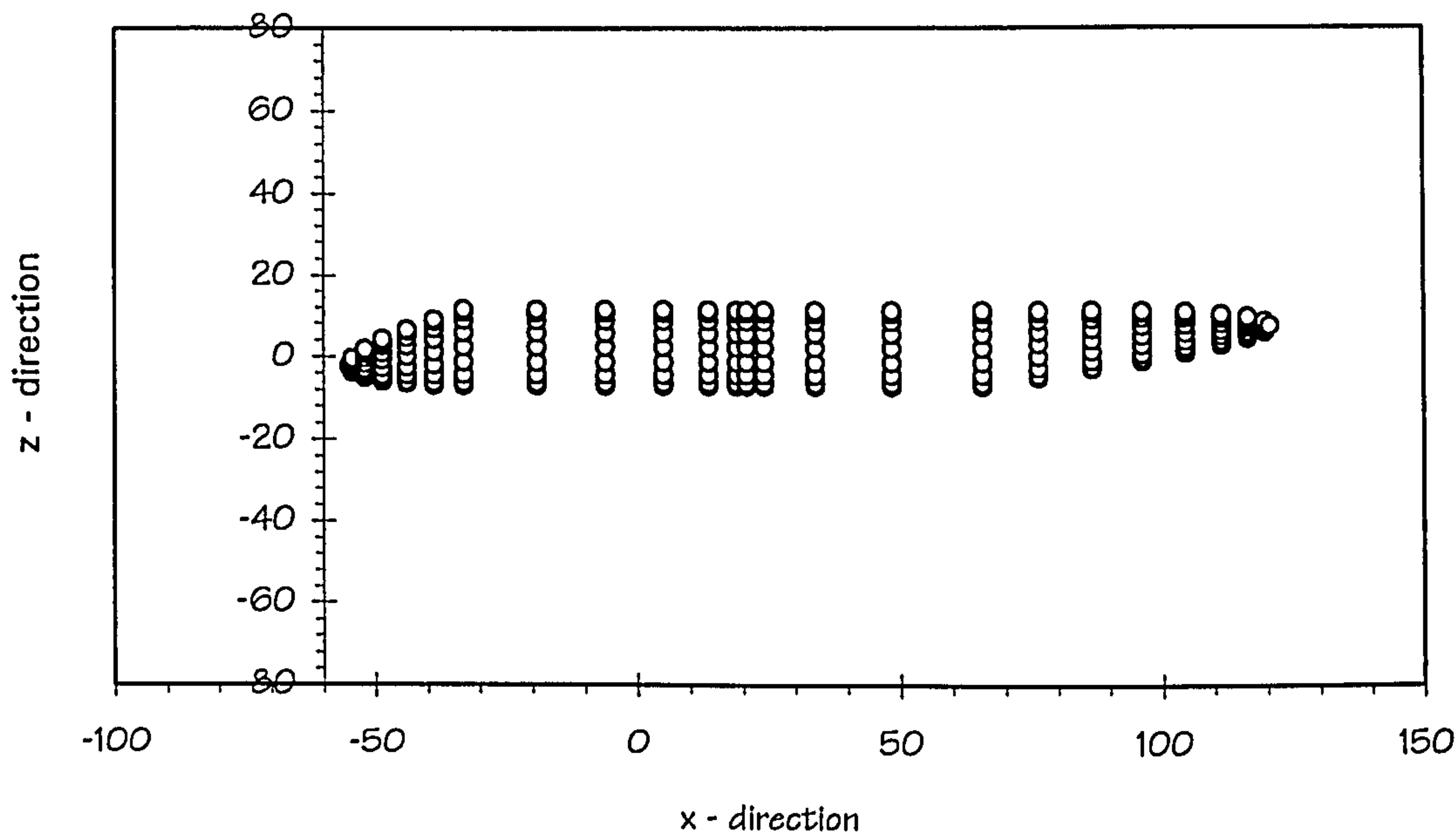


Figure C.8 Fuselage panels

C.3.3 HTP points generation

Horizontal tail plane panels are generated by using the same method as the wing. Thickness ratio, taper, and sweep effect on the HTP are calculated using the same method and sine distribution panels are also modelled for the HTP.



C.3.4 VTP points generation

Vertical tail plane panels are generated using a similar method as the wing and HTP panels are generated. The only difference is that the VTP is treated as half of a whole wing.

Table C.1 Example output of PRESPARV

A300-600				
0				
1	1	1	0	
0	0			
4	0			
1				
WING				
21	21	1		
2800	15.4	0	0	0
0	0	1		
0	1	2		
FUSELAGE				
17	19	2		
2800	15.4	0	0	0
0	0	2		
HTP				
11	13	1		
2800	15.4	0	0	0
0	0	3		
0	1	2		
VTP				
13	11	1		
2800	15.4	0	0	0
0	0	4		
0	0	2		
0	0	0		
0.79				
0				
0	0			
1				
0				
43.5209	-73.4	9.08921		
43.5687	-73.4	9.2129		
43.7014	-73.4	9.29631		
43.9181	-73.4	9.34336		
44.2176	-73.4	9.37639		
44.5979	-73.4	9.40007		
-----deleted-----				
co-ordinate points of wing, fuselage, http, and vtp				
-----deleted-----				
99.1511-6.575	10.7073			
99.4162	-6.575	10.4772		
100.202	-6.575	10.27		
101.484	-6.575	10.1106		
103.255	-6.575	10.034		
105.889	-6.575	10.1323		
115.75	26.3	12.7445		
0				



The output file generated from PRESPARV module is in the form of the required input format of SPARV program. For more information, Ref. 12 should be consulted.

#### C.4 Co-ordinate points of deflected wing.

As explained previously, the calculation of SPARV and NASTRAN is done in several iterations in order to study the static aeroelasticity of the wing. The co-ordinate points explained in the previous section are only used for the first iteration. The next iteration requires a deflection caused by the pressure distribution to be modelled. The deflection is calculated by using the NASTRAN program. The wing points are generated by calculating the deflection caused by the load and translates the co-ordinate of 'rigid wing' accordingly.

#### C.5 PRESPARV stand alone program

A stand alone program which can be run manually is developed and it uses 'GnuPlot' program to display the outputs. This program is used to make sure that the points generated by the program are correct.

#### C.6 POST SPARV

The input file required by the POST SPARV module is the output file of SPARV. The data required by the NASTRAN program such as pressure distribution, is extracted from the SPARV output file. This pressure distribution is then



transferred to the PRE NASTRAN program in order to generate a NASTRAN input file. More detail of this process can be found in next appendix, in the PRE NASTRAN section.



# *Appendix D*



## D. NASTRAN PRE AND POST PROCESSORS

### D.1 Introduction

In this appendix the method of transferring the pressure distribution from the SPARV output file is explained. Modelling of the NASTRAN is also explained and example files are given.

The pre-processor of NASTRAN (PRENASTRAN) uses bi-linear interpolation to extract the pressure distribution from the SPARV output. This is due to the fact that NASTRAN and SPARV use different panels for modelling the problem. SPARV uses panels that are parallel to the streamwise direction, and NASTRAN uses panels that are perpendicular to the rear spar.

The post-processor of NASTRAN (POSTNASTRAN) is required to extract the required data from the NASTRAN output such as defections and weight.

### D.2 PRENASTRAN input file

In order to be able to execute the PRENASTRAN module independently, the PRENASTRAN module is programmed to read input from an input file. Although in the normal case the input file is written by the aircraft synthesis module, it can be written manually by user. The required files in order to run PRENASTRAN module are the INITIAL.DAT file and SPARV.CPX (Sparv output file).



The SPARV output file is needed in order to obtain the air pressure. The INITIAL.DAT file contains other information that was needed such as the spars location, ribs location, kink location, engine location, dynamic pressure, engine weight, etc. The required input can be seen in Table D.1.

The pressure distribution of the wing is extracted from the SPARV output file SPARV.CPX. This pressure is in the form of pressure coefficients  $C_p$ , which have to be converted to the actual pressures by multiplying by the dynamic pressure  $q_\infty$ . This dynamic pressure is calculated earlier at the design case where speed is at maximum diving speed. Example of Sparv output can be seen in Table D.2.

**Table D.1    Example of INITIAL.DAT**

AIRBUS 300-B2    lambda = 30		title
21	sparv_NX	
29	sparv_NY	number of panels
5	nas_NX	
26	nas_NY	
20	eng_loc	panel location in the chord direction
16	spar_percent[1]	
28.3	spar_percent[2]	
40.5	spar_percent[3]	
52.8	spar_percent[4]	
65	spar_percent[5]	kink location
33.424	Croot_st	
21.6803	Cb	
16.383	C_kink	
5.78863	Ctip	
163.336	span	
37.8	kink_percent(%)	
18.5	fuse_diam(ft)	
202.982	dynamic_pressure	
10535.2	eng_weight_lb_each	
3.75	maximum_g_accltion	
0.0	deltay[1]	
2.5	deltay[2]	
5.0	deltay[3]	
7.5	deltay[4]	
10.0	deltay[5]	
12.5	deltay[6]	
15.0	deltay[7]	
17.5	deltay[8]	
20.0	deltay[9]	



22.5	deltay[10]
25.0	deltay[11]
27.5	deltay[12]
30.0	deltay[13]
32.5	deltay[14]
35.0	deltay[15]
37.5	deltay[16]
40.2	deltay[17]
43.1	deltay[18]
47.0	deltay[19]
0.0	deltay[20] eng
0.0	deltay[21]
57.5	deltay[22]
60.0	deltay[23]
62.5	deltay[24]
65.2	deltay[25]
0.0	deltay[26]

ribs location



### Table D.2 Example of SPARV.CPX file

[illegible]

**alpha = 0.0**

```

MACH NUMBER = 0.650
HEWITT USED ON COMPONENTS: 1 3
DOUBLET OPTION 1
REFLECTION OPTION 1
NO OF PANELS 1984
NO OF OLD PANELS 0

```

```

*****
* SPARV AXIS SYSTEM *****
*
*
* ALPHA +VE NOSE UP *
*
* BETA +VE NOSE TO STBD *
*
* X +VE AFT *
*
* Y +VE STBD *
*
* Z +VE UP *
*
* Cl +VE STBD WING UP *
*
* Cm +VE NOSE UP *
*
* Cn +VE NOSE TO PORT *
*****

```

1  
1\*\*\*\*\*NON-VISCOUS SOLUTION\*\*\*\*\*

COMPONENT 1 WING		ONSET FLOW=					-----				
STATION 1 U/S											
N	X	Y	Z	VX	VY	VZ	X/C	CP	MU		
1	51.265923	-81.417435	5.749708	0.563400	-0.470979	0.536692	0.002573	0.175895	0.006903		



2	51.323395	-81.417435	5.845395	1.092954	-0.107869	0.823308	0.012592	-0.804528	0.020759
3	51.437782	-81.417435	5.909352	1.452986	0.143482	0.488644	0.032294	-1.183448	0.044383
4	51.608055	-81.417435	5.953320	1.357006	0.145134	0.267494	0.061526	-0.845524	0.063843
5	51.832863	-81.417435	5.989363	1.262134	0.153964	0.166224	0.100078	-0.601654	0.077337
6	52.110825	-81.417435	6.019048	1.208250	0.175429	0.101976	0.147717	-0.475085	0.087476
7	52.441120	-81.417435	6.042520	1.174605	0.198270	0.062981	0.204303	-0.404415	0.094770
8	52.824966	-81.417435	6.059660	1.153257	0.221731	0.029580	0.270045	-0.365030	0.100289
9	53.270271	-81.417435	6.069205	1.135780	0.243939	0.000932	0.346293	-0.336791	0.102553
10	53.840958	-81.417435	6.067513	1.114110	0.267795	-0.031483	0.443983	-0.303674	0.100510
11	54.503040	-81.417435	6.048920	1.100937	0.305832	-0.070082	0.557288	-0.300457	0.100705
12	55.073730	-81.417435	6.018420	1.096594	0.358927	-0.105442	0.654924	-0.330256	0.118391
13	55.519028	-81.417435	5.983875	1.089258	0.408279	-0.134132	0.731088	-0.356842	0.139336
14	55.902870	-81.417435	5.946723	1.085331	0.455507	-0.159921	0.796726	-0.393471	0.159387
15	56.233154	-81.417435	5.908438	1.085686	0.497048	-0.189185	0.853194	-0.439496	0.177084
16	56.511101	-81.417435	5.869360	1.084623	0.527739	-0.228256	0.900701	-0.480444	0.192002
17	56.735893	-81.417435	5.831265	1.082446	0.548263	-0.264335	0.939111	-0.511815	0.204455
18	56.906158	-81.417435	5.798192	1.048214	0.545515	-0.282464	0.968195	-0.452660	0.215502
19	57.020523	-81.417435	5.773925	0.965596	0.489771	-0.276507	0.987727	-0.242242	0.220848
20	57.077988	-81.417435	5.761120	0.888224	0.415492	-0.255593	0.997540	-0.026826	0.219563
STATION 2 U/S									
N	X	Y	Z	VX	VY	VZ	X/C	CP	MU
21	50.637329	-80.417984	5.683067	0.526465	-0.387798	0.581086	0.002574	0.240666	0.008157
22	50.696922	-80.417984	5.782570	1.090409	-0.014389	0.862021	0.012595	-0.844055	0.025672
23	50.815434	-80.417984	5.849027	1.486221	0.237692	0.509726	0.032298	-1.295046	0.055790
24	50.991814	-80.417984	5.894653	1.428816	0.223258	0.283067	0.061530	-1.033615	0.084338
25	51.224670	-80.417984	5.931995	1.355126	0.193505	0.177190	0.100083	-0.821935	0.108475
26	51.512569	-80.417984	5.962690	1.299582	0.173013	0.108655	0.147722	-0.675991	0.129429
27	51.854671	-80.417984	5.986885	1.253008	0.160477	0.067564	0.204310	-0.563238	0.146399
28	52.252224	-80.417984	6.004455	1.216600	0.156931	0.033390	0.270051	-0.479404	0.159951
29	52.713425	-80.417984	6.014085	1.186824	0.159199	0.004958	0.346299	-0.414395	0.168236
30	53.304482	-80.417984	6.011942	1.158088	0.164762	-0.026551	0.443990	-0.354858	0.170257
31	53.990177	-80.417984	5.992154	1.144476	0.179320	-0.063495	0.557294	-0.333551	0.175114
32	54.581215	-80.417984	5.960038	1.136524	0.195511	-0.095586	0.654930	-0.327080	0.203159
33	55.042381	-80.417984	5.923800	1.124851	0.207303	-0.120429	0.731094	-0.311912	0.237020
34	55.439888	-80.417984	5.884895	1.114353	0.218329	-0.142006	0.796730	-0.299622	0.271457
35	55.781937	-80.417984	5.844845	1.104436	0.227325	-0.166496	0.853198	-0.289841	0.303597
36	56.069775	-80.417984	5.804006	1.080536	0.225966	-0.197752	0.900704	-0.250784	0.330852
37	56.302567	-80.417984	5.764223	1.032706	0.207562	-0.219486	0.939113	-0.155127	0.350148
38	56.478886	-80.417984	5.729702	0.974852	0.174656	-0.225937	0.968197	-0.031782	0.360289
39	56.597321	-80.417984	5.704382	0.927572	0.138890	-0.225556	0.987730	0.069954	0.363673
40	56.656818	-80.417984	5.691023	0.896124	0.112275	-0.219042	0.997541	0.138353	0.363638

=====deleted =====



The data that needs to be extracted from the SPARV.CPX file (see Table D.2) is the co-ordinate point of the pressure location , and the pressure itself. The co-ordinate point is in the form of x co-ordinate (column 2), y co-ordinate (column 3), and z co-ordinate (column 3). The pressure coefficient is CP at column 9. These co-ordinates with the corresponding pressure coefficient are required to find the pressure at certain finite element mesh points. Four pressure and co-ordinate points are required in order to interpolate and find a pressure load at one single point of the mesh.

### D.3 PRENASTRAN output file

This module works together with POSTSPARV to fulfil the task of extracting the pressure distribution from SPARV output. The second task of this module is to generate an input file for NASTRAN. The method of generating the co-ordinate points for NASTRAN model is similar to the method for generating the points for SPARV panel. The location of front spar, rear spar, and ribs are known from the previous module and are passed to the PRENASTRAN module in the INITIAL.DAT file. The co-ordinate of the finite element mesh is generated by using interpolation from the known geometric points set up previously by PRESVARV program. Example output of PRENASTRAN module can be seen in Table D.3.



Table D.3 Example output of PRENASTRAN

```
ID      MSC-XL, MSC-NASTRAN
SOL     200 $ V66 - Static Analysis
TIME 300
CEND
TITLE = MSC/NASTRAN ----- MSC/XL
SUBTITLE = STATICS CASE CONTROL
LABEL = DEFAULT SUBCASE STRUCTURE
DISP = ALL
STRESS = ALL
FORCE = ALL
STRAIN = ALL
ESE = ALL
    SUBCASE 1
    PARAM,APPC,STATICS
    SPC = 1
    LOAD = 1
BEGIN BULK
PARAM   POST      0
PARAM   AUTOSPC YES
$
$      GRID DATA
$
$23456781234567812345678123456781234567812345678123
$
GRID    1          55.1237 -78.04  8.52309
GRID    2          56.5828 -77.30228.46758
GRID    3          58.1564 -76.56448.30018
GRID    4          38.3808 -52.04  6.1705
GRID    5          41.4239 -50.46446.00316
GRID    6          44.7081 -48.88885.58875
GRID    7          25.5488 -31.99054.44039
GRID    8          30.6183 -30.83734.28122
GRID    9          35.9551 -29.68413.73438
GRID   10          21.8684 -26.01854.0493
GRID   11          27.051  -23.60443.78327
GRID   12          32.8043 -21.19032.9948
GRID   13          18.787  -21.01853.72186
GRID   14          24.5055 -18.44333.42795
GRID   15          30.8299 -15.86812.53138
GRID   16          15.3422 -15.42893.35581
GRID   17          21.6599 -12.67353.03073
GRID   18          28.6228 -9.918182.0133
GRID   19          55.1014 -78.04  7.82576
GRID   20          56.5568 -77.30227.65491
GRID   21          58.1391 -76.56447.73467
GRID   22          38.3154 -52.04  4.69079
GRID   23          41.3466 -50.46444.27682
GRID   24          44.6553 -48.88884.38621
GRID   25          25.4278 -31.99052.21762
GRID   26          30.4749 -30.83731.66818
GRID   27          35.8565 -29.68411.9012
GRID   28          21.7125 -26.01851.36211
GRID   29          26.86   -23.60440.533982
GRID   30          32.6686 -21.19030.656694
GRID   31          18.6018 -21.01850.645844
GRID   32          24.2805 -18.4433-0.27534
GRID   33          30.6711 -15.8681-0.12311
GRID   34          15.1243 -15.4289-0.1549
GRID   35          21.3968 -12.6735-1.18011
GRID   36          28.438  -9.91818-0.99490
GRID   37          56.9996 -78.04  8.5351
GRID   38          58.8735 -78.04  8.44277
GRID   39          56.9748 -78.04  7.7473
GRID   40          58.8577 -78.04  7.91084
GRID   41          10.918  -8.25   2.88568
GRID   42          19.4782 -8.25   2.7262
```



```

GRID      43      10.918  0      2.88568
GRID      44      19.4782 0      2.7262
GRID      45      28.6228 0      2.0133
GRID      46      10.6581 -8.25  -1.1833
GRID      47      19.1859 -8.25  -1.87377
GRID      48      10.6581 0      -1.1833
GRID      49      19.1859 0      -1.87377
GRID      50      28.438  0      -0.99490
$
$      CQUAD4
$
$      upper wing skin
$234567812345678123456781234567812345678123456
$
CQUAD4    1      1      1      2      5      4
CQUAD4    2      1      2      3      6      5
CQUAD4    3      1      4      5      8      7
CQUAD4    4      1      5      6      9      8
CQUAD4    5      1      7      8     11     10
CQUAD4    6      1      8      9     12     11
CQUAD4    7      1     10     11     14     13
CQUAD4    8      1     11     12     15     14
CQUAD4    9      1     13     14     17     16
CQUAD4   10      1     14     15     18     17
$
$      lower wing skin
$
CQUAD4   11      2     19     20     23     22
CQUAD4   12      2     20     21     24     23
CQUAD4   13      2     22     23     26     25
CQUAD4   14      2     23     24     27     26
CQUAD4   15      2     25     26     29     28
CQUAD4   16      2     26     27     30     29
CQUAD4   17      2     28     29     32     31
CQUAD4   18      2     29     30     33     32
CQUAD4   19      2     31     32     35     34
CQUAD4   20      2     32     33     36     35
$
$      upper wing root
$
CQUAD4   21      3     41     42     44     43
CQUAD4   22      3     42     18     45     44
CQUAD4   23      1     16     17     42     41
$
$      lower wing root
$
CQUAD4   24      4     46     47     49     48
CQUAD4   25      4     47     36     50     49
CQUAD4   26      2     34     35     47     46
$
$      upper wing tip
$
CQUAD4   27      1     37     38      3      2
$
$      lower wing tip
$
CQUAD4   28      2     39     40     21     20
$
$      front spar
$
$23456781234567812345678123456781234567812345
$
CQUAD4  101      5      1      19      22      4
CQUAD4  102      5      4      22      25      7
CQUAD4  103      5      7      25      28     10
CQUAD4  104      5     10      28      31     13
CQUAD4  105      5     13      31      34     16
CQUAD4  106      5     16      34      46     41
CQUAD4  107      5     41      46      48     43
$
```



```
$          REAR spar
$
$234567812345678123456781234567812345678123456781234
$
CQUAD4  201      6      38      40      21      3
CQUAD4  202      6      3      21      24      6
CQUAD4  203      6      6      24      27      9
CQUAD4  204      6      9      27      30     12
CQUAD4  205      6     12      30      33     15
CQUAD4  206      6     15      33      36     18
CQUAD4  207      6     18      36      50     45
$
$          ribs
$
$23456781234567812345678123456781234567812345678123456
$
CQUAD4  301      7      1      19      39      37
CQUAD4  302      7     37      39      40      38
$
CQUAD4  303      7      1      19      20      2
CQUAD4  304      7      2      20      21      3
$
CQUAD4  305      7      4      22      23      5
CQUAD4  306      7      5      23      24      6
$
CQUAD4  307      7      7      25      26      8
CQUAD4  308      7      8      26      27      9
$
CQUAD4  309      7     10      28      29     11
CQUAD4  310      7     11      29      30     12
$
CQUAD4  311      7     13      31      32     14
CQUAD4  312      7     14      32      33     15
$
CQUAD4  313      7     16      34      35     17
CQUAD4  314      7     17      35      36     18
$
CQUAD4  315      7     41      46      47     42
CQUAD4  316      7     42      47      36     18
$
CQUAD4  317      7     43      48      49     44
CQUAD4  318      7     44      49      50     45
$
$          CTRIA3
$
$          upper wing tip
$2345678123456781234567812345678123456781234567
$
CTRIA3  29      1      1      37      2
$
$          lower wing tip
$
CTRIA3  30      2      19      39      20
$
$          upper wing root
$
CTRIA3  31      1      17      18      42
$
$          lower wing root
$
CTRIA3  32      2      35      36      47
$
$          PLOAD4
$
$          upper wing skin
$2345678123456781234567812345678123456781234567812
$
PLOAD4      1      1-59.1427-61.8878-50.3685-78.2301
PLOAD4      1      2-61.8878-31.3934-41.596 -50.3685
PLOAD4      1      3-78.2301-50.3685-50.8665-72.8449
```



PLOAD4 1 4-50.3685-41.596 -43.6491-50.8665  
PLOAD4 1 5-72.8449-50.8665-51.1307-69.1618  
PLOAD4 1 6-50.8665-43.6491-45.8575-51.1307  
PLOAD4 1 7-69.1618-51.1307-51.3193-66.0781  
PLOAD4 1 8-51.1307-45.8575-47.2413-51.3193  
PLOAD4 1 9-66.0781-51.3193-51.5301-62.6308  
PLOAD4 1 10-51.3193-47.2413-3.95672-51.5301  
\$  
\$ lower wing skin  
\$  
PLOAD4 1 11 -22.0547-19.1066-12.6888-2.19356  
PLOAD4 1 12 -19.10666.51559 12.9525 -12.6888  
PLOAD4 1 13 -2.19356-12.6888-18.702 -10.6256  
PLOAD4 1 14 -12.688812.9525 10.6057 -18.702  
PLOAD4 1 15 -10.6256-18.702 -23.581 -14.1669  
PLOAD4 1 16 -18.702 10.6057 7.98227 -23.581  
PLOAD4 1 17 -14.1669-23.581 -27.0626-17.1318  
PLOAD4 1 18 -23.581 7.98227 6.33843 -27.0626  
PLOAD4 1 19 -17.1318-27.0626-30.9547-20.4463  
PLOAD4 1 20 -27.06266.33843 0.776339-30.9547  
\$  
\$ upper wing root  
\$  
PLOAD4 1 23 -62.6308-51.5301-3.47473-6.76076  
\$  
\$ lower wing root  
\$  
PLOAD4 1 26 -20.4463-30.9547-1.92518-1.90992  
\$  
\$ upper wing tip  
\$  
PLOAD4 1 27 -59.1427-28.9713-31.3934-61.8878  
\$  
\$ lower wing tip  
\$  
PLOAD4 1 28 -22.05474.7782 6.51559 -19.1066  
\$  
\$ upper wing tip - ctria !!!  
\$  
PLOAD4 1 29 -59.1427-59.1427-61.8878  
\$  
\$ lower wing tip - ctria  
\$  
PLOAD4 1 30 -22.0547-22.0547-19.1066  
\$  
\$ upper wing root - ctria  
\$  
PLOAD4 1 31 -51.5301-3.95672-3.47473  
\$  
\$ lower wing root  
\$  
PLOAD4 1 32 -30.95470.776339-1.92518  
\$  
\$ SPC  
\$  
\$2345678123456781234567812345678123456  
\$  
SPC 1 41 246 0.0  
SPC 1 42 246 0.0  
SPC 1 18 246 0.0  
SPC 1 46 246 0.0  
SPC 1 47 246 0.0  
SPC 1 36 246 0.0  
SPC 1 43 123456 0.0  
SPC 1 44 123456 0.0  
SPC 1 45 123456 0.0  
SPC 1 48 123456 0.0  
SPC 1 49 123456 0.0  
SPC 1 50 123456 0.0  
\$



```

$          PSHELL
$
$23456781234567812345678123456781234567812345678123456
$
PSHELL  1      1      0.007  1      1.      1
PSHELL  2      1      0.007  1      1.      1
PSHELL  3      1      0.017  1      1.      1
PSHELL  4      1      0.017  1      1.      1
PSHELL  5      1      0.017  1      1.      1
PSHELL  6      1      0.017  1      1.      1
PSHELL  7      1      0.017  1      1.      1
$
$          MAT1
$
$234567812345678123456781234567812345678123456781234
$
MAT1     1      1.6E9      0.33  1.73E2
$
$          FORCE
$
$234567812345678123456781234567812345678123456781234
$
FORCE    1      30      0      2000.0  0.0      0.0      1.0
FORCE    1      31      0      2000.0  0.0      0.0      1.0
$
$=====
$          DESIGN MODEL SOL-200
$
$
$          DESVAR
$
$2345678123456781234567812345678123456781234567
$
DESVAR   1      THICK1  0.007  0.001  1.0
DESVAR   2      THICK2  0.007  0.001  1.0
DESVAR   3      THICK3  0.017  0.001  1.0
DESVAR   4      THICK4  0.017  0.001  1.0
DESVAR   5      THICK5  0.017  0.001  1.0
DESVAR   6      THICK6  0.017  0.001  1.0
DESVAR   7      THICK7  0.017  0.001  1.0
$
$          DLINK
$
$2345678123456781234567812345678123456781234567812345
$
DLINK    1      1      0.0      1.0      2      1.0
$
$          DVPREL1
$ DEFINITION OF DESIGN VARIABLE TO ANALYSIS MODEL PARAMETER RELATIONS
$
$2345678123456781234567812345678123456781234567812345678123
$
DVPREL1  1      PSHELL  1      4      +THICK1
+THICK1  1      1.0
DVPREL1  2      PSHELL  2      4      +THICK2
+THICK2  2      1.0
DVPREL1  3      PSHELL  3      4      +THICK3
+THICK3  3      1.0
DVPREL1  4      PSHELL  4      4      +THICK4
+THICK4  4      1.0
DVPREL1  5      PSHELL  5      4      +THICK5
+THICK5  5      1.0
DVPREL1  6      PSHELL  6      4      +THICK6
+THICK6  6      1.0
DVPREL1  7      PSHELL  7      4      +THICK7
+THICK7  7      1.0
$
$  STRUCTURAL RESPONSE IDENTIFICATION
$
$23456781234567812345678123456781234567812345678123456781234

```



```

$
DRESP1  20      W      WEIGHT
DRESP1  21      DZ1     DISP           1           1
DRESP1  22      DZ2     DISP           2          38
DRESP1  23      S1      STRESS  PSHELL   2           1
DRESP1  24      S1      STRESS  PSHELL   2           2
DRESP1  25      S1      STRESS  PSHELL   2           3
$
$ DESIGN OBJECTIVE IDENTIFICATION (WEIGHT MINIMIZATION)
$
DESOBJ  20      WEIGHT           MIN
$
$ CONSTRAINTS
$
$2345678123456781234567812345678123456
$
DCONSTR 21      ALL      -100.0  100.0
DCONSTR 22      ALL      -100.0  100.0
DCONSTR 23      ALL      -15000. 20000.0
DCONSTR 24      ALL      -15000. 20000.0
DCONSTR 25      ALL      -15000. 20000.0
$
$ OPTIMIZATION CONTROL
$
DSCREEN 1      DISP
DSCREEN 2      STRESS
DOPTPRM 2      2
$
ENDDATA

```

## D.4 POSTNASTRAN

The task of this module is to extract the deflection of the wing and to extract the weight of the wing calculated by NASTRAN. Together with the PRESERV module, the deflection of the wing is used to model the SPARV co-ordinate points which are used in the second, third and fourth iterations. The deflection of each rib and spar is needed to calculate the deflected wing in the SPARV input.